The use of multiparameter flow cytometry to examine the state of *Escherichia coli* during a bioprocess

Jennifer Olajumoke Shitu
BSc. MSc.

A thesis submitted to the University of London
for the degree of Doctor of Philosophy

July 2005

Advanced Center for Biochemical Engineering
Department of Biochemical Engineering
University College London
Torrington Place
London WC1E 7JE

ProQuest LLC
789 East Eisenhower Parkway
P.O. Box 1346
Ann Arbor, MI 48106-1346

Abstract

The use of multiparameter flow cytometry to examine the state of *Escherichia coli* during a bioprocess

Traditional monitoring methods of cellular status, such as reproductive viability studies and optical density measurements tend to be time consuming and unable to give any insight into the physiological state of the cell beyond culturability. Multiparameter flow cytometry, a powerful investigative tool that allows the rapid, optical, quantitative measurement of cellular physiology via intrinsic and evoked optical signals from single cell or cell-sized particles in a moving fluid stream, was used as an alternative to provide valuable insights into the effects of bioprocesses on *E.coli.*

Batch fermentation processes and batch and fed batch biocatalytic processes were investigated for this thesis. Multiparameter flow cytometry was used in the characterisation of batch fermentations of *E.coli* IL-13 during the production of the recombinant human interleukin 13, in conjunction with fermentation profiling by traditional means and recombinant protein characterisation. It was established, via flow cytometric analysis of cell samples stained with a combination of three fluorescent stains, propidium iodide, PI; Bis- (1,3-dibutylbarbituric acid) trimethine oxonol, BOX, and Syto Red 63, SR; that induction with IPTG during the exponential phase, with controlled dissolved oxygen (above 30%) and pH (7± 0.2) were the optimum conditions for this fermentation.

The changing physiological and metabolic state of the whole cell biocatalyst *E.coli* TOP10 pQR239 during the Baeyer-Villiger monooxygenase mediated stereo-selective oxidation of bicyclo (3.2.0.) hept-2-en-6-one to yield (-)-1(S) 5(R)-2-oxabicyclo (3.3.0) oct-6-en-3-one and (-) 1 (R) 5(S)-3-oxabicyclo (3.3.0) oct-6-en-2-one was investigated in

batch and fed-batch biocatalytic processes as well as in shake flask bioconversions. The effects of bioconversion media, storage temperature, reaction pH, substrate and product concentration and the influence of the co-substrate glycerol on cell quality and enzyme activity were investigated. Whole cell biocatalyst quality was found to be affected by all of the above mentioned investigated parameters and the presence of the co-substrate was established to be essential for optimum enzyme activity.

Multiparameter flow cytometry was successfully applied to an industrially significant fermentation and biocatalytic process and facilitated the rapid analysis of cell quality in both instances to monitor the changes to cell cytoplasmic membrane integrity and polarisation, cell respiration capacity, the production of a recombinant therapeutic protein and a biocatalytic enzyme; thus establishing its feasibility as a tool for process definition and optimisation, during both the research and developmental stages of a bioprocess.

Acknowledgements

I would like to express my gratitude to my supervisors: Prof. John Woodley (UCL) and Dr. Michel Chartrain (Merck & Co Inc). John for his generous support, encouragement and valuable ideas into this project and Michel for his immense contributions to the project and being accessible despite being 'across the pond' in New Jersey.

I would like to thank the BBSRC and Merck & Co Inc. for their financial support.

I am grateful to my parents for their love, support and putting up with me during the course of my studies. To my sister Tracy, for making sure I was fed, being proud of me and keeping me motivated. Special thanks to my baby brother Jason, without whom this thesis would never have been written. And to Reg who gave me the light to run the last lap.

And to my colleagues in Foster Court for making it a thoroughly remarkable experience.

For my grandmothers

Alhaja Alimot Olajumoke Shitu

Mrs Mary Christiana Rock

Contents

Abbreviations

Abbreviation	
ADH	Alcohol dehydrogenase
ADP	Adenine diphosphate
ATP	Adenine triphosphate
BOX	Bis-(1, 3-dibutylbarbituric acid) trimethine oxonol
BVMO	Baeyer-Villiger monooxygenase
CCP	Carbonyl cyanide m-chlorophenylhydrazone
CER	Carbon-dioxide evolution rate ($mmolL^{-1}\ h^{-1}$)
CHMO	Cyclohexanone monooxygenase
CM	Cytoplasmic membrane
DBS	Dulbecco's buffered saline
DCW	Dry cell weight
DMSO	Dimethyl sulphoxide
DNA	Deoxyribonucleic acid
dsDNA	Double strand deoxyribonucleic acid
DOT	Dissolved oxygen tension (%)
EDTA	Ethylenediaminetetraacetic acid
FID	Flame ionisation detector
GC	Gas chromatography
IL-13	Interleukin 13
IPTG	Isopropyl-β-D-thiogalactopyranoside
OD	Optical density
OUR	Oxygen uptake rate ($mmolL^{-1}\ h^{-1}$)
RO	Reverse osmosis
RNA	Ribonucleic acid
PAGE	Polyacrylamide gel electrophoresis
PI	Propidium iodide
SDS	Sodium dodecyl sulphate

SR	Syto red 63
STR	Stirred tank reactor
TH2	T helper 2

List of Figures

List of Tables

Chapter 1

Introduction

1.0. Introduction

The production of fine chemicals and pharmaceutical grade therapeutic molecules from microbial systems is the core of modern biotechnology. Consequently there is a great deal of interest in strategies which increase their efficiency and output. Flow cytometry is a powerful investigative tool which could provide valuable insights into the effects of bioprocess conditions and parameters on the stability of the microorganisms involved in such processes.

1.1. Fermentation Processes

The foundations of biotechnological processes are rooted in fermentation; many of which are traditionally geared towards the production of foods and beverages. Microorganisms may be engineered to express non-host proteins during the fermentation process in response to certain induction strategies, which initiate the expression of the host or non-host protein(s). The proteins expressed range from therapeutic agents such as antibiotics and monoclonal antibodies to enzymes which maybe used in biocatalytic processes.

A great many biotechnological experiments are carried out in shake flasks, which impart the advantage of facilitating high densities of experimental data and simplicity of the apparatus (Freyer *et al* 2004). However, this approach is hindered by the fact that online monitoring of reaction parameters and trends as well as stringent control of cultivation or process conditions within the vessel are difficult to carry out. Consequently bacteria are cultivated in fermentation vessels (bioreactors) which allow rigorous online control and

monitoring. There are three main kinds of fermentation processes: Batch, fed-batch and continuous processes. Batch fermentations are the most basic and commonly used fermentation processes. Here all the nutrients required for growth are present at the start of the cultivation process. Nothing is added or removed from the bioreactor for the entire duration of cultivation i.e. it is a closed system. The cost of running a batch reactor depends on the time taken to achieve the desired biomass, product concentration or substrate conversion (Doran 1999). While this route has the advantage of being relatively easy to operate, depletion of a vital growth media component or accumulation of fermentation by-products such as acetate or citric acid may pose significant problems to cell quality and/or recombinant protein expression, via the inhibition of cell growth and downstream processing complications. Fed-batch processes are run a little differently in that nutrient composition is maintained via its intermittent or continuous addition into the bioreactor. This confers the advantage of avoiding high growth rates in cases where oxygen demand during fast growth may be too high for the mass transfer capabilities of the bioreactor (Doran 1999) or avoiding the build-up of inhibitory concentrations of acetic acid produced via overflow metabolic pathways (Hewitt *et al* 1999b, Andersson *et al* 1996). Bakers yeast is produced via fed-batch cultures to overcome catabolite repression and control oxygen demand (Doran 1999). However the problem of waste product accumulation still remains as nothing is removed from the fermentation. Continuous processes on the other hand employ a strategy where as a consequence of continuous nutrient addition and product and/or waste removal the fermentation process can continue indefinitely. This method is not commonly used.

The primary aim of fermentation processes is the production of cell biomass. This biomass may then be used to facilitate biocatalytic reactions or as a conduit for host or non-host protein expression. Fermentation control is important as it can have a significant impact on biomass concentration and quality, which may in turn affect overall system productivity.

1.1.1. Non-host protein expression

The expression of non-host protein(s) in recombinant bacteria usually occurs during the fermentation step; and can be achieved by either of two methods: extensively by an increase in gene copy number usually by plasmid amplification or intensively by the use of strong inducible promoters (Teich *et al* 1998). Inducible promoters may be activated by a variety of means, such as changes to the cellular environment. Increasing the cultivation temperature from 30°C to 38-42°C in *E.coli* containing thermoinducible promoters has been reported to induce foreign gene expression (Chen *et al* 1995; Ryan *et al* 1996), as has the addition of methanol to the culture medium (Hohenblum *et al* 2003) and exposure to light (Keyes and Mills 2003). Chemical induction of foreign gene expression is also possible. This is usually achieved by the addition of a compound which is not actively metabolised by the cell such as L-arabinose (Doig *et al* 2001) and Isopropyl-β-D-thiogalactopyranoside (IPTG) (Kosinski *et al* 1992; Anderson *et al* 1996; Lewis *et al* 2004). Either of these routes will induce the expression of the recombinant protein and the concomitant diversion of cellular metabolism away from normal cellular activity (Bentley *et al* 1990; Andersson *et al* 1996; Soriano *et al* 2002) thus eliciting a stress response.

Tight regulation, characterised by an absence of gene expression in the absence of the inducer (Keyes and Mills 2003), high-levels of expression and homogeneous induction are desired characteristics of inducible gene expression systems for biotechnological use, IPTG inducible promoters such as the one used in this study have the two latter characteristics (Chao *et al* 2003). While it is desired that gene expression should be to levels high enough to observe the desired physiological response, it is paramount that the inducer not be toxic to the host organism (Keyes and Mills 2003), thus control of the levels of the inducing agent which the host organism, is exposed to and when induction is implemented requires close monitoring and regulation.

The location of the non-host protein, whether it is intracellular or extracellular is governed by the kind of protein being expressed. For instance, in *Escherichia coli* TOP10

pQR239 expressing the recombinant cyclohexanone monooxygenase from *Acinectobacter calcoaceticus* (Doig *et al* 2001; 2002) the enzyme is located in the cell membrane as it is oxygenase (Held *et al* 2000). Other proteins may be located freely in the cytoplasmic space or as inclusion bodies.

1.2. Biocatalytic Processes

Biocatalytic processes include fermentations, enzyme catalysis and whole cell systems.

1.2.1. Biocatalysis

Biocatalysis involves the use of enzymes to mediate the approach to equilibrium of a given reaction. Although the concept of biocatalysis is not a new science, it nevertheless poses an integral part of modern bioprocess engineering. The natural diversity of enzymes along with high throughput screening techniques are exploited to access enzymes with greater industrial potential (Rozzell 1998). An estimated 2500 enzymes have been identified, with only 10% having commercial applications, of this number only 25 account for 80% of applications (Woodley 2000). Biocatalysis is used to facilitate two main types of transformations, the resolution of pairs of enantiomers and the asymmetric transformation of a racemic compound into a single isomer derivative (McCoy, 2001).

1.2.1.1. Biocatalysts

Biocatalysts generally consist of one or more enzymes, with respect to the number of catalytic steps required. There are a number of features that make the use of biocatalysts more desirable in contrast to chemical or conventional catalysts.

The most significant feature of biocatalysts is the exhibition of stereo-, regio- and chemo-specificity (Van den Burg *et al* 1999; Rasor and Voss 2001; Faber 2000), which facilitate reaction precision, minimizing side reactions and maximizing yield (Shaw *et al* 1999).

This is of great importance in the manufacture of pharmaceutical molecules and fine chemicals, as the production of an optically pure molecule is more likely to occur under the said conditions. Being biological in nature, biocatalysts are capable of working under mild operating conditions, typically neutral pH, ambient temperature, atmospheric pressure and in aqueous environments (Shaw *et al* 1999; Faber 2000). Biocatalysts are also increasingly being used in non-aqueous systems (de Bont 1998; Klibanov 2001). As a consequence of the mild operating conditions favored by biocatalysts, which are characterized by processes requiring lower energy inputs, biocatalyst mediated reactions are more energy efficient and environmentally friendly than those mediated by chemical catalysts. Biocatalysts are capable of sequential operation in the presence of an enzyme series, as this commonly occurs in nature. Enzyme mediated processes reduce the occurrence of by-product synthesis and thus the cost of product isolation and purification.

While the more positive characteristics of biocatalysts are significant so too are the less positive features. These include: the high cost of biocatalyst identification and development, this process is often expensive and time consuming; natural substrates and/or environments are often required, though it should be said that some enzymes, such as lipases can use inorganic solvents as substrates. The lack of operational stability of the biocatalyst also poses a significant problem where enzyme recycling is required. The development of thermostable enzymes via directed evolution and screening of thermophilic microorganisms is aiding in the creation of more robust catalysts; immobilization and isolation may also help to improve biocatalyst stability within a process setting. Low volumetric productivity is also a problem associated with biocatalysts (Thayer 2001), however this is not always the case, single step enzymatic transformations have been shown to produce tens or hundreds of grams of product ($L^{-1}h^{-1}$). An example of a highly productive biocatalytic process is the production of L-phenylalanine using an amidase or transaminase (Rozzell 1998).

1.2.1.2. Biocatalyst forms

The form of enzyme used can have a significant impact on the bioprocess, as everything from the initial upstream stage of fermentation to the recovery and purification stages have to be taken into account when establishing the best process route. Biocatalysts may be used in the form of isolated enzymes or as whole cells; which are either immobilized on an inert support or free within the process fluid. The form of biocatalyst used for a given biotransformation depends on a number of factors including, reaction type, co-factor requirement and reaction scale (Faber 2000).

1.2.1.3. Whole cell biocatalysts

The whole cell biocatalysts used tend to be bacterial and are characterized by large surface-area to volume ratios, which lead to high substrate biotransformation rates and the capacity to metabolize an extensive range of substrates and are easier to culture, being generally less fastidious in nature, than yeast or mammalian cells (Roberts *et al* 1995).

There are undoubted benefits of using enzymes in their natural environments (i.e. in the microbial cell); these benefits constitute the principal driving force behind the use of whole cell catalysts; since the removal of the enzyme from its natural environment confers no real advantages on it and may in fact adversely affect the enzyme by destabilizing it or hindering its activity in some manner. Whole cell processes have the dual function of introducing chirality and mediating multi-step processes (Buckland *et al* 2000). Whole cells can be free or immobilized on an inert base; although immobilizing whole cells may result in oxygen transfer limitations, which can potentially compromise enzyme activity.

Whole cell biocatalytic processes have the advantage of being reasonably cost effective, since the cost of preparation of cell free intracellular enzymes is often expensive and laborious in terms of the time and resources required for the isolation and purification. It

is therefore more economical to use whole cell biocatalysts in instances where it is a feasible alternative. Whole cell biocatalysts also confer the advantage of ensuring complete enzyme activity; since enzyme instability may be induced outside the cellular environment, due to the alteration or loss of the natural conformation required for enzyme activity. Removing an enzyme from a membrane bound environment may result in a partial or total loss of enzyme activity as seen in alkane hydrolase (Duetz *et al* 2001).

One of the principal driving forces behind the use of whole cell biocatalytic systems is the ease of meeting co-factor requirements. In biotransformations involving growing or resting cells co-factor regeneration is accomplished by the complete enzyme apparatus of the cell (Eckstein *et al* 2004), thus eliminating the need to provide the stochiometric quantities of co-factors required. Such co-factor requiring reactions include redox reactions which require pyridines such as nicotinamide adenine dinucleotide phosphate (NADPH) as cofactors and adenine triphosphate (ATP) requiring phosphorylations (Endo and Koizumi 2001). Co-factors are often expensive and the use of whole cells that already possess the cofactors such as NADPH circumvents the necessity of purchasing these co-factors (Held *et al* 2000). The number of enzymes, co-factors and substrates involved in a reaction may also result in it being too complicated to perform *in vitro* as seen in the asymmetric reduction of prochiral carbon molecules (Duetz *et al* 2001; Buckland *et al* 2001).

Whole cells may be used in any one of the following four forms. As growing cells where the cells are actively undergoing cell growth and proliferation during the course of the biocatalytic process (Woodley 2000), which is typically based on conventional fermentation practices. While growing cells facilitate higher biocatalytic activities these biotransformations are commonly accompanied by increased by-product concentrations and process control difficulties as a result of the high biomass achieved (Faber 2000). Alternatively the cells may be resting (non-growing) i.e. they are not actively exhibiting growth or proliferation but are metabolically active (Woodley 2000; Simpson *et al* 2001). This method has been shown by Walton and Stewart (2002) to present a number of process advantages to large scale bioconversions which include simplification of reactor

scheduling, extended reaction times and avoidance of substrate and/or product toxicity issues, in the Baeyer-Villiger oxidation mediated by recombinant *E.coli* BL21 (DE3). However, biocatalyst activity may be decreased. The resting cells may also be re-suspended in buffered pre-defined media such as phosphate buffers (Walton and Stewart 2004). The use of re-suspended resting cells may help eliminate problems associated with product isolation from the process medium (Woodley 2000). Spore cultures may also be used; they may be reactivated by re-suspension in water or dilute buffer. They are incubated in the absence of nutrients and are capable of maintaining useful biotransformations for up to 30 days (Roberts *et al* 1995).

Immobilization of whole cells, usually bacterial or yeast, increases the chances of the cells remaining metabolically active for longer than if they were an actively growing culture. However, this can also lead to a reduction in catalytic activity, possibly as a result of substrate diffusion and oxygen transfer limitations. This can be overcome by increasing cell density. This trend of decreasing enzyme activity may also be observed if an isolated enzyme has been immobilized.

1.2.1.4. Isolated enzymes

Enzymes that are free of the membrane-induced confines of the cell are said to be isolated. These enzymes may either be free within the process or immobilized on an inert support matrix. Isolated enzymes are generally used for simpler reactions such as hydrolysis, that do not require the involvement of multiple enzymes or co-factors and in cases where there is a limited transport into the cells and competing enzyme-catalysed reactions are present (Buckland *et al* 2001; Woodley 2000).

The fact that isolated enzymes can be purified, immobilized and stabilized implies that their performance margins can be improved upon and enzyme recovery and re-use is possible. Isolated enzymes are characterized by high specificity and selectivity. However

because the enzymes are free of the cell confines any required co-factors need to be supplied, at significant expense.

1.2.1.5. Immobilized enzymes

Isolated enzymes and whole cell catalysts may be immobilized in order to facilitate re-use or promote ease of product recovery and purification. Immobilization of isolated enzymes generally facilitates ease of product recovery and purification and may encourage high product formation as the enzyme can be configured so that the active site is constantly exposed to the substrate.

Immobilization can be achieved by any one of four means; Entrapment in a polymer matrix, surface adsorption onto a water insoluble solid support, covalent attachment to a water-insoluble solid support and chemical cross-linking with bi-functional agents (Roberts *et al* 1995).

1.2.1.6. Co-factor requirement in biocatalysis

Co-factors such as the pyridine dinucleotides e.g. NADPH or phosphorylated trinucleotides e.g. ATP are expensive but vital to some biocatalytic processes and thus must be recycled or regenerated. This may be achieved by *in vivo* co-factor recycling; an approach, which is being industrially exploited, via the use of intact, metabolically active cells as biocatalysts. There are two methods of NADPH regeneration. The first of these utilizes an ancillary enzymatic reaction e.g. glucose dehydrogenase to regenerate NADPH from NADP produced in the principal enzymatic reaction. The second method is a substrate-coupled approach, where a reduced substrate is oxidized to product by the same enzyme in the presence of NADP produced in the former reaction (Pereira *et al* 1994). As well as regeneration of the co-factor the co-substrate may also provide metabolic maintenance energy (Meinander and Hahn-Hägerdal 1997).

Among the principle driving forces for the use of whole cell biocatalyst in industrially important biocatalytic processes is the ease of co-factor regeneration. This is especially essential in the case of redox biocatalysis since product formation is inextricably linked with co-factor regeneration (Walton and Stewart 2004). The introduction of oxygen by biocatalysts is co-factor dependent and while *in vitro* co-factor regeneration is feasible it is costly (Held *et al* 2000). Co-factor consumption is usually stochiometric and as such may add significant expense to the process. Important NADPH-dependent processes include hydroxylations, epoxidations and the reduction of ketones to chiral alcohols (Duetz *et al* 2001). CHMO is an example of an enzyme that utilizes the expensive and unstable cofactor, NADPH, in stochiometric quantities (Hogan and Woodley, 2000).

1.2.1.7. Biocatalyst deterioration

It is expected that a certain amount of biocatalyst deterioration will occur during the progression of a biocatalyst through a bioprocess. This deterioration will be as a result of any number of associated and independent factors which include natural cell death, cell damage due to process conditions and substrate and/or product inhibition. Consequently any deterioration needs to be monitored and controlled to maintain optimum biocatalyst efficiency and productivity for as long as possible.

1.2.1.8. Biocatalyst limitations

Biocatalyst use within the process industry is not without limitations and there are usually strategies in place to ensure optimum process conditions without compromising biocatalyst activity and product titers. Thus the choice of catalyst form requires careful consideration in order to minimize compromising biocatalyst activity.

One of the most common forms of biocatalyst limitation is inhibition caused by substrate and/or product accumulation in the system. Substrate inhibition may be overcome by

keeping substrate concentrations low via controlled addition during the bioprocess (Faber 2000), while removal of accumulating product via *in-situ* product removal methods may circumvent product inhibition issues (Lye and Woodley 1999; Simpson *et al* 2001; Hilker *et al* 2004). Substrate and/or product toxicity to the whole cell biocatalyst may also be a problem, as seen in an indene bioconversion mediated by a *Rhodococcus* strain (Amanullah *et al* 2002a). Despite possessing mechanisms which allow them to cope with unfavorable conditions, many microorganisms are unable to cope with the high concentrations of non-natural substrates and products which may be used in industrial biocatalytic processes (Held *et al* 2000).

The fact that enzymes are only naturally present in one enantiomeric form, mean that it is impossible to invert the chiral induction of a given enzyme reaction by choosing the other enantiomers of the biocatalyst (Faber 2000), thus catalytic activity may be compromised. Enzymes may also exhibit narrow operation parameters, and only exhibit optimal activity within certain pH, temperature and salt concentration ranges beyond which they become deactivated (Prescott *et al* 1996; Faber *et al* 2000).

When free whole cells are the biocatalyst form of choice, cell density within the process can be a problem, especially as high cell density growth is the norm for culturing whole cell biocatalysts (Woodley 2000). High densities may result in oxygen transfer limitations within the bioreactor (Doran 1999) this can be overcome by fed-batch fermentation processes, where the controlled addition of a carbon source may slow down growth rates.

1.3. The model processes

Two model processes, each representative of the two halves that could constitute upstream biotechnological processes were investigated in this study. The rationale behind this was based on the fact that for many bioprocesses the fermentation and subsequent biotransformation stages are separate entities, which may on occasion require different process conditions. In the case of fermentation processes where natural carbon sources are used for production of biomass and for *de novo* synthesis of products such as alcohols

and vitamins (Held *et al* 2000), the process usually has a single upstream step. However, when whole cell biocatalysis is the process aim, the fermentation step's primary function is the generation of biomass which is subsequently used to facilitate the biotransformation; resulting in two upstream process steps (three, if primary recovery or separation is included). Combining the two model processes allowed a realistic representation of the upstream process(s) of a bioprocess to be examined and acquired. Possible upstream process steps are outlined in Figure 1.1.

1.3.1. The fermentation process

The fermentation process investigated was the expression of human interleukin 13 by recombinant *Escherichia coli.*

1.3.1.1 The bacterial strain

Human interleukin 13 was expressed as inclusion bodies in *E.coli* strain BL21 (DE3) (Novagen, Madison, WI, USA). This strain is subsequently referred to as *E.coli* IL-13. This strain contained a pET11a plasmid (Novagen, Madison, WI, USA) into which the IL-13 gene had been cloned. *E.coli* IL-13 carries the T7 RNA polymerase gene in an isopropyl-β-D-thiogalactopyranoside (IPTG) inducible form, under the control of the *lac* UV5 promoter (Dumon-Seignovert *et al* 2004). *lac* UV5 is a variant of the lac promoter (Pan and Malcolm 2000). IPTG, a *lac* operon inducer, permits transcription by binding to the *lac* repressor and substantially decreasing its binding ability to the *lac* operator (Novy and Morris 2001). The pET11a plasmid configuration is shown in Figure 1.2. This strain was kindly donated by Dr. Michel Chartrain (Merck and Co Pharmaceuticals Inc. Bioprocessing Research and Development, Rahway, N.J. USA).

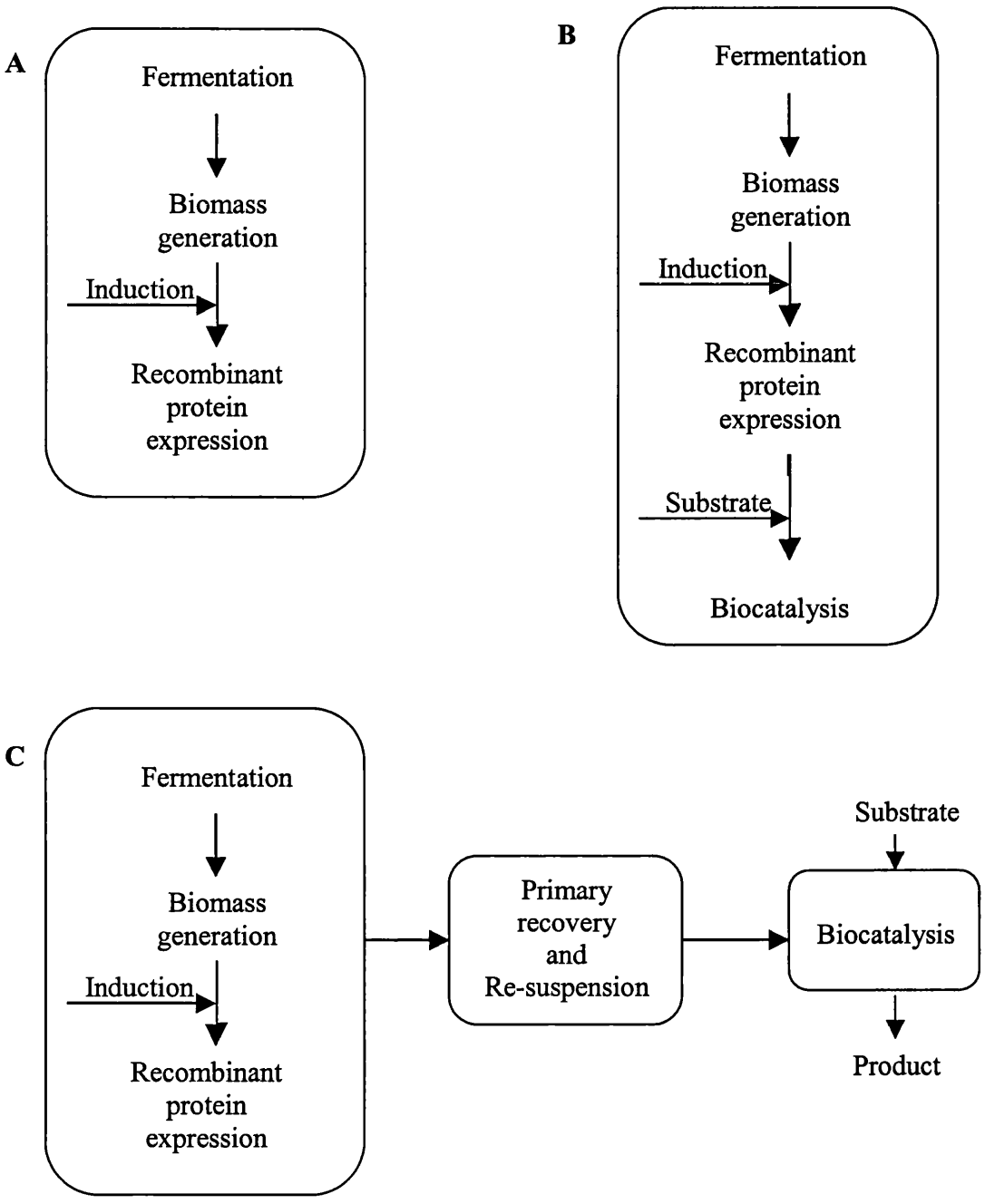

Figure 1.1. Possible process routes. A. Single upstream process step: fermentation; B. Two step upstream process: The biocatalytic reaction occurs sequentially in the same vessel. C. Three step upstream process: The fermentation step is followed by a primary recovery step then the biocatalytic reaction, the two are separate entities.

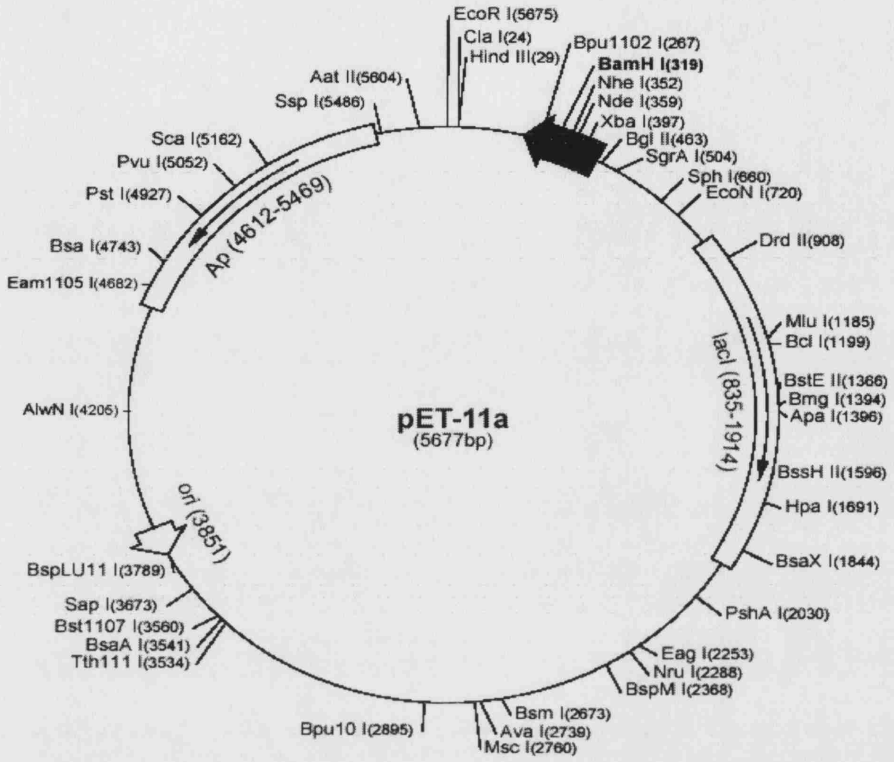

Figure 1.2. The pET11a vector
(Novagen. http://www.emdbiosciences.com/docs/NDIS/TB042-000.pdf)

1.3.1.2. Interleukins

The human immune system utilises a number of specialised cells in its defence against infection among which are the cytokines, a number of which are referred to as interleukins. Interleukins (IL) are low molecular weight glycoproteins secreted by leukocytes to activate and regulate important biological processes such as cell growth, immunity and morphogenesis, and are produced mainly by leukocytes (nucleated haemoglobin-free blood cells) (Goldsby *et al* 2000) although some are produced by polymorphonuclear phagocytes or auxiliary cells.

Interleukins are involved in directing other immune cells to divide and differentiate; with each interleukin acting on a specific group of cells which in turn express the correct receptors for that interleukin. IL-13 is a member of the short-four-helix-bundle cytokines, one of several classes of helical cytokines that include IL-2, IL-3, IL-4, IL-5 and granulocyte macrophage colony stimulating factor. It is a pleiotropic cytokine which elicits pro-inflammatory and anti-inflammatory immune responses (Eisenmesser *et al* 2000). In the human body the main source of IL-13 are the T helper 2 (TH2) cells (interleukin producing $CD4^+$ cells). IL-13 stimulates proliferation of antibody producing B-cells (immunoglobin producing lymphocytes) cumulating in the production of IgG and IgE. It also promotes $CD8^+$ cell growth and TH2 cell differentiation. IL-13 is structurally similar to IL-4, with which it shares ~25% sequence identity, and has similar effects (Malabarba *et al* 1996; Goldsby *et al* 2000; Eisenmesser *et al* 2000; Eales 2003).

Previous studies have reported the expression of interleukins in *E.coli* systems, for example Dean *et al* (2005) expressed feline interleukin 15 while Joshi and Puri (2005) expressed human interleukin 13. Thompson and Debinski (1999) also reported on the expression of human interleukin 13 in *E.coli*. The human IL-13 expressed by *E.coli* IL-13 is between 10.3 and 15kDa.

1.3.2. The biocatalytic process

The biocatalytic process investigated was the Baeyer-Villiger monooxygenase (BVMO) mediated stereo-selective oxidation of a cyclic ketone, bicyclo (3.2.0.) hept-2-en-6-one to yield two chiral lactone products, (-)-1(S) 5(R)-2-oxabicyclo (3.3.0) oct-6-en-3-one and (-) 1 (R) 5(S)-3-oxabicyclo (3.3.0) oct-6-en-2-one. This bioconversion was facilitated by the use of the whole cell biocatalyst *Escherichia coli* TOP10 pQR239.

1.3.2.1. The bacterial strain

The strain used was a modified *E.coli* strain containing a plasmid, pQR239 into which the cyclohexanone monooxygenase (CHMO) gene bearing the araBAD promoter, from *Acinetobacter calcoaceticus* NCIMB 9871, a class 2 pathogen (Doig *et al* 2001) had been cloned. This is a non-pathogenic recombinant *E.coli* strain. The CHMO gene in *E. coli* TOP10 pQR239 is under the control of an L (+) arabinose inducible promoter. This strain has the advantage of lacking the lactone hydrolase present in *A. calcoaceticus*, thus eliminating product degradation by that route (Doig *et al* 2001). This strain was kindly donated by Dr. John Ward (Biochemistry and Molecular Biology Department, UCL).

1.3.2.2. The Baeyer-Villiger reaction

The Baeyer-Villiger reaction is an example of an academically and industrially significant chemical reaction, which involves the transformation of a cyclic ketone to a lactone in a reaction mediated by a hydroxyl-peroxide or peroxyacid (Kelly 1996; Roberts and Wan 1998), this reaction was first discovered in 1899 by Baeyer and Villiger. The enzymatic Baeyer-Villiger reaction as exemplified in this investigation is an efficient way of obtaining enantiopure lactones from racemic or prochiral cyclic ketones (Simpson *et al* 2001).

The Baeyer-Villiger reaction is believed to occur via a two-step process, Figure 1.3. In this process the addition of peroxyacid to the carbonyl group of the ketone (step 1) creates a tetrahedral Criegee-intermediate, which subsequently (step 2) rearranges, via the expulsion of a carboxylate ion and migration of a carbon-carbon bond, to form the corresponding lactone (Roberts and Wan 1998; Faber 2000).

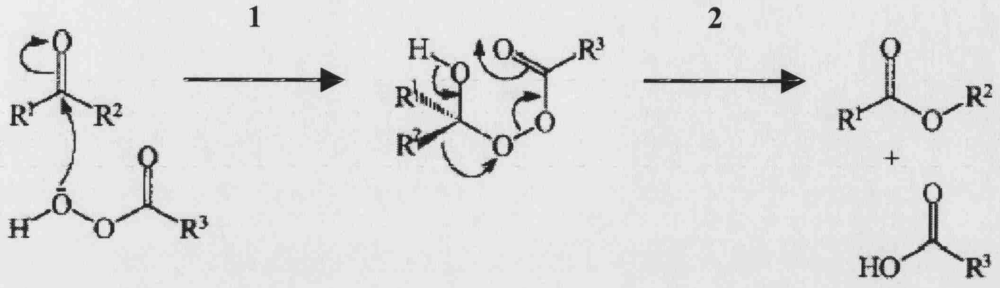

Figure 1.3. The two-step mechanism for the Baeyer-Villiger reaction. (Modified from Roberts and Wan 1998).

A significant number of the enzymes capable of mediating Baeyer-Villiger reactions are monooxygenases. Monooxygenases incorporate a single oxygen atom derived from molecular oxygen into the substrate with the accompanying reduction of the second oxygen atom into a water molecule (Held *et al* 2000). This activation of molecular oxygen is via reduction at the expense of a reductant, usually NADH or NADPH (Faber 2000). The Baeyer-Villiger monooxygenases (BVMOs) catalyse the nucleophilic oxygenation of a wide variety of linear or cyclic ketones to their corresponding optically pure esters and ketones (Willetts 1997; Bird *et al* 2002). BVMOs are classified with respect to the nature of their flavin cofactor, (which is present in all BVMOs) (Malito *et al* 2004).

The type I enzymes are flavin adenine dinucleotide, FAD binding and NADPH dependent, both enzymes plus the substrate bind to the same polypeptide subunit and may have a monomeric or homo-oligomeric structure (Willetts 1997; Alphand *et al* 2003). The type I enzymes, which include cyclohexanone monooxygenase from *A. calcoaceticus* and phenylacetone monooxygenase from *Thermobifida* fusca (Malito *et al* 2004) are the most extensively investigated (Mihovilovic *et al* 2002). The type II enzymes on the other hand are flavin mononucleotide, FMN binding and NADH dependent. They consist of two distinct kinds of subunits, one of which binds the carbonyl substrate and the other

nicotinamide nucleotide, thus serving as an NADH dehydrogenase (Willetts 1997; Alphand *et al* 2003).

In addition to catalyzing Baeyer-Villiger type transformations, the BVMO group of enzymes has been shown to catalyse other transformations including sulfoxidation (Beecher and Willetts 1998; Zambianchi *et al* 2002) and amine oxidation (Stevens and Vanderhoydonck, 2001). Several bacteria e.g. *Acinetobacter sp.* (Doig *et al* 2001) and *Rhodococcus sp.* (Van Der Werf 2000) and fungi e.g. *Cylindrocarpon radicicola* ATCC 11011 (Itagaki 1986), produce BVMOs. In bacteria these oxidations are typically part of catabolic pathways for non-carbohydrate ketone energy sources such as cyclohexanone and camphor; in fungi they are involved in the switch from primary to secondary metabolism (Willetts 1997; Walton and Stewart 2002).

The most well characterized of the BVMOs is cyclohexanone monooxygenase (CHMO) from *A. calcoaceticus* NCIMB 9871 (Mihovilovic *et al* 2001; Alphand *et al* 2003). This enzyme is a 59 kDa monomeric FAD and NADPH dependent oxidoreductase (Stewart 1998). Owing to its capacity to catalyse the Baeyer-Villiger type oxidation of over 80 different ketones (Stewart 1998), it has great potential in industrial catalysis.

The BVMO reaction investigated in this study is the stereo-selective oxidation of the cyclic ketone, bicyclo (3.2.0.) hept-2-en-6-one to yield two chiral lactone products, (-)-1(S) 5(R)-2-oxabicyclo (3.3.0) oct-6-en-3-one and (-) 1 (R) 5(S)-3-oxabicyclo (3.3.0) oct-6-en-2-one. The bioconversion is catalysed by the CHMO expressed by the whole cell biocatalyst *E.coli* TOP10 pQR239. This is the only route for the production of the enzymatic lactone, (-) 1 (R) 5(S)-3-oxabicyclo (3.3.0) oct-6-en-2-one. A reaction scheme of this bioconversion is illustrated in Figure 1.4.

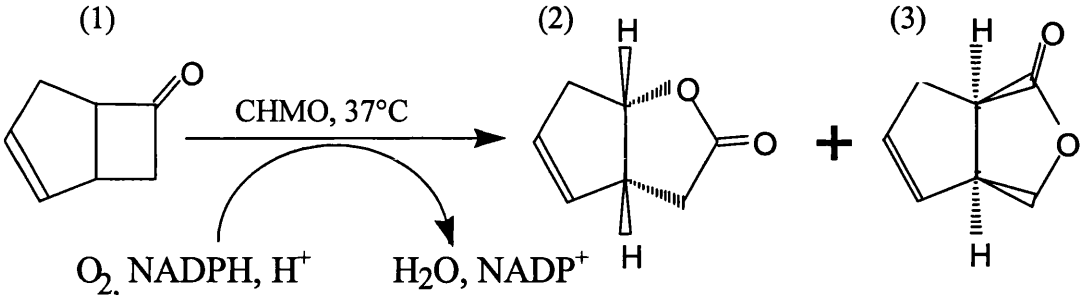

Figure 1.4. The Baeyer -Villiger CHMO mediated stereoselective oxidation of bicyclo (3.2.0.) hept-2-en-6-one (1) yielding (-)-1(S) 5(R)-2-oxabicyclo (3.3.0) oct-6-en-3-one (2) and (-) 1(R) 5(S)-3-oxabicyclo (3.3.0) oct-6-en-2-one (3).

1.4. The *E.coli* systems

While the two model processes investigated in this study, the production of a recombinant protein following induction during fermentation and the whole cell biocatalyst mediated BVMO bioconversion, are representative of the two processes that could constitute upstream biotechnological processes they are further related in a number of ways.

The first of these common links is the fact that both processes involve recombinant *E.coli* strains. *E.coli* systems containing a variety of expression vectors are commonly used in academia and in industrially and commercially relevant processes. Thus data and conclusions obtained may be applied to *E.coli* systems utilizing similar plasmids and processes as well as to other similar organisms.

Induction of recombinant gene expression is vital for control of plasmid expression with regard to preventing random and directed expression of the recombinant protein during the bioprocess. It is a key parameter for optimization in the development of processes where expression of the recombinant protein is the ultimate aim. Induction frequently

precedes whole cell biocatalysis as the expression of the recombinant enzyme needs to occur prior to bioconversion initiation. This is certainly the case in the BVMO mediated oxidation of bicyclo (3.2.0.) hept-2-en-6-one into (-)-1(S) 5(R)-2-oxabicyclo (3.3.0) oct-6-en-3-one and (-) 1(R) 5(S)-3-oxabicyclo (3.3.0) oct-6-en-2-one.

Flow cytometric profiling of both potential factions of the upstream stage of a bioprocess has been achieved, facilitating insights into process characterization and optimization using a non-traditional technique. A detailed discussion on flow cytometry can be seen in chapter 2.

1.5. Flow cytometry

Flow cytometry measures intrinsic and evoked optical signals from single cell or cell-size particles in a moving fluid stream (Weaver 2000). It allows the characterization of heterogeneous cell populations using scattered light; this characterization is with respect to distributions in their physiological status and metabolic activities such as DNA content, viability, protein content and enzyme activity (Kell *et al* 1991).

1.5.1. Applications of flow cytometry

Flow cytometry has significant advantages over conventional microscopic analysis, principally because it is capable of rapid single cell analysis and thus gives accurate accounts on the physiological state of the said cells. Perhaps the most important of these is its capacity for analysis of cellular status 'beyond culturability'.

One of the principal applications of flow cytometry is the determination of viability, which tends to be rather complex to define and measure (Nebe-Von-Caron *et al* 1999; Winson and Davey 2000; Parthuisot *et al* 2003). Traditional methods for determining this include the plate count method which is based on the reproductive ability of the cells and

takes 2-5 days despite its high sensitivity and the determination of colony counting units (Deere *et al* 1998). Another method is to evaluate cell viability is via membrane integrity assessment using tryphan blue exclusion; this method is not sensitive (Cunningham 2001). Total microscopic counts may also be used but they lack the capacity to discriminate between living, dead and viable but non-culturable cells (Thusitha *et al* 2000). Typically microbial cells are said to be viable if they are capable of proliferation (Nebe-von Caron and Badley 1995) or of performing all cell functions necessary for survival under given conditions (Breeuwer and Abee 2000). Owing to the heterogeneity encountered within microbial populations, cells cannot be simply classified as dead or alive as these definitions of cell viability does not take into account injured or stressed cells which have reached this state as a result of culture conditions or extended lag phases and may otherwise recover and become capable of reproduction. It is also possible for viable cells to enter a viable but non-culturable state (Parthuisot *et al* 2003). Consequently a second definition, used for vital cells, is the presence of cellular metabolism such as membrane potential and enzyme activities (Nebe-von Caron and Badley, 1995). Work by Nebe-von Caron *et al* (1998) identified four physiological states following flow cytometric analysis of *Salmonella typhimurium*: reproductively viable, metabolically active, intact and permeabilised.

High speed analysis is another advantage of flow cytometry. In light of the necessity of avoiding physical damage to the cells, the combination of cell concentrations and linear flow rates allow most flow cytometers to analyse between 100 and 1000 cells sec^{-1} (Davey and Kell 1996; Braga *et al* 2003). Typical flow cytometric analysis rates are in the region of 10^4 to 10^5 particles min^{-1} (van Dilla *et al* 1969; Robertson *et al* 1998). Sample preparation times are determined by the fluorescent stains used, their targets within the cell and any cell preparation requirements such as fixing or washing. A single cell crosses the light beam in 15 to 20 μsec, this is period corresponds to the duration of the fluorescent light pulse (van Dilla *et al* 1969). Sample analysis typically takes 1-2 minutes.

While the advantages of flow cytometry are many, the technology is not without disadvantages. The first of these is the cost of the flow cytometers which can cost anything up to $200,000 depending on specification and capacity. The second potential shortcoming is that skilled personnel are usually required to operate and maintain the instruments in order to obtain acceptable or optimum performance; as a consequence newer machines are designed to be more user friendly (Davey and Kell 1996; Fu *et al* 1999).

1.5.2. Process applications of flow cytometry

The optimisation and control of bioprocesses requires the stringent monitoring and skillful manipulation of environmental variables to maintain the culture at conditions which are optimal for product synthesis. The physiological state of the growing biomass and the distribution of different physiological and metabolic states within the cell population can have a significant impact on the productivity of a biotechnological process (Porro and Srienc 1995). Multiparameter flow cytometry provides a robust method of gathering information on the distribution of a given parameter within the cell population. The characterization of the various sub-populations present at any given time especially with respect to metabolic activity or status would greatly enhance bioprocess optimisation capacity (Reiseberg *et al* 2001). All of the above advantages and applications (Section 1.5.1) work in conjunction to promote the application of multiparameter flow cytometry to process characterization studies and process optimisation, thus facilitating its use as a process tool.

When coupled with cell sorting, flow cytometry may be used in the selection of biotechnologically valuable bacterial strains. Cell sorters separate a heterogeneous suspension of particles into purified fractions based on their fluorescence and light scattering properties following flow cytometric analysis (Ibrahim and Van den Engh 2003). Cell sorting is accomplished by the application of an electric charge to a droplet containing the cell of interest which is then passed through an electrostatic field and

subsequently deflected right or left (Horan and Wheeless 1977). This confers the advantage of physically isolating different sub-populations of cells for further analysis. This has been demonstrated by Nebe-von Caron *et al* (1998) who identified four physiological states following flow cytometric analysis and cell sorting onto solid growth medium, of *Salmonella typhimurium.* In light of this, flow cytometry coupled cell sorting may be used to isolate high yielding biotechnological strains or sub-populations that show a low sensitivity to toxic substrates or harsh processing conditions.

Flow cytometric analysis has been applied to the investigation of microorganisms in batch (Hewitt *et al* 1999a, b; Amanullah *et al* 2002a, b; 2003) and continuous cultures (Lú Chau *et al* 2001) and may be used to provide the rapid online microbial monitoring that is essential in industrial process systems (Harding 2000). Zhao *et al* (1999) have applied a flow injection flow cytometry system to the online monitoring of bioreactors. The quantitative and qualitative representation of what is happening within a culture during cultivation and/or a reaction that can be obtained from flow cytometric analysis is inestimable. Since flow cytometry can be used to monitor the effects of process parameters on microbial systems, its use as a process condition optimisation tool, via investigation of the process organism, is the next logical step. This study aims to demonstrate the use of multiparameter flow cytometry as a feasible process monitoring and optimisation tool.

1.6. Summary

The microbial bioprocess is a multifaceted entity, involving the optimization of many process parameters. Of these the optimization of the microorganism in use is possibly one of the most crucial as its physiological and metabolic status is paramount to system productivity. This project aims to investigate the effects of a range of parameters on the stability of two *E.coli* strains involved in a fermentation and biocatalytic process via the use of multiparameter flow cytometry. These parameters are also assessed in terms of their impact on overall process productivity.

Chapter 2

Flow Cytometry and Method Development

2.0. Introduction

Microbial cultures are dynamic systems, at any given time during culture in liquid media, there is a lack of equilibrium as the cell population is composed of several sub-populations of cells at different stages of the cell cycle which exhibit a range of physiological and metabolic states.

Microbial heterogeneity within a culture, excluding natural mixed populations, is due to three major sources (Davey and Kell, 1996; Zhao *et al,* 1999; Winson and Davey, 2000). The first of these is changes in the microbial genotype as a result of mutations. Mutations are known to occur randomly or in response to environmental changes in microbial populations and may be lethal or advantageous to the organism (Weaver 1995). Mutations can contribute to physiological alterations via selection if the new mutation is advantageous or dominant. The effects on the population are greater if the mutation occurs early in the growth of the culture. These mutations can alter microbial genotypes as seen in populations of *E.coli* where mutations arise on average in $5x\ 10^{-3}$ of the population in each generation (Davey and Kell, 1996). Plasmid loss in recombinant strains can also have the same effect.

Progression through the prokaryotic cell cycle may also contribute to heterogeneity within a microbial population ultimately resulting in phenotypic alterations (Srienc and Dien 1992). Overlapping cycles of DNA replication can result in a variable gene copy number and cause further increases in heterogeneity within the population. Since protein expression can be dependent on phases of the cell cycle it follows that the distribution of cells in the cell cycle will significantly affect microbial activity (Davey and Kell 1996).

Environmental changes during cultivation may also cause phenotypic alterations (Dunlop and Ye 1990, Shapiro 2000a). Conditions such as nutrient availability (Muller *et al* 1999) and pH variation (Onyeaka *et al* 2003) can also have a significant impact on culture heterogeneity.

In industrial biotechnological processes this heterogeneity within cultures can have a significant impact on growth associated parameters such as protein synthesis or substrate uptake (Zhao *et al* 1999) and may considerably influence the overall productivity and stability of the microbial process. However, it is difficult to identify and quantify these sub-populations rapidly and continually in a process environment. This is where flow cytometry comes into its own as a tool for quantitative and qualitative estimation of these dynamics.

The principle of flow cytometry is to pass a narrow stream of cells, stained with a fluorescent dye which binds quantitatively to the cellular constituent being investigated, through a beam of exciting light and to measure the intensity of the resulting pulses of fluorescence (Steen and Lindmo 1979; Veal *et al* 2003).

2.1. Flow Cytometry

Flow cytometry is a method that measures intrinsic and evoked optical signals from single cell or cell-size particles in a moving fluid stream (Weaver 2000). It allows the characterization of heterogeneous cell populations using scattered light; this characterisation is with respect to distributions in their physiological status and metabolic activities such as DNA content, viability, protein content and enzyme activity (Kell *et al* 1991). Intracellular component specific fluorescent stains allow acquisition of information on cellular characteristics, such as size, membrane potential, viability and metabolism, which in the terminology of single-cell analysis are usually referred to as parameters (Shapiro 2000a). This term is also used to refer to the physical characteristics measured by instruments such as flow cytometers.

Initially developed in the late 1940s by Gucker *at al* (1947) to detect bacteria in aerosols for military applications flow cytometry has since been applied to the study of mammalian cells (Harding *et al* 2000; Borth *et al* 2001), yeasts (e.g. Fowler and Dunlop 1989; Deere *et al* 1998; Bouchez *et al* 2004), bacteria (e.g. Skarstad *et al* 1983; Muller *et al* 2000 and 2002; Amanullah *et al* 2002a, b; 2003) virus detection (Patterson *et al* 1993) and sub-microscopic particles (Steen 2004). Flow cytometry can also be applied to the measurement of prepared cellular components such as organelles and nuclei (Joroszeski and Radcliff 1999).

The 1960s (van Dilla *et al* 1969) and 1970s (Steen and Lindmo, 1979; Shapiro *et al* 1979) reported on applications of flow cytometry to the study of mammalian cells however applications to bacterial systems were limited by the smaller size and consequently low concentrations of cellular constituents of microbial cells (Davey and Kell 1996; Hewitt *et al* 1999a; Winson and Davey 2000). The smaller size of bacterial cells causes a decrease in the sensitivity of the technique due to a decreased signal, typically 1000X less than animal cells (Amanullah *et al* 2003). Work by van Dilla *et al* (1969) who incorporated a laminar sheath- flow technique and an argon laser was an important step in application of this technique to microbiology as was work by Steen and Lindmo (1979), who developed a sensitive arc-lamp based instrument. In the late 1970s development of better fluorescent stains and optics technology facilitated the successful application of flow cytometry to microorganisms (Hutter and Eipel 1979; Steen and Boye 1980).

2.2. Fluorescent stains

The ability to quantify particle-associated fluorescence is a powerful flow cytometric feature, which gives it an edge over techniques that use light scattering methods alone, such as confocal imaging. Flow cytometry relies heavily on the use of fluorescent stains, which in conjunction with scattered light can generate information on cell physiology and cellular metabolism (Amanullah *et al* 2002a, b; 2003). Through increasing availability of

fluorescent dyes which exhibit specific binding to intracellular components and are capable of facilitating analysis of cell structure and function, flow cytometry is already making significant inroads into bacterial cell physiology studies (Amanullah *et al* 2002a, b; 2003; Hewitt *et al*, 1999a, b; Shapiro 2003). Cellular component specificity coupled with the rapid throughput of cells possible in flow cytometry allows statistically feasible information about cell number, physiology and viability to be obtained (Hewitt *et al* 1999a, b). Using a mixture of stains as seen in multiparameter flow cytometry further enhances this and aids the identification of the sub-populations within a heterogeneous population of cells.

2.2.1. Characteristics of flow cytometric stains

In order to function efficiently in flow cytometry, potential fluorescent probes must exhibit a number of characteristics. Photostability, the number of times a stain can be excited before decomposition begins, is an important concern when choosing a stain to use in a flow cytometric analysis. However, if handled properly the photostability of the dye is not usually a problem (Davey and Kell 1996).

The excitation coefficient of the stain is also important. The extinction coefficient of a dye is a measure of the amount of light that can be absorbed at a common wavelength. Most useful fluorescent stains have their maximum absorption wavelength close to the spectral lines of the most common flow cytometer light sources but distant from the excitation maximum of auto-fluorescent molecules present within the cells being investigated. The quantum yield of a dye is the number of photons emitted per photon absorbed. It is also a crucial quality as fluorescence intensity is proportional to the product of the excitation coefficient and the quantum yield. It may be influenced by environmental factors such as pH and solvent polarity (Shapiro 2003).

In order to facilitate staining of intact cells, dyes must be capable of crossing the cell membrane by either passive (diffusion), active or carrier mediated transport (Shapiro

2003). Ease of entry can significantly affect staining ability. Other factors that could influence the use of a fluorescent stain in cytometry is its solubility in water and its chemical toxicity. A number of vital stains (e.g. the oxonol dyes) may cause cellular damage. The amount of time between excitation and emission is also a factor, which requires consideration, as this may allow multiple excitation of the stain molecule within a small period of time (Davey and Kell 1996).

2.2.2. Fluorescent stains commonly used in flow cytometry

Fluorescent stains such as propidium iodide and fluorescein diacetate are commonly used as indicators of cell viability in fluorescent microscopy (Mason *et al* 1995) and have been shown to be equally useful in flow cytometry. The number of stains available for flow cytometric analysis runs into hundreds; and are categorised with respect to which intracellular components they stain and whether they are membrane permeant or not.

There are a number of fluorescent stains used specifically for flow cytometry; some of the more widely used ones are listed in Table 2.1.

Class of stain	Example and binding ability	Characteristics	Measured parameter	Excitation minima (nm)	Emission maxima (nm)	Reference
Nucleic acid stains	Propidium iodide(PI): Non-selective DNA and RNA	Cannot cross intact CM Non-permanent	Cell viability CM integrity	530	625	Amanullah *et al* 2002b
Nucleic acid stains	Syto dyes: Non-selective DNA, RNA	Can cross intact CM Permeant	Nucleic acid content	657	673	Mason *et al* 1998 Braga *et al* 2003
Nucleic acid stains	Ethidium Bromide (EB): dsDNA intercalator	Can cross intact CM; Actively pumped out of most cells.	CM integrity	518	605	Nebe-von Caron *et al*, 1998 Hewitt *et al* 1999a Amanullah *et al* 2002a
Potential sensitive probes	Oxonol dyes e.g. bis (1, 3-dibutylbarbituric acid) trimethine oxonol ($DiBAC_4(3)$) (BOX) Depolarized CM	Anionic, Lipophilic, Non-toxic Intracellular accumulation in depolarized CM	Membrane energization CM potential Heterogeneity in sub-populations	490	529	Amanullah *et al* 2002a,b Shapiro 2000a,b
Potential sensitive probes	Cyanine dyes e.g. 3,3'-dihexylocarbocyanine iodide ($DiOC_6$ (3))	Polarised CM	CM potential	484	501	Novo *et al*, 1999 Shapiro *et al* 1979; 2000b Lewis *et al* 2004
Lipophillic membrane probes	Rhodamine 123 (Rh123): Polarized CM	Cationic, Lipophilic Intracellular accumulation in polarised CM	Membrane energization CM potential Cell viability	485	530	Winson and Davey 2000
Protein stains and labels	Fluorescein isothiocyanate (FITC)	Cannot cross intact CM	Total protein content	495	520	Herrera *et al* 2002
pH indicators	5 (6) carboxy-fluorescein	Can cross intact CM	Cell viability	490	520	Breeuwer *et al* 1995

Table 2.1. Commonly used stains in flow cytometry. (CM: cytoplasmic membrane)

2.2.3. Fluorescent stains used in this study

2.2.3.1. Syto Red

Nucleic acids are frequently the cellular targets of fluorescent stains used in flow cytometry and can provide information on parameters such as nucleic acid content in relation to cell cycle phase and cell viability.

The SYTO dyes are low-affinity cyanine dyes that can passively diffuse across the membrane of most cells and are capable of non-selective staining of DNA and dsRNA via the formation of fluorescent complexes (Haugland 2002; Shapiro, 2003). The SYTO dyes lack the quartenary ammonium groups that are also absent in thiazole orange, which they were derived from. This feature contributes significantly to their permeancy (Shapiro 2003). SYTO dyes will also stain most Gram-positive and Gram-negative bacteria as well as eukaryotic cells.

The SYTO dyes are characterised by low extinction coefficients and low quantum yields and a net positive charge at neutral pH. They also differ from each other in characteristics, which include cell permeability and excitation and emission spectra.

Syto Red 63 (SR), the SYTO dye used in this study is a red fluorescent, membrane permeant vital stain and was used to label whole cells. SR stains all bacteria in a population regardless of the condition of their cytoplasmic membranes. This ensures that the flow cytometric events recorded were actual cells and not attributed to debris. SR can be excited with a xenon or mercury-arc lamp or with the 488 nm line of an argon-ion laser. SR has an excitation maximum of 655 nm, an emission maximum of 675 nm (Haugland 2002). The absorption and fluorescence emission spectra of SR are shown in Figure 2.1.

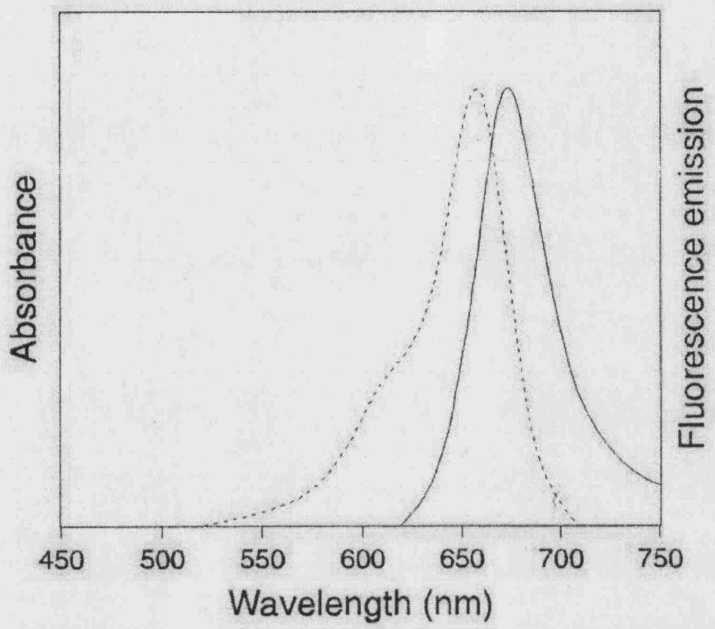

Figure 2.1. Absorption and fluorescence emission spectra of Syto Red 63 (SR) bound to dsDNA (Modified from Haugland 2002).

2.2.3.2. Propidium iodide

The integrity of the cytoplasmic membrane has been routinely characterised by the use of biological stains such as methylene blue and Congo red (Rozack and Colwell 1987). These stains work on the principle of dye exclusion or retention; viable cells with intact membranes are not stained; however if the cell membrane has been compromised these stains can enter and thus stain the cells. Cells that lack an intact membrane cannot maintain an electrochemical gradient and can be classified as dead (Nebe-Von-Caron *et al* 1999). Fluorescent stains such as propidium iodide and ethidium bromide work on this principle for the assessment of cell viability.

Propidium iodide (PI) is a commonly used nucleic acid stain for cell viability assessment and is used in this study for this purpose. PI's chemical structure can be seen in Figure 2.2A. PI is a membrane-impermeant non selective nucleic acid dye (DNA and RNA), which stains by intercalating into nucleic acid molecules with negligible sequence preference (Crissman *et al* 1979) and with a stochiometry of one dye molecule per 4-5 base pairs of DNA (Haugland 2002). It has a molecular weight (MW) of 668.4 and accumulates in cells that have lost membrane integrity. Since it cannot cross the intact cell membrane it can be used as an indicator of membrane integrity and hence, cell viability (Amanullah *et al* 2002a). It is commonly used as a counter stain in multifluorochrome flow cytometry (PI and BOX, Amanullah *et al* 2003; PI and SYTO 9, Bunthof *et al* 2001 and Braga *et al* 2003; PI, EB and BOX Hewitt *et al* 1999a).

PI can be exited with a xenon or mercury-arc lamp or with the 488nm line of an argon-ion laser. PI has an excitation maximum of 535 nm, an emission maximum of 617 nm, illustrated in Figure 2.2B; and exhibits red fluorescence at 488nm when bound to nucleic acids (Haugland 2002) PI's low fluorescence caused by its low extinction coefficient is a limitation of this dye (Breeuwer and Abee 2000).

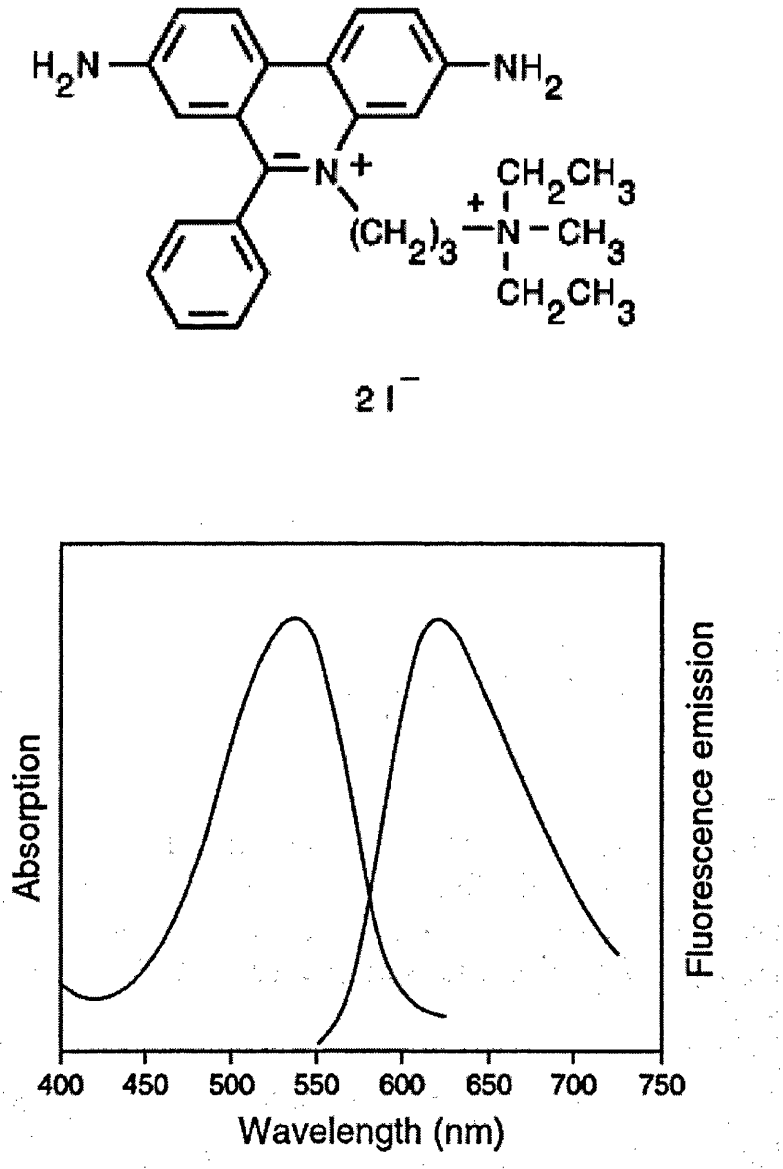

Figure 2.2. Chemical structure (A) and absorption and fluorescence emission spectra of propidium iodide (PI) bound to dsDNA (B); (Modified from Haugland 2002).

2.2.3.3. Bis (1, 3-dibutylbarbituric acid) trimethine oxonol

Membrane potential is generated and maintained by the concentration gradients of ions such as sodium, potassium, hydrogen and chlorides (Shapiro 2000b). The extrusion of H^+ ions by the H^+ ATPase or the electron transfer chain is generally responsible for membrane potential generation in bacteria (Breeuwer and Abee 2000). Membrane potential is an indication of the state of the energy metabolism and the physical integrity of the cytoplasmic membrane.

Potential differences across the cytoplasmic membrane of bacteria are reduced when energy metabolism is inhibited (Shapiro 2000b) and is indicative of metabolic stress (Amanullah *et al* 2002a, b; 2003). The cellular apparatus for energy metabolism in bacteria is located in the cytoplasmic membrane (Jepras *et al* 1997). When bacteria are metabolically active and their cytoplasmic membranes intact, the electrical potential difference across the membrane is between 100 and 200 mV with respect to the exterior, the interior is negative (Novo *et al* 1999). Membrane depolarisation occurs when this membrane potential is reduced and the interior becomes less negative, the opposite occurs when the membrane potential increases and is referred to as hyper-polarisation. Chemical or physical rupture of the cytoplasmic membrane allows the free movement of inorganic ions and can reduce the membrane potential to zero (Novo *et al* 1999; Shapiro, 2000b and 2003). Membrane depolarisation has been reported to be transient (Shapiro 2003). Chemical substances such as carbonyl cyanide m-chlorophenylhydrazone (CCCP), which eliminates the proton gradient across the membrane, can be used to induce membrane depolarisation for investigative purposes (Novo *et al* 1999; Shapiro 2000b).

Membrane potential can be measured via implanted electrodes (direct measurement) which is impractical for bacterial cells but has been previously been applied to artificially enlarged *E.coli* (*Novo et al 1999),* the use of lipid soluble indicator substances for cells in suspension (Shapiro *et al* 1979) and the flux of potassium or rubidium ions across the membrane (Novo *et al* 1999). The last two methods are incapable of individual cell

measurements and instead give an average membrane potential of the entire cell suspension.

Flow cytometric techniques for determining the polarisation status of the bacterial cytoplasmic membrane permit the acquisition of information on the cell-to-cell variations in membrane potential. This can be achieved by the use of fluorescent anionic and cationic lipophillic dyes such as the cyanine and oxonol dyes (Mason *et al* 1995; Shapiro 2000b, 2003). This study uses an oxonol dye, bis(1,3-dibutly barbituric acid) trimethine oxonol, $DiBAC_4(3)$ (BOX), for this purpose.

Membrane potential measurements can be compromised by the presence of efflux pumps, active transport systems which actively pump out the fluorescent stain, disruption to these systems could cause membrane depolarisation (Shapiro 2000b; Hewitt and Nebe-Von Caron 2001). However anionic stains such as BOX only enter the cell once these active transport systems are no longer functioning and membrane potential has been lost.

The oxonols fall into the category of slow potential sensitive dyes, which include the carbocyanines and rhodamine derivatives (Plasek and Sigler 1996). They are negatively charged and undergo a potential dependent distribution between the cytoplasm and the extracellular medium in eukaryotic cells (Jepras *et al* 1997). The oxonols do not accumulate extensively in bacteria with negative transmembrane electrochemical potential (Mason *et al* 1995). The bis-barbituric acid oxonols are commonly referred to as bis-oxonol (BOX) in the literature; the most commonly used of which is bis(1,3-dibutly barbituric acid) trimethine oxonol, $DiBAC_4(3)$, (Haugland 2002).

BOX has a MW of 516.64 and is composed of two heterocyclic rings separated by a polymethine bridge (Shapiro 2003). The structure of bis (1,3-dibutylbarbituric acid) trimethine oxonol ($DiBAC_4$ (3)) is shown below in Figure 2.3A. This is an anionic, lipophilic, non-toxic dye, which accumulates in the depolarised cell membrane, where it binds to lipid rich intracellular components and exhibits enhanced fluorescence and

spectral shifts (Amanullah *et al* 2002a, b; 2003; Shapiro, 2000a, b; Haugland 2002). Cells with membrane potential will exclude BOX and fluorescence weakly (Jepras *et al* 1997; Shapiro 2000a, b), with the fluorescent response decreasing with increases in membrane potential (Mason *et al* 1995). BOX also exhibits high voltage sensitivity (Jepras *et al,* 1997). BOX has been used for the study of bacterial and eukaryotic cells in this capacity.

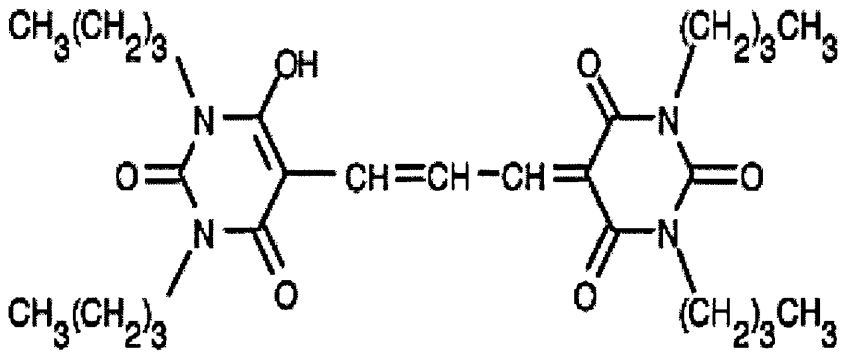

Figure 2.3. Chemical structure of bis(1,3-dibutly barbituric acid) trimethine oxonol, $DiBAC_4(3)$, (BOX). (Modified from Haugland 2002)

2.2.3.4. Multi-fluorochrome staining

The presence of a high percentage of dead, dormant or compromised cells at any point in a bioprocess will adversely affect the process in terms of product yield and overall process efficiency, consequently necessitating precise information on the physiological state(s) of cells that make up that population. This can be achieved rapidly and with greater accuracy by multi-fluorochrome staining.

The simultaneous use of different fluorochromes (fluorescent stains) allows a more in-depth definition of conventional viability by allowing the detection of growth as well as complex cellular activities, such as metabolic activity, membrane integrity and

reproductive growth (Nebe-von Caron *et al* 2000). Cells investigated in this way can be separated into the categories of viable but non-culturable cells or viable and culturable cells. The use of multiple stains can also help to understand functional differences and interactions highlighted by individual stains.

Stain combinations are chosen in such away that the dyes compliment and compensate for each other. For instance the use of two DNA stains with different permeabilities can be used for membrane integrity measurements. The advantages of this is that efflux pumps that may remove dyes can be overcome without affecting membrane integrity measurements (Nebe-von Caron *et al* 1999) and total counts are possible as permeabilised as well as dead cells are identified (Nebe-von Caron and Badley 1995). An example of this is the combination of SYTO 9 and PI (Braga *et al* 2003), for the investigation of the microbiological effect of two macrolides. Syto 9 stains all bacteria indiscriminately, and PI stains bacteria with damaged cell membranes. A combination of BOX and PI was used by Amanullah *et al* (2003) to measure strain dependent toxicity in the indene bioconversion, allowing the identification of three distinct cell populations, dead, depolarised and viable. Double staining with two fluorochromes of different membrane permeability as illustrated above, allows more stringent determination of viability (Nebe-von-Caron *et al* 1999). An example of triple fluorochrome staining was demonstrated by Nebe-von Caron *et al* (1998), who used a combination of ethidium bromide (EB), PI and BOX to identify four physiological states in *Salmonella typhimurium* cells.

The principal limitations of multi-fluorochrome staining are the availability of the fluorescent dyes and equipment limitations however increasingly sophisticated flow cytometers with sophisticated compensation software is making this easier.

2.2.3.5. The bacterial cell wall and stain exclusion and retention

Microbial systems show a broad array of transport mechanisms, including active transport and facilitated diffusion, some of which are absent from mammalian cells. Therefore it cannot be assumed that flow cytometric stain interactions in bacterial and mammalian cells will be the same. These stain-cytoplasmic membrane interactions further differ between Gram-negative and Gram-positive bacteria. Figure 2.4 illustrates the differences between the cell membranes of these bacteria.

The bacterial cell membrane is important in regulating which molecules enter or leave the cytoplasm (Mortimer *et al* 2000). Significant differences in cell envelopes and substrate uptake exist between Gram positive and Gram negative bacteria (Comas-Riu and Vives-Rego 1999), which have a marked impact on their interactions with the dyes used in flow cytometry. The majority of Gram-positive bacteria are surrounded by a thick peptidoglycan cell wall, which offers scant resistance to the diffusion of small molecules into the intracellular compartment despite being mechanistically strong. The Gram negative bacteria on the other hand have a second outer membrane which offers significant resistance to diffusion of small molecules such as antibiotics (Nikaido 1994) and a number of fluorescent dyes. The structure of the bacterial cell wall imposes restrictions on the entry of vital dyes, this is especially important in Gram negative bacteria, which as a consequence of their asymmetric lipid composition are fairly impermeable to hydrophilic and moderately hydrophobic compounds (Herrera *et al* 2002). The intact membranes of Gram negative bacteria exclude cyanines (e.g. BOX) and other lipophillic compounds, thus membrane potential estimation in these bacteria requires that the outer membrane be permeabilised by the addition of a chelating agent such as ethylediaminetetraacetic acid (EDTA); this treatment does not adversely affect cell viability in the short term (Mason *et al* 1995; Hewitt *et al* 1999b; Nebe-Von-Caron *et al* 1999; Shapiro 2000b). The chelating agent serves to remove the lipopolysaccharide from the outer membrane (Davey and Kell 1996). Bacterial efflux pumps, such as the glycoprotein drug efflux pumps actively transport cyanine dyes and other lipophillic cations out of the cell and have also been associated with the expulsion of EB, owing to

the similarity of this molecule to PI it may be inferred that a similar occurrence may occur with PI (Mortimer *et al* 2000; Shapiro 2000b).

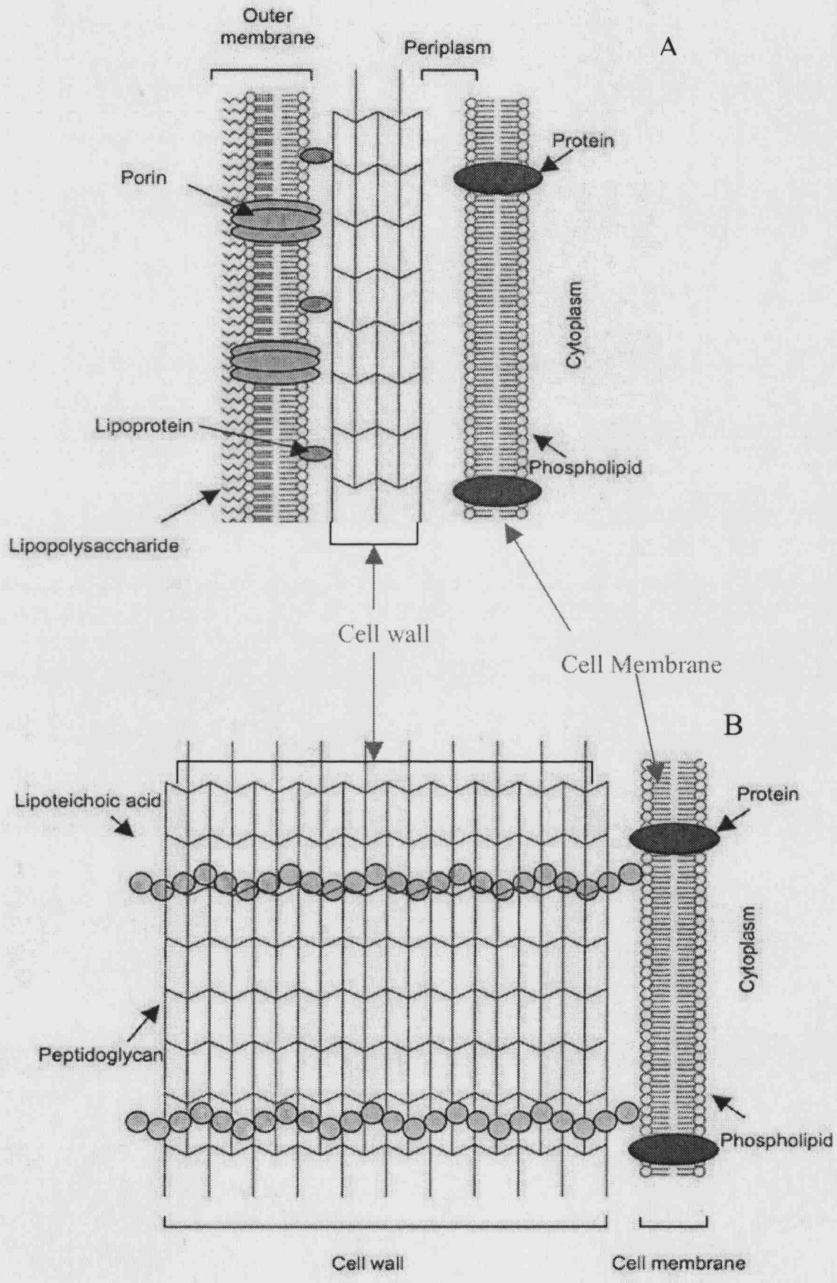

Figure 2.4. The Gram-negative cell wall (A); The Gram-positive cell wall (B) (Modified from Green 2002).

2.3. Flow cytometric optics

2.3.1. Light sources

The illumination of particles as they flow past a light source generates the signals used in flow cytometric analysis (Givan 2001). The quantitative aspects of flow cytometry are based on the measurement of light, which can be fluorescent, scattered or absorbed (Watson 1991). A characteristic required for a good light source is the radiance, the analogous radiometric quantity. Radiance (L) measures power emitted from, transmitted through or reflected by a surface, per unit of its area per unit solid angle and is the quality used to compare light outputs of extended sources (Shapiro 2003).

$$L = \varphi / A\Omega$$

Where φ = radiant flux, Ω = intensity and A = unit area. The units of radiance are Wm^{-2} sr^{-1}.

High light fluxes, where large numbers of photons pass through a small volume of space, are required at the intersection of the cell stream with the illumination as a result of the small number of fluorescent molecules per cell and the short time that each cell is exposed to the exciting light. The light flux is generated at the illumination source and must be as small and as bright as possible. As a prerequisite for obtaining sufficiently high energy photons (ultra violet (UV), violet and blues) an incandescent source must be very hot, typically 6000 K. As energy is emitted as heat, some kind of cooling mechanism is required (Watson 1991).

Light used in flow cytometry is available from either of two primary sources, a laser or an arc lamp (Watson 1991; Ormerod 2000; Givan 2001; Shapiro 2003). In both light sources electrons are raised to high-energy orbitals via electricity and energy is given off in the form of photons when the electrons fall back to their lower energy orbitals (Givan

2001). Deuterium, xenon and mercury lamps are available, their light emission spectra is between 300 and 550 nm. The mercury lamps have a higher radiance in the UV to low blue region of the spectrum (365, 405, 436, 546 and 578 nm) than the xenon lamp, which has no strong lines in the near UV, or visible spectrum. The Deuterium lamp is not suitable for flow cytometry (Watson 1991; Shapiro 2003).

Van Dilla *et al* first reported the use of lasers in flow cytometry in 1969. The beams emitted by lasers are coherent i.e. the light is polarised, the beam generated remains compact and shows minimal divergence (it is parallel), and exhibit spectral purity (Watson 1991; Ormerod 2000; Givan 2001). It is this directional coherence that makes lasers so valuable for flow cytometry, as they provide a very bright fine beam of light, which permits particles flowing in a stream to be strongly illuminated for a short period of time so that measurable signals from single particles can be generated (Givan 2001). Argon lasers operated at 488 nm permit the excitation of a number of fluorescent stains including PI and the cyanine dyes and are the most commonly used lasers for flow cytometry. Argon lasers are typically air-cooled. Other lasers such as dye, helium-neon and diode lasers are also used (Shapiro 2003; Harding *et al* 2000).

Flow cytometers can have single or multiple lasers allowing for analysis of different wavelengths. Single laser flow cytometers typically have argon ion lasers operated at 488 nm; these can be coupled with a red diode laser outputting at 635 nm. This has the advantage of high sensitivity and minimal compensation requirements. The former is available in the Beckman Coulter EPICS XL-MCL and the later is available in the Beckman Dickinson FACSCalibur™ flow cytometer.

The intensity of emission is dependent on the number of fluorophores present at constant laser power; this makes flow cytometry both a qualitative and highly quantitative analysis tool (Ibrahim and Van den Engh 2003).

2.3.2. Fluorescence detectors and optical filters

Scattered light and fluorescence are measured by an electronic detector such as a photomultiplier tube (PMT) (Horan and Wheeless 1977; Lawry 1998; Shapiro 2000a). Three or more of these may be present, measuring light emitted at right angles from the cells in the illuminating stream (Givan 2001). These fluorescence detectors are numbered e.g. FL1, FL2 etc (see Figure 2.5). Photodiodes are used as detectors for absorption, extinction and forward scatter signals (Shapiro 2003). Photomultipliers are capable of intensifying a signal by many orders of magnitude thus allowing the measurement of low levels of fluorescence and determination of sensitivity and detection limits (Watson 1991). Thus individual particles in a heterogeneous sample can be measured and with the use of software packages, data clusters identifying sub-populations within the sample may be identified (Lawry 1998). Photodetectors are placed at different positions in the cytometer consequently a combination of mirrors and filters are used to define the spectral responses of the detectors (Figure 2.5). A barrier filter blocks laser illumination while dichroic mirrors and filters are used to select bands of fluorescence for measurement (Horan and Wheeless 1977).

Dichroic and band pass filters (Figure 2.5) are based on interference filters and are used in flow cytometers which use arc light sources. Dichroic filters are angle sensitive and are usually used at an angle of 45° and split the light beam according to colour. They are short wavelength pass filters and transmit light below a given wavelength whilst reflecting light of longer wave lengths (Ormerod 1994; Givan 2001). Bandpass filters on the other hand transmit light over a narrow band and are typically placed directly in front of the detector (Ormerod 1994); they are used at 90° to the light path. Filter and mirror selection is influenced by the fluorescence and emission spectra of the fluorochromes being used (Givan 2001).

Figure 2.5 is an illustration of the flow cytometric optic system incorporating various detectors and filters.

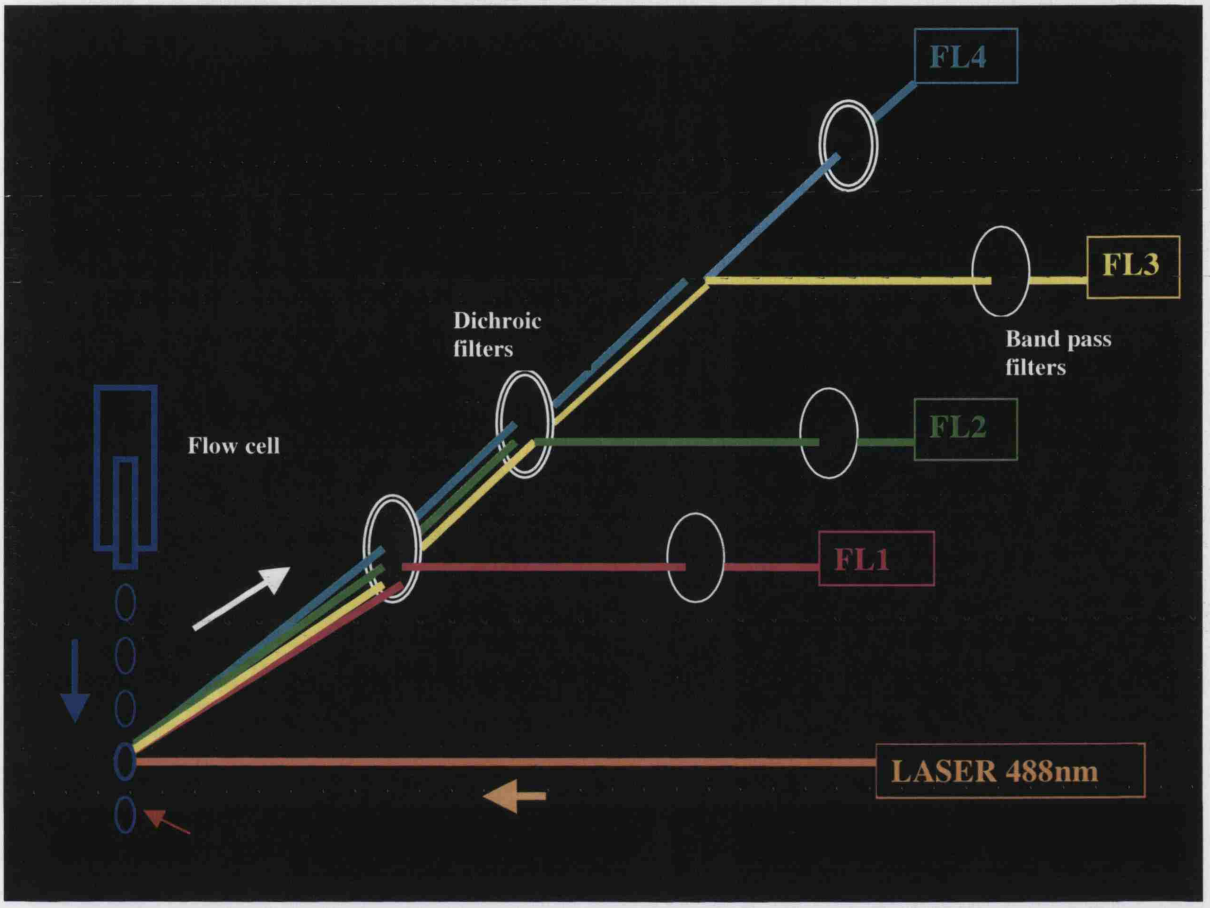

Figure 2.5. The flow cytometric optic system incorporating the various detectors and filters. FL1-FL4 are the fluorescence detectors.

Cells which are being analysed are placed in suspension, usually in a buffered medium (sheath fluid) and focussed into a directed fluid stream, from which they emerge in single file (Ibrahim and Van den Engh 2003). This sheath flow technique was first described by Crosland-Taylor in 1953 and was incorporated into flow cytometer set ups by Van Dilla *et al* in 1969 who incorporated a laminar sheath flow technique and an argon laser to the analysis of volume and Feulgen-DNA distributions of Chinese Hamster Ovary cells growing asynchronously in suspension culture. Cells in suspension emerge from the flow cell (Figure 2.5) confined to the center of the flow stream, which in conjunction with laminar-sheath flow reduces clogging due to clumps (Horan and Wheeless 1977). They

are then intersected by light from the laser beam, which is typically placed orthogonal to the flow. If the cell has retained the fluorescent stain it will fluoresce emitting a measurable pulse of photons at specific wavelengths and this will be detected by the fluorescence detectors (FL1-FL4). Signals are collected by photodetectors, processed, digitised and stored (Ibrahim and Van den Engh 2003).

2.4. Light scatter

Light scattering is an integral flow cytometric parameter. It can be used for size estimation, differentiation of cell types on the basis of size and morphology, detection of fluorescence negative cells and gating of fluorescence measurements (Steen 2004). Light scattering involves a brief interaction between a photon and an electron in which the photon is destroyed and its energy transferred to the electron, which almost immediately releases this energy as a new photon. Scattered light has the same wavelength or colour as the incident light. Scattered light usually appears to be at an angle to the incident beam as the new photon does not always travel in the same direction as the old one (Shapiro 2003).

Light scattering, via the measurement of optical density is widely used in microbiology as a means microbial biomass determination. These measurements do not attempt to discriminate photons scattered at different angles (Davey and Kell 1996). Multi-angle light scattering has significant impact on the accuracy of flow cytometric characterizations.

The intensity of light scattered by a particle is a function of its shape, size and internal structure (Patkar *et al* 2002). The relationship between cell morphology and light scatter is dependent on the configuration of the optical system and can under certain conditions be used for biomass estimation (Robertson *et al* 1998). Bacteria can be detected from the background signal based on their intrinsic light scattering properties in the forward angle light scatter (FALS) and the orthogonal or right angle light scatter (RALS) direction (Amanullah *et al* 2002a).

2.4.1. Forward angle light scatter

Forward angle light scatter (FALS) is defined as light of the same colour as the illuminating beam that has been bent to a small angle, typically 0.5 – 1.5°, from the direction of the original beam (Watson 1991; Givan 2001). FALS is seen when light from the laser beam is deflected by the surface of the particle(s) being analysed. The majority of light is scattered at small forward angles, this is observed at low concentrations similar to flow cytometric conditions and it is possible to differentiate the various physiological states of organisms within a population based on their differential light scattering behaviour (Davey and Kell 1996). Detectors convert the light into voltage pulses, which are relative to the particle size and volume. Smaller particles produce smaller pulses while larger particles generate larger ones. FALS can be used to measure microbial cell size provided only physiologically similar cells are compared, but limitations caused by differences in the refractive index between the cells and the suspending medium as well as cellular orientation may occur (Davey and Kell 1996; Amanullah *et al* 2002a). FALS is a measure of the cell volume and is largely dependent on the mass or volume of the cell (Patkar *et al* 2002; Davey and Kell 1996). It is also used as a gating parameter to exclude aggregates and debris from further analysis.

2.4.2. Right angle light scatter

Right angle light scatter (RALS) is defined as a light of the same colour as the illuminating beam that is scattered by a particle to an angle of 90° (large angle) from the illuminating beam, this is also known as side scatter or orthogonal light scatter (Givan 2001; Shapiro 2003). Light scattered at wider angles can generate information on the surface and internal structure of the cell with higher intensity signals being obtained from cells with the highest levels of cytoplasmic granularity (Davey and Kell 1996). RALS is affected by intracellular structures and inclusion body formation in *E. coli* K-12 JC 5183 (Patkar *et al* 2002). In cells which have been engineered to produce intracellular products which accumulate in the cytoplasm an increase in light scattering at right angles to the

incident beam may be expected as a result of product accumulation, allowing the isolation of such cells without damage to the intracellular contents (Davey and Kell, 1996). Patkar *et al* (2002) demonstrates this when they confirm the link between intracellular GVGIP production and cell light scattering properties. Thus RALS could be a potential process tool, permitting rapid evaluation of expression systems in terms of product formation. Figure 2.6 shows the interactions of light with a cell during flow cytometric analysis.

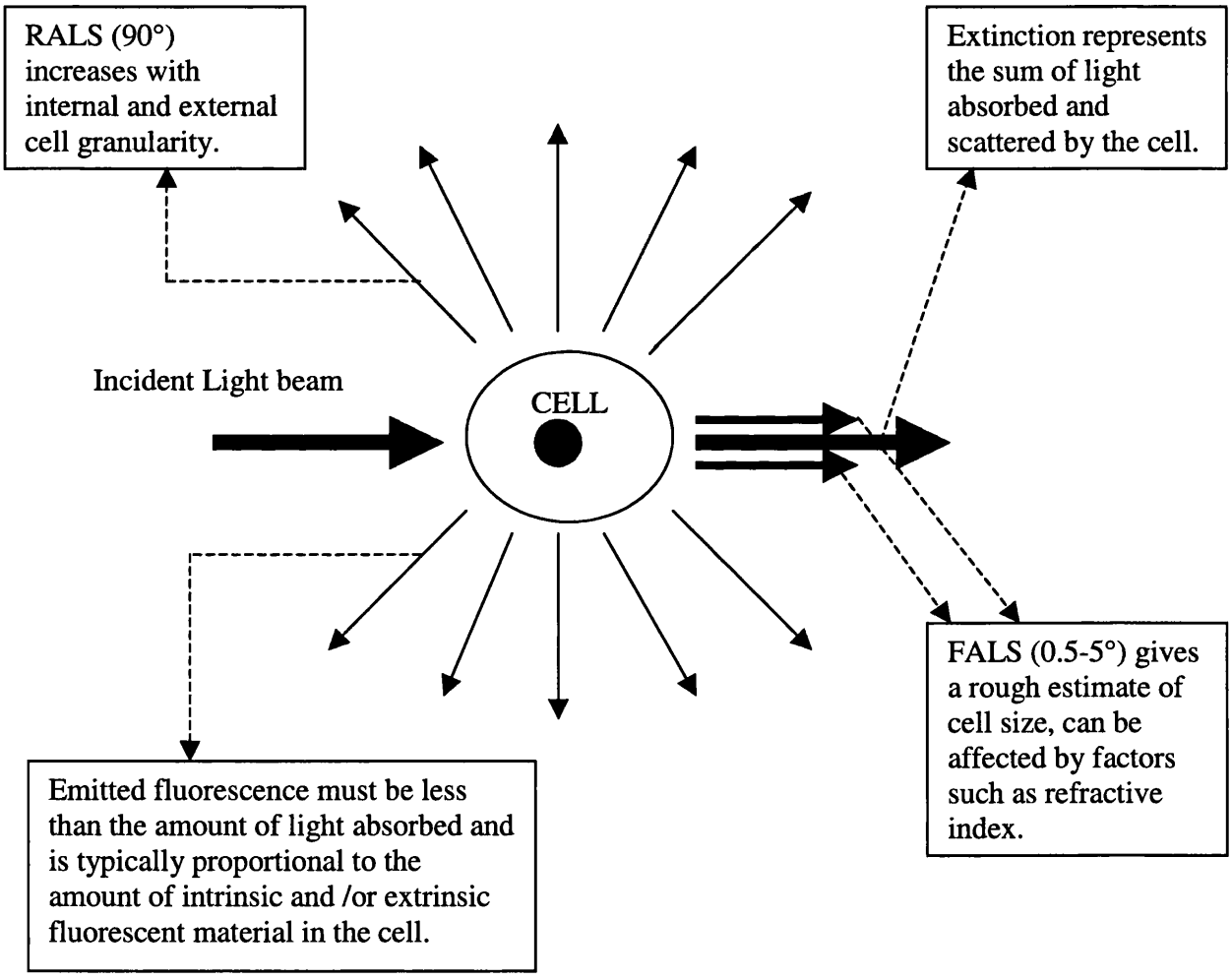

Figure 2.6. The interaction of light with a cell during flow cytometric analysis. (Modified from Shapiro 2003)

2.4.3. Spectral overlap and compensation

The filter and mirror combinations (Figure 2.5 and section 2..3.2) used in flow cytometry though useful in separating fluorescence of different wavelengths are not capable of totally eliminating spectral overlap between the fluorescence emissions when two or more fluorescent stains are used. Figure 2.7 shows the spectral overlap of Fluorescein isothiocyanate (FITC) and phycoerythrin (PE). This principle holds true for other stain combinations such PI and BOX, as used in this study.

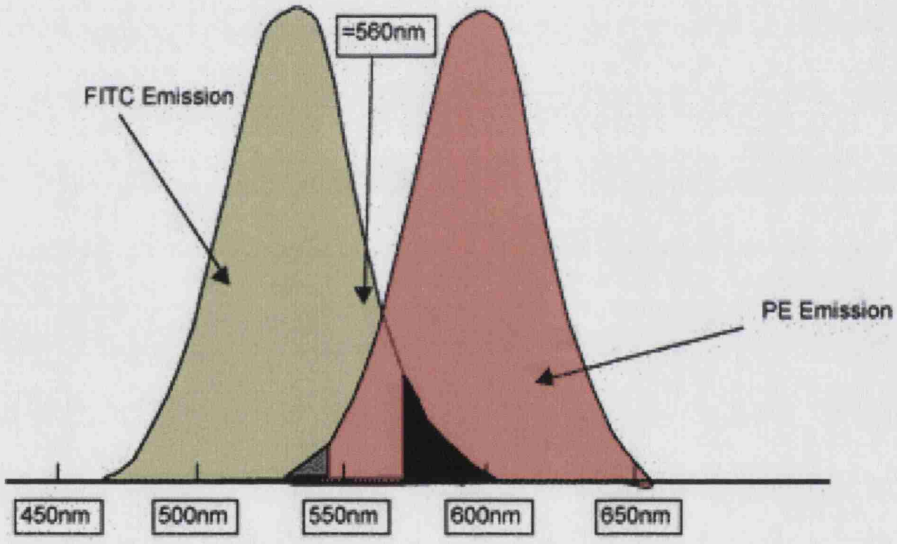

Figure 2.7. A close up view of FITC and PE fluorescence overlap. ▓ Overlap of PE fluorescence into FITC-PMT. ▓ Overlap of FITC fluorescence into PE-PMT. (Modified from http://biology.berkeley.edu/crl/compensation.html)

Flow cytometers are equipped with compensation networks, which measure the signal on one photodetector and subtract a certain percentage of that signal from the signal of another photodetector; these percentages are empirically derived (Ormerod 1994; Givan 2001). In multiparameter flow cytometry where more than two stains are being used the

signals from the detectors need to be compensated individually for each fluorescent stain. It should be noted that compensation values are valid only for a given set of fluorescent stains with a particular set of filters, mirrors and voltages applied to specific detectors (Givan 2001). As the number of fluorochromes increases extra care needs to be taken to accommodate for compensation artefacts and limitations (Shapiro 2003), using compensation software such as the Beckman Coulter Advanced Digital Compensation System (ADCS) can make this easier. However, it should be noted that the coefficient of variance (CV) of population clusters can increase slightly after software compensation has been applied. This results in a decrease in resolution which is primarily due to the loss of analog signals when signals are digitised (Bagwell and Adams 1993).

2.4.4. Quenching

Quenching occurs when there is a reduction in the fluorescence yield as a result of a loss of the absorbed excitation energy. It is usually due to a number of mechanisms by any pathway other than light emission. These include: reversion of the fluorophore to the ground state by non-radiative energy transfer within the fluorophore carrier complex, dissipation of the energy into the microenvironment and bleaching, which occurs as a result of a second photon being absorbed by the fluorochrome before it has discharged the energy from the first (Watson 1991 and 1992). In order to prevent or minimise quenching of intracellular dyes lower concentrations of fluorescent dyes are used in flow cytometry than in bulk measurements, these are typically in the range of 50 nM to 1-2 μM (Shapiro 2000b).

2.5. Flow Cytometric data representation

2.5.1. Gating

Populations of cells for analysis are selected by gating. This technique is essential for the selection of the cell population (or sub-population) to be analysed and debris exclusion.

Gating is essential for the correct quantification and analysis of the different cellular sub-populations which may be present in the sample being analysed (Bryne *et al* 2000). Proper gating is achieved by a combination of flow cytometry software and operator proficiency to select the population that is to be analysed. Gates may be applied to histogram and bivariate data plots. Figure 2.8 illustrates a gated population. The gated population in plot A is represented, and analysed on plot B.

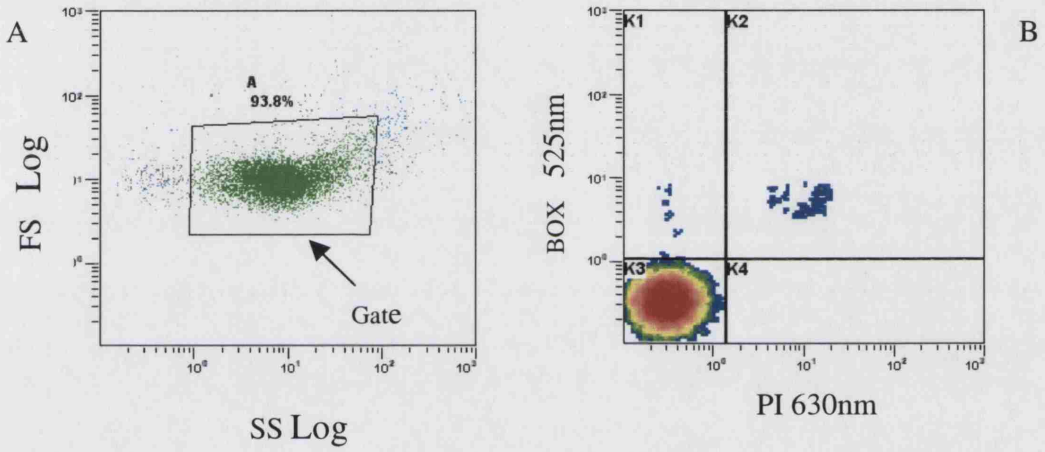

Figure 2.8. Bivariate data plots showing gated populations of *E. coli* TOP10 pQR239.

2.5.2. Data representation

There are a number of accepted ways of presenting flow cytometric data, these are influenced to an extent by the number of fluorochromes in use, what parameters are being measured and to an extent what the investigator is trying to portray. The main objective is to display the data accurately without compromising analytical integrity. To accommodate the large numbers of events being recorded results are usually reported and displayed on a logarithmic scale, which has the advantage of intensifying weak signals and compressing strong signals (Ormerod 1994; Shapiro 2003).

Common methods of data representation are illustrated in Figure 2.9A-E which represents data obtained from analysis of *E.coli* TOP10 pQR239 cells which have been heat treated and stained with a combination of PI and BOX prior to analysis. The most basic of these is the single parameter histogram plot, Figure 2.9A, which gives a representation of the number of events (arbitrary units) in relation to the emitted fluorescence detected by a given detector. This gives an indication of negative and positive events. Histogram plots are used to display data from a single acquired parameter (Radcliff and Jaroszeski 1998), e.g. analysis following staining with a single dye.

Data may also be represented as a two parameter (bivariate) histogram as illustrated in Figures 2.9 B to E. These allow the visualisation of relative levels of other parameters collected at the same time. Bivariate data plots allow the discrimination of dual labelled populations which may be hidden if histograms are used to display the data (Radcliff and Jaroszeski 1998). Dot plots such as that shown in Figure 2.9B are another common method of data representation and shows distinct populations of cells. This dot plot is divided into four quadrants into which cells which are positive or negative for the two stains used, whether individual or double positive or negative, are distributed. The lower left (LL) quadrant shows double negative cells; the upper left quadrant (UL) shows cells positive for only one stain, BOX; the upper right quadrant (UR) shows double positives while the population in the lower right (LR) quadrant show events positive for only the second stain, PI. This distribution pattern holds true for Figures 2.9 B-D. Figure 2.9 C is a colour density plot representation of the same data; the different colours represent different frequencies of occurrences. This data is also represented as a contour plot, Figure 2.9 D. Here the frequency of events is not displayed for each point but are instead linked to form contour lines of points for which data values occur with equivalent frequency. In isomeric plots as seen in Figure 2.9E, the apparent height or Z-value corresponding to any pair of x and y coordinates is made proportional to the frequency of occurrence of the corresponding paired data values in the sample (Shapiro 2003). In this investigation data is represented as bivariate histograms, principally dot (chapter 3) and density (chapter 4 and 5) plots.

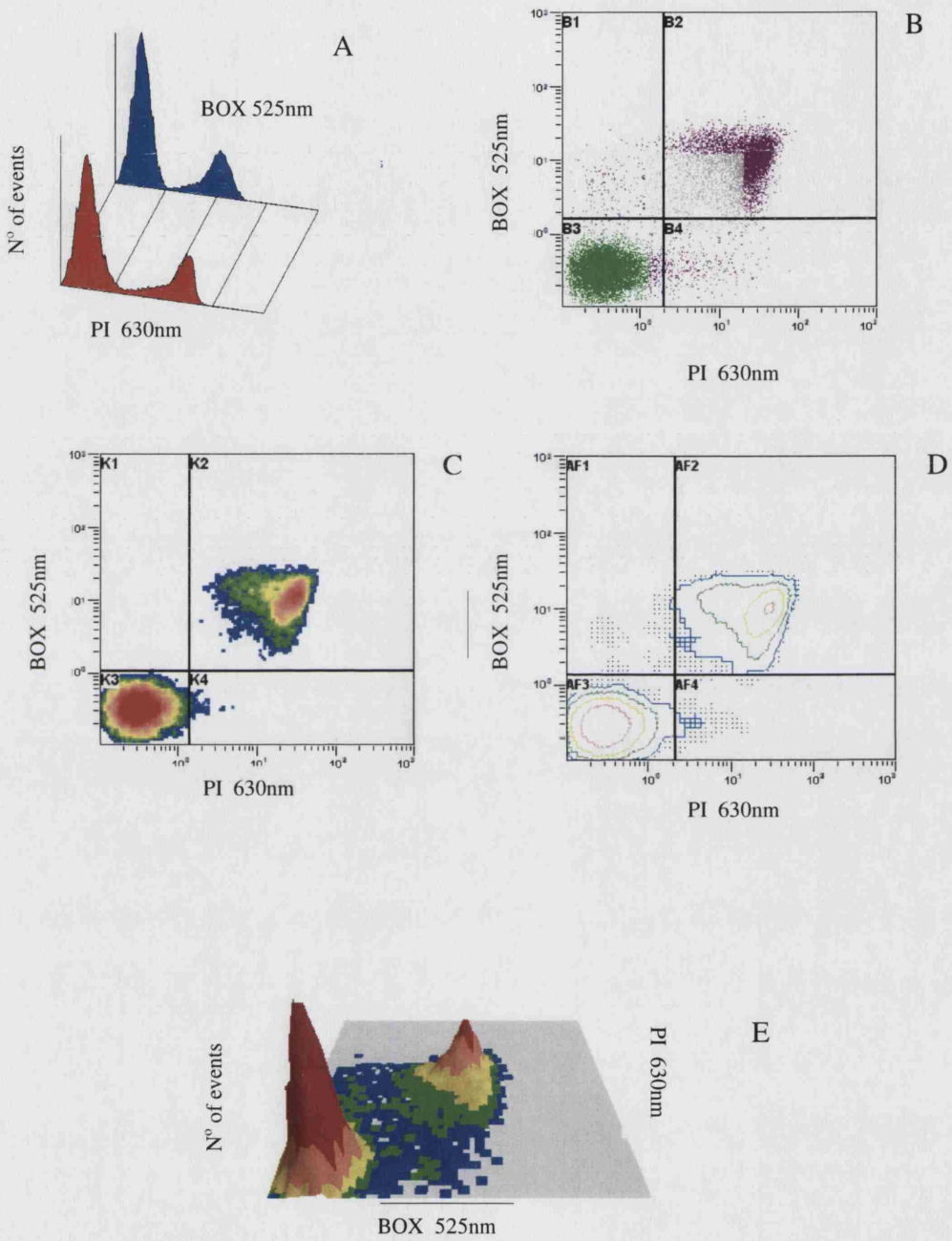

Figure 2.9. Methods of flow cytometric data representation. Single parameter histograms (A). Bivariate data plots: Dot plot (B), Colour density plot (C), Colour contour plot (D) and Isometric plot (E). The data is of *E.coli* TOP10 pQR239 cells stained with a combination of PI and BOX.

2.5.3. Multiparameter data acquisition

Multiparameter data acquisition and multivariate data analysis is a key feature of flow cytometric analysis which has made it an increasingly valuable analytical tool. Most microbiological investigations tend to measure only one factor per sample at a time. Multiparameter flow cytometry is the simultaneous measurement of a number of different substances or characteristics in cells, multiparameter data analysis is the collection and manipulation of the data obtained from such measurements (Shapiro 2003). The use of suitable fluorescent stains or combination of stains with different cellular targets coupled with wavelength combinations allows the estimation of multiple parameters in single cells, such as membrane integrity and membrane potential, within a given population. This allows sub-populations within the population to be identified and the determination of the relationships between different cellular variables. Experimental systems described by Bigos *et al* (1999) simultaneously measured nine fluorescence and two scatter parameters in each cell. This approach has been used in the identification of mutants and contaminants, which under the appropriate measurement conditions, appear as a separate sub-population of cells (Winson and Davey 2000). The choice of reagent-dye combinations and the ability to compensate in multi-parameter measurement space were determined to be crucial to obtaining satisfactory results. Pumps that actively remove some fluorescent dyes from internal cellular compartments are a major obstacle to multiparametric measurements, with highly energized cells being capable of removing supravital stains like ethidium bromide (Nebe-von Caron *et al* 1998). Flow cytometry specific data analysis packages, such as CellQuest Pro software (Beckman Dickinson) and the EPICS XL software (Beckman Coulter), are used to analyse the data obtained. It is also possible to acquire multivariate data from each cell.

2.6. Flow cytometry method development

2.6.1. Instrumentation

The flow cytometers used in this study were the EPICS XL-MCL (autoloader) 4 Colour Bench Top Flow Cytometer with Flow Centre II Acquisition Workstation, with 488 nm excitation from an argon-ion laser at 15mW (Beckman Coulter, High Wycombe, Bucks, U.K.) and the FACSCalibur™ dual laser flow, bench top analyser with optional fluidic sorter, cytometer (Beckman Dickinson, San Jose, CA. USA).

This section details the development of a protocol for the analysis of *E.coli* TOP10 pQR239 stained with a combination of PI and BOX on the Beckman Coulter EPICS XL-MCL (Chapters 4 and 5). The protocol used in chapter 3 for the analysis of *E.coli* IL-13 was developed on the FACSCalibur™ and kindly donated by Rich Wnek, Bioprocessing R & D Department, Merck & Co Inc. NJ. USA.

2.6.1.1. Instrument set up

This protocol for the analysis of *E.coli* TOP10 pQR239 on the EPICS XL-MCL (Beckman Coulter, High Wycombe, Bucks, U.K) was developed. The first thing was to establish particle size limits within the protocol. This was done by running a series of beads of known diameter through the machine. Once the laser had been allowed to heat up and all the pressures stabilised the Flowcheck™ protocol was run. Flowcheck™ Fluorospheres (Beckman Coulter, High Wycombe, Bucks, U.K) are 10μm in diameter, latex particles, which are fluorescent on all of the four fluorescent detectors in the EPICS XL Flow Cytometer. They were used to check laser alignment; this was achieved by confirming that the coefficient of variance (CV), the relative standard deviation, values was less than 2% on all the detectors. Variations in laser power and PMT sensitivity were also assessed by daily monitoring of the mean channel for each parameter.

3.6 μm diameter fluorospheres were used to set the upper size limits. These fluorospheres are seen in a tight population in the upper right hand corner of the Log FS v Log SS plot and are shown in Figure 2.10. All other particles can be attributed to broken beads or particles from the sheath fluid or dilution buffer (Dulbecco's phosphate buffered saline) and were excluded from the gate which was set up around the 3.6μm fluorospheres. Typical CV values for the 3.6μm fluorospheres under these conditions were 0.8-0.9. In bivariate data plots these fluorospheres are located on the bottom left hand corner of the plot. Increasing the discriminator setting to 3 did not significantly alter the distribution pattern of the fluorospheres and as such was maintained at 2. The 3.6μm fluorospheres were taken to be the upper size limit for the bacterial cells. 1.0μm fluorospheres were used to set the lower size threshold. In this instance the fluorospheres are positioned in the center of the Log FS v Log SS plot and are gated. They also had a mean CV of 1.1.

When a mixture of 3.6 and 1.0μm fluorospheres were run under the same conditions two distinct populations were observed. The 3.6μm fluorospheres are in the top right hand corner while the 1.0μm fluorospheres are in the centre of the Log FS v Log SS plot.

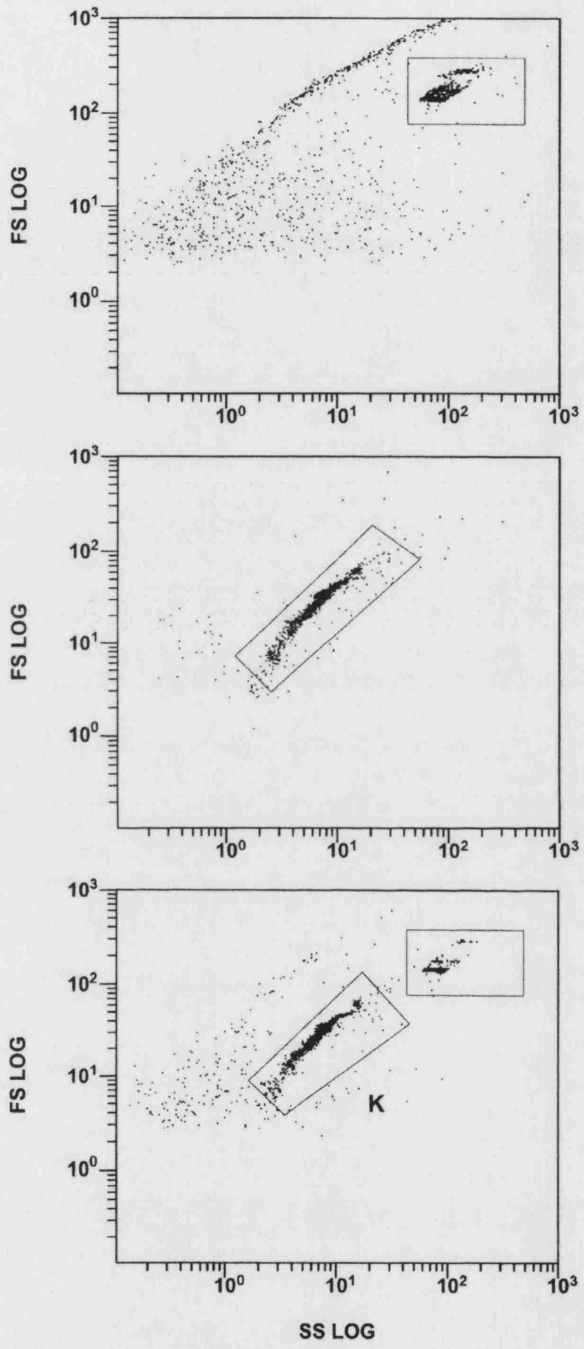

Figure 2.10. Forward scatter against side scatter plots of 3.6μm (A) and 1.0μm (B) fluorospheres and a mixture of both sized fluorospheres (C).

In order to confirm the above data, samples of filtered Dulbecco's buffered saline (DBS) (Sigma-Aldrich, Poole, Dorset, U.K) and Isoton II (sheath fluid in which the cells being analysed are typically suspended) (Beckman Coulter, High Wycombe, Bucks, U.K) were put through the flow cytometer in place of the fluorospheres (Figure 2.11). Neither solution showed the presence of 3.6μm particles, however smaller particles were observed, suggesting the presence of salt crystals. Thus suggesting that while filtering would eliminate a large percentage of particulate matter some would still remain.

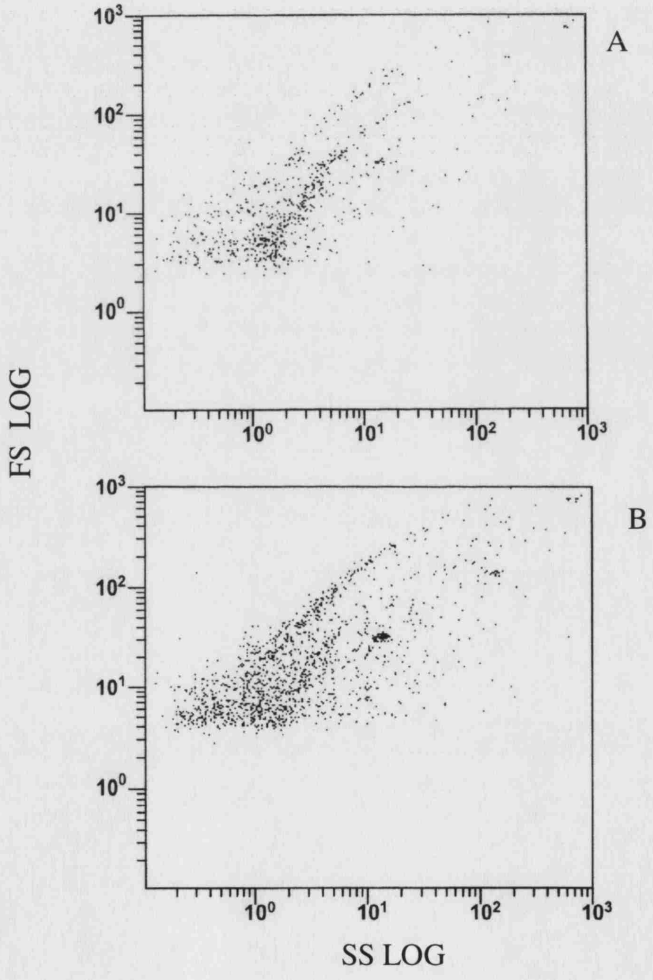

Figure 2.11. Forward scatter against side scatter plot of filtered DBS (A) and Isoton II (B)

2.6.2. Protocol development

In order to analyse *E.coli* TOP10 pQR239 cells a discriminator setting of 2 was used, this is the level which the signal must exceed in order to be recorded and is a means of reducing the background noise. The FL1 and FL3 detectors, which detected and measured BOX and PI fluorescence respectively, were set at voltages of 585 and 807 respectively. Forward and side scatter voltages were set at 55 and 185 volts. The gains were set at 1.0 for both the FL1 and FL3 detectors; for forward and side scatter these were set at 5.0 and 10.0.

Compensation using the ADCS software was set at 16% for the FL1 detector and at 23% for the FL3 detector.

2.6.2.1. Data acquisition and representation

A total of 50,000 gated events per sample were analysed (Amanullah *et al* 2002, 2003). This conferred the advantage of reducing the errors below 1% and allowed detection of subtle changes within the population (Nebe-von-Caron and Badley 1995). The statistical abundance of an event and the signal intensity that separates it from background noise are limitations of optical systems. As a result at least 100 cells with the desired characteristic must be acquired so that cell clustering can be visualised and statistical robustness achieved (Nebe-von-Caron *et al* 1999).

Density and dot plots were used to represent the data obtained. All plots display data over 4 log decades. During protocol development it was found that when using a linear scale only background noise showed up on the plots. Though density and dot plots were used to display the data it should be said that there is no difference in information between the two forms of bivariate data representation (Shapiro 2003).

2.7. Flow cytometry controls

2.7.1. Sample preparation

The driving principle behind flow cytometry is single cell analysis; consequently it is vital that cells being passed through the flow cell be as free as possible from aggregates or clumps. The reason for this is that depending on the orientation with which the clump enters the flow cell, a clump containing just one non-viable cell and a number of viable cells may register as a single event of non-viable cells (Nebe-von-Caron *et al* 1999; Winson and Davey 2000).

Cell samples were taken from the culture or reaction vessel and prepared for flow cytometric analysis. First they were diluted in filtered 1x DBS to a concentration of 10^5 cells ml^{-1} (Appendix 1). The samples were also vortexed for ~30 sec to disrupt any aggregates that may be present prior to analysis.

PI and BOX were added to the cell suspension at a final concentration of 5.0 and 10.0μgml^{-1} and incubated for 10min at 25°C (Amanullah *et al* 2002a, b; 2003).

2.7.1.1. *E.coli* TOP10 pQR239 single and double stain controls

Control flow cytometric analyses were carried out to determine the distribution of *E.coli* TOP10 pQR239 cells following staining with PI and BOX, individually and in combination. Cells which had been grown under process conditions for 6 hours (Luria Bertani (LB) media, at 37°C, 1000rpm, air supplied at 0.66vvm and pH 7.0; see chapter 4 and 5) and were thus expected to be intact and viable were analysed. Heat stressed cells were prepared by boiling a cell sample at 100°C for 10 min before analysis. Figure 2.12 shows the expected intact and compromised cell distribution on bivariate data plots following staining with PI and BOX. Figure 2.13 shows the forward and side scatter profile of untreated *E.coli* TOP10 pQR239 stained with PI and BOX. The 50,000 events

analysed are from the gated region. Following heat treatment the population of dead cells would be expected to have increased significantly, this was also observed. The single parameter and bivariate histogram representations of heat treated and non-heat treated cells are shown in Figures 2.14 to 2.18.

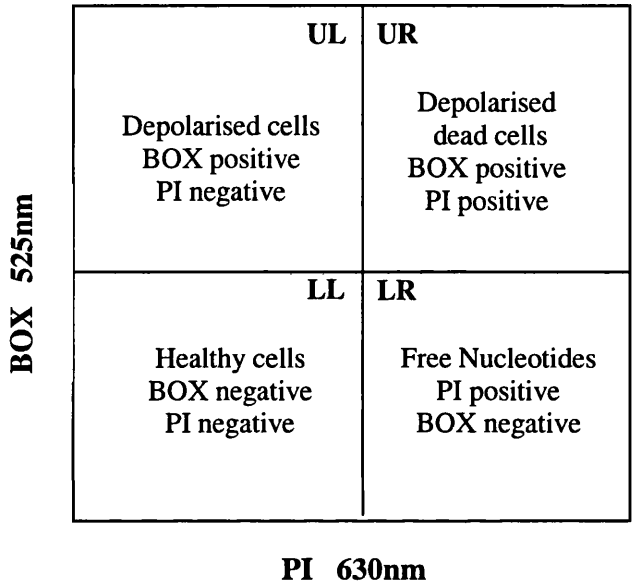

Figure 2.12. Expected distribution of intact and compromised *E.coli* TOP10 pQR239 on bivariate data plots (dot and density plots) following staining with PI and BOX. This staining pattern also holds true for *E.coli* IL-13.

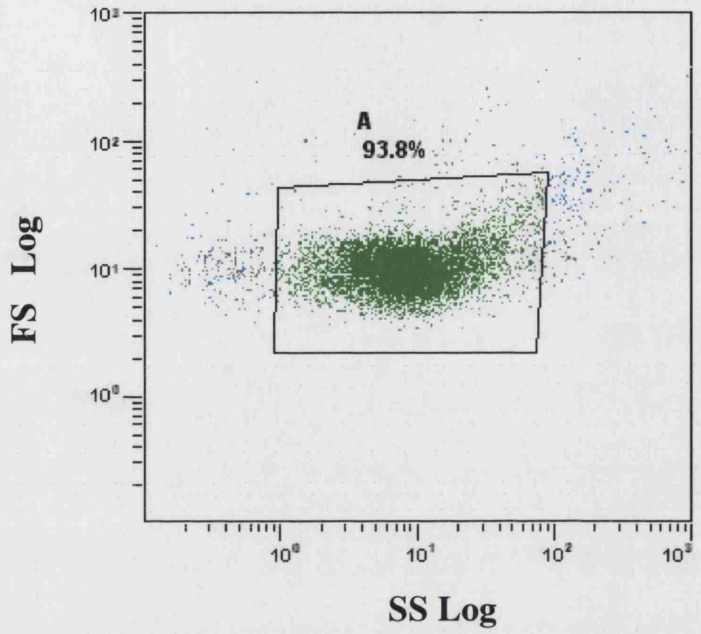

Figure 2.13. Forward and side scatter dot plot of untreated *E.coli* TOP10 pQR239 cells stained with PI and BOX after 6h growth.

Flow cytometry staining controls were carried out for each cell sample. This was to establish that the staining patterns observed when experimental data were being collected were accurate. Theoretically, following staining with PI, two distinct populations should be observed following analysis of cell sample. These would be dead cells (lacking membrane integrity) and viable cells (with intact membranes). Following heat treatment the population of dead cells would be expected to have increased significantly. This was observed. Single staining with BOX should also present two populations, a viable population with intact, polarised membranes and a second population of cells with depolarized membranes. Following heat treatment the population of cells with depolarized membranes would be expected to have increased significantly, this was also

observed. Staining with a PI and BOX combination should present a third population of cells, which are characterized by non-intact depolarized cytoplasmic membranes. These cells are dead and unlike cells that have depolarized but intact membranes these cells do not recover their viable status. They would be located in the upper right hand quadrant (UR) of a bivariate data plot.

Figure 2.14 depicts untreated and unstained cells, as shown all they all appear to be healthy and intact. The addition of fluorescent stains, a combination of PI and BOX to the same sample showed a different profile, Figure 2.15. Here the cells are shown to be predominantly healthy (LL quadrant) with only a small percentage of the population taking up the fluorescent stains. The UL quadrant of the density plot shows a small percentage of metabolically stressed cells which stain positively for BOX only. The UR quadrant also shows a small population, these cells have stained positively for both PI and BOX indicating that membrane polarity has been lost and the cell membrane is no longer intact essentially these cells are dead.

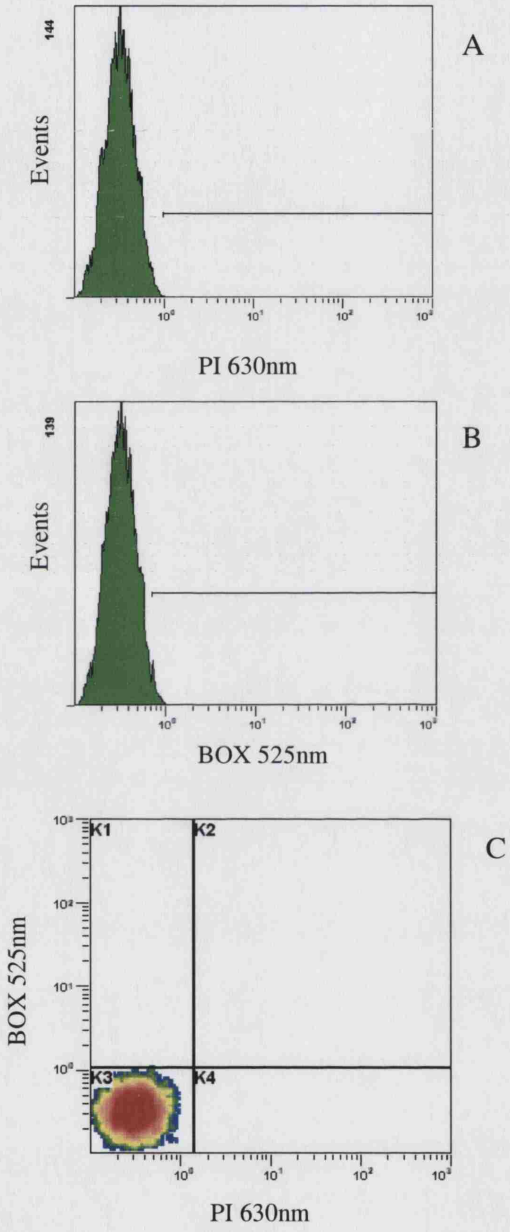

Figure 2.14. Untreated and unstained *E. coli* TOP10 pQR239 cells, from a 6 h culture. The data acquired is represented as histogram plots (A for PI and B for BOX) and as a density plot (C).

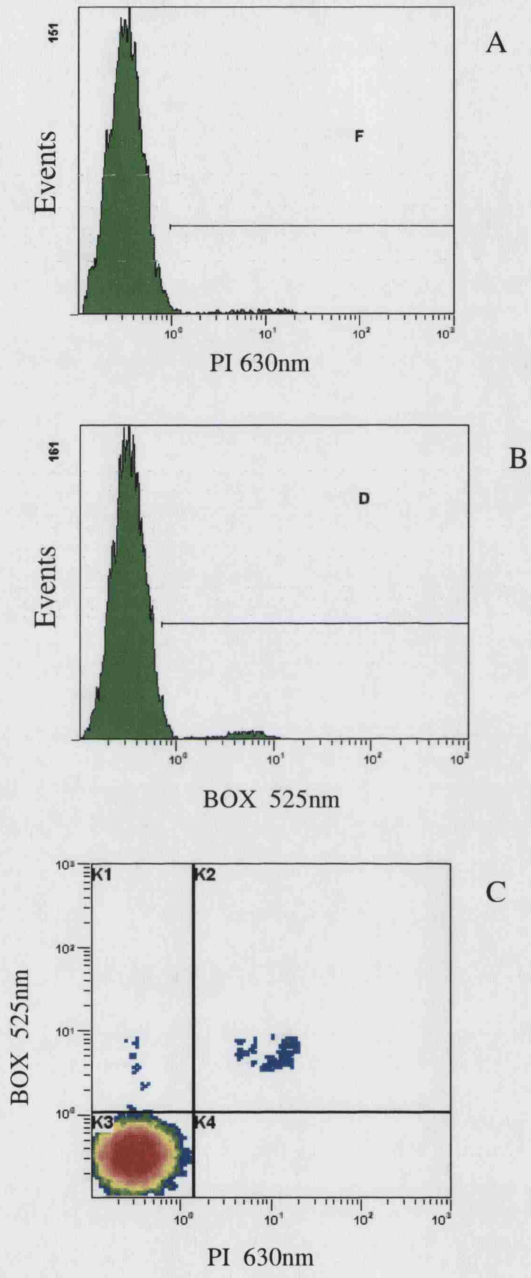

Figure 2.15. PI and BOX stained untreated *E. coli* TOP10 pQR239 cells from a 6 h culture. The data acquired is represented as histogram plots (A for PI and B for BOX) and as a density plot (C).

Heat-treated cells were stained with PI. This was to illustrate the location of PI positive, dead cells following single fluorochrome staining. Figure 2.16 shows the distribution of these cells. The histogram plot (Figure 2.16) shows two distinct peaks. The higher peak is of intact viable cells and the smaller peak corresponds to the dead cells. It is obvious that heat stress caused significant loss of cell viability. Cells killed by other means and stained with PI only are expected to display a similar distribution.

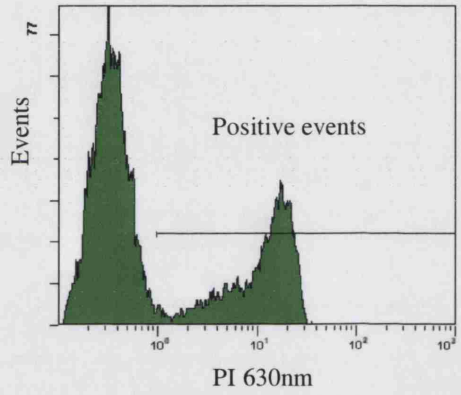

Figure 2.16. Heat treated *E. coli* TOP10 pQR239 stained with PI only. The data acquired is represented as a histogram plot.

Heat treated cells were also stained with BOX. This was to illustrate the location of BOX positive cells which had lost their membrane potential, following single fluorochrome staining. Figure 2.17 shows the distribution of these cells. The histogram plot (Figure 2.17) shows two distinct peaks. The higher peak is of intact viable cells and the smaller peak corresponds to the depolarised cell population. It is obvious that heat stress caused significant loss of cell membrane potential. Cells which have lost membrane polarisation as a result of other conditions and stained with BOX are expected to display a similar distribution.

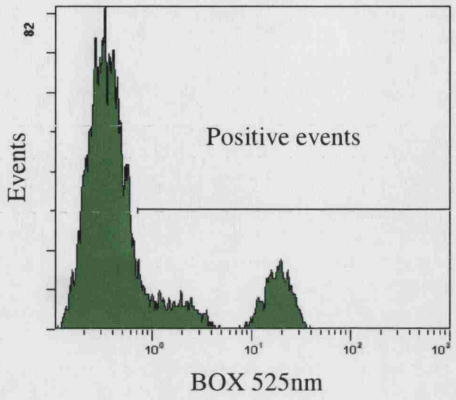

Figure 2.17. Heat treated *E. coli* TOP10 pQR239 stained with BOX only. The data acquired is represented as a histogram plot A.

A mixed cell sample of heat treated and untreated cells was also assessed. These cells were stained with a combination of PI and BOX, the data obtained is illustrated in Figure 2.18. Figure 2.18A shows the the distribution of cells which been stained by either stain. The dennsity plot, Figure 2.18B, clearly depicts two distinct cell populations; The intact viable cells in the LL quadrant and a population of dead cells in the UR quadrant.

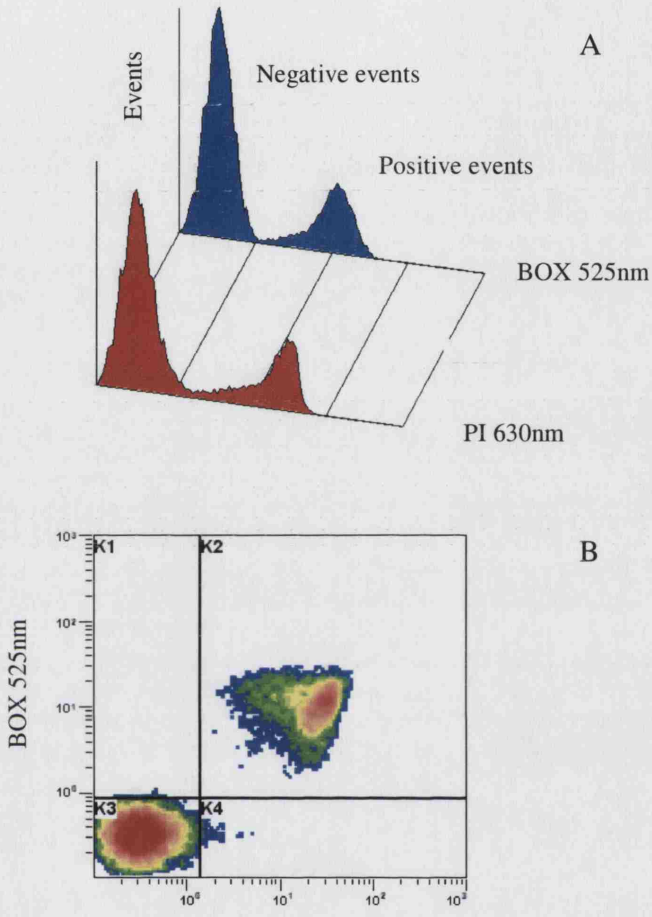

Figure 2.18. Heat treated and untreated *E. coli* TOP10 pQR239 stained with PI and BOX. The data acquired is represented as a histogram plot, A (PI and BOX event histograms) and as a density plot B.

2.7.1.2. *E.coli* IL-13 single and double stain controls

Control flow cytometric analyses were carried out to determine the distribution of *E.coli* IL-13 cells following staining with PI, BOX and Syto Red 63, on the FACSCalibur. Cells

which had been grown under process conditions for 6 hours (Luria Bertani (LB) media, at 37°C, 300-700rpm, air flow of 10slpm, pressure at 5psig and pH 7.0; see chapter 3) and were thus expected to be intact and viable were analysed.

Flow cytometry staining controls were carried out with each stain. This was to establish that the staining patterns observed when experimental data were being collected were accurate. Figure 2.19 shows the forward and side scatter dot plot of *E.coli* IL-13 cells stained with a combination of SR, PI and BOX at a culture age of 6 h.

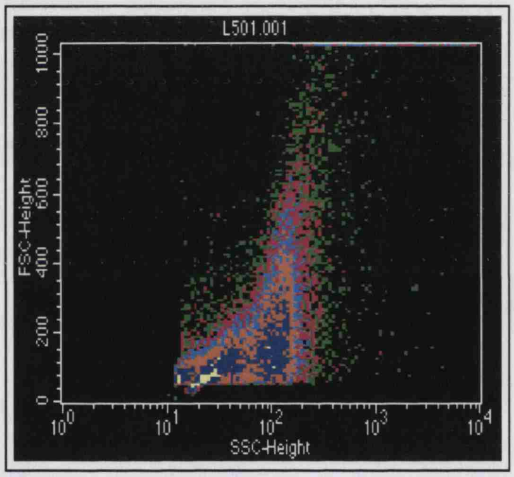

Figure 2.19. Forward and side scatter plot of *E.coli* IL-13 stained with a combination of SR, PI and BOX at a culture age of 6 h. 20,000 cells were analysed.

The distribution of *E.coli*-1L-13 untreated cells following staining with PI and BOX as conforms to the expected distribution patterns for cells exposed to the said stains (Figure 2.20).

A

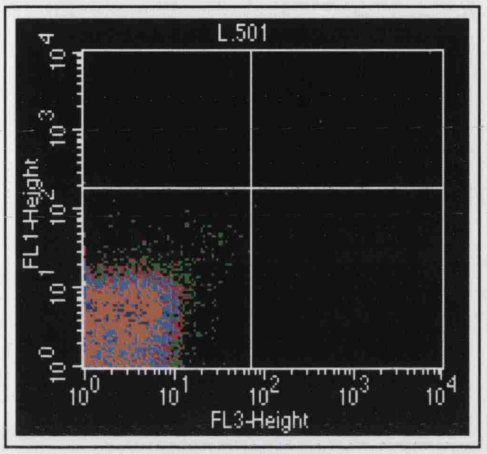

B

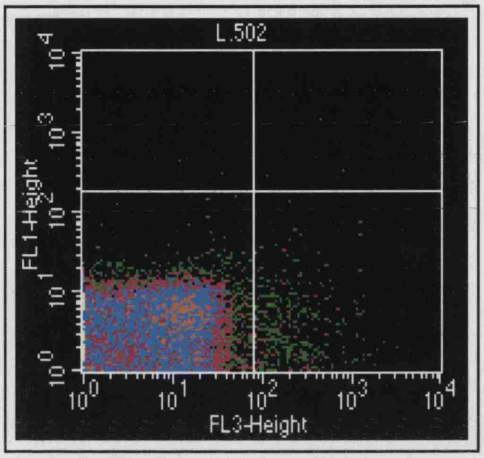

C

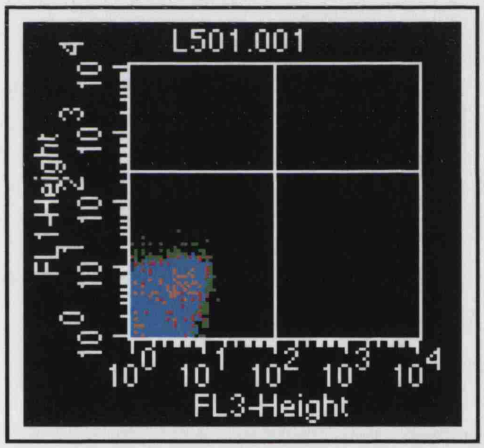

D

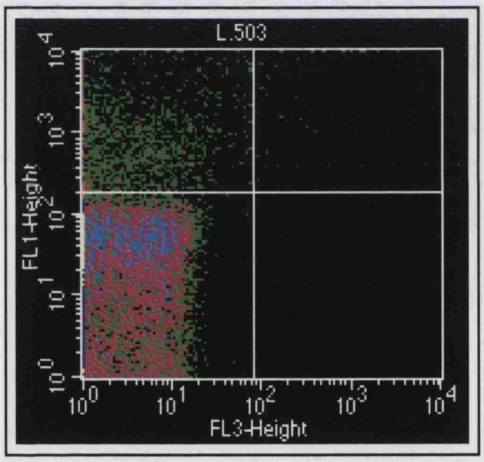

Figure 2.20. DOT plots of unstained (A) and stained untreated *E.coli* IL-13 (PI (B), SR (C), and BOX (D)) at a culture age of 6 h. 20,000 cells were analysed per sample. The cell population was predominantly intact and viable at this time.

2.8. Rationale for choice of organism

The basic requirement for flow cytometry is the presence of single cells that can flow separately along the flow channel (Bragga *et al* 2003) for this reason studies of bacteria have mainly been concentrated on *E.coli* (Skarstad *et al* 1983; Jepras *et al* 1997; Hewitt *et al* 1999a, b) and *Staphylococcus aureus* (Comas and Vives-Rego 1998; Novo *et al* 2000) both of which grow as single cells without too much aggregation.

This study investigated two *Escherichia coli* strains: *E.coli* IL-13 and *E.coli* TOP10 pQR239. *E.coli* IL-3 is a recombinant strain which following induction with Isopropyl-β-D-thiogalactopyranoside (IPTG) expresses the human interleukin IL-13. *E. coli* TOP10 pQR239 is a whole cell biocatalyst which is involved in the BVMO mediated stereo-selective oxidation of bicyclo (3.2.0.) hept-2-en-6-one to yield (-)-1(S) 5(R)-2-oxabicyclo (3.3.0) oct-6-en-3-one and (-) 1(R) 5(S)-3-oxabicyclo (3.3.0) oct-6-en-2-one in a example of an industrially significant biocatalytic reaction.

Using these strains allowed the application of flow cytometry to both a batch fermentation process, *E.coli* IL-13's expression of human IL-13; and to a batch and fed-batch biocatalytic process, *E.coli* TOP10 pQR239 in the BVMO mediated bioconversion.

2.9. Summary

Flow cytometry is a specialised technique that can pose significant insights into the way bacteria are characterised, analysed and optimised during biotechnological processes.

Chapter 3

Flow Cytometric Profiling of Induction Condition Optimisation during an *Escherichia coli* IL-13 Fermentation

3.0. Introduction

Modern biotechnological research has made the creation of genetically engineered bacterial strains capable of high-level expression of recombinant target proteins a standard feature in biotechnological process development. Strains with these aptitudes are of immense benefit to commercial ventures, for the production of large quantities of the desired product(s), and in academic research. The host-vector relationship and promoter strength are important parameters, which are routinely optimised to induce the most favourable levels of foreign gene expression by the host cell. Nutritional and metabolic parameters, plasmid segregational instability and the extent of cellular stress responses also play a vital role in recombinant protein expression (Andersson *et al* 1996; Bhattacharya and Dubey 1997).

The over expression of recombinant proteins in *Escherichia coli* often results in severe growth inhibition of the host cells, accompanied by severe metabolic changes. These adverse effects characterised by an increased metabolic burden are mainly attributed to the presence of plasmid replication systems, rDNA transcription and plasmid-encoded mRNA translation, to which cellular resources are redirected at the expense of normal host cell metabolic processes (Bentley *et al* 1990; Andersson *et al* 1996; Soriano *et al* 2002). These changes may be characterised by a decrease in growth rates, enhanced production of heat-shock proteins and inclusion body formation (Kurland and Dong 1996). This growth and metabolic process inhibition usually become apparent following transcriptional induction of the foreign gene.

This study investigated the effects of IPTG induction on *E.coli* IL-13 at different times during the exponential growth phase and the effects of fermentation condition variation (DOT and pH changes) using multiparameter flow cytometry in conjunction with traditional fermentation profiling methods. The aim was to two fold, a. to determine when during the exponential phase would induction have the least detrimental effect on cell physiology, metabolism and protein expression and b. to determine DOT and pH conditions under which maximum cell quality would be maintained without compromising recombinant protein expression.

3.1. Materials and Methods

3.1.1. Strain

The strain used was a modified *Escherichia coli* strain BL21 (DE3) containing a pET11a vector (Novagen, Madison, WI, USA) into which had been cloned the human interleukin 13 gene under the control of an isopropyl-β-D-thiogalactoside (IPTG) inducible promoter. This strain referred to as *E.coli* IL –13, was kindly donated by Dr. Michel Chartrain (Merck and Co Pharmaceuticals Inc. Bioprocessing Research and Development Rahway, NJ. USA).

3.1.2. Culture media

E.coli IL-13 was cultured in Luria Bertani (LB) media (Sigma, St. Louis, MO, USA) 25 gL^{-1} and ampicillin (Sigma, St. Louis, MO, USA) at a final concentration of 100mg L^{-1}. All media components except ampicillin were sterilized *in-situ* in the fermenter by heating to 123°C at 1.2 bar pressure for 30 min. 0.15 ml L^{-1} antifoam, polypropylene glycol '2000 (Fluka Chemie, Buches, Switzerland) was added to the bioreactor prior to media sterilization. Ampicillin was filter sterilized using a sterile 0.2 μm filter and aseptically added to the media immediately prior to inoculation.

3.1.3. *E.coli* IL-13 cultivation

E.coli IL-13 was cultivated in a 30L stirred tank reactor (STR) (B-braun Biotechnology, PA, USA), with a working volume of 20 L. The STR was inoculated with a 2.5% overnight (16h) culture. Culture pH was maintained at 7.0 ± 0.2 by the controlled addition of 1M sodium hydroxide (NaOH) and temperature was maintained at 37°C. An agitation speed of 300 rpm was maintained. Dissolved oxygen tension (DOT) within the culture was measured with a polarographic probe (Ingold, Messtechnick, Urdorf, Switzerland) and maintained at above 30% by agitation speed control (300-700 rpm). The culture was aerated via a submerged sparger, which introduced air (standard composition: 78.13% oxygen, 20.92% nitrogen and 0.03% argon) into the vessel at the rate of 10slpm. Vessel pressure was maintained at 300-500psig.

The cell culture was induced with 1mM IPTG, biotechnology grade (Fisher Biotech, NJ, USA), at early, midway and late in the exponential phase, when $OD_{600\,nm}$ reached 0.5 ± 0.05, 1 ± 0.2 and 3 ± 0.2 respectively. Samples were taken prior to and post induction. IPTG was dissolved in RO water and filter sterilized using a 0.2µm sterile disposable filter, before being aseptically added to the fermentation vessel.

3.1.4. Biomass measurement

Biomass increase during cultivation of *E.coli* IL-13 was measured via optical density (OD) measurements at 600 nm using a GENESYS 5 thermo spectroscopic (Rochester, NY, USA) variable wavelength spectrophotometer (Appendix II). Dry cell weight (DCW) (gL^{-1}) measurements were also taken. 5 ml samples of the fermentation broth were filtered using a vacuum pump and pre-weighed 0.22 µm filter paper (Whatman, Maidstone, U.K.), the filtrate was washed twice with an equal volume of RO water and the samples dried for 3 min in a microwave oven on high setting (650 watts). The weight differences were recorded.

3.1.5. Analytical

3.1.5.1. Fermentation Profiling

Dissolved oxygen tension (DOT), was monitored using a polarographic DOT probe. (Ingold, Messtechnick, Urdorf, Switzerland). The carbon-dioxide evolution rate (CER) and oxygen uptake rate (OUR) were measured and recorded via mass spectroscopic analysis of exit gases from the fermenter. DOT, CER and OUR data were collected using the FIX software (GE Fanuc, NY, USA).

3.1.5.2. Recombinant protein identification

The presence of IL-13 protein in *E.coli* IL-13 following induction with IPTG was determined via sodium dodecyl sulphate polyacrylamide gel electrophoresis (SDS PAGE) (Laemmli 1970) followed by silver staining to visualise the protein bands.

10 ml samples of fermentation broth were harvested from the fermentation vessel prior to and post induction, the cell mass was separated from the fermentation by centrifugation at 7000 rpm for 30min. Samples were standardised to 1 OD unit before SDS PAGE analysis. Protein was extracted from the cell pellet using the BugBuster® Protein Extraction Reagent kit as directed by the manufacturers protocol for protein extraction and inclusion body purification (IL-13 is present in inclusion bodies), this was a chemical lysis process. 10µl of a 1 in 10 dilution of the purified protein suspension was added to 10µl of Laemmli buffer and incubated at 90°C for 5 min, to denature the protein, prior to being loaded onto a pre-cast 4 - 20%, 10 well, Novex® Tris–Glycine–SDS gel (Invitrogen, Carisband, CA, USA). The gel was run in 1X Novex® Tris-Glycine SDS Running Buffer, for 90 min at 150volts. 10µl of protein size markers, of size range 10-255 kDa (Perfect protein™ markers, Novagen, USA) in an equal volume of Laemmli buffer, was also loaded on to the gel to determine the size of the protein bands seen following silver staining of the SDS PAGE gels.

Silver staining for protein visualisation was achieved using the SilverXpress® Silver Staining kit (Invitrogen, Carisband, CA, USA).

3.1.5.3. Flow cytometry

Flow cytometric analysis was carried out using a FACSCalibur™ dual laser flow, bench top analyser with optional fluidic sorter, cytometer (Beckman Dickinson, San Jose, CA, USA). The excitation light source was an air-cooled argon ion laser (488nm). Data analysis was accomplished with the CellQuest Pro software (BD Biosciences San Jose, CA, USA), which allows protocol definition and batch analysis. All solutions were filtered prior to use using a 0.2μm filter to remove any particulate matter that could interfere with analysis. Culture samples were diluted in Dulbecco's Phosphate buffered saline, pH 7.2 (DBS) (Sigma, St. Louis, MO, USA) to a final concentration of 1 x 10^{-5} cells per ml (Appendix I) and stained with propidium iodide (PI) (Sigma, St. Louis, MO, USA), bis- (1,3-dibutylbarbituric acid) trimethine oxonol (BOX) (Molecular Probes, Eugene, OR, USA) and Syto Red 63 (SR) (Molecular Probes, Eugene, OR, USA) at a final concentration of 5μgml^{-1}, 10μgml^{-1} and 1μ$Molml^{-1}$ respectively. Ethylenediaminetetraacetic acid (EDTA) was added at a final concentration of 4mMml^{-1} to facilitate BOX straining. The systems' compensation was set up in such a way as to minimize the spectral overlap between the PI, BOX and SR emitted fluorescence detectors. BOX, PI and SR fluorescence were measured at 525, 630 and 655 nm respectively following a 10 min incubation period at room temperature (25°C). A total of 20,000 cells were analysed per sample. Flow cytometric data is represented in dot plots.

SR stains nucleic material in whole cells and was used to ensure that every registered event was a cell. This allowed 20,000 cells to be analysed.

3.2. Results

Environmental conditions during fermentations can significantly impact recombinant protein expression and thus need to be optimised. This section reports on the effects of when, during the cell cycle, induction took place and variations in DOT and pH during the fermentation. Analyses were carried out using flow cytometry to quantitatively establish the metabolic and physiological status of the cells and SDS PAGE gel analysis to identify and characterise the recombinant IL-13 protein.

Cell quality was assessed pre and post induction. Figure 3.1 is a schematic of the induction period optimisation fermentations, showing the times before and after induction for all conditions investigated as well as for the non-induced fermentation. The flow cytometric analysis used employs three fluorescent stains, PI, BOX and SR, all of which work together to establish the quality of *E.coli* IL-13. PI is a vital fluorescent probe that binds to DNA but is unable to cross the intact cytoplasmic membrane. Intact cells show selective membrane permeability. Cells that have lost membrane integrity therefore take up PI and are classified as dead cells (Amanullah, *et al* 2002a, b). The second stain, BOX, binds to the cell membrane following its depolarization, where it distributes according to the membrane potential gradient, provided the free stain gradient is below the saturation point for the available binding points (Nebe-von-Caron and Badley 1995). SR binds all nucleic material and its function was to identify whole cells, and as a result every one of the 20,000 events analysed can be assumed to be a single cell as opposed to fermentation debris or cell fragments. However, SR staining is not represented in the dot plots, as its function is cell identification. Together these stains give a clear indication of the metabolic and physiological condition of *E.coli* IL-13 during the fermentation.

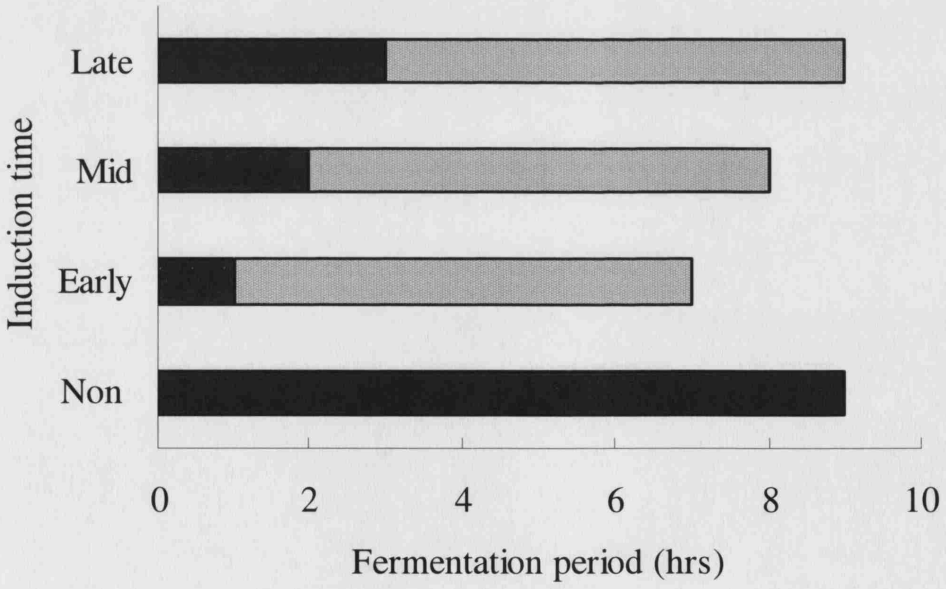

Figure 3.1. Induction period. ▮ Time period prior to induction, ▒ time period post induction.

3.2.1. Control fermentations

3.2.1.1. Fermentation profiles

Control fermentations of non-induced *E.coli* IL-13 were carried out to give an indication of normal cell growth parameters, as well as to identify the different growth phases during which induction would take place. Figure 3.2A shows the optical density profile of non-induced cells during the 9 h duration of the fermentation. A short lag phase followed by an exponential phase, which lasts approximately 3 h ensued, following this the cells enter a stationary phase where they remain for the duration of the fermentation. This figure also shows the change in the dissolved oxygen tension, DOT, profile of the fermentation. The DOT dropped linearly until half way through the exponential phase, then it appeared to stabilise. It began to rise again after 6 h and finally stabilised at ~80% indicating that the cells were no longer growing, i.e. they are in the stationary growth phase. Figure 3.2B shows the oxygen uptake and carbon dioxide evolution rates (OUR and CER) of the cells during the fermentation. These profiles also clearly identified the different growth stages of *E.coli* IL-13 with respect to cellular respiration. A final dry cell weight of $2.13gL^{-1}$ was obtained and a specific growth rate of $0.71h^{-1}$ was recorded for non-induced cells, in the control fermentation.

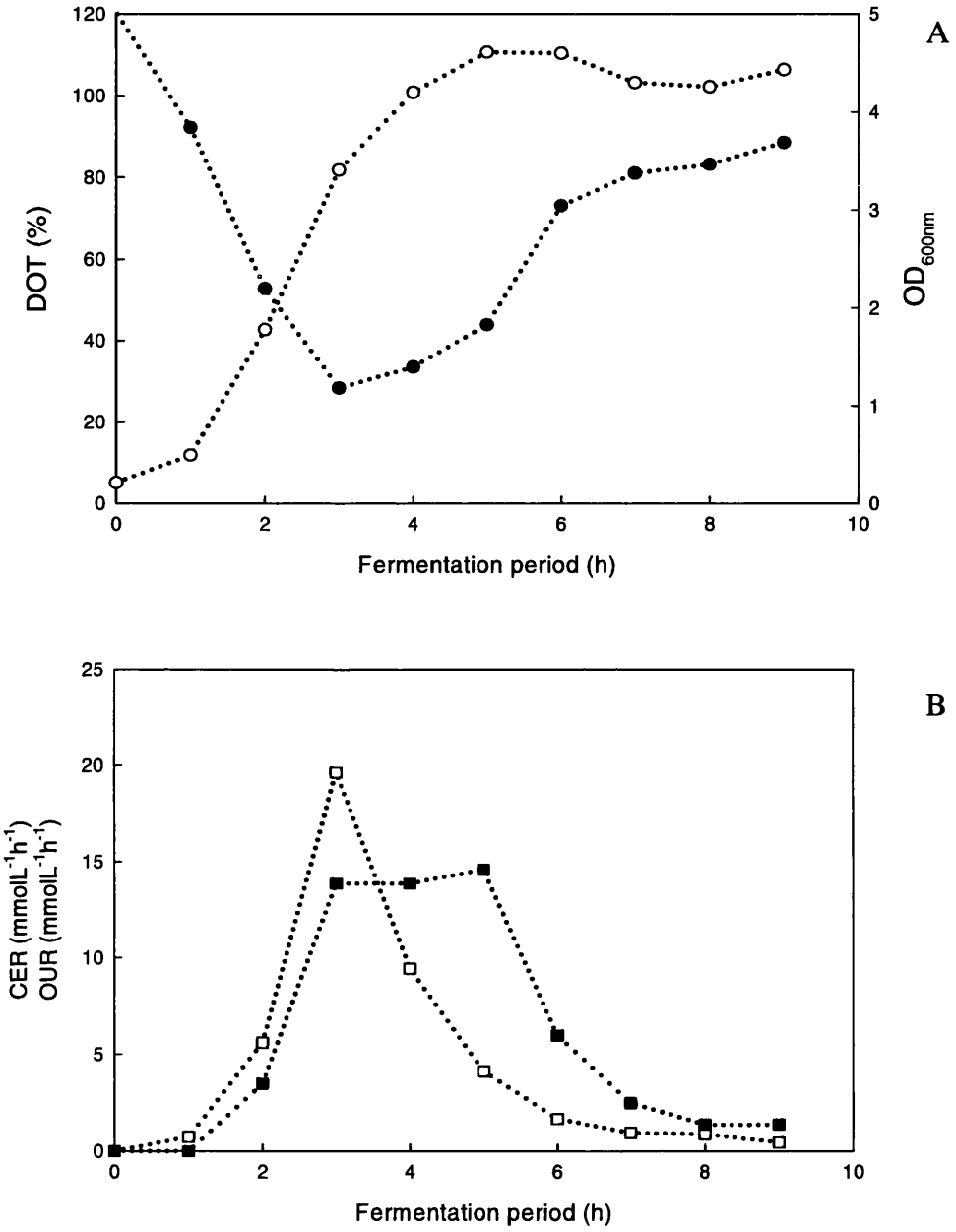

Figure 3.2. Fermentation (A) and respiratory (B) profiles of non-induced *E.coli* IL-13 (○) OD_{600nm}, (●) DOT, (□) OUR, (■) CER.

3.2.1.2. Flow cytometry

Tri-stain flow cytometry, utilising PI, BOX and SR was used to investigate the physiological and metabolic status of *E.coli* IL-13 during the fermentation prior to and post induction with 1mM IPTG during the exponential growth phase, see Figure 3.4. Flow cytometric analysis was carried out on samples taken from non-induced fermentations to act as controls. These corresponded time-wise with samples from the induced fermentations and were run under the same fermentation conditions (Figure 3.1).

The non-induced cell population were predominantly healthy at all the time points examined. Before induction when OD_{600nm} was 0.5 ± 0.05 96% of the cells were intact, staining negatively for PI and BOX, and 1.8% were dead staining positively for the said stains. 6 hours later, when the cells are of the same culture age as they would be 6h post early exponential phase induction (see Figure 3.1) the percentage of healthy intact cells had slightly increased to 96.4%, these can be seen in the LL quadrant of the 7 h dot plot in Figure 3.3. At 2 h culture age when an OD of 1 ± 0.5 had been achieved, which corresponds to the initiation of mid exponential growth phase induction, 95.8% of the population were found to be viable and 2.7% dead. This population of intact cells had significantly reduced by almost 8%, to 88% when the culture age reached 8h (corresponding to 6 h post mid exponential phase induction), this population can be seen in the 8h dot plot in Figure 3.3.

When the culture OD had reached 3 ± 0.5, samples corresponding to pre late exponential phase induction were removed from the fermenter and analysed. Here the percentage of viable, physiologically and metabolically stable cells was lower than previously recorded at 92.7%; with a correlating higher percentage of dead cells of 4.7% at the end of the fermentation (corresponding to 6h post late exponential phase induction) when culture age had reached 9h, the percentage of intact cells had risen slightly to 96%. This may be attributed to cell proliferation. The population of metabolically stressed, depolarised cells, which stained positively for BOX only (located in the UL quadrant of the dot plots) remained relatively low (<3%) in all samples from the non-induced fermentations.

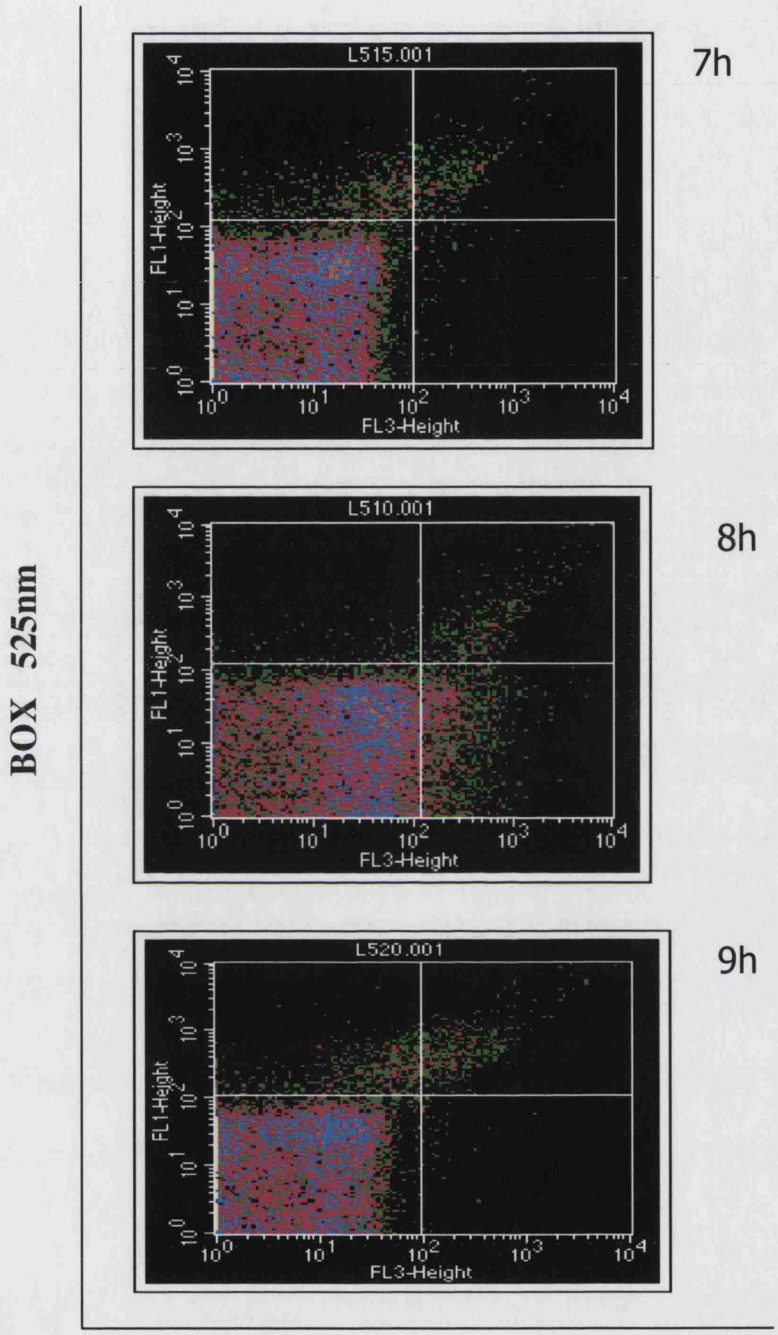

Figure 3.3. Flow cytometric profile of non-induced *E.coli* IL-13 at 7, 8 and 9 h post inoculation corresponding to 6 h after induction early, midway and late in the exponential growth phase.

3.2.2. Induction time optimisation

Chemical induction is a common method of initiating the expression of foreign genes in recombinant bacterial systems (Kosinski *et al* 1992; Andersson *et al* 1996; Lewis *et al* 2004), when this occurs during the growth period and under what conditions, such as concentrations of the inducing agent, can significantly affect the final quantity and quality of recombinant protein product (Patkar *et al* 2002), as well as the physical and metabolic status of the host cell. This study investigated the effects of inducing IL-13 production in *E.coli* IL-13 at different stages of the exponential growth phase using multiparameter flow cytometry in conjunction with traditional methods of fermentation monitoring (cell respiration monitoring and biomass increase measurements). Inductions early, midway and late in the exponential phase were assessed.

3.2.2.1. Early exponential growth phase induction

20 L fermentations were carried out and non-host gene expression induced at different times during the exponential growth phase. Figure 3.4A shows the OD_{600nm} and DOT measurements, for a culture induced early in the exponential phase, when an OD of 0.5 ± 0.05 had been attained. Here the OD measurements show a short lag phase as in Figure 3.2A; however following induction there was a very slow entry into the exponential growth phase. The DOT data also shows a slower decrease, not reaching the 30% minimum until 5 h after inoculation, this occurred 2 h earlier in non-induced cells (see Figure 3.3). The respiratory profile on the other hand was significantly different from the control fermentation; this can be seen in Figure 3.4B. Two lag and exponential growth phases were observed, the first following inoculation and a second one following induction. A decrease in the cell growth rate was observed one hour post induction after which the cells appeared to enter a second lag phase before entering a prolonged, 2 h exponential phase. The specific growth rate of the first exponential phase was $0.74\ h^{-1}$, the second had a lower specific growth rate at $0.41\ h^{-1}$. The respiratory profile implied a decline in cell growth after this; in the control fermentation this decline was more gradual. The biomass accumulation under these

conditions was lower than in the control fermentation with the final DCW being 1.48 gL^{-1}.

Flow cytometry was used to investigate the physiological and metabolic status of *E.coli* IL-13 prior to and post induction with 1mM IPTG early in the exponential phase, dot plots are shown in Figure 3.5. Post induction samples were taken 6 h post induction. Prior to induction the cells were predominantly viable, staining negatively for PI and BOX and located in the LL quadrant (95%). 2.5% of the cells stained positively for PI and BOX were located in the UR quadrant, these cells were dead. Following induction a high percentage of the cells were still intact and viable (92%), however the percentage of dead cells had increased to 3.5%. A population of depolarised cells was observed, in the UL quadrant and accounted for 4.3% of the compromised cell population. At the end of the fermentation, less than 10% of the total cell population was compromised. This is just 3% more than were compromised at the end of the non-induced fermentation.

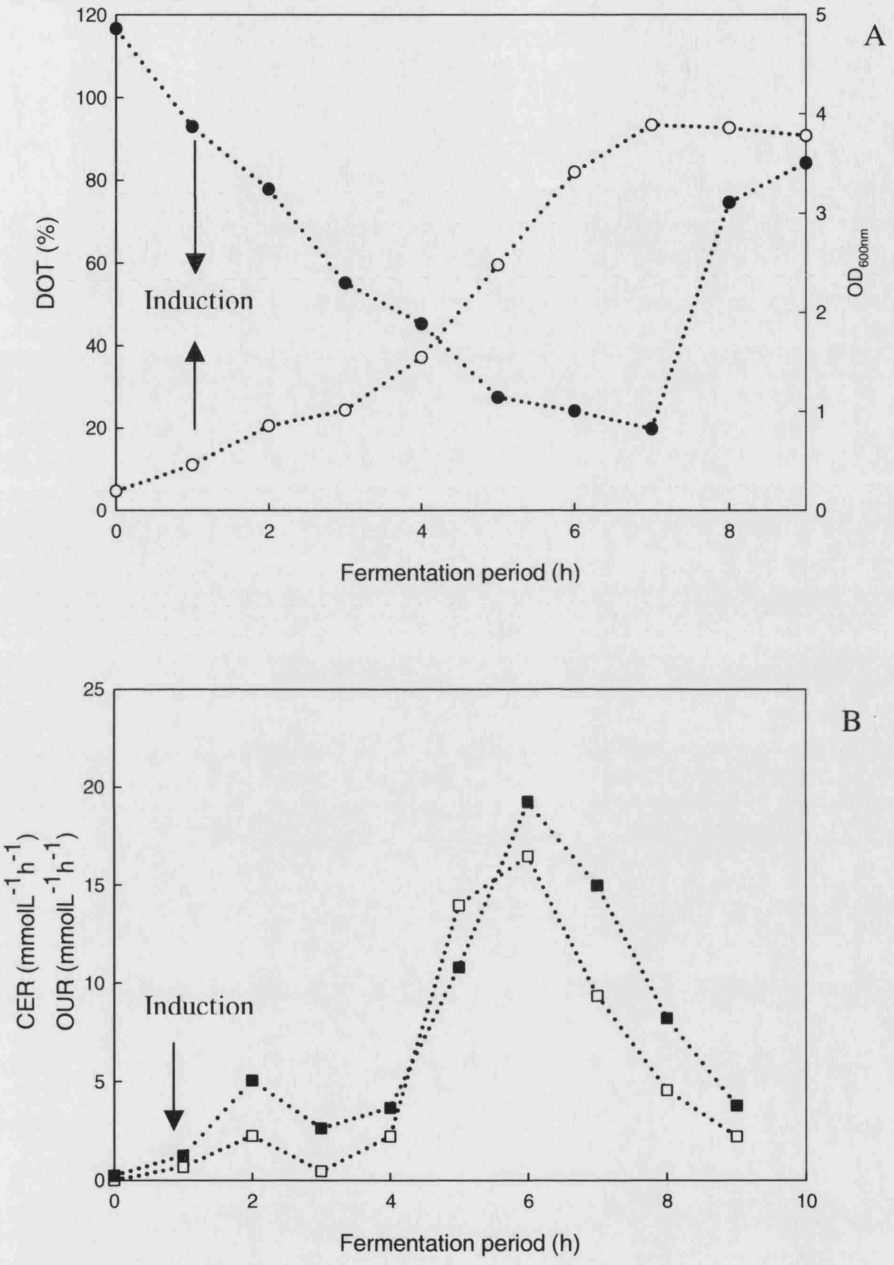

Figure 3.4. Fermentation (A) and respiratory (B) profiles of *E.coli* IL-13 induced early during the exponential growth phase. (○) OD_{600nm}, (●) DOT, (□) OUR, (■) CER.

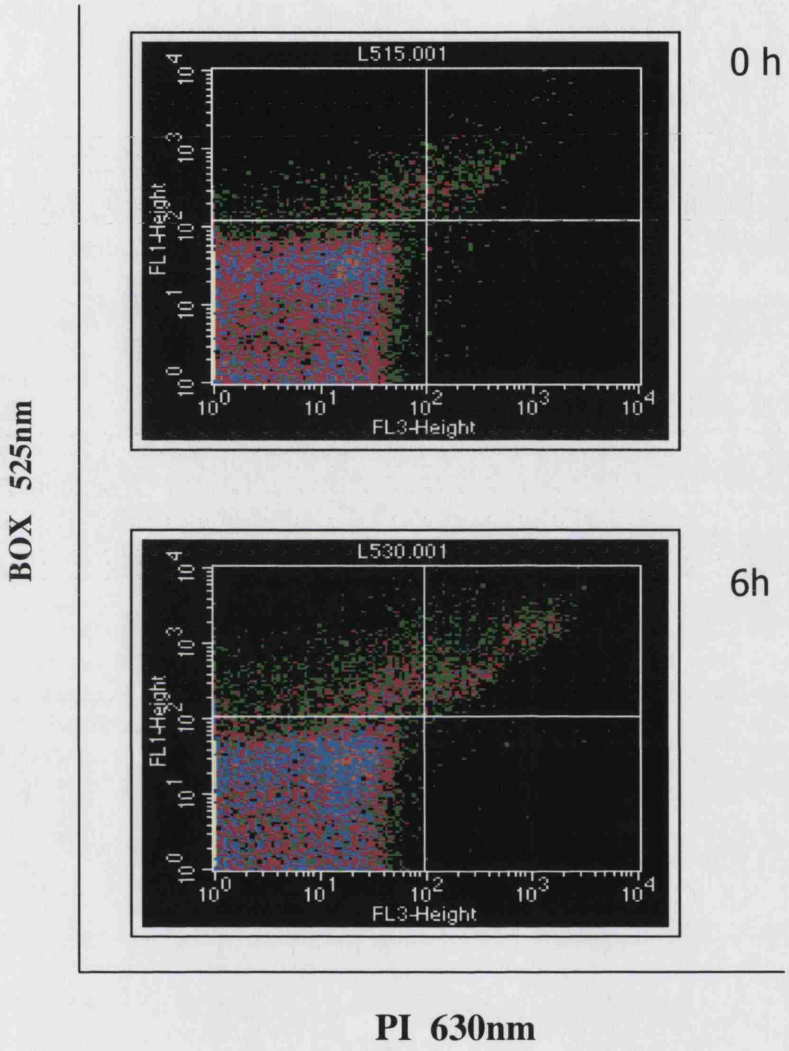

Figure 3.5. Flow cytometric profiles of *E.coli* IL-13 pre and post early exponential phase induction.

3.2.2.2. Mid exponential growth phase induction

20 L fermentations were induced midway through the exponential growth phase, when the OD_{600nm} had reached 1.0 ± 0.5, 2h post inoculation. Figure 3.6A shows the OD and DOT profiles under the said condition. Cell biomass increased exponentially for the first 3h of the fermentation after which the culture entered the stationary phase rather abruptly and remained there for the remainder of the fermentation. The DOT profile shows that DOT reached 30% within 2 h and then slowly increased to 70% where it remained for the last 2 h of the fermentation; Indicating that cellular respiration had slowed down, hence the increased concentration of dissolved oxygen in the fermentation vessel. This is further reinforced by the cellular respiration profile in Figure 3.6B. The OUR and CER profiles are almost identical and show an initial lag phase as seen in the control fermentation and followed by a short exponential phase. A specific growth rate of $0.64h^{-1}$ was recorded; this was lower than the rate recorded for the control fermentation and the initial specific growth rate of the fermentation which was inoculated early in the exponential phase but higher than the latter fermentation's second specific growth rate. However, there was an almost instantaneous drop in cell respiration following induction shown by the low rates (< $10mmolL^{-1}\ h^{-1}$) of OUR and CER. A final DCW of $1.32gL^{-1}$ was recorded; this also was lower than the final DCW of the control fermentation.

Flow cytometry was used to investigate the physiological and metabolic status of *E.coli* IL-13 prior to and post induction with 1mM IPTG midway through the exponential phase, Figure 3.7. Before induction just 2% of the cell population was dead, thus most of the cells were viable and intact (91.3%). However, this percentage had increased significantly 6 h post induction to 18%, UR quadrant of the 6 h dot plot in Figure 3.7. In total 30% of cells were compromised 6 hours after induction.

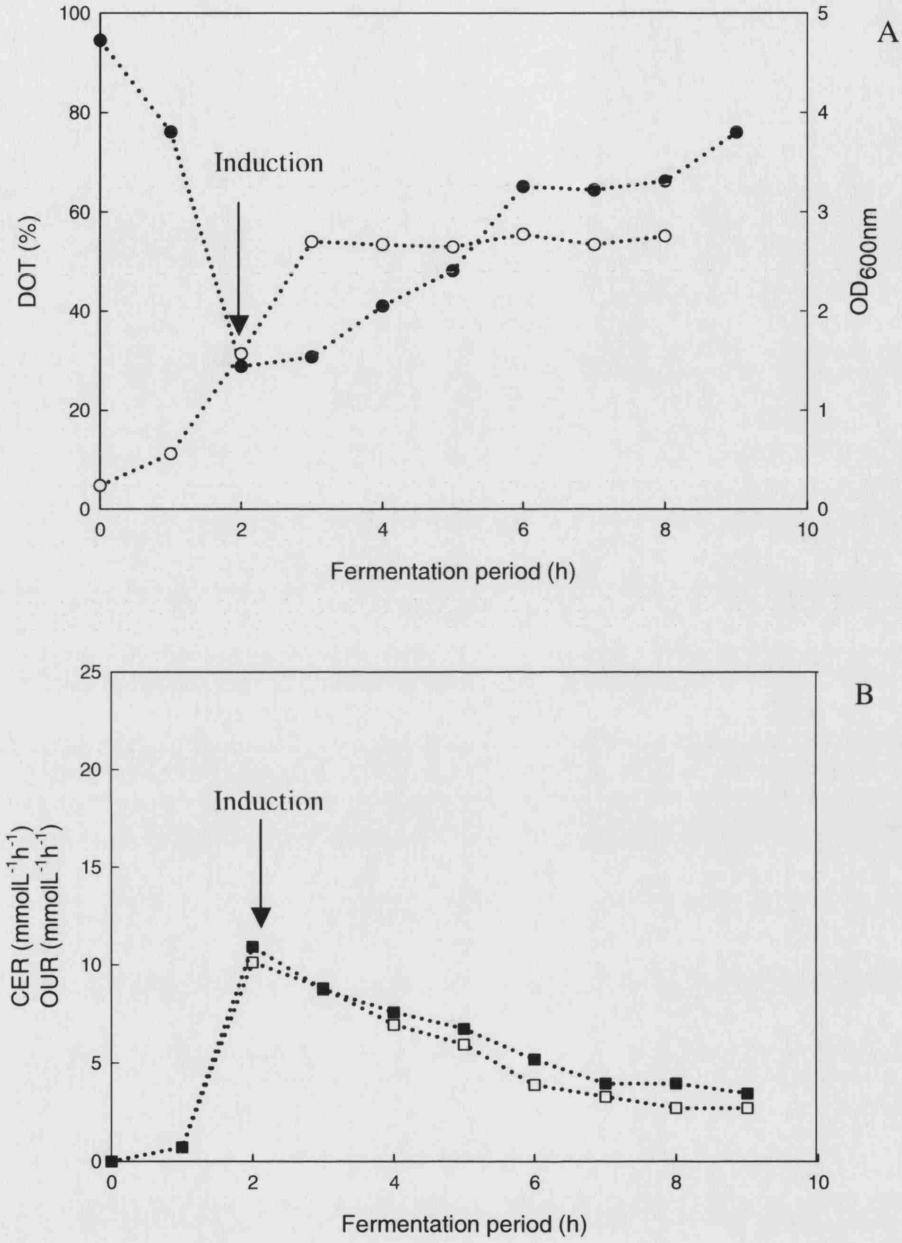

Figure 3.6. Fermentation, A, and respiratory, B, profiles of *E.coli* IL-13 induced mid-way through the exponential growth phase. (○) OD_{600nm}, (●) DOT, (□) OUR, (■) CER.

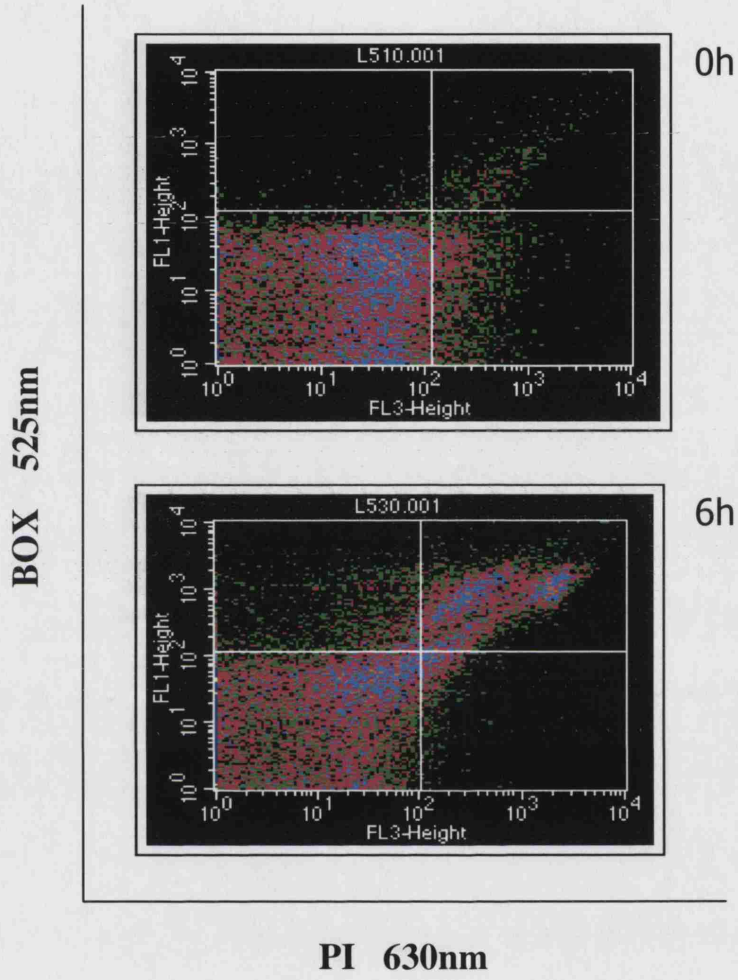

Figure 3.7. Flow cytometric profiles of *E.coli* IL-13 pre and post mid exponential phase induction.

3.2.2.3. Late exponential growth phase induction

20 L fermentations were induced late in the exponential growth phase with 1mM IPTG, when the OD_{600nm} had reached 3.0 ± 0.5. Figure 3.8A shows the OD and DOT profiles under this condition, these closely mimic the OD and DOT profiles of the control fermentation, as did the cellular respiration profiles, Figure 3.8B. The specific growth rate observed here, $0.72h^{-1}$, was also quite close to the growth rate of the control fermentation, the final DCW recorded was slightly higher at $2.20gLh^{-1}$.

Flow cytometry was used to investigate the physiological and metabolic status of *E.coli* IL-13 prior to and post induction with 1mM IPTG late in the exponential phase (Figure 3.9). Flow cytometric analysis showed that prior to induction the cell population was predominantly intact, >95%. 6h post induction the percentage of dead and damaged cells was still low, less than 5% (Figure 3.9, 6 h dot plot), suggesting that in terms of cell quality, induction during the late exponential growth stage was optimal. Mid exponential induction was the most detrimental to cell viability, with close to 30% of the cell population being compromised 6 h post induction.

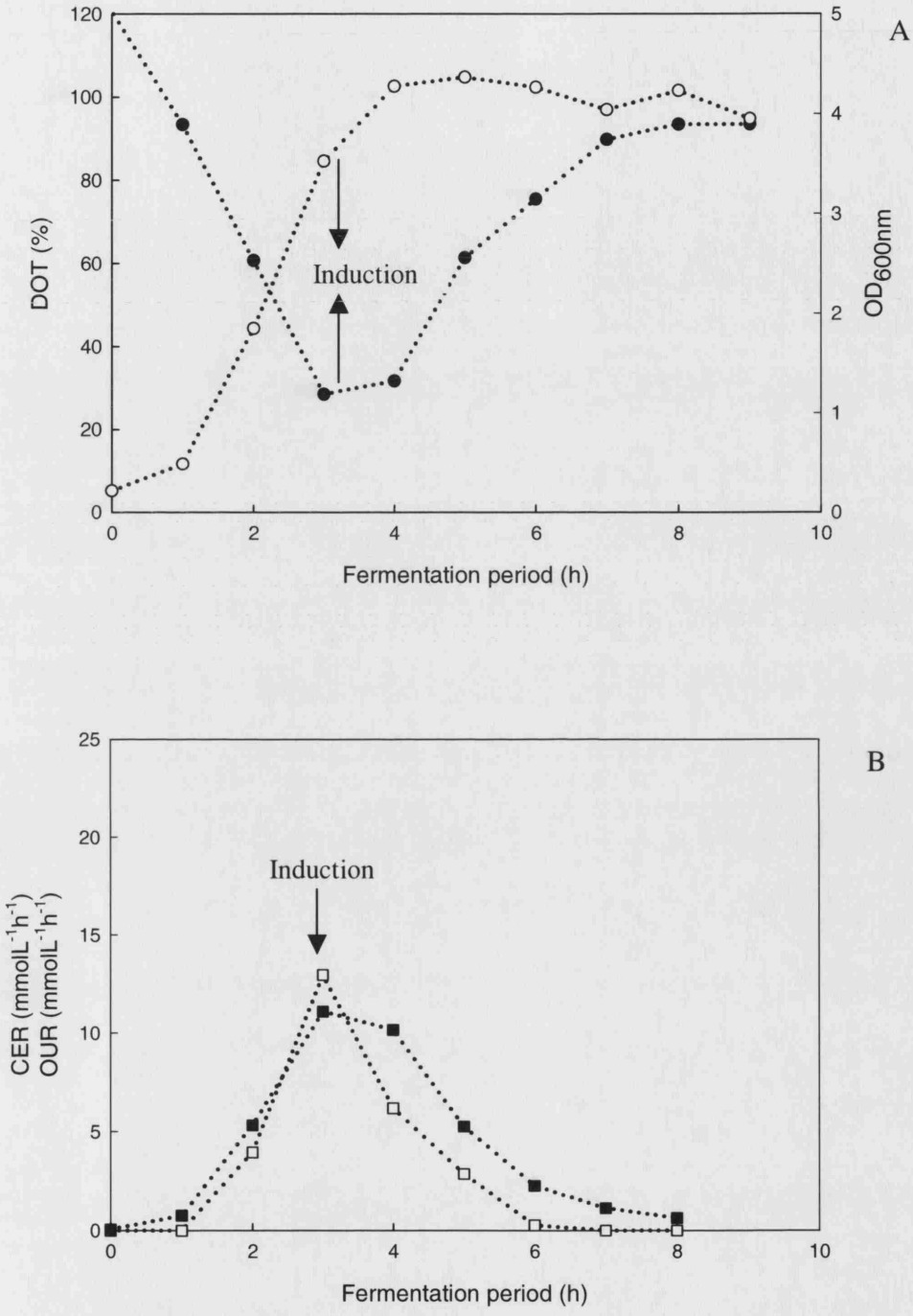

Figure 3.8. Fermentation (A) and respiratory (B) profiles of *E.coli* IL-13 induced late during the exponential growth phase. (○) OD600nm, (●) DOT, (□) OUR, (■) CER.

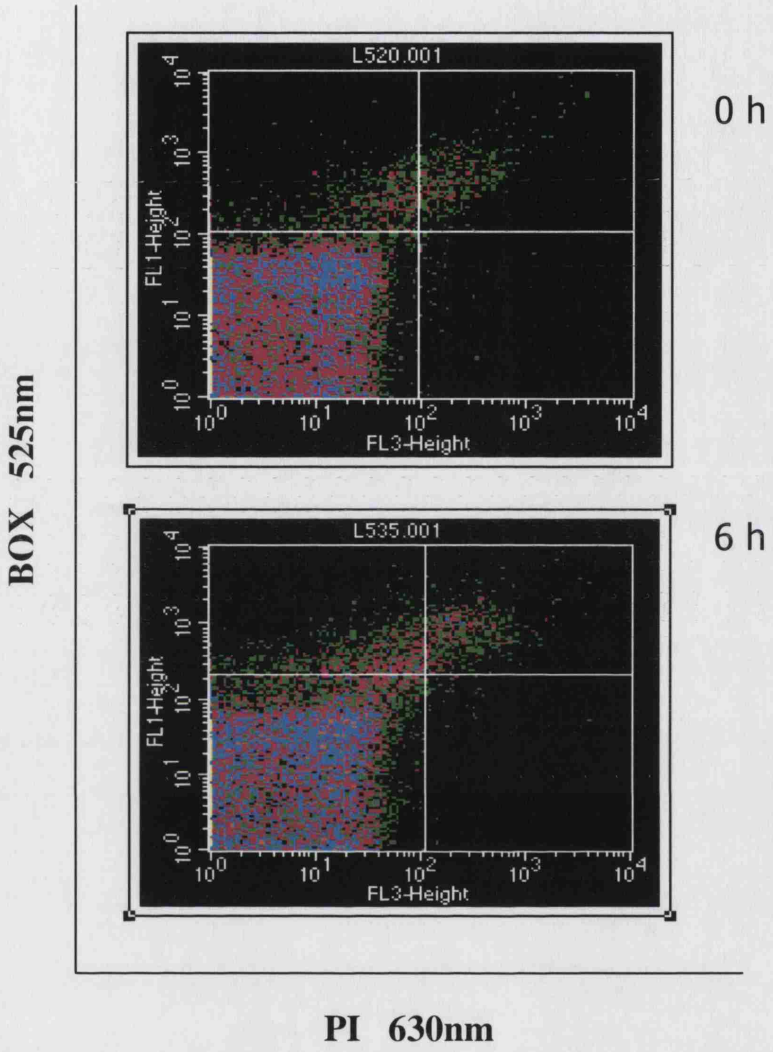

Figure 3.9. Flow cytometric profiles of *E.coli* IL-13 pre and post late exponential phase induction.

3.2.2.4. Recombinant protein identification

Protein extracted and purified from *E.coli* IL-13 induced under the three conditions and the non-induced control was analysed on a 4–20% Tris – Glycine – SDS PAGE gel for the presence of the recombinant interleukin 13 (IL-13) protein. IL-13 is typically between 10.3 and 15 kDa in size. Joshi and Puri (2005) report the expression of a 12KDa human IL-13 in *E.coli.*

The protein solute from the non-induced fermentation was not expected to present a band indicative of the presence of IL-13, or in the event that it did the band was expected to be faint, as only minute amounts would have been produced. Induced fermentations were expected to show the presence of the recombinant IL-13 protein.

All protein purified from the induced fermentation samples showed the presence of a 12.5KDa band, which is within the appropriate band size range (Figure 3.10) signifying that foreign protein expression had occurred. The IL-13 band was absent from the lanes containing the protein purified from the non-induced fermentations. This suggests tightly controlled expression of the recombinant protein, i.e. there is no significant basal expression.

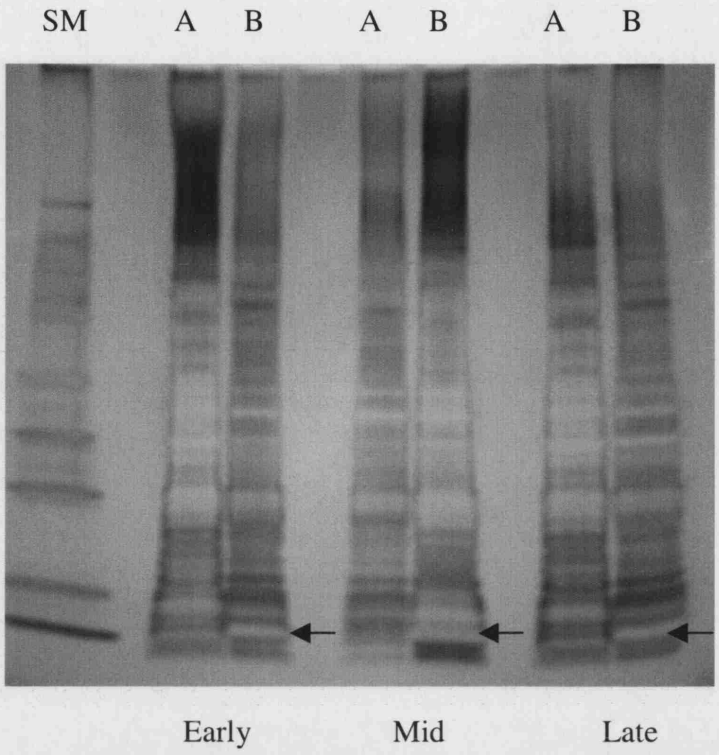

Figure 3.10. SDS PAGE gel of protein purified from non-induced and induced *E.coli* IL-13 fermentations. (SM) Protein size marker, (A) Non-induced samples, (B) Induced samples. Arrows point to the IL-13 band, which is 12.5kDa in size. Protein bands are visualised with silver staining.

3.2.3. Optimisation of fermentation conditions for the expression of IL-13

The previous set of experiments was used to establish the point during the exponential growth phase when induction would cause the least damage to the cells with respect to viability and membrane quality. It was determined that induction early in the exponential phase resulted in the lowest levels of metabolic stress and cell death in *E.coli* IL-13. This section investigates the effects of fermentation conditions on the physical and metabolic status of *E.coli* IL-13 and recombinant protein production. The effects of pH and dissolved oxygen tension (DOT) during the fermentations were investigated using multiparameter flow cytometry in conjunction with conventional methods of fermentation profiling.

3.2.3.1. Control *E.coli* IL-13 fermentation with DOT and pH control

Having established that induction early in the exponential growth phase promoted the most favourable levels of cell viability, this induction condition was used in all subsequent investigations.

During the fermentation DOT was maintained above 30% air saturation by automatic agitator speed modification and pH was maintained at 7 ± 0.2 throughout the fermentation via the controlled addition of 1M NaOH; Recombinant protein expression was induced by the addition of 1mM IPTG. Figure 3.11A shows the OD_{600nm} and DOT profiles, following induction early in the exponential phase, when an OD of 0.5 ± 0.05 had been attained. The cell respiratory profile, Figure 3.11B shows two lag and exponential phases; pre and post induction, with the first and second exponential growth phases having specific growth rates of 0.74 and $0.41h^{-1}$ respectively.

Figure 3.12 shows the result of flow cytometric analysis of fermentation samples taken at 2 and 6 h post induction. The cells were stained with a combination of SR, PI and BOX. The second lag phase, which the culture enters at 2-3 h post induction, was characterised by a significant population of metabolically stressed, depolarised cells situated in the UL quadrant, which accounted for 7.2% of the total cell population. This sub-population was found to be transient, as the depolarised BOX positive population was observed to have decreased 6 hours after induction to 4.2%, by which time the cells had resumed normal respiration and exponential growth. The percentage of dead cells, located in the UR quadrants was also low, 2.4 and 3.5% respectively at 2 and 6 h post induction. At the end of the fermentation (6 h after induction) 92% of the cell population was still intact and viable; these cells can be seen in the LL quadrant of the 6h dot plot in Figure 3.12.

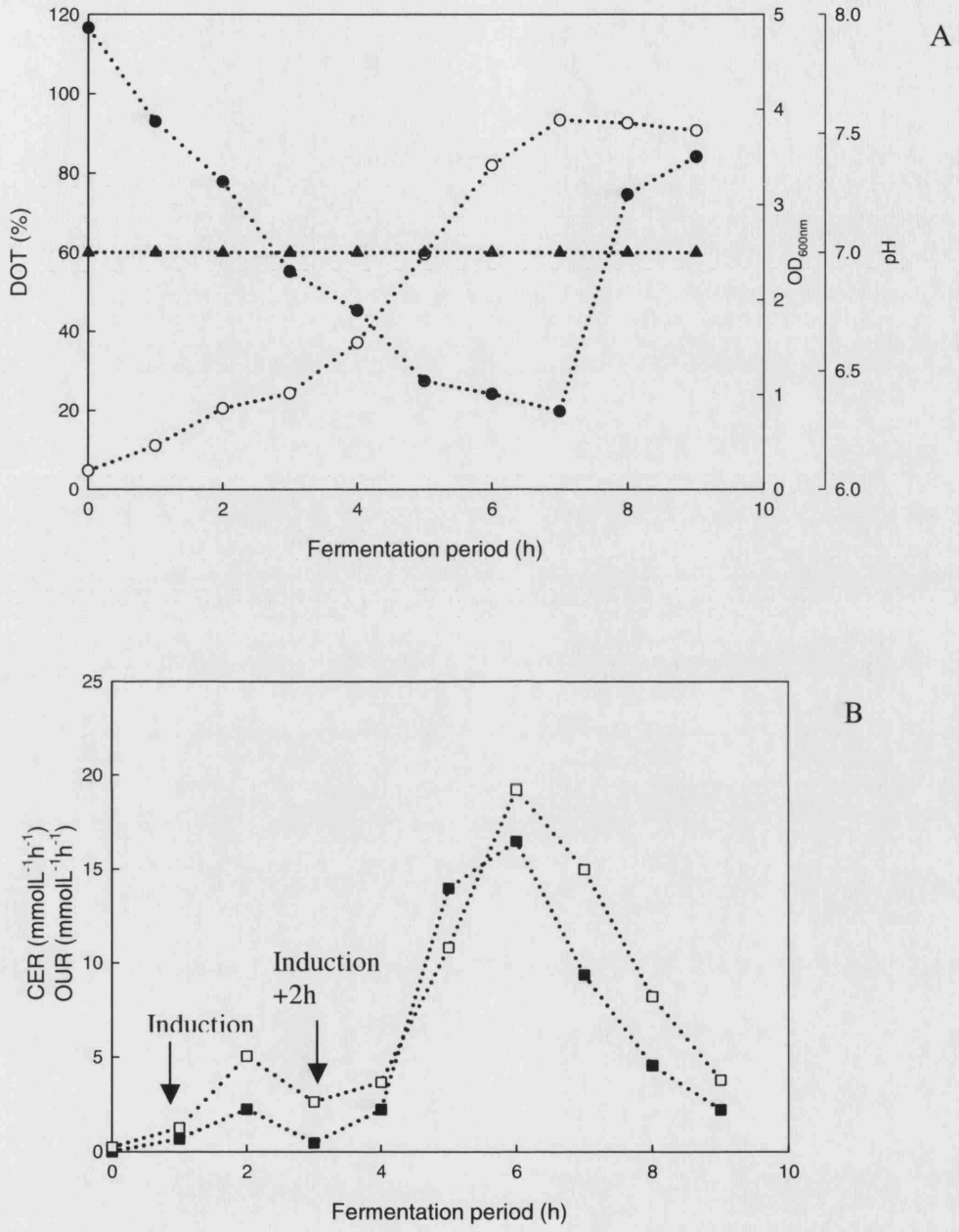

Figure 3.11. Fermentation (A) and respiratory (B) profiles *E.coli* IL-13 induced early in the exponential phase with DOT (●) maintained above 30% air saturation and pH (▲) at 7 ± 0.2. (○) OD_{600nm}, (□) OUR, (■) CER.

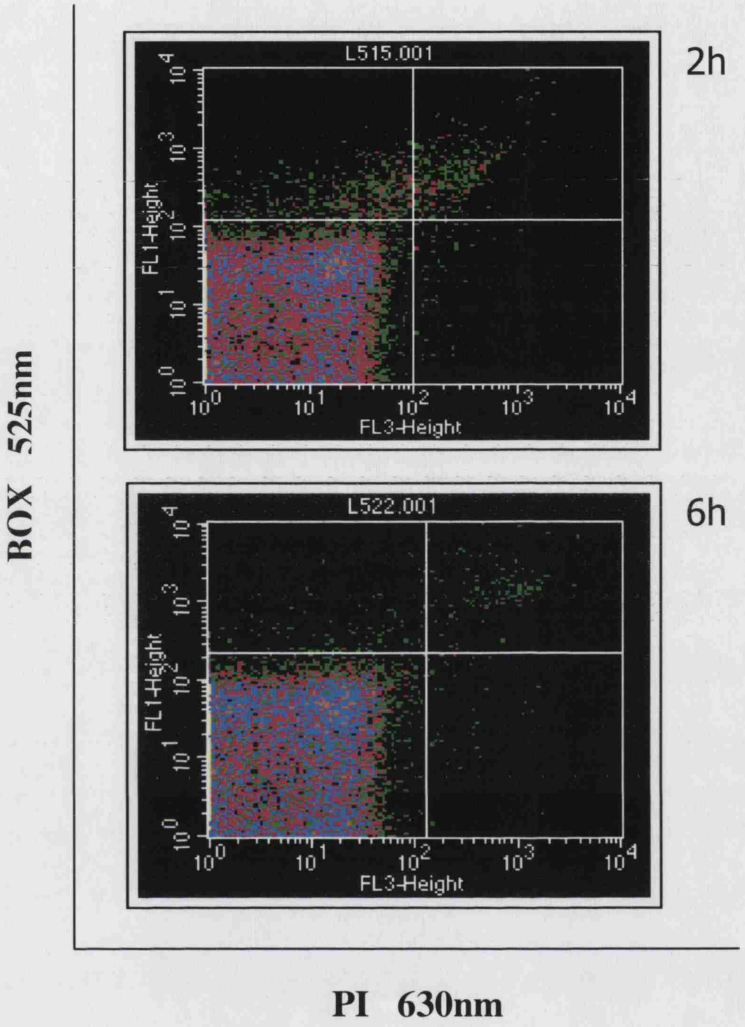

Figure 3.12. Flow cytometric profiles of *E.coli* IL-13, induced early in the exponential phase. The fermentation was run with DOT maintained at 30% above air saturation and pH maintained at 7.0 ± 0.2. 20,000 cells were analysed per sample.

3.2.3.2. *E.coli* IL-13 fermentation without DOT or pH control

In previous fermentations DOT and pH control were implemented to aviod oxygen limitation and maintain a neutral fermentation pH, both of which would minimise cell quality deterioration. Running the fermentation without DOT or pH control allowed the effects of these parameters on cell quality and recombinant protein production to be investigated.

The fermentation profile of *E.coli* IL-13 under the above conditions was very diffrerent from that seen in the control fermentation, this is illustrated in Figure 3.13. Figure 3.13A shows the pH, DOT and OD profiles. As in the control fermentations (Figure 3.11A) the DOT began to decrease following inoculation as cell proliferation began to transpire, however this decrease was reversed once the cells had been induced. After a further 2 h the DOT began to decrease again and then once more began to increase 4 h post induction. However the DOT within the fermentation does not reach zero, instead it only reaches a low of ~20% suggesting that not all cells were actively respiring. Cell biomass increase, as measured by OD measurements appeared to slow down after induction but picked up again ~5 h post induction, with a final DCW of 2.18gL^{-1} being recorded. In the absence of any control the culture pH increased during the fermentation, possibly due to amino acid breakdown.

The OUR and CER profiles, shown in Figure 3.13B, shows an abrupt decline in cell respiration following induction. After this respiration remains relatively stable but low for ~2.5 h after induction before it began to rise again implying a second, shorter exponential phase which lasted for a little over 1.5 h with a specific growth rate of 0.25 h^{-1}. This was significantly lower than the specific growth rate of 0.68 h^{-1} recorded for the initial exponential growth phase.

Flow cytometric analysis of *E.coli* IL-13 cells mirrored the pattern observed in the cellular respiration data (Figure 3.14). Samples taken 2 h post induction, shown in Figure 3.14, during what appeared to be a second lag phase, show a significantly high percentage of metabolically stressed cells, 26% of the cell population, which presented with depolarised cytoplasmic membranes and thus stained positively for BOX only. A large percentage of the cells, ~17%, were dead as can be seen in the UR

quadrant of the 2 h plot. 4 hours later (6 h post induction) the metabolically stressed population had considerably decreased to 13.2%, almost half the original value. This decrease corresponds with the entry into the stationary phase following the 'recovery' of the cells in the second exponential phase. At 6 h post induction, 82% of the population was still intact and viable.

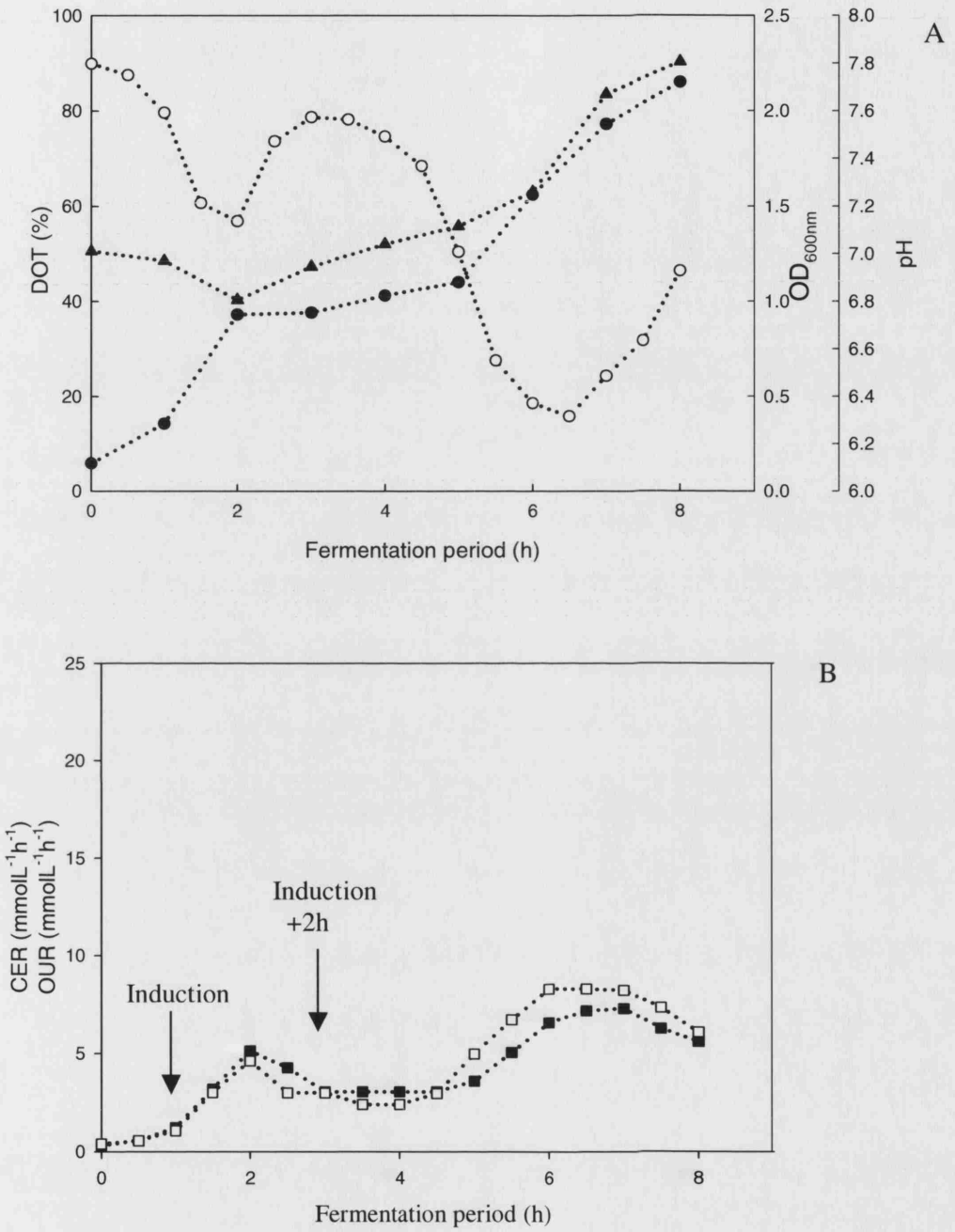

Figure 3.13. Fermentation (A) and respiratory (B) profiles *E.coli* IL-13 induced early in the exponential phase without DOT (○) or pH (▲) at 7 ± 0.2 control. (●) OD_{600nm}, (□) OUR, (■) CER.

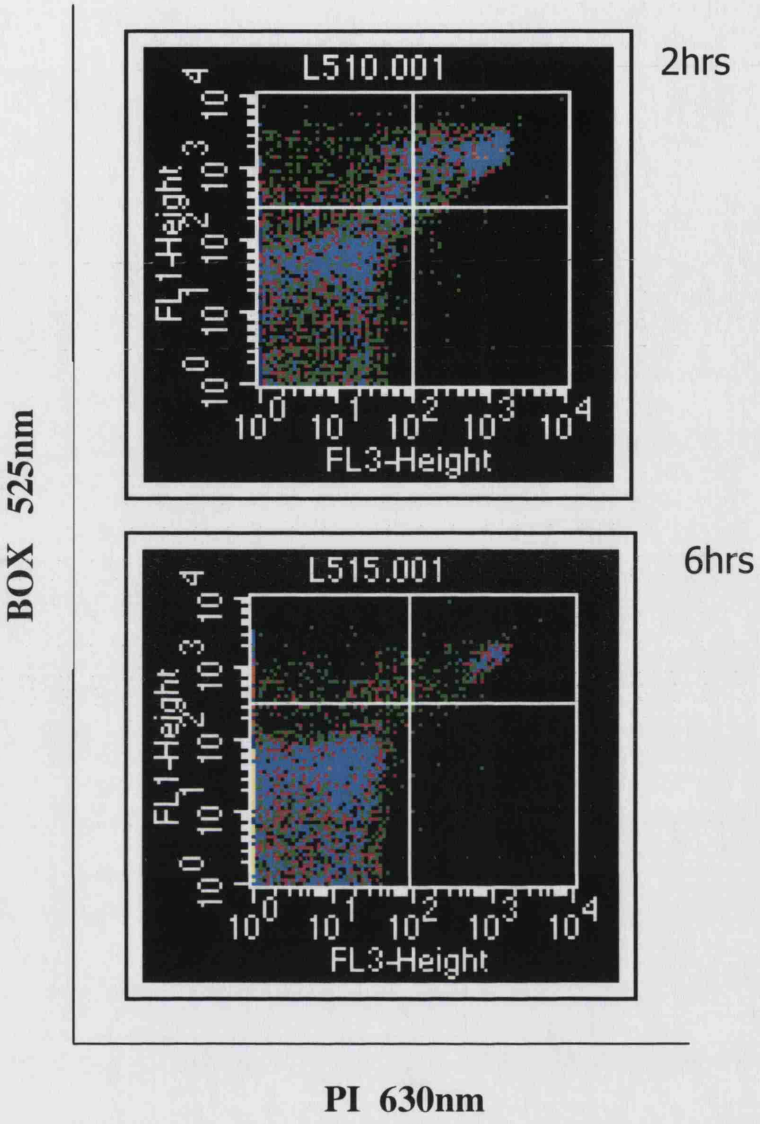

Figure 3.14. Flow cytometric profiles of *E.coli* IL-13, induced early in the exponential phase. Fermentation was run without DOT or pH control. 20,000 cells were analysed per sample.

3.2.3.3. *E.coli* IL-13 fermentation with DOT control only

DOT within the fermentation vessel was maintained above 30% air saturation to ensure enough oxygen was available to maintain normal cell activity and growth. DOT was maintained above 30% by agitation speed modification (300-700 rpm) during the fermentation.

The DOT profile, seen in Figure 3.15A, closely mimics the profile when DOT was not controlled (Figure 3.13A), with a slow increase following induction and then a steady decline. However, DOT did not fall below 30%. Cell biomass increases steadily prior to induction after which the rate of biomass increase slowed down, the final biomass recorded under these conditions was 1.74 gL^{-1}. pH during the fermentation initially decreased as biomass increased and stabilised at 7.2 for 3 h before steadily increasing, finally peaking at 7.95 by the end of the fermentation. This may be attributed to an increasing ammonia concentration as amino acids within the media are broken down.

Figure 3.15B shows cell respiration (OUR and CER) measurements during the fermentation when DOT was maintained above 30%. The initial specific growth was 0.63 h^{-1}, following induction there was a drop in both the OUR and CER rates, once again signifying a second lag phase after which the cells entered a second period of exponential growth with a lower specific growth rate of 0.28 h^{-1}. Cell respiration began to decline after 6 h, this had also been the case in the control fermentation.

Cells were removed from the fermentation at 2 and 6 hours post induction with 1mM IPTG and their metabolic and physiological status analysed using multiparameter flow cytometry, the results are depicted in Figure 3.16. Here also the analysis illustrated that metabolic stress once again accounted for a significant proportion of the compromised cells within the population at 2 h post induction with 31.1% being depolarised and just 55.9% being intact and viable. 4 hours later this depolarised population had decreased to 12.4%. At 6 h post induction 82% of the cell population was still viable.

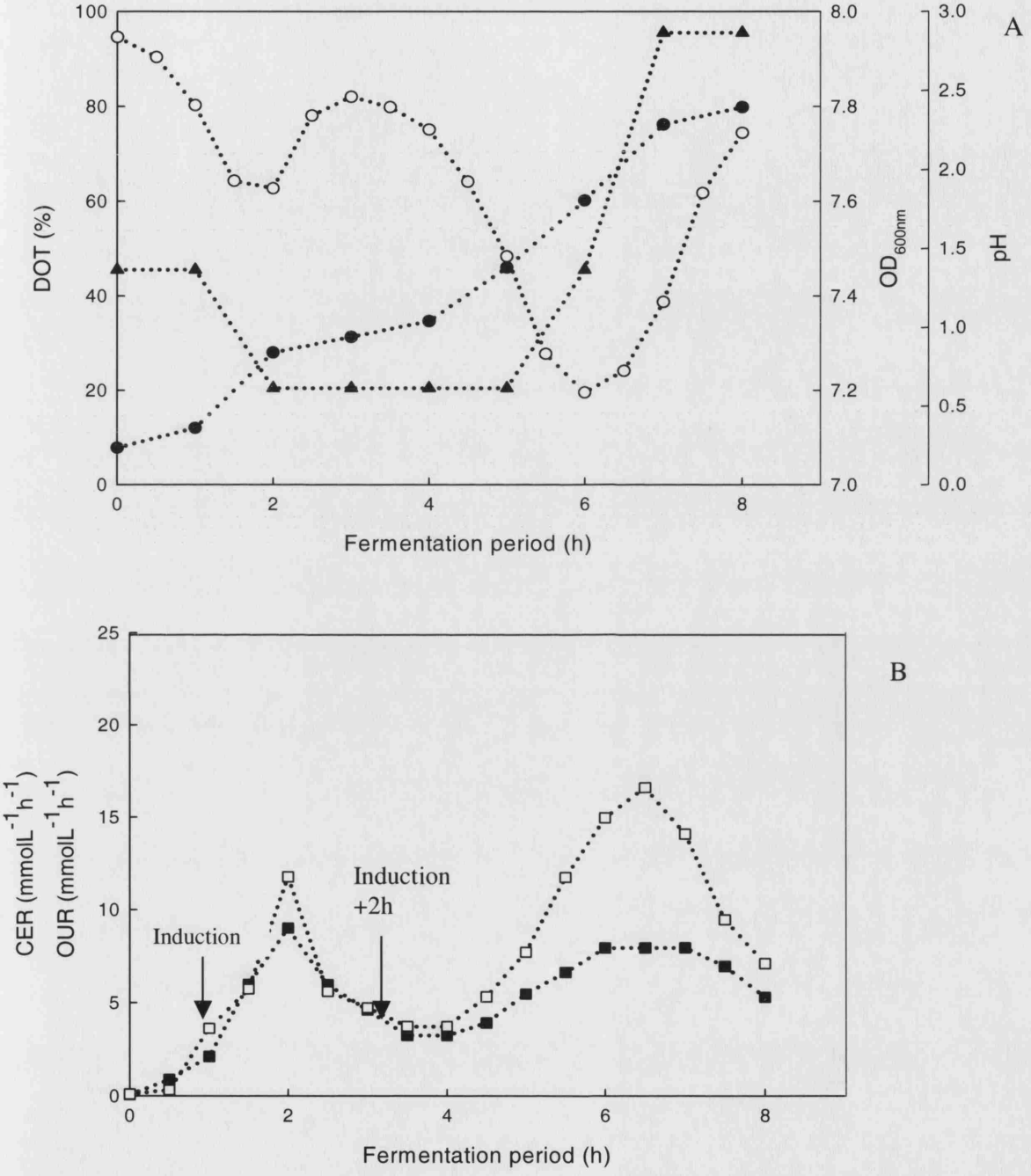

Figure 3.15. Fermentation (A) and respiratory (B) profiles *E.coli* IL-13 induced early in the exponential phase with DOT (●) control only. (▲) pH, (○) OD_{600nm}, (□) OUR, (■) CER.

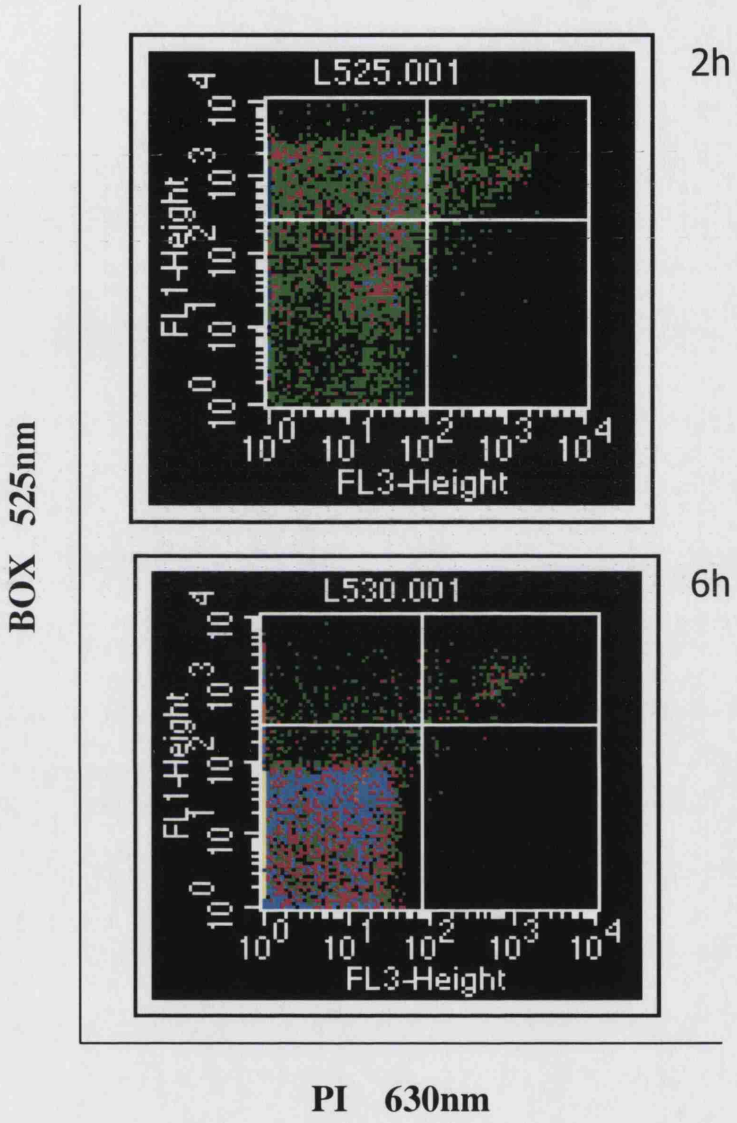

Figure 3.16. Flow cytometric profiles of *E.coli* IL-13, induced early in the exponential phase. Fermentation was run with DOT control only, DOT was maintained at 30% above air saturation. 20,000 cells were analysed per sample.

3.2.3.4. *E.coli* IL-13 fermentation with pH control only

The pH during the fermentation was controlled to eliminate any potential effects of pH on the stability and recombinant protein production capacity of *E.coli* IL-13. Culture pH was maintained at 7.0 ± 0.2 by the controlled addition of 1M NaOH.

pH remained constant throughout this fermentation, Figure 3.17A. The DOT profile here mimicked the others seen under the previous conditions investigated. However due to the lack of control of this parameter, low levels of ~10% were recorded, these were the lowest levels recorded in all experiments. Cell biomass also increased in a similar fashion to those observed in the other conditions. In Figure 3.17B, which shows the OUR and CER changes during the fermentation with active pH control, two lag and exponential phases were once again recorded and specific growth rates of 0.74 and 0.23 h^{-1} were recorded for each exponential growth phase, characterised by the increase in cellular respiratory activity following the first lag period (post innoculation) and the second post induction one. However, the cells appeared to be in better condition following second lag phase than when DOT and pH control were not implemented.

Cells were removed from the fermentation at 2 and 6 hours after induction with 1mM IPTG and their metabolic and physiological status evaluated using multiparameter flow cytometry following staining with a combination of PI, BOX, and SR, this is portrayed in Figure 3.18. At two hours after induction 48.4% the cell population were found to stain positively for BOX only, indicating metabolic stress characterised by cytoplasmic membrane depolarisation, a further 10.6% were dead and stained positively for PI and BOX; viable cells constituted the remaining 49% of thr population. By 6h post induction the population of depolarised cells had reduced to 10.6%, thus increasing the percentage of viable, intact cells to 88%.

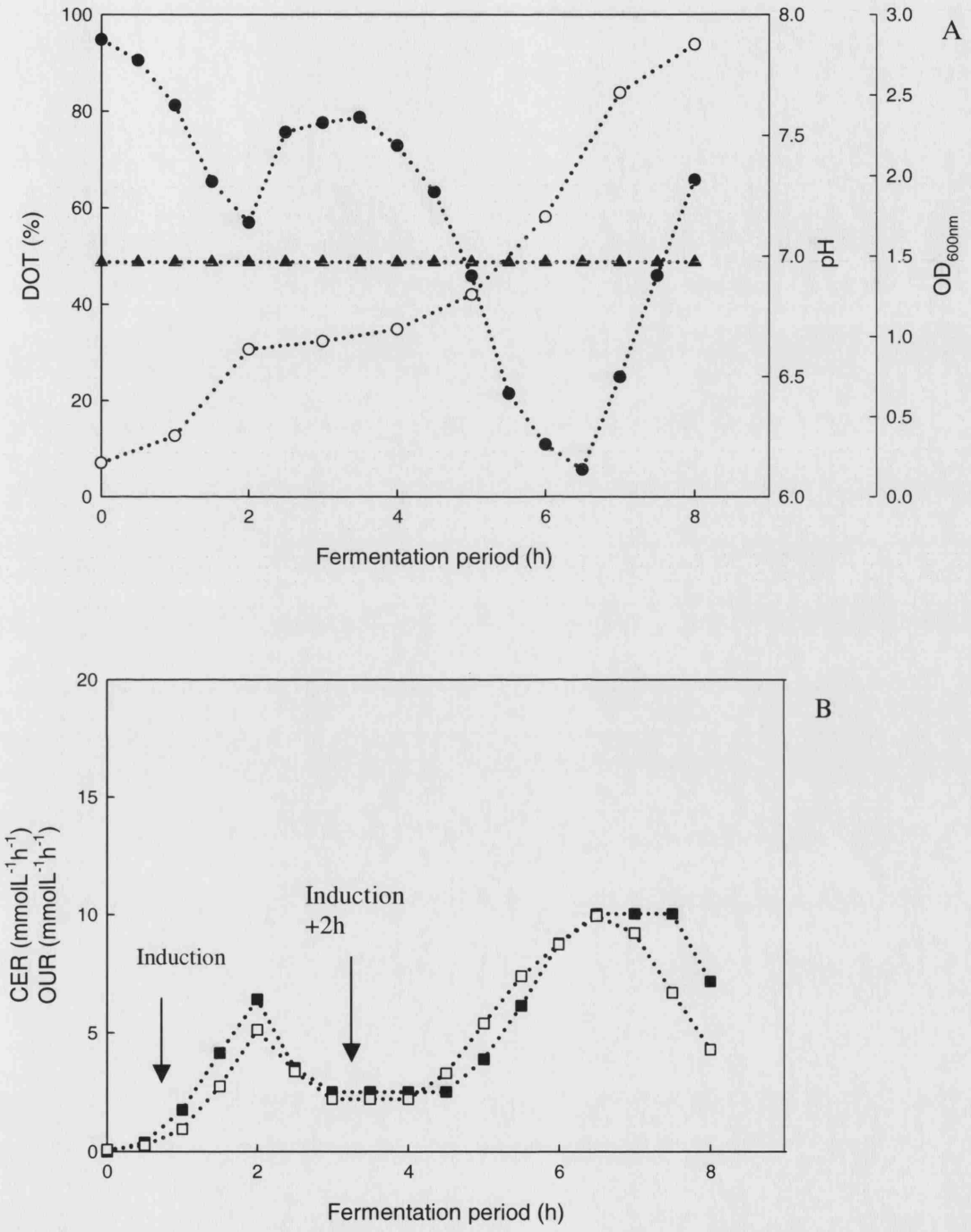

Figure 3.17. Fermentation (A) and respiratory (B) profiles *E.coli* IL-13 induced early in the exponential phase with pH (▲) control only. (○) OD_{600nm}, (●) DOT, (□) OUR, (■) CER.

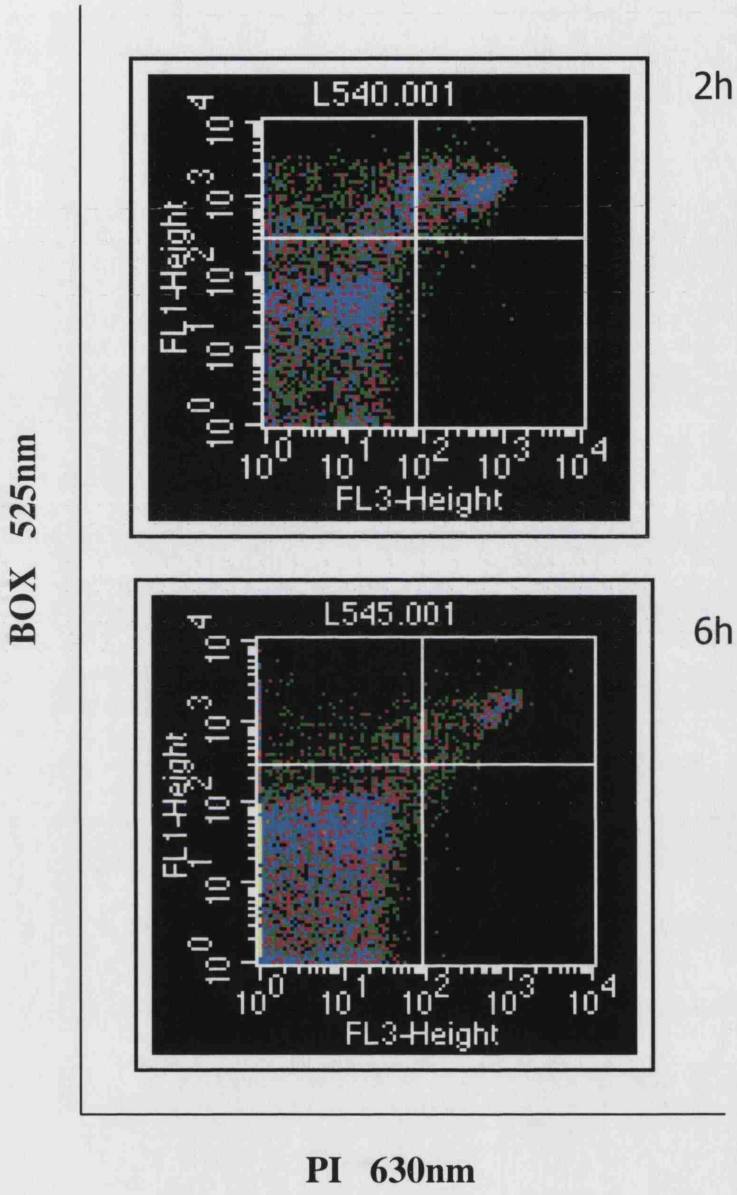

Figure 3.18. Flow cytometric profiles of *E.coli* IL-13, induced early in the exponential phase. Fermentation was run with pH control only. 20,000 cells were analysed per sample.

3.2.3.5. Recombinant protein identification

Protein extracted and purified from *E.coli* IL-13 following induction under the different DOT and pH conditions was analysed on a 4–20% Tris – Glycine – SDS gel for the presence of the recombinant IL-13 protein. IL-13 is typically between 10.3 and 15 kDa in size. Samples were taken at 6h post induction.

Recombinant IL-13 was expressed under all conditions, presenting with a band of 12.5kDa, which fell within the appropriate size range. Protein expression, as shown in Figure 3.19, was not affected when DOT and/or pH was not regulated during the fermentation.

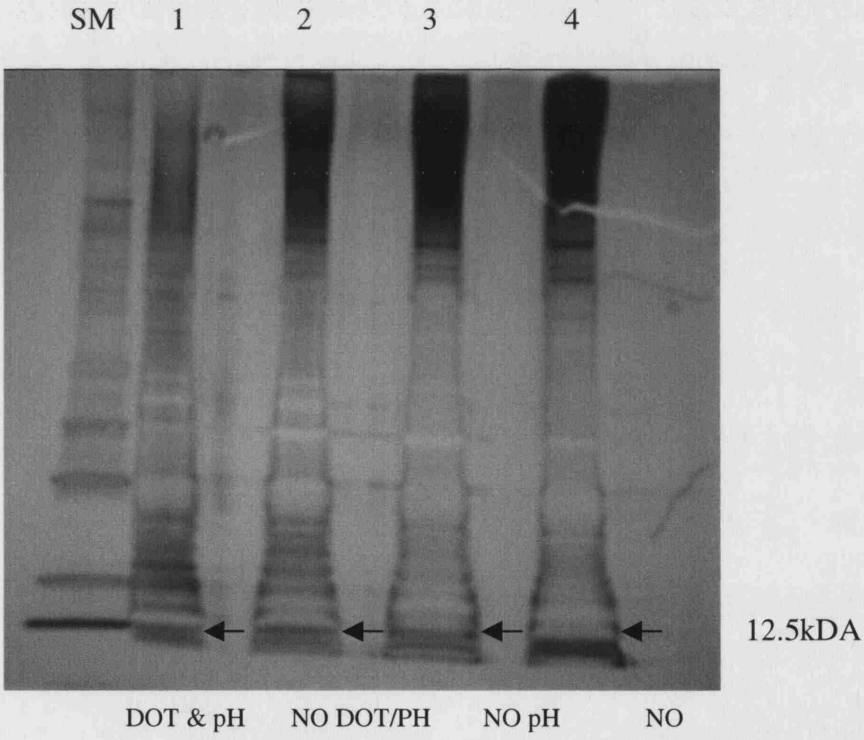

Figure 3.19. SDS PAGE gel of protein purified from cultures induced under different DOT and pH conditions. Arrows point to the IL-13 band, which is 12.5kDa in size. Protein bands are visualised with silver staining. Protein size marker (SM).

3.3. Discussion

Foreign protein synthesis in the host cell has been found to enhance the maintenance coefficient and has been reported to impose a metabolic burden on the normal functioning of the host cell, thus inducing severe metabolic stress (Bentley *et al* 1990; Bhattacharya and Dubey 1997; Soriano *et al* 2002). Hence it is important to induce the cells during phases of the growth cycle that are most physiologically and metabolically favourable for the host cell to commence and maintain expression of the foreign protein, without compromise to normal cellular function. This study investigated metabolic and environmental conditions, which may impact cell quality, with respect to viability and metabolic stress response in *E.coli* IL-13; and expression of recombinant IL-13. Specifically effects of induction with 1mM IPTG during the exponential growth phase, pH and DOT on cell quality during the exponential growth phase were investigated using traditional fermentation monitoring methods and multiparameter, flow cytometric analysis.

IPTG inducible systems are widely used in recombinant systems and are characterised by high product yields (Soriano *et al* 2002). Recombinant IL-13 protein expression by *E.coli* IL-13 was induced with 1mM IPTG at different time points during the exponential growth phase. All induced fermentations were found to produce IL-13; however cellular physiology during the fermentations varied considerably. In comparison to the non-induced fermentation, the induced fermentations exhibited 'atypical' respiratory profiles and cell quality. It has been previously documented that induced bacteria grow slowly, may eventually stop growing all together and may accumulate inclusion bodies (Fouchet *et al* 1994; Kurland and Dong 1996). This was found to be the case following IPTG induction of *E.coli* IL-13.

Cellular respiration, as indicated by carbon-dioxide evolution and oxygen uptake rates (CER and OUR), slowed down in all induced fermentations regardless of when during the exponential phase they were induced. However, following early exponential phase induction the cells exhibited a 'recovery'; this could be attributed to a number of reasons.

The OD at induction was quite low at 0.5± 0.05; at this OD the concentration of IPTG available per cell may be assumed to be higher than in the other two fermentations with higher optical densities. As a consequence, the decline in cellular respiration may be attributed to IPTG toxicity, reduction of the synthesis of cellular proteins present in exponential growth or an increased synthesis of major stress proteins. Kosinski *et al* (1992) report a reduction in synthesis of prominent host cell exponential growth proteins following IPTG induction of *E.coli* MG1655. The cells which were least susceptible to the toxic effects of the inducing agent entered a second lag phase during which they adapted to their environment and subsequently resumed exponential growth. The optical density of the fermentations subjected to these conditions increased, reaching a final OD of 3.8; however the final DCW (gL^{-1}) was low at 1.48 gL^{-1} when compared to the final DCW of the non-induced control, which was 2.13 gL^{-1}. The high OD but low DCW observed may be due to an increase in cell size following induction, which together with the apparent decline in cell proliferation appears to be characteristic of the induction of the IL-13 plasmid, Soriano *et al* 2002 reported a similar trend for *E.coli* containing an IPTG inducible lacUV5 promoter for the expression of the T7 RNA polymerase gene. They found that upon induction with IPTG *E.coli* stopped active cell division and instead increased in size, total protein and DNA content as well as recombinant protein content. The presence of a pET plasmid (*E.coli* IL-13 contains the pET11a plasmid, Novagen, Madison, WI, USA) may also contribute to the severe growth retardation following IPTG induction at this stage in the exponential growth phase (Soriano *et al* 1999). It may be that induction midway through the exponential growth phase may result in a greater susceptibility to induction associated growth retardation when this plasmid type is used.

Late exponential phase induction had the least damaging effect on host cell metabolism, the respiratory and biomass increase profiles illustrate this, as they closely mimic the control fermentation profile. However, the decline in cellular respiration was not very pronounced implying that IPTG toxicity here is not a major issue. This may be due to the higher cell density at induction or as a result of normal cell division having slowed down and cellular energies now being redirected to maintaining current cell status and not non-host protein expression. A more pronounced sensitivity was noted following induction midway during the exponential

phase. This was indicated by an abrupt decline in cellular respiration from which the cells do not 'recover'. This absence of 'recovery' could be attributed to the rapid re-direction of cellular ATP reserves to the production of recombinant IL-13. However it has been shown that induction of T7-based expression strains can lead to growth cessation (Miroux and Walker 1996).

Multiparameter flow cytometry was used to show how *E. coli* IL-13 cell quality and metabolism may be compromised by induction with IPTG. Comparisons of cells taken from the control and test fermentations indicated that early during the exponential growth phase was the most favourable point for induction and mid exponential phase induction the most detrimental with respect to maintaining high cell viability and metabolic status.

The flow cytometric data from the fermentations were averaged and are compared in Figure 3.20, which shows the percentage of dead cells prior to and post induction under all conditions and in the control. Prior to induction dead cells account for less than 5% of the total cell population, a 7-fold increase was noted following mid exponential phase induction.

Protein expression occurred following induction at all three phases during the exponential growth. Work by Bhattacharya and Dubey (1997) showed that most foreign protein was synthesised during the post induction lag; a very distinct lag was observed following induction early in the exponential growth phase. This implies that this condition may be the most favourable, in terms of protein expression levels. High level expression of recombinant proteins in *E.coli* often accumulates as insoluble aggregates *in vivo* as inclusion bodies. This is mainly attributed to the over-expression of proteins in the cell lacking the required accessories for its folding to the native form (Patra *et al* 2000). The IL-13 expressed by *E.coli* IL-13 was in inclusion body form and was not quantified in titreL^{-1}.

Dissolved oxygen tension significantly influences fermentation performance and the negative effect of its limitation on maximum cell concentration and growth of aerobic organisms is recognised to follow Monod-type kinetics (De León *et al* 2003). DOT

can also affect plasmid copy number and stability in *E.coli* fermentations (Chou *et al* 2000) and consequently product expression. During this investigation sub-optimal DOT and pH conditions were shown to have a significantly adverse effect on the physiological and metabolic status of *E.coli* IL-13, and to a lesser extent recombinant IL-13 expression.

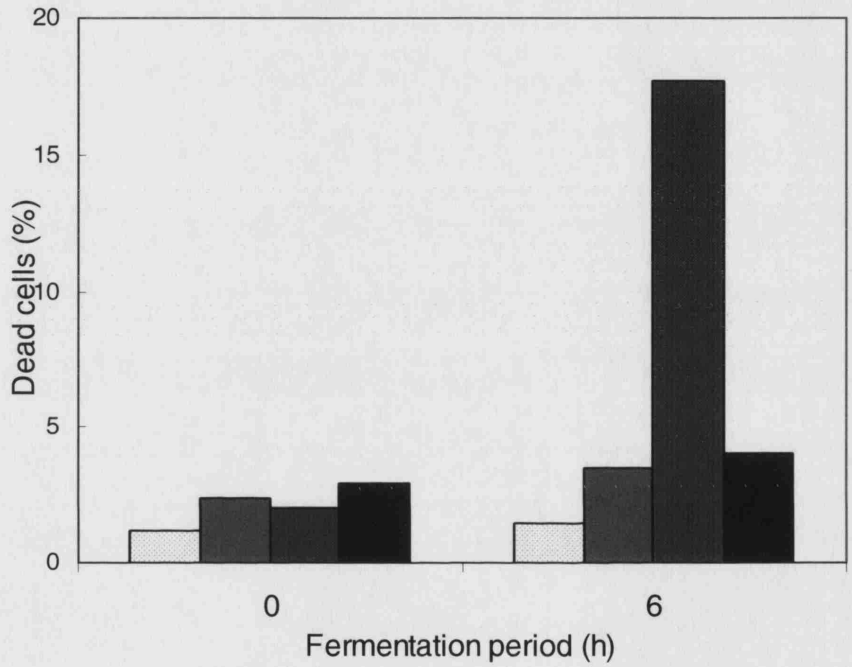

Figure 3.20. Percentage of dead cells following flow cytometric analysis of *E.coli* IL-13 induced at various points during the exponential growth phase. ▒ Non - induced, ▒ early induction, ▒ mid induction, ▒ late induction. Cells were stained with a combination of PI, BOX and SR. 20,000 cells were analysed per sample.

In all fermentation condition optimisation experiments, flow cytometric analysis showed a significant population of metabolically stressed cells two hours post induction when DOT and pH deviated from the standard operating conditions of DOT at 30% above air saturation and pH 7.0 ± 0.2. This cellular metabolic stress was indicated by a high percentage of BOX positive cells following flow cytometric analysis. These cells exhibited a loss in membrane polarisation, which coincided with when the cellular respiration rates showed a decrease. This trend could be a response

to the toxic effect of the inducing agent or a decrease in cell respiration as the cells began IL-13 expression. Bacterial respiratory enzymes are not compartmentalised within mitochondria, as they are in eukaryotic cells, existing instead on the inner surface of the cytoplasmic membrane.

Membrane potential changes rapidly in response to the availability or lack of suitable energy sources and may be dissipated when the organism is killed or injured (Shapiro 2003). The increased pH as a result of the accumulation of fermentation metabolites would encourage the cells to actively pump out hydrogen ions to balance the internal cell pH, the pace of this activity or losing this battle could trigger abnormal metabolic stress levels and possible cell death until the cells adapted to this new condition. The breakdown of amino acids within the fermentation media would also contribute to an increasing pH.

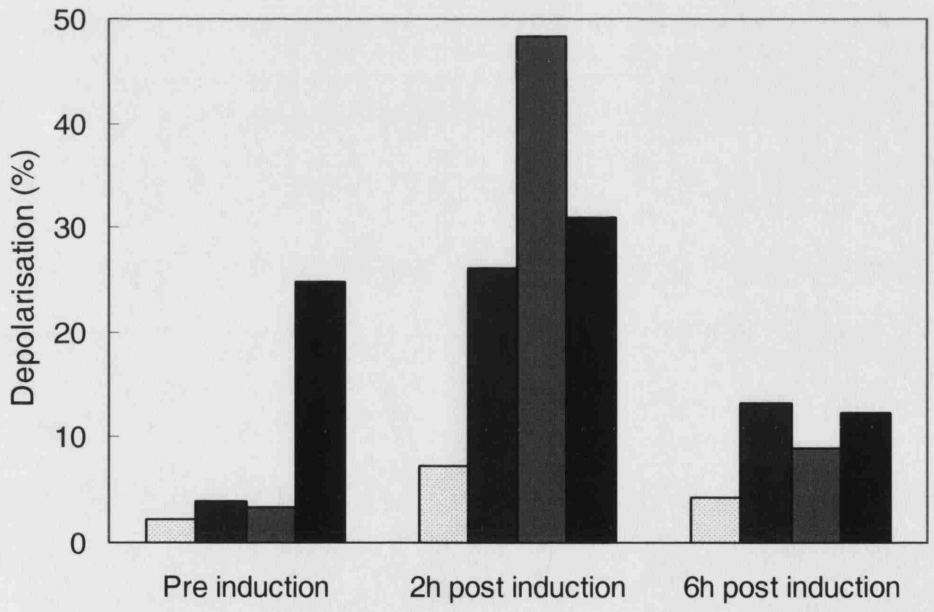

Figure 3.21. Percentage of depolarised cells following flow cytometric analysis of *E.coli* IL-13 induced early during the exponential growth phase under different DOT and pH regimes. ▒ DOT and pH control, ▓ No DOT or pH control, ▒ No DOT control ▉ No pH control. Cells were stained with a combination of PI, BOX and SR. 20,000 cells were analysed per sample

Controlling DOT and pH reduced the quantity of metabolically stressed cells during the fermentation when compared to when neither parameter was controlled. DOT is known to strongly affect fermentation performance and the production of different recombinant proteins may be affected by DOT limitation (De León *et al* 2003). This held true for IL-13 expression, as DOT decreasing to below the 30% did not prevent IL-13 expression; neither did the increasing pH observed when pH control was not implemented. A trend of cytoplasmic membrane recovery from depolarisation was seen in each instance, (Figure 3.22), indicating that membrane depolarisation is transient and that given suitable conditions normal membrane potential can be re-established. This is supported by findings by Shapiro 2000b and 2003, which establishes the transient nature bacterial cytoplasmic membrane depolarisation. Environmental conditions during the fermentation may also account for the high levels of depolarisation observed; with uncontrolled levels of dissolved oxygen contributing to high levels of depolarisation (Figure 3.22), more so than when neither DOT nor pH were controlled.

3.4. Summary

Multiparameter flow cytometry has been successfully applied to a fermentation process for the production of a recombinant protein, human interleukin 13. Early in the exponential phase was established as being the least detrimental stage of the exponential phase for the induction of *E.coli* IL-13, in terms of cell viability and metabolic status, respiratory capacity and protein production. However these can be adversely affected by sub-optimal DOT and pH conditions during fermentation. Optimum conditions for cell quality and protein expression were found to be early exponential phase induction with DOT maintained above 30% and a culture pH of 7± 0.2. The findings are such that they can be applied to other IPTG inducible systems especially those involving *E.coli* strains as the host cell.

Chapter 4

Whole Cell Biocatalyst Stability: A Flow Cytometric Approach

4.0. Introduction

Microorganisms used within the fermentation and pharmaceutical industries may have been rendered inherently unstable as a consequence of selection, genetic manipulation and mutation (Breese and Sharp 1980) and as such may require a number of maintenance strategies to improve stability. Environmental conditions play a key role in the stability of microorganisms and can significantly affect cell proliferation and quality during the fermentation and bioconversion stages. Consequently these conditions are carefully controlled to optimise cell proliferation, and in the case of microbial systems used as whole cell biocatalysts, optimise and maintain cell quality during the biocatalytic reaction.

There is an increasing industrial demand for biocatalysts as they are capable of catalysing reactions with high reaction specificity, stereo-selectivity and reaction rates (Van den Burg *et al* 1999). The capacity of a biocatalyst to retain activity over time is one of the most prominent limiting factors in most biocatalytic processes, with biocatalyst operational stability being a significant determinant of bioprocess viability (Illanes 1999). Thus, ensuring the stability of the biocatalyst involved in any process is an integral part of process development as biocatalyst stability is closely linked to system productivity. Biocatalyst (enzyme) stability may be optimised by a number of methods such as, reversing the charge on a side chain on the surface of the protein (Grimsley *et al* 1999), crystallisation of the enzyme followed by subsequent cross-linking (Govardhan 1999), covalent modification (De Santis and Jones 1999), as well as by studying the unfolding energetics of enzymes as a function of parameters such as pH, temperature and concentrations of co-solutes. However, whole cell biocatalysts do not encounter the same

problems as soluble or immobilized enzymes and as such are subject to different methods of investigating and promoting stability. Genetic engineering, for example, via the efficient transformation of mutated genes and the expression of the enzyme of interest in a suitable host usually *Escherichia coli* (Van den Burg *et al* 1999), which in turn exhibits increased expression of target proteins and increased ability to withstand process conditions is one way of improving whole cell biocatalyst stability. Protein engineering is also another route for biocatalyst improvement.

The whole cell biocatalyst *Escherichia coli* TOP10 pQR239 was used in the BVMO mediated stereo-selective oxidation of bicyclo (3.2.0.) hept-2-en-6-one to yield (-)-1(S) 5(R)-2-oxabicyclo (3.3.0) oct-6-en-3-one and (-) 1 (R) 5(S)-3-oxabicyclo (3.3.0) oct-6-en-2-one. This is a non-pathogenic recombinant *E.coli* strain containing the cyclohexanone monooxygenase (CHMO) gene from *Acinetobacter calcoaceticus* NCIMB 9871, a class 2 pathogen. The CHMO gene in *E. coli* TOP10 pQR239 is under the control of an L (+) arabinose inducible promoter and is ampicillin resistant. This strain has the advantage of lacking the lactone hydrolase present in *A. calcoaceticus*, thus eliminating product degradation by that route (Doig *et al* 2001).

This system was chosen for flow cytometric analysis because while the BVMO bioconversion has been well characterised in terms of the process, enzyme activity and some reaction parameters, no work had previously been done to examine the physiological state of the whole cell biocatalyst during the course of the bioconversion.

As a whole cell biocatalyst, *E. coli* TOP10 pQR239 would be susceptible to a range of environmental conditions. These could potentially have an adverse impact on the metabolic and physiological condition of the cells during the course of the fermentation and bioconversion processes, consequently affecting its capacity to carry out the reaction. The effects of non-growth aqueous bioconversion media, temperature storage conditions and pH on biocatalyst stability and enzyme activity were examined using multiparameter flow cytometry, which established the metabolic and physiological status of the whole cell biocatalyst under the said conditions.

4.1. Materials and methods

4.1.1. Biocatalyst

The strain used was a modified *Escherichia coli* strain containing a plasmid, pQR239 into which the cyclohexanone monooxygenase (CHMO) gene bearing the araBAD promoter, from *Acinetobacter calcoaceticus* NCIMB 9871 (Doig *et al* 2001) had been cloned. The expression of the CHMO gene is induced by L (+) arabinose. This strain, *E. coli* TOP10 pQR239 was kindly donated by Dr. John Ward (Biochemistry and Molecular Biology Department, UCL).

4.1.2. Culture media

E.coli TOP10 pQR239 was cultured in modified Luria Bertani (LB) media; composed of soya bean peptone (enzymatic digest) (Fluka Chemie, Buchs, Switzerland), glycerol and sodium chloride (NaCl) at 10 gL^{-1} (Sigma-Aldrich, Poole, Dorset, UK); 25 gL^{-1} yeast extract and 400mgL^{-1}ampicillin (Sigma-Aldrich, Poole, Dorset, UK). All media components except ampicillin were sterilized *in-situ* in the fermenter by autoclaving at 121°C for 20 min. Ampicillin was filter sterilized using a sterile 0.2 μm filter and added to the media immediately prior to inoculation. 0.5 mlL^{-1} antifoam, polypropylene glycol '2000 (Fluka Chemie, Buchs, Switzerland) was added to the fermenter prior to media sterilization.

4.1.3. Routine storage of *E.coli* TOP10 pQR239

Stock cultures of *E.coli* TOP10 pQR239, were prepared by inoculating a 1litre (L) shake flask, working volume 100 ml, with an individual colony grown overnight on a modified LB and ampicillin agar plate at 37°C. The shake flask was incubated at 37°C for ~6 h, until an optical density (OD_{670nm}) of 3-4 had been attained. The cell suspension was then

aseptically mixed with 50% v/v of sterile glycerol and 1ml aliquots were dispensed into 2 ml sterile eppendorf tubes and stored at – 80°C. These stocks were used throughout this work.

4.1.4. Whole cell biocatalyst cultivation

Whole cell biocatalyst cultivation took place in a 2L LH 210 stirred tank reactor, working volume 1.5 L (Bioprocessing Engineering Services, Charing, Kent, U.K). The reactor was operated with an agitation speed of 900 rpm at 37°C and aeration was maintained at 0.66 vvm via the introduction of air (standard mixture of 21% oxygen and 79% nitrogen) from a submerged sparger. Culture pH was monitored using a pH probe (Ingold, Messtechnick, Urdorf, Switzerland), and maintained at 7.0 by the controlled addition of 3 M hydrogen phosphate (H_3PO_4) and 3 M sodium hydroxide (NaOH).

The bioreactor was inoculated with an overnight (16 h) 150 ml (10% of the total working volume) shake flask culture cultivated from a 1ml frozen glycerol stock aliquot. CHMO production was induced by the addition of 2.5 gL^{-1} L-arabinose, approximately 3 hours after inoculation, during the exponential phase when an optical density (OD_{670nm}) of 7-8 had been attained.

4.1.5. Biomass separation

Cells were separated from the culture medium by centrifugation in a laboratory scale centrifuge (J21 M1 Beckman, Palo Alto, CA, USA) at 7000 rpm for 20 min at 4°C. The pellet was re-suspended in the aqueous bioconversion media to a cell concentration of 10 gL^{-1} before the bioconversion was initiated.

4.1.6. Whole cell biocatalyst stability at different storage temperatures

The whole cell biocatalyst was cultured as in section 4.1.4, and stored at -80, 4 and 25°C for a 168 h period (one week), in 2 ml aliquots and assayed for enzyme activity and cell quality at regular time points. The cells stored at -80°C, were suspended in 70% glycerol in a 1:1 ratio prior to storage, in order to minimize damage to the cell membrane during freezing (El- Kest and Marth 1991; Koening 2003.) Frozen cells were thawed slowly at 25°C, cells stored at 4°C were allowed to reach 25°C before flow cytometric analysis. The cells were then re-suspended in 18 ml 50 mM phosphate buffer pH 7.0, in a 500 ml baffled shake flask and put into an incubator at 37°C for 10 min, to bring the cell suspension up to the reaction temperature before the bioconversion was initiated by the addition of racemic (+/-) bicyclo [3.2.0] hept-2-en-6-one to a final concentration of 1 gL^{-1} and glycerol at a final concentration of 10 gL^{-1} (no glycerol was added to the reactions with cells stored at -80°C. The bioconversion took place at 37°C, 200 rpm for 30 min in a rotary shaker.

4.1.7. Whole cell biocatalyst stability in aqueous (non- growth) bioconversion media

The bioconversion media investigated were: Phosphate buffer (10mM, 50mM, 100mM) (Sigma-Aldrich, Poole, Dorset, U.K), sodium chloride (NaCl) (10mM, 50mM, 100mM) (Sigma-Aldrich, Poole, Dorset, U.K), reverse osmosis (RO) water, fresh fermentation media and spent fermentation media. All bioconversion reactions were carried out in aqueous bioconversion medium adjusted to pH 7.0 to minimise any possible effects of pH on the enzyme and whole cell biocatalyst during the bioconversion. The bioconversion was initiated by the addition of racemic (+/-) bicyclo [3.2.0] hept-2-en-6-one at a final concentration of 0.5 gL^{-1} and glycerol at 10 gL^{-1} to 20 ml of re-suspended cells in a 500 ml baffled shake flask. Cells were used at a final concentration of 10 gL^{-1}. The shake flasks were agitated at 200 rpm at 37°C in a rotary shaker for the 4 h duration of the bioconversion.

4.1.8. Whole cell biocatalyst stability at different bioconversion pHs

Whole cell stability and enzyme activity at different bioconversion pHs: 6.5, 7.0, 7.5 and 8.0 were investigated The whole cell biocatalyst was cultured as in section 4.1.4. Cells were harvested (section 4.1.5), rinsed in pH 7.0 RO water and re-suspended in 50 mM phosphate buffer of the appropriate pH before being returned to a 2L bioreactor, 1L working volume, where the bioconversion took place. Before initiation of the bioconversion the cell suspensions were allowed to reach the bioconversion temperature of 37°C and stabilized to the required pH. The bioconversion was initiated by the addition of 1.0 gL^{-1} racemic (+/-) bicyclo [3.2.0] hept-2-en-3-one and glycerol at a final concentration of 10 gL^{-1}. Cells were used at a final concentration of 10 gL^{-1}. The reactions took place at 800 rpm, 37°C over a 4 h period. Bioconversion pH was maintained by the controlled addition of 3M H_3PO_4 and 3M NaOH to the reaction vessel. Initial product formation rates were measured via 20 ml shake flask reactions over a 30 min period with 1 gL^{-1} substrate, 10 gL^{-1} glycerol at 200 rpm and 37 ° C.

4.1.9. Analytical

4.1.9.1. Biomass measurement

Biomass increase during cultivation of *E.coli* TOP10 pQR239 was measured via optical density (OD) and dry cell weight (DCW) measurements. DCW concentrations (gL^{-1}) were determined from a calibration curve of known DCW and OD, measured at 670nm with a variable wavelength spectrophotometer (Unicam, Cambridge U.K). The DCW calibration curve was determined from the weight difference of cell pellets from 1 ml of fermentation broth taken at regular time intervals during the fermentation, which had been washed with 5 ml RO water and dried at 100°C for 24 h (Appendix IV).

4.1.9.2. Flow cytometry

Flow cytometric analysis was conducted using an EPICS XL-MCL (autoloader) 4 Colour Bench Top Flow Cytometer with Flow Centre II Acquisition Workstation, with 488 nm excitation from an argon-ion laser at 15 mW (Beckman Coulter, High Wycombe, Bucks, U.K.). FL1 and FL3 detectors, which measured bis-(1,3-dibutylbarbituric acid) trimethine oxonol (BOX) and propidium iodide (PI) fluorescence respectively, were set at 585 and 807 volts respectively, with a corresponding compensation of 24 and 16% to minimize spectral overlap during analysis.

Stock solutions of each dye were prepared as follows: PI was made up at 200 $\mu g ml^{-1}$ in 1x Dulbecco's Phosphate buffered saline, pH 7.2 (DBS) (Sigma-Aldrich, Poole, Dorset, UK). BOX was made up at 10mg ml^{-1} in dimethyl sulphoxide (DMSO). The DMSO stock was maintained at -20°C. The DBS stocks were maintained at -4°C.

All solutions were filtered prior to use using a 0.2 µm filter to remove any particulate matter that could interfere with analysis. Culture samples were diluted in 1x DBS to a final concentration of 1 x 10^{-5} cells ml^{-1} and stained with PI and BOX at a final concentration of 5 and 10 $\mu g ml^{-1}$ respectively. Ethylenediaminetetraacetic acid (EDTA) was added to the working solution at a final concentration of 4 mM to facilitate BOX staining. PI and BOX fluorescence were measured at 630 and 525 nm respectively following a 10 min incubation period at room temperature (25°C). A total of 50,000 events were analysed per sample. The data obtained is represented in density plots.

4.1.9.3. Gas Chromatography

Bicyclo (3.2.0.) hept-2-en-6-one (substrate) depletion and the accumulation of the products (-)-1(S) 5(R)-2-oxabicyclo (3.3.0) oct-6-en-3-one and (-)1(R) 5(S)-3-oxabicyclo (3.3.0) oct-6-en-2-one was measured using an XL-2 gas chromatograph (GC) with flame ionisation detector (FID) (Perkin-Elmer, Norwalk, CT, USA) with an AT-1 column 30m x 0.2mm x 0.25µm (Alltech, Deerfield, IL, USA) with helium as the mobile phase.

A 2 ml sample was removed from the bioconversion vessel and centrifuged in a bench top centrifuge (Biofuge, Hanau, Germany) at 1300 rpm for 2 min to separate the cell biomass from the supernatant. 1 ml of the supernatant was added to an equal volume of ethyl acetate containing naphthalene ($1mgml^{-1}$) as an internal standard and centrifuged for a further 2 min. The supernatant was analysed.

The GC was operated with an injector and column temperature of 250°C and an oven temperature of 110°C. Retention times for bicyclo (3.2.0.) hept-2-en-6-one, (-)-1(S) 5(R)-2-oxabicyclo (3.3.0) oct-6-en-3-one, (-)1(R) 5(S)-3-oxabicyclo (3.3.0) oct-6-en-2-one and the internal standard were at 1.8, 3.5, 3.55 and 3.9, respectively.

4.2. Results

4.2.1. Introduction

When establishing the operating parameters for a given whole cell biocatalytic process, the physiological condition of the whole cell biocatalyst is one of the most significant parameters which needs to be determined and optimized. This section reports on the stability of the whole cell biocatalyst *E.coli* TOP10 pQR239 during the BVMO mediated stereo-selective oxidation of bicyclo (3.2.0.) hept-2-en-6-one to yield (-)-1(S) 5(R)-2-oxabicyclo (3.3.0) oct-6-en-3-one and (-) 1 (R) 5(S)-3-oxabicyclo (3.3.0) oct-6-en-2-one, in a number of aqueous bioconversion media, at different pHs and following storage at different temperatures over a period of time. Analyses were carried out using flow cytometry, to quantitatively establish the metabolic and physiological status of the cells and with gas chromatography to monitor enzyme activity.

The fermentation and bioconversion are two separate stages. This section addresses the bioconversion stage. Doig *et al* (2001; 2002 and 2003) have previously established the

fermentation conditions for the whole cell biocatalyst. Figure 4.1 illustrates these two stages and the experimental scheme.

As previously stated, the flow cytometric analysis used employs two fluorescent stains, PI and BOX; both of which work together to establish the quality of the whole cell biocatalyst. Membrane integrity is measured with respect to exclusion or retention of fluorescent dyes; PI is a vital fluorescent probe that binds to DNA but is unable to cross the intact cytoplasmic membrane. Intact cells show selective membrane permeability. Cells that have lost membrane integrity therefore take up PI and are classified as dead cells (Amanullah *et al* 2002a, b). The second stain, BOX, binds to the cell membrane following its depolarization, where it distributes according to the membrane potential gradient, provided the free stain gradient is below the saturation point for the available binding points (Nebe-von-Caron and Badley 1995). Together these stains give a clear indication of the metabolic and physiological condition of the whole cell biocatalyst.

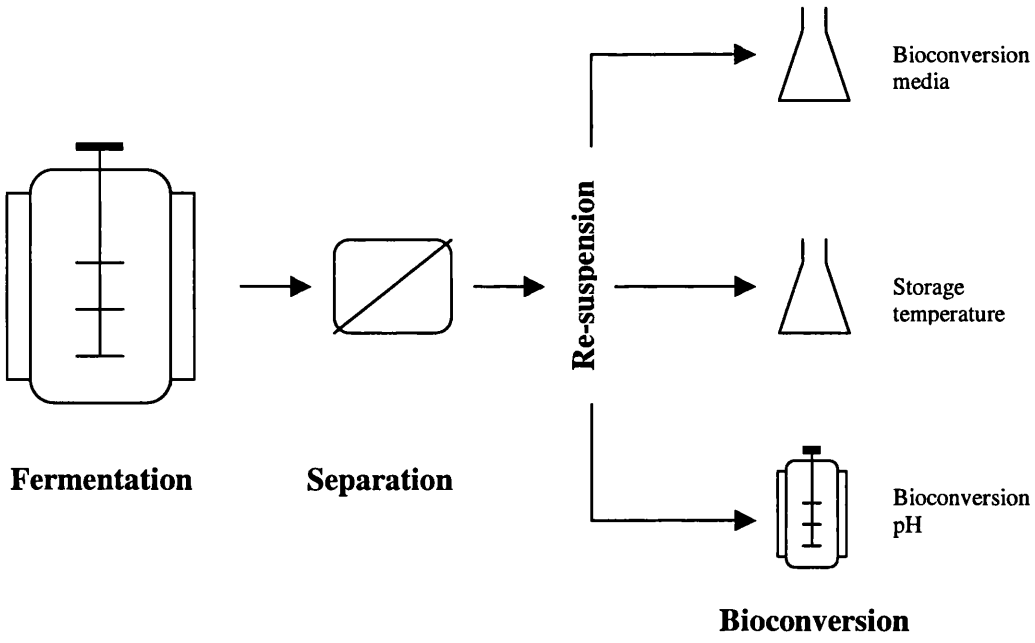

Figure 4.1. Fermentation and bioconversion process

4.2.2. Biomass separation and the whole cell biocatalyst

The whole cell biocatalyst was separated from the fermentation broth at the end of the fermentation stage by centrifugation and the cell mass re-suspended in the bioconversion media. Separation was achieved in a laboratory scale centrifuge. It was found that at the speed used, 7000 rpm, there was no significant damage to the whole cell biocatalyst. Prior to centrifugation a total cell viability of 90.2% was recorded, this decreased by just 2.5% following centrifugation. This is depicted in the density plots in Figure 4.2. This illustrates the robustness of *E.coli* strains and the fact that the centrifugation conditions were not excessively harsh. Damage during re-suspension was also minimal as a low impact re-suspension method was used. Thus it can be safely assumed that this step is only responsible for a negligible amount of cell damage.

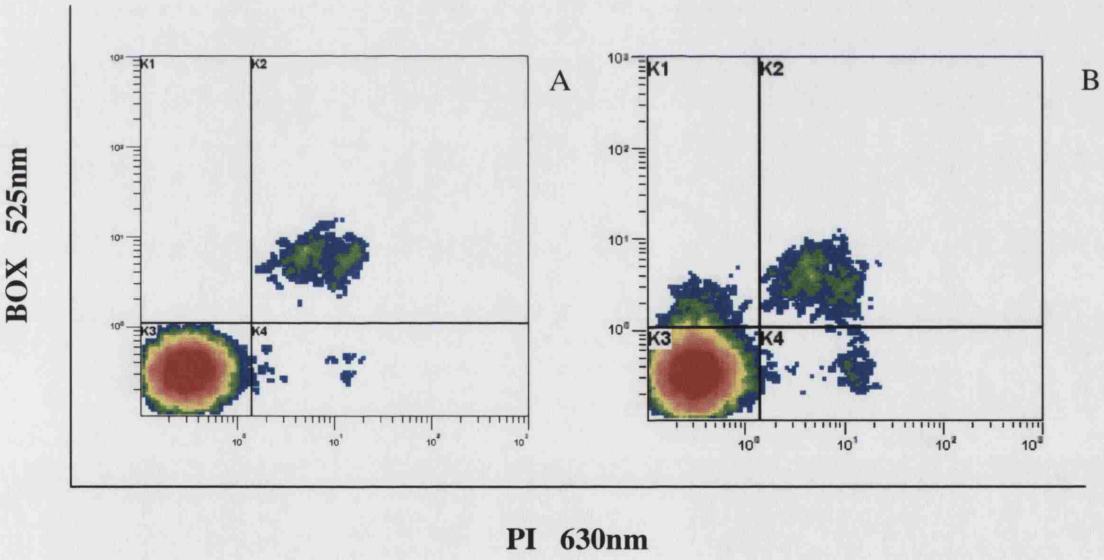

Figure 4.2. *E.coli* TOP10 pQR239 at harvest (A) culture age 6 h and post separation by centrifugation (B). Cells were stained with a combination of PI and BOX. 50,000 events were analysed.

4.2.3. Whole cell biocatalyst stability at different storage temperatures

It may be necessary under certain circumstances, such as when there is an unforeseen break in the process chain, to store the whole cell biocatalyst prior to the bioconversion step, after completion of the fermentation stage. In these instances it is important that the whole cell biocatalyst remain stable and predominantly intact. It is also important that levels of enzyme activity be maintained during any storage. The ultimate aim of these storage processes is to put the cell into a state of stasis at a temperature below their optimum growth and reaction temperature, from which they can be reactivated with little or no detrimental effects. Bacterial cultures are routinely stored at 4°C for short periods of time and at –70 to –80°C for extended periods of time. Storage at 25°C, room temperature is less common, as there is nothing to prevent cell degradation at this temperature, further cell proliferation, albeit slowly, may occur.

4.2.3.1. Flow cytometric analysis

Multiparameter flow cytometry was used to visualize the differences in the biocatalyst's stability with respect to the percentage of viable, depolarized and dead cells present in the population following storage at different temperatures (-80, 4, and 25°C) over a 168 h period, when compared to a sample of cells analyzed by flow cytometry immediately after the fermentation step as seen in Figure 4.2A. The metabolic and physiological status of *E.coli* TOP10 pQR239 varied significantly between the different temperatures with time. These variations can be seen in Figures 4.3 to 4.5, which show the alterations to cellular status following storage at -80, 4, and 25°C at 16, 72 and 168 h post storage.

Cell stability was high at -80°C, with 58% of the population being intact and viable following 168 h storage. An initial drop to 70% viability was observed after the first 16 h of storage, after this the percentage of intact cells remained relatively stable for the duration of storage, Figures 4.6 and 4.8. A significant population of BOX positive cells, which were depolarized, accounted for ~8% of the compromised cells.

Storage at 4°C caused the least damage to the whole cell biocatalyst with a high percentage (80%) of viable, intact cells still being present after 168 h. An initial drop in cell viability was recorded following overnight storage, as may be observed in Figure 4.4 plots B and C, as well as in Figure 4.7. As with the cells stored at –80°C the population of dead cells also remained fairly constant, although a lower percentage was observed.

Storage at 25°C was established to be the most damaging to the whole cell biocatalyst. This was indicated by the decline in cell viability observed during the storage period at this temperature, Figures 4.5 and 4.8. Just 46.5% of cells were intact after 168 h. The increase in cell deterioration was continuous and prolific at this temperature. As well as a significant population of depolarized cells in the UL quadrant, which increased and then decreased during storage the storage period (cytoplasmic membrane depolarization is transient, Shapiro 2001), two populations of dead cells were observed in the UR quadrant (Figure 4.5 B and C).

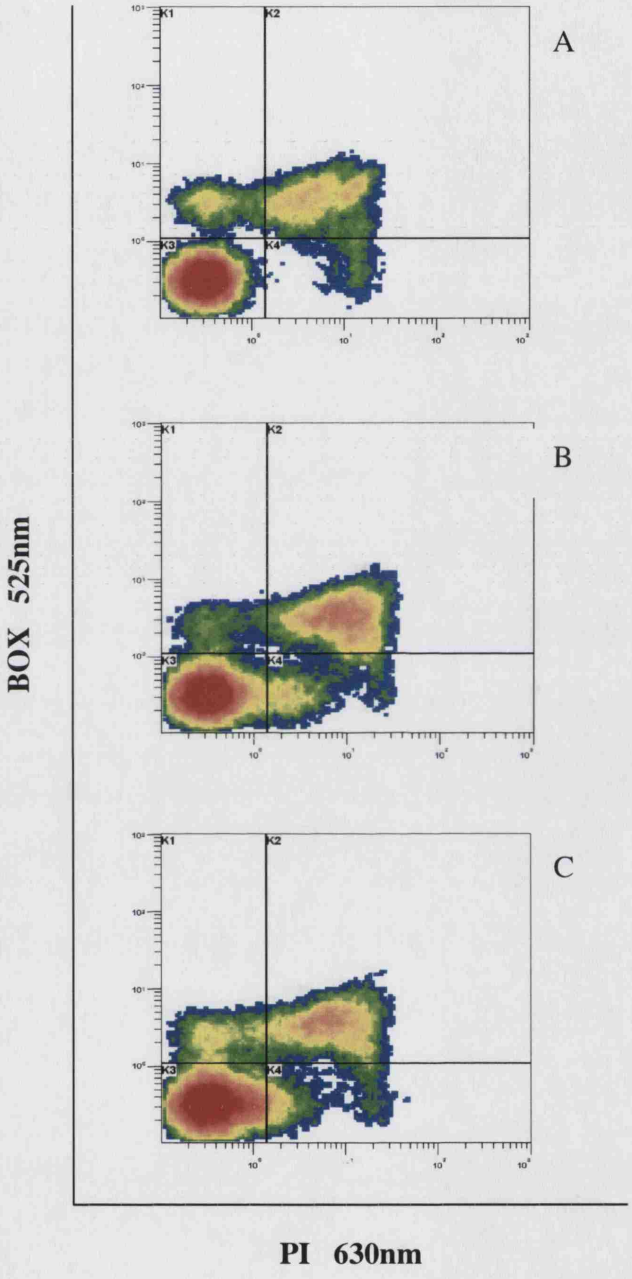

Figure 4.3. Flow cytometry profile of the effects of storage at –80ºC on *E.coli* TOP10 pQR239 over a 168 h period. 16 h (A), 72 h (B) and 168 h (C) after storage. 50,000 events were analyzed.

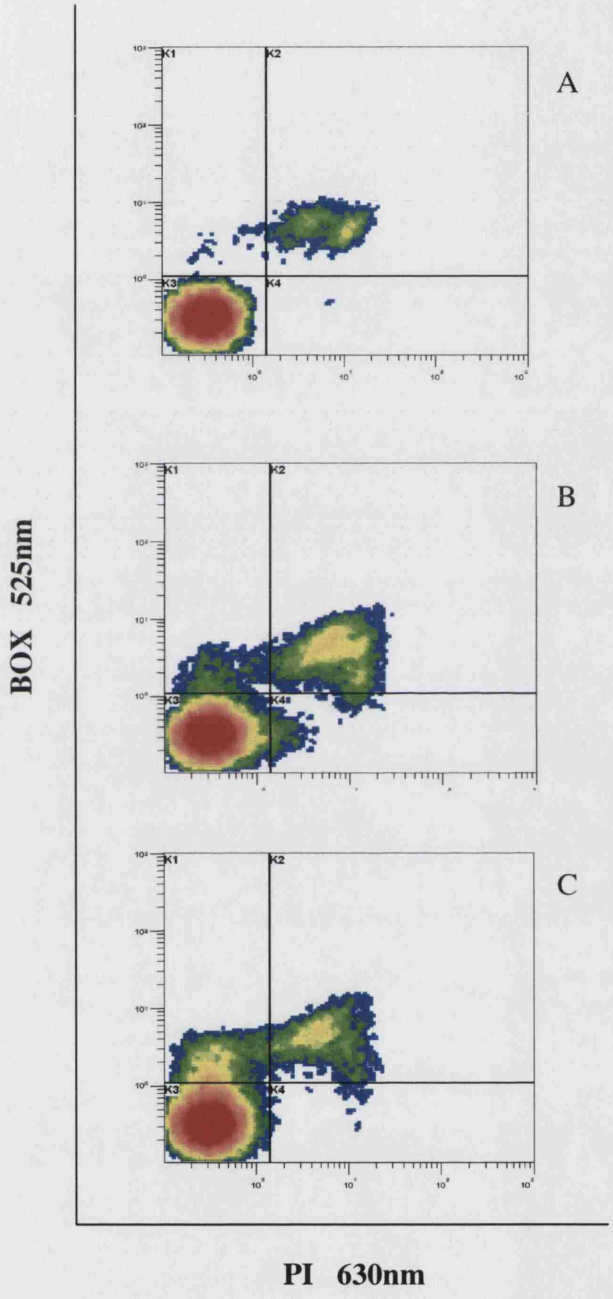

Figure 4.4. Flow cytometry profile of the effect of storage at 4ºC on *E.coli* TOP10 pQR239 over a 168 h period. 16 h (A), 72 h (B) and 168 h (C) after storage. 50,000 events were analyzed.

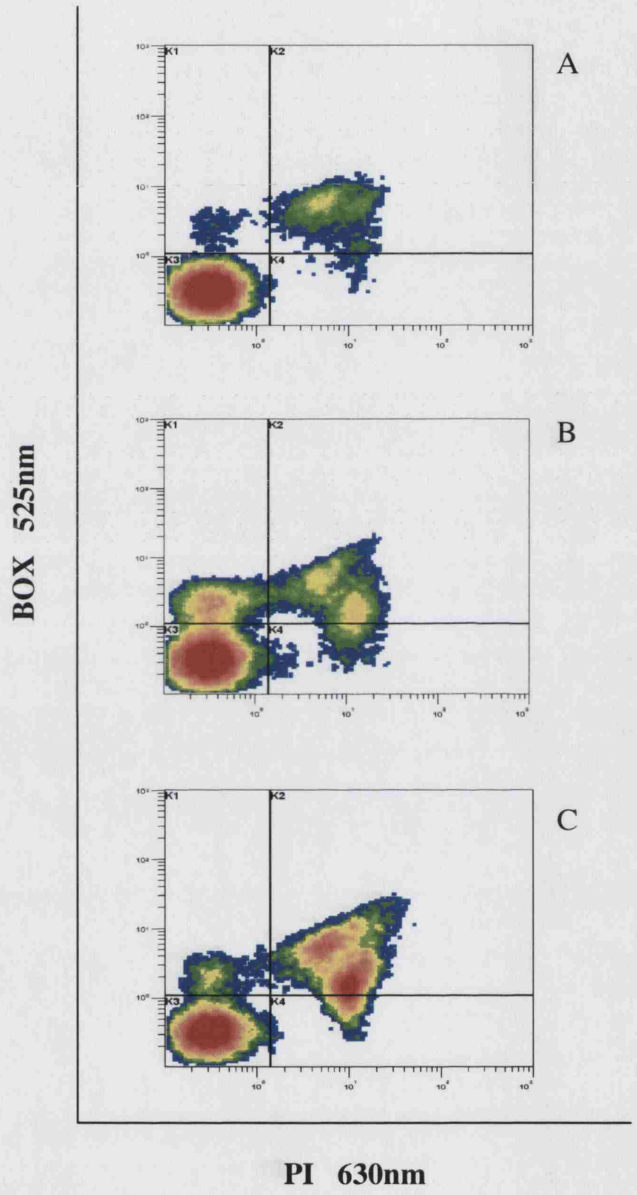

Figure 4.5. Flow cytometry profile of the effects of storage at 25°C on *E.coli* TOP10 pQR239 over a 168 h period. 16 h (A), 72 h (B) and 168 h (C) after storage. 50,000 events were analysed.

4.2.3.2. Residual enzyme activity following storage at different temperatures

The bioconversion was initiated by the addition of 1 gL^{-1} substrate, and glycerol at a final concentration of 10 gL^{-1}. It was observed that all the cells, regardless of storage temperatures retained biocatalytic activity indicating that the enzyme was still functional following storage. However there were significant differences in initial product formation rates (Figures 4.6 to 4.8). In the control bioconversion, where the whole cell biocatalyst was used immediately after the fermentation step, a product formation rate of 7.4 gL^{-1} h^{-1} was observed.

All storage conditions exhibited a decrease in enzyme activity indicated by a decreased product formation rate when compared to the product formation rate prior to storage. Following storage of the whole cell biocatalyst at all temperatures, there was a sharp drop in enzyme activity in the first 16 h of storage. At –80°C (Figure 4.6) enzyme activity remained stable over the entire duration of the storage period, between 2.6 and 3.0 gL^{-1} h^{-1}. This trend was also observed following storage at –4°C, (Figure 4.7) where following the initial drop in product formation rate, the enzyme activity rates remained between 3.0 and 3.8 gL^{-1} h^{-1}. The enzyme activity profile following storage at 25°C was very different; a steady decline in the rate of product formation over the 168 hour period was observed (Figure 4.8), starting at 3.2 gL^{-1} h^{-1} following overnight storage until enzyme activity was lost completely after 144 h. This loss of enzyme activity may be attributed to a number of reasons, firstly any free enzyme which may have been present as a result of cell lysis may have been denatured at this temperature and secondly some of the intact cells in the population may be new cells which have grown during storage. These cells may lack the plasmid as no ampicillin is present to select for plasmid containing cells. Also, if the plasmid is replicated induction of CHMO expression did not take place. Thus the likelihood of there being any active enzyme present was low.

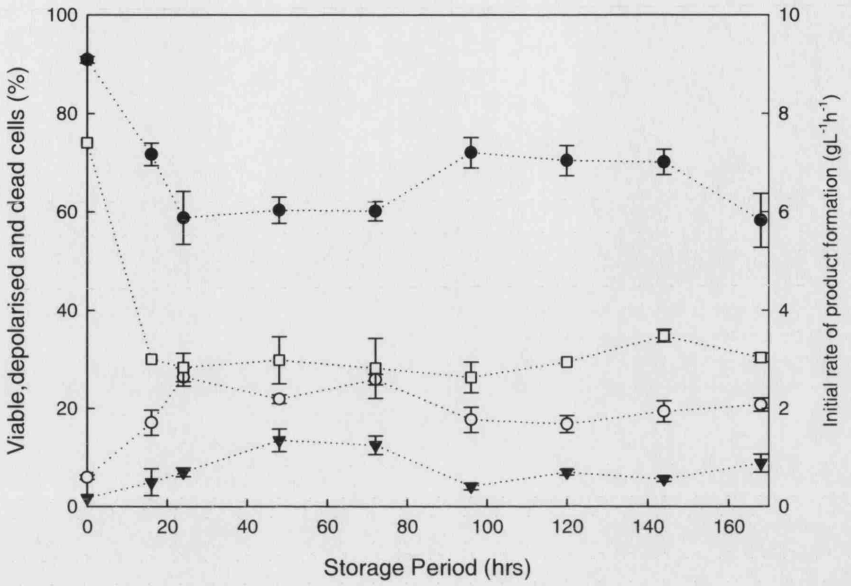

Figure 4.6. Cell quality of *E.coli* TOP10 pQR239 following storage at –80ºC. (●) viable cells, (▼) depolarized cells, (○) dead cells and initial product formation rates (□).

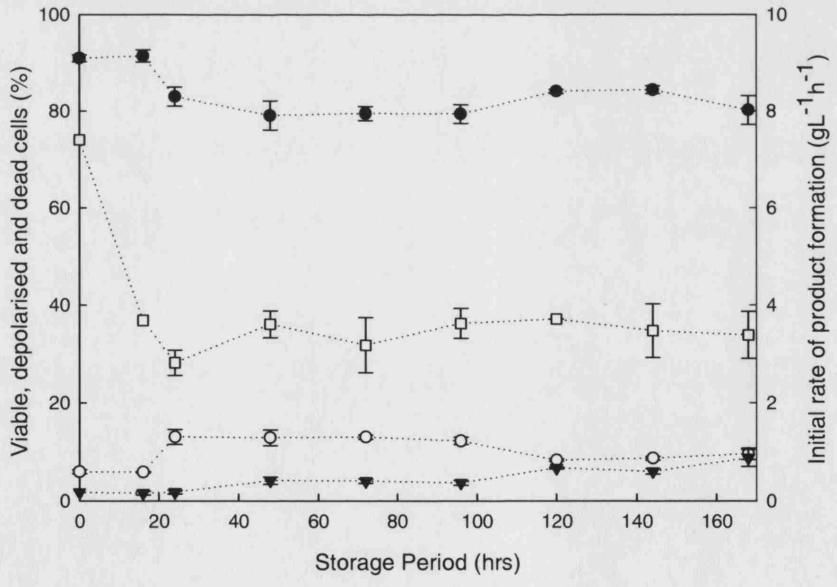

Figure 4.7. Cell quality of *E.coli* TOP10 pQR239 following storage at 4ºC. (●) viable cells, (▼) depolarized cells, (○) dead cells and initial product formation rates (□).

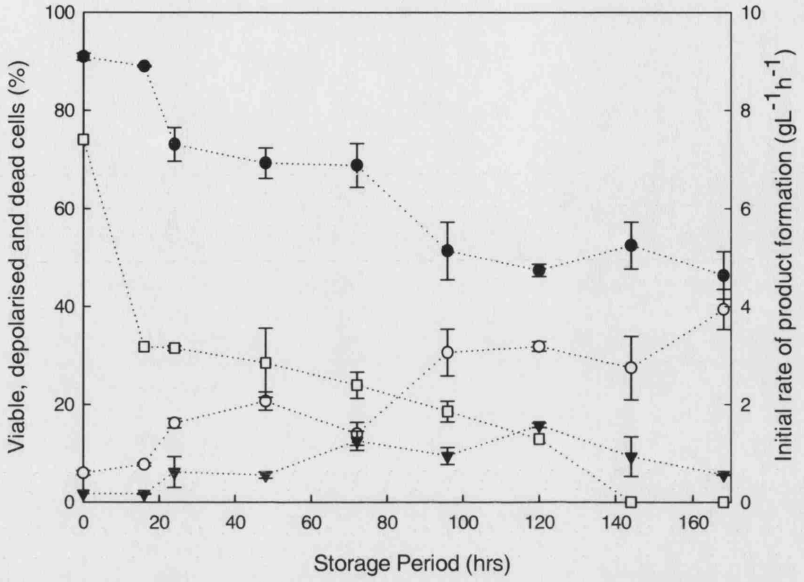

Figure 4.8. Cell quality of *E.coli* TOP10 pQR239 following storage at 25°C. (●) viable cells, (▼) depolarized cells, (○) dead cells and initial product formation rates (□).

4.2.4. Whole cell biocatalyst stability in aqueous (non-growth) bioconversion media.

The use of chemically defined media is becoming more feasible for bacterial cultures (Wang and Lee 1998; Petry *et al* 2000; Niccolai *et al* 2003). This has the advantage of reducing the number of ill-defined contaminants, which may be present as a result of culture in biologically defined media. The use of chemically defined media as the fermentation or bioconversion media can significantly decrease the cost and number of steps of the down stream processing stage whilst ensuring high whole cell biocatalyst quality for the duration of the reaction.

The BVMO reaction was carried out after a fermentation stage where the cell biomass required for the bioconversion was generated. It was during this bioconversion step that

the quality of the whole cell biocatalyst was of greatest importance. High biocatalyst stability would allow the reaction to be carried out for an extended period of time, facilitating good levels of product formation and accumulation. Using a range of commonly used microbiological solutions and buffers, such as phosphate buffer (Walton and Stewart 2004) allowed the impact of non-growth media on the metabolic and physiological condition of *E.coli* TOP10 pQR239 during the BVMO reaction to be investigated.

4.2.4.1. Flow cytometric analysis

Multiparameter flow cytometry was used to visualise the differences in the biocatalyst's response to performing the bioconversion in different aqueous media. Figures 4.10 to 4.15 depict these responses in comparison to cellular status at harvest, Figure 4.2, and a control reaction in fermentation broth, from which glycerol and substrate were excluded, Figure 4.9. Prior to bioconversion initiation, while the cells were still in spent fermentation broth at the end of the fermentation stage, ~6% of the cell population were dead; this can be seen in the upper right quadrant (UR) of the density plot in Figure 4.2. This indicated that there were a high percentage of viable cells at the end of the fermentation. It was expected that exposure to different bioconversion media would alter the percentage of viable, depolarised and dead cells within the population.

The control reaction also showed a high percentage of viable cells, 93.3% following the 4 h bioconversion period, Figure 4.9. A small population of the cells also stained positively for BOX, indicating intact but depolarised cytoplasmic membranes.

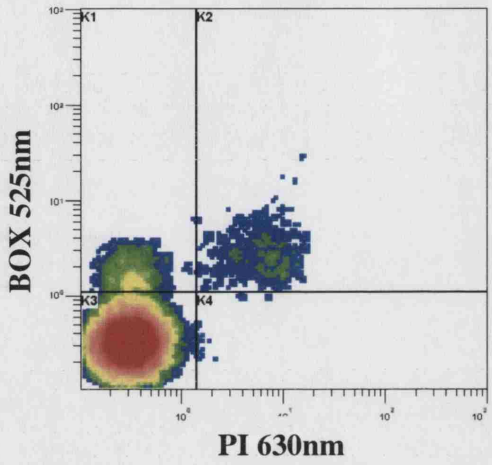

Figure 4.9. *E.coli* TOP10 pQR239 bioconversion control. Cells were incubated at 37°C and 200 rpm with substrate and glycerol precluded for 4 h. Cells were stained with a combination of PI and BOX. 50,000 events were analysed.

In Figure 4.10 the state of the biocatalyst performing the bioconversion in phosphate buffers of different ionic strength, 10, 50 and 100mM, all at pH 7.0, are depicted. The cells were predominantly intact at the end of the 4 h bioconversion, with less than 10% loss of cell viability. 10mM and 100mM phosphate buffers caused the highest and least cellular damage respectively after 4 hours.

Figure 4.11 shows the state of the biocatalyst carrying out the reaction in NaCl solutions of different ionic strength; 10, 50 and 100mM. Here again the biocatalyst was predominantly intact, 85%, 4 hours after the bioconversion was initiated. 50mM NaCl was least detrimental to biocatalyst integrity. Cellular damage in RO water, spent and fresh fermentation media were low with the percentage of intact cells being 88.2%, 91% and 94.6% respectively, after 4 h (Figure 4.12).

E.coli TOP10 pQR239 viability remained high in all aqueous bioconversion media assessed. This can be seen in Figures 4.13 to 4.15, which are graphical representations of the percentage of viable cells during the bioconversion reactions in the different bioconversion media assessed as a function of time. *E.coli* TOP10 pQR239 viability remained greater than 80% for the 4 hour duration of the bioconversions when compared to the control reaction, which had a final intact cell percentage of 93.3%. The neutral pH and the low substrate concentration minimized any potential adverse effects of pH differences, substrate or product toxicity on the biocatalyst and inhibition of the enzyme.

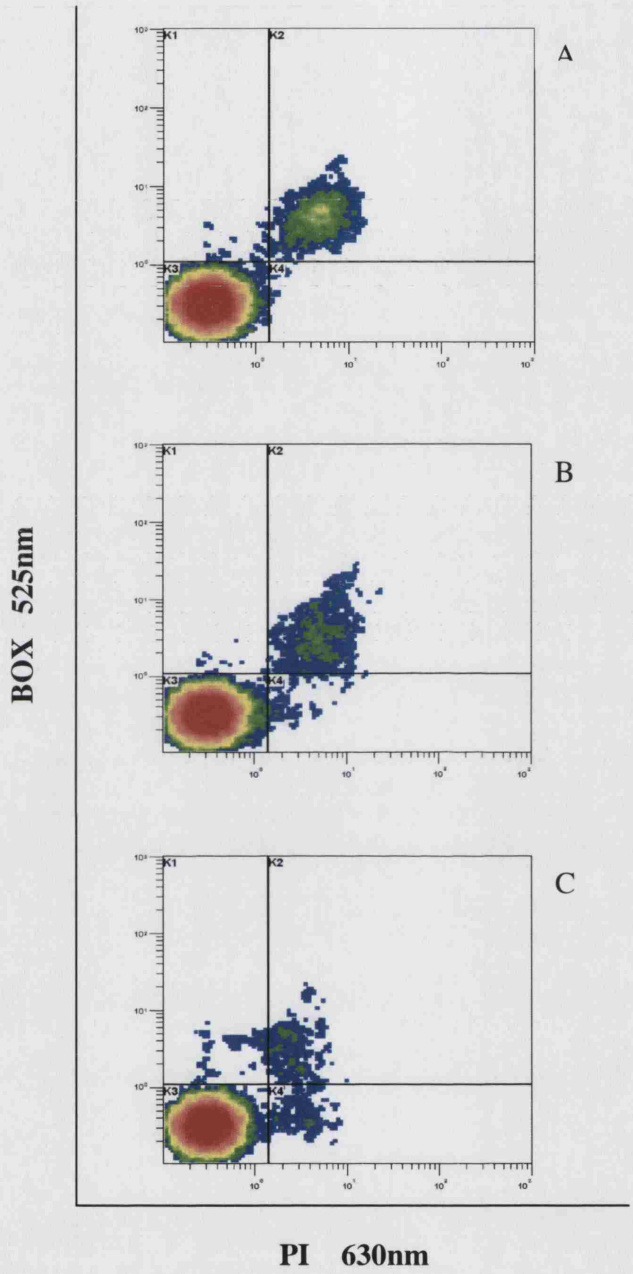

Figure 4.10. The effects of aqueous non-growth media on cell quality of *E.coli* TOP10 pQR239 during the bioconversion of bicyclo (3.2.0.) hept-2-en-6-one into (-)-1(S) 5(R)-2-oxabicyclo (3.3.0) oct-6-en-3-one and (-) 1(R) 5(S)-3-oxabicyclo (3.3.0) oct-6-en-2-one. Cells were stained with a combination of PI and BOX. 10 mM phosphate buffer (A), 50 mM phosphate buffer (B), 100 mM phosphate buffer (C). 50,000 events were analyzed.

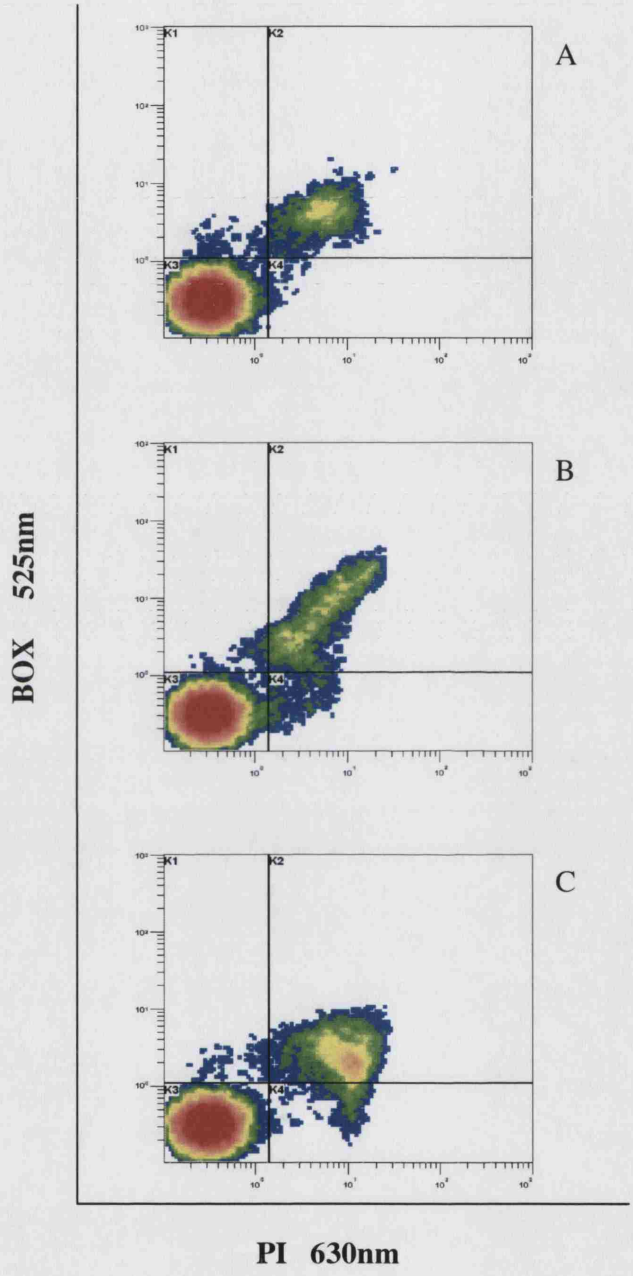

Figure 4.11. The effects of aqueous non-growth media on cell quality of *E.coli* TOP10 pQR239 during the bioconversion of bicyclo (3.2.0.) hept-2-en-6-one into (-)-1(S) 5(R)-2-oxabicyclo (3.3.0) oct-6-en-3-one and (-) 1(R) 5(S)-3-oxabicyclo (3.3.0) oct-6-en-2-one. Cells were stained with a combination of PI and BOX. 10 mM NaCl solution (A), 50 mM NaCl solution (B), 100 mM NaCl solution (C). 50, 000 events were analyzed.

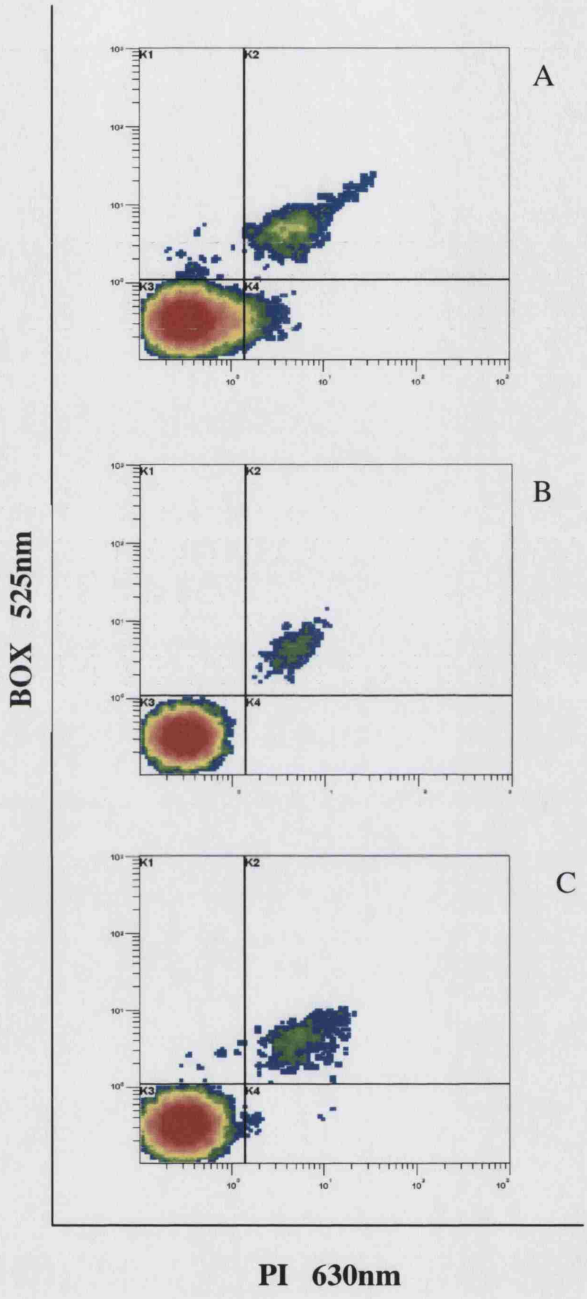

Figure 4.12. The effects of aqueous media on cell quality of *E.coli* TOP10 pQR239 during the bioconversion of bicyclo (3.2.0.) hept-2-en-6-one into (-)-1(S) 5(R)-2-oxabicyclo (3.3.0) oct-6-en-3-one and (-) 1(R) 5(S)-3-oxabicyclo (3.3.0) oct-6-en-2-one. Cells were stained with a combination of PI and BOX. Reverse osmosis water (RO) (A), Spent fermentation media (B), Fresh fermentation media (C). 50,000 events were analyzed.

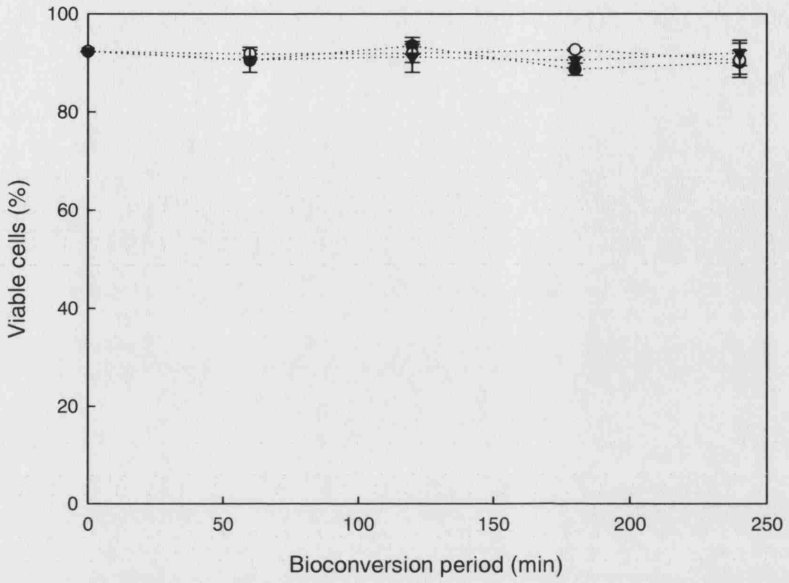

Figure 4.13. Cell viability in phosphate buffers during a 4 h bioconversion. (●) 10 mM phosphate buffer; (○) 50 mM phosphate buffer; (▼) 100 mM phosphate buffer. 50,000 events were analyzed.

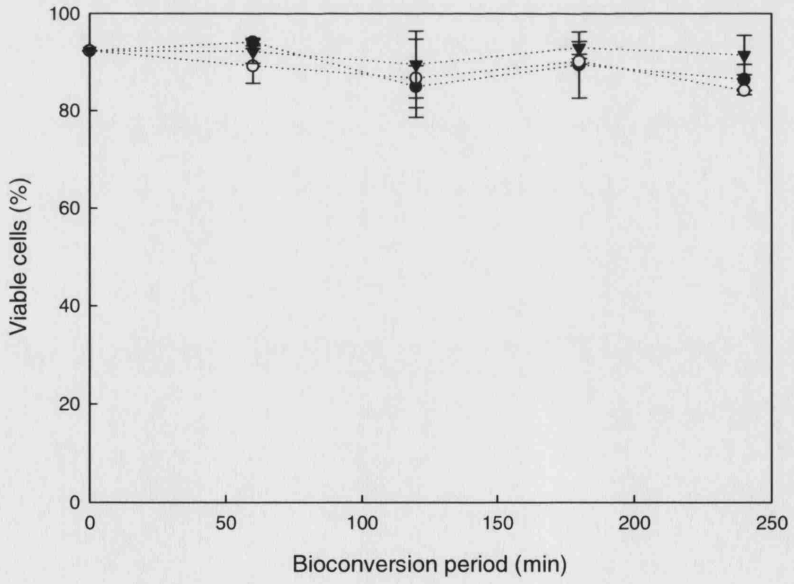

Figure 4.14. Cell viability in NaCl solutions during a 4 h bioconversion. (●) 10 mM NaCl; (○) 50 mM NaCl; (▼) 100 mM NaCl. 50,000 events were analyzed.

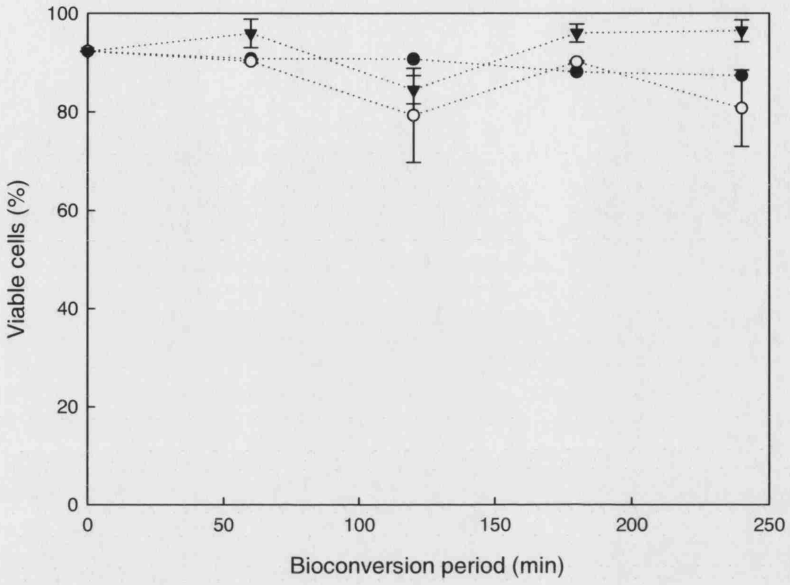

Figure 4.15. Cell viability in Reverse osmosis water and fermentation media during a 4h bioconversion. (●) RO water; (○) Spent fermentation media; (▼) fresh fermentation media. 50,000 events were analysed.

4.2.4.2. Enzyme activity assay

The enzyme which mediates the Baeyer-Villiger reaction, cyclohexanone monooxygenase (CHMO) was produced by *E.coli* TOP10 pQR239 following induction with L-arabinose, during the exponential growth phase (section 4.1.4). Enzyme activity was measured during the initial 30 min of the bioconversion; the rate of product formation during this period (quantified by GC analysis, section 4.1.9.2.) gave an indication of enzyme activity.

The bioconversion was initiated by the addition of 0.5 gL^{-1}substrate and glycerol at a final concentration of 10 gL^{-1}. It was observed that the bioconversion proceeded in all aqueous bioconversion media investigated, however there were notable differences in

product yields, as shown in Figures 4.16 to 4.18. The phosphate buffers supported the highest product formation rates, with 50 and 100 mM phosphate buffer exhibiting the highest product formation rates (14.7 and 14.1 $gL^{-1}h^{-1}$).

In NaCl solutions the highest initial conversion rate was observed in 50 mM NaCl, 10.5 $gL^{-1}h^{-1}$, as illustrated in Figure 4.17. In both 10 mM phosphate buffer and NaCl solution the initial rates of bioconversion were low, 9.9 and 7.8 $gL^{-1}h^{-1}$. The bioconversion in RO water had the lowest initial bioconversion rate 5.3 $gL^{-1}h^{-1}$; the bioconversion rate in spent and fresh fermentation media was also at the lower end of the scale, at 6.8 and 9.4 $gL^{-1}h^{-1}$, this data is shown in Figure 4.18.

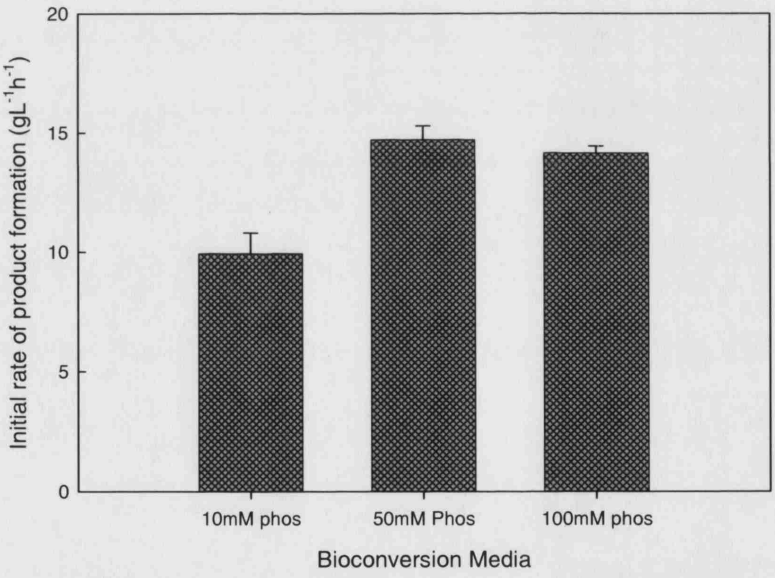

Figure 4.16. Initial product formation rates in pH 7 phosphate buffers, 30 min bioconversion period.

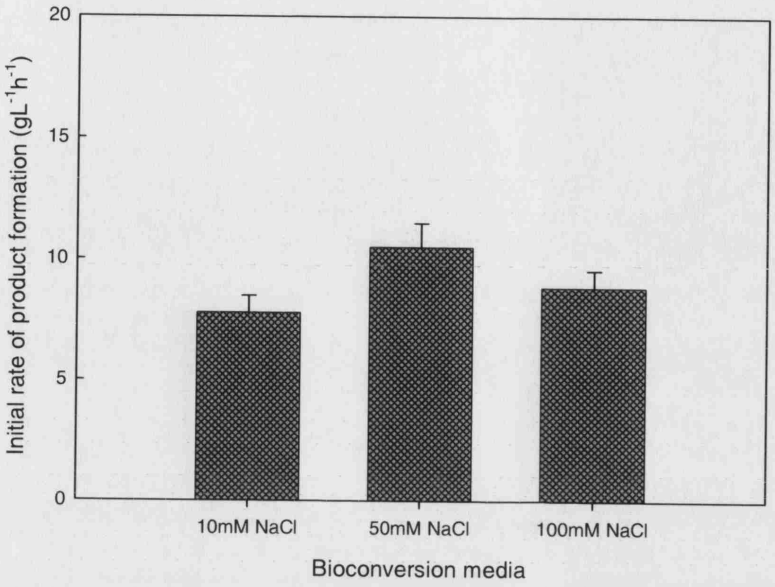

Figure 4.17. Initial product formation rates in pH 7 NaCl solutions, 30 min bioconversion period.

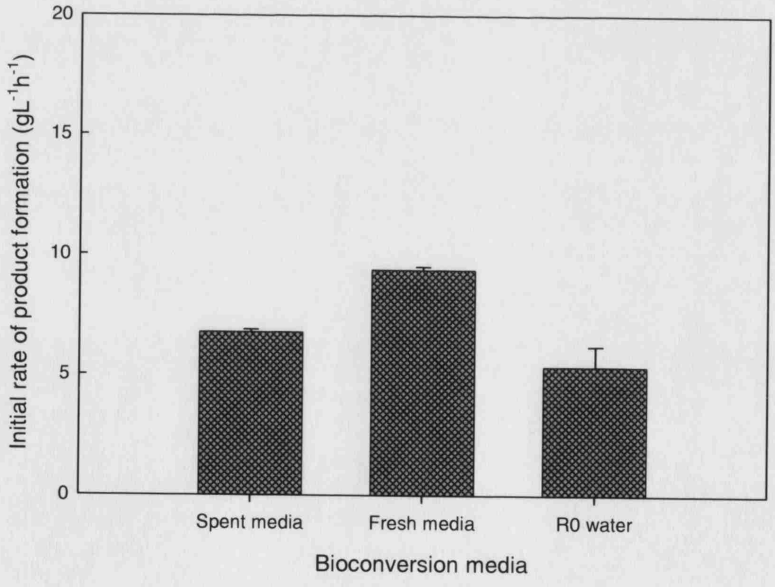

Figure 4.18. Initial product formation rates in spent and fresh fermentation media and pH 7 RO water, 30 min bioconversion period.

4.2.5. Whole cell biocatalyst stability at different bioconversion pHs

Microbial systems are susceptible to damage or death as a result of sub-optimal pH conditions, with a significant number of bacteria, including *E.coli* growing and working best at neutral pH (Bearson *et al* 1997). Therefore buffered media are used to minimise growth inhibition as a result of pH changes, which may occur, for example in fermentative bacteria which form organic acids from carbohydrates (Prescott *et al* 1996) during the fermentation stage. During bioconversion reactions pH control is implemented in order to maintain whole cell biocatalyst stability and enzyme activity. The whole cell biocatalyst, like any other microbial system may be compromised by sub-optimal environmental parameters. The effects of a range of pHs (6.5, 7.0, 7.5 and 8.0) during the bioconversion on the whole cell biocatalyst were investigated. Typically, the bioconversion was carried out in spent fermentation media at pH 7 (Doig *et al* 2002).

4.2.5.1. Flow cytometric analysis

Multiparameter flow cytometry was used to visualize the differences in the biocatalyst's stability following bioconversion reactions in 50 mM phosphate buffer at different pHs. The results obtained clearly indicated that pH has a significant effect on the stability of *E.coli* TOP10 pQR239 during the bioconversion. The metabolic and physiological status of the cells varied significantly during the bioconversion period at different pHs. These variations are shown in Figures 4.19 to 4.22.

Carrying out the bioconversion at pH 6.5 did not appear to cause exceptionally high levels of cellular damage or metabolic stress in the whole cell biocatalyst during the 4h duration of the reaction (Figure 4.19), a 10% decrease in cell viability was observed, from 89% 30 min after initiation of the bioconversion to 79% at completion. At pH 7.0, the pH at which the reaction is typically carried out, cell deterioration levels were comparatively low. A 4% drop in cell viability was recorded during the entire duration of the bioconversion (Figure 4.20). A 0.5 increase in pH to pH 7.5 caused a 17% decrease in

viability over the same time period, however at this pH a significant increase in cells which stained positively for BOX was observed during the bioconversion and accounted for 8% of compromised cells by the end of the bioconversion, suggesting a slow decline in cell quality (Figure 4.21). In Figure 4.22, of cells carrying out the bioconversion at pH 8.0, the pattern was very different. There are no intact, depolarised cells (UL quadrant); instead there is an increasing population of dual positive, dead cells. A 20% decrease in viability was observed at this pH during the bioconversion.

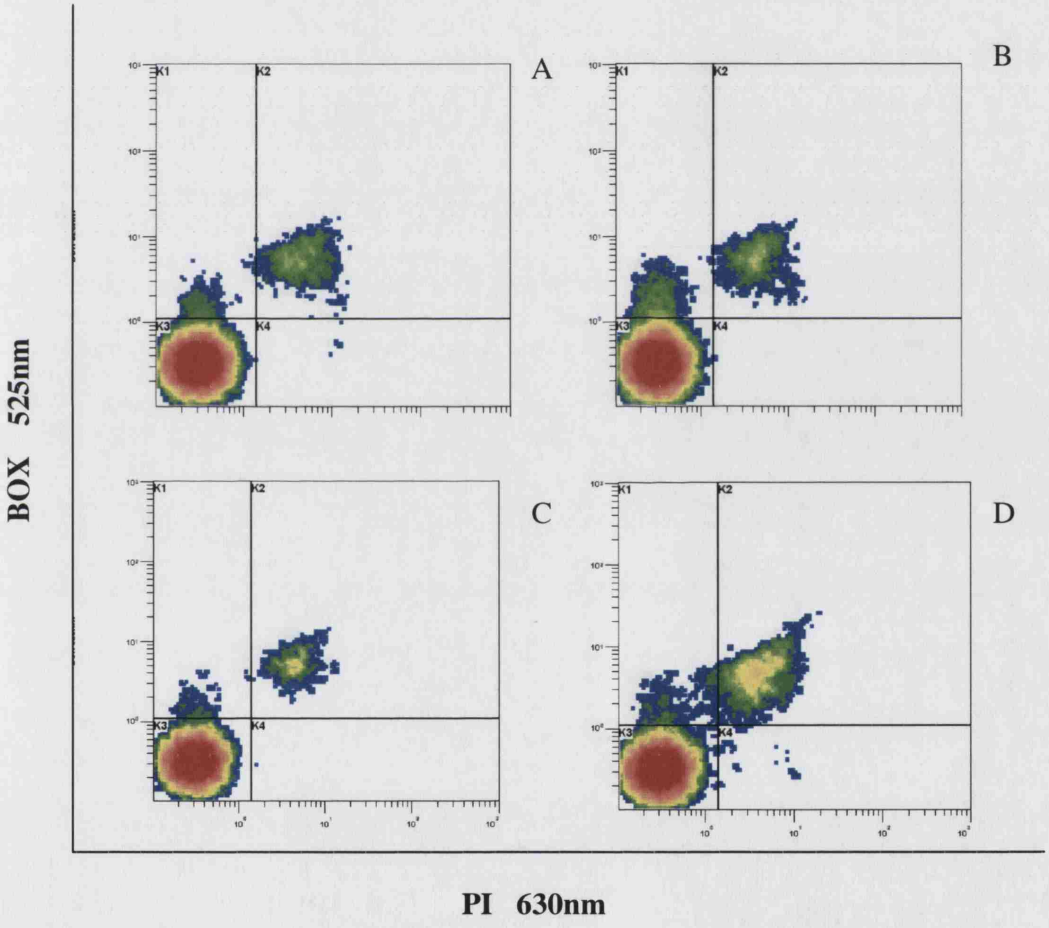

Figure 4.19. Flow cytometry profiles of *E.coli* TOP10 pQR239 during the bioconversion of bicyclo (3.2.0.) hept-2-en-6-one into (-)-1(S) 5(R)-2-oxabicyclo (3.3.0) oct-6-en-3-one and (-) 1(R) 5(S)-3-oxabicyclo (3.3.0) oct-6-en-2-one at pH 6.5. Cells were stained with PI and BOX. 0 min (A), 30min (B), 120min (C), 240min (D). 50,000 events were analyzed.

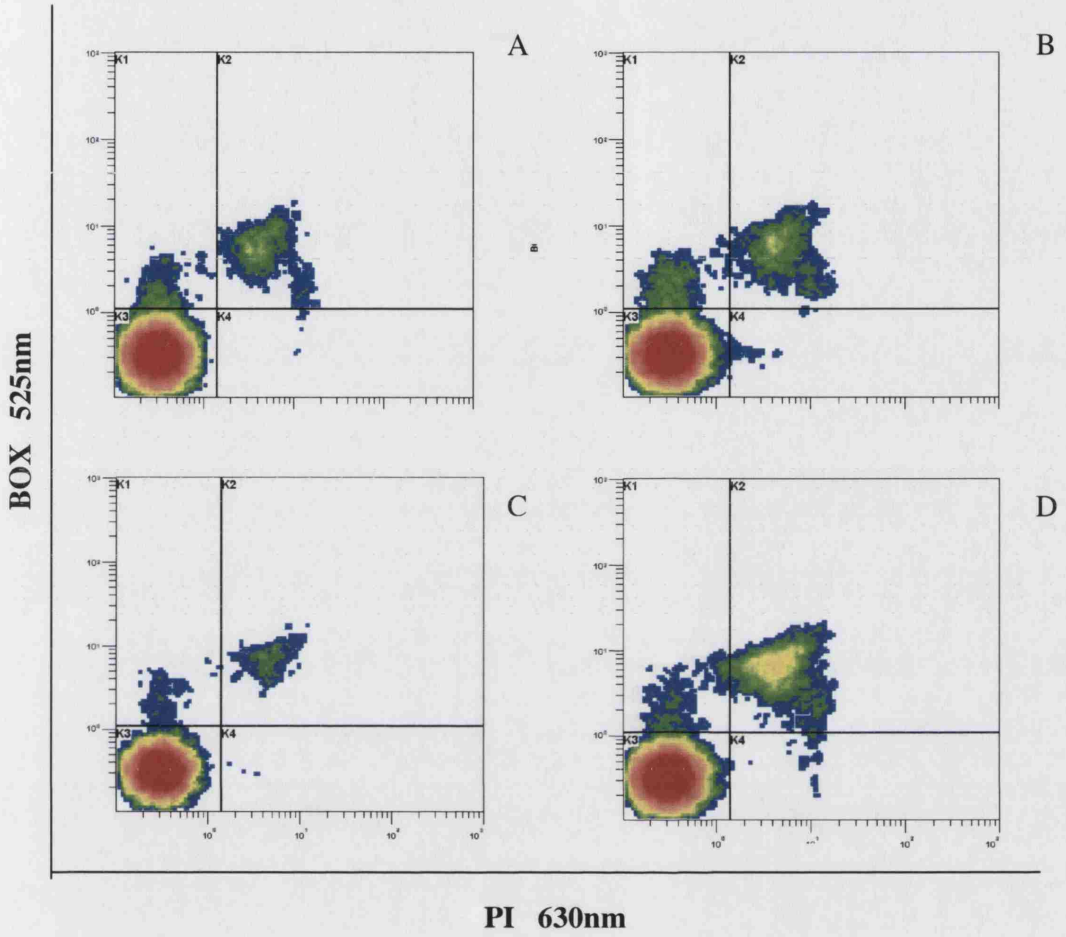

Figure 4.20. Flow cytometry profiles of *E.coli* TOP10 pQR239 during the bioconversion of bicyclo (3.2.0.) hept-2-en-6-one into (-)-1(S) 5(R)-2-oxabicyclo (3.3.0) oct-6-en-3-one and (-) 1(R) 5(S)-3-oxabicyclo (3.3.0) oct-6-en-2-one at pH 7.0. Cells were stained with PI and BOX. 0 min (A), 30min (B), 120min (C), 240min (D). 50,000 events were analyzed.

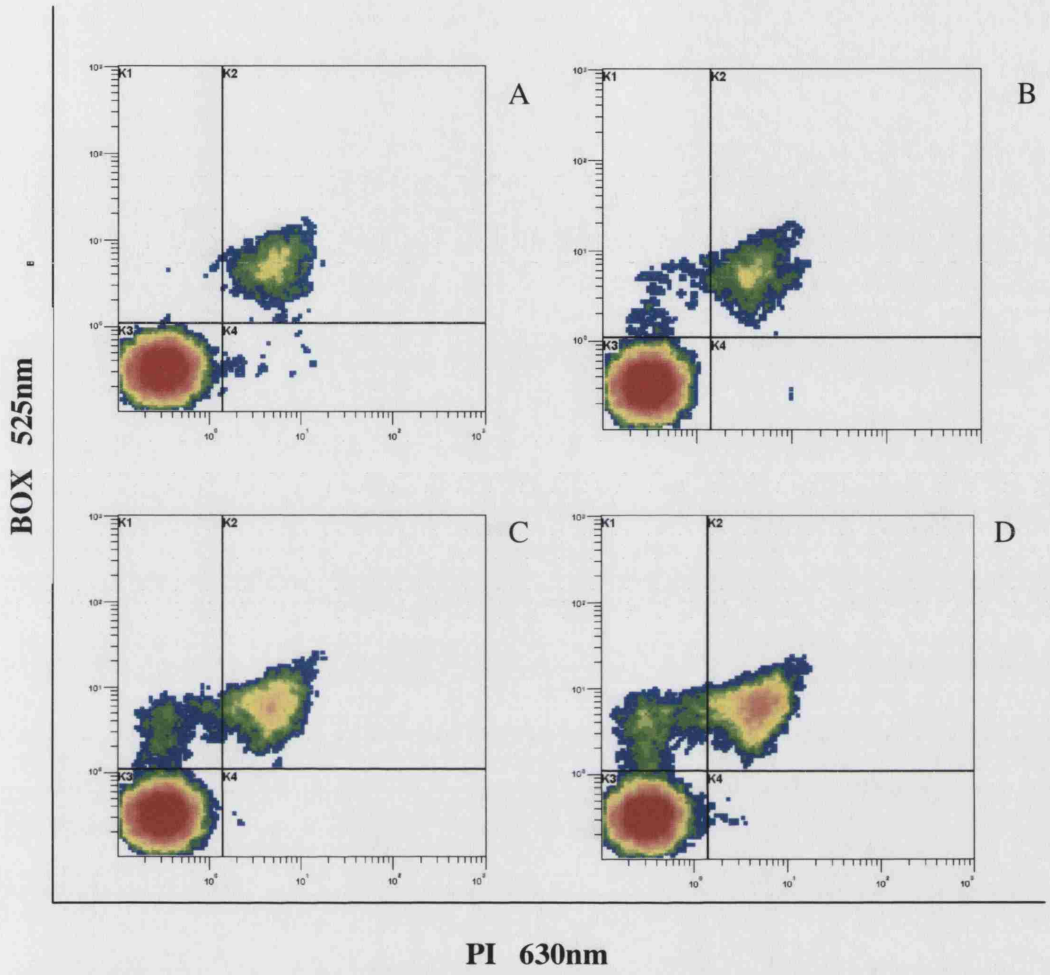

Figure 4.21. Flow cytometry profiles of *E.coli* TOP10 pQR239 during the bioconversion of bicyclo (3.2.0.) hept-2-en-6-one into (-)-1(S) 5(R)-2-oxabicyclo (3.3.0) oct-6-en-3-one and (-) 1(R) 5(S)-3-oxabicyclo (3.3.0) oct-6-en-2-one at pH 7.5. Cells were stained with PI and BOX. 0 min (A), 30min (B), 120min (C), 240min (D). 50,000 events were analyzed.

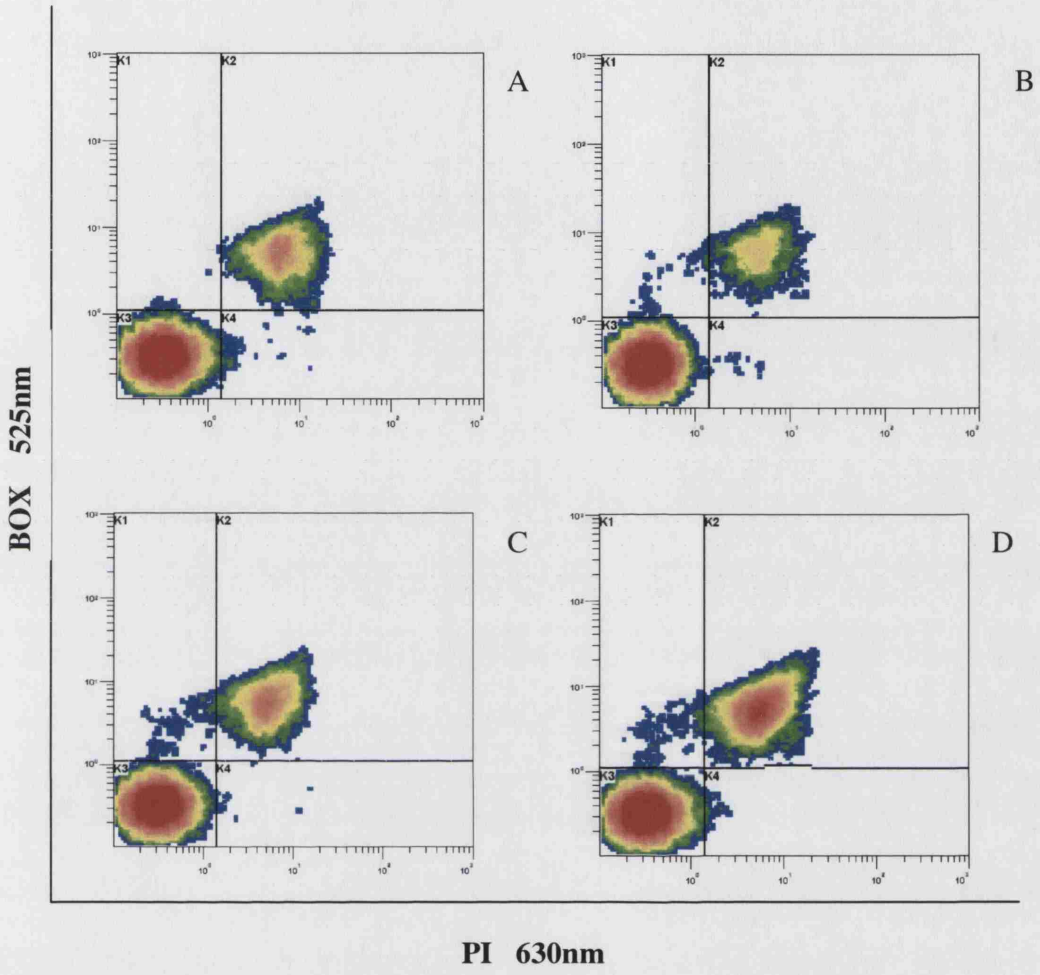

Figure 4.22. Flow cytometry profiles of *E.coli* TOP10 pQR239 during the bioconversion of bicyclo (3.2.0.) hept-2-en-6-one into (-)-1(S) 5(R)-2-oxabicyclo (3.3.0) oct-6-en-3-one and (-) 1(R) 5(S)-3-oxabicyclo (3.3.0) oct-6-en-2-one at pH 8.0. Cells were stained with PI and BOX. 0 min (A), 30min (B), 120min (C), 240min (D). 50,000 events were analyzed.

4.2.5.1. Enzyme activity at different bioconversion pHs

The bioconversion was initiated by the batch addition of 1gL^{-1}substrate and 10 gL^{-1} glycerol, when the cell suspension had reached the reaction temperature of 37°C and the pH had stabilized. It was recorded that the bioconversion reaction proceeded at all pHs, however the levels of enzyme activity recorded varied (Figures 4.23 to 4.26).

The highest rate of initial enzyme activity, 24.4 gL^{-1}h^{-1} was recorded for the reaction at 7.0, followed by 7.9 gL^{-1} h^{-1} at pH 7.5. The lowest rate of initial enzyme activity, 3.73 gL^{-1} h^{-1} was observed at pH 8.0, with initial enzyme activity at pH 6.5 only slightly higher at 4.10 gL^{-1} h^{-1}. In all instances, as indicated by the final product concentrations, greater than 85% substrate conversion was observed.

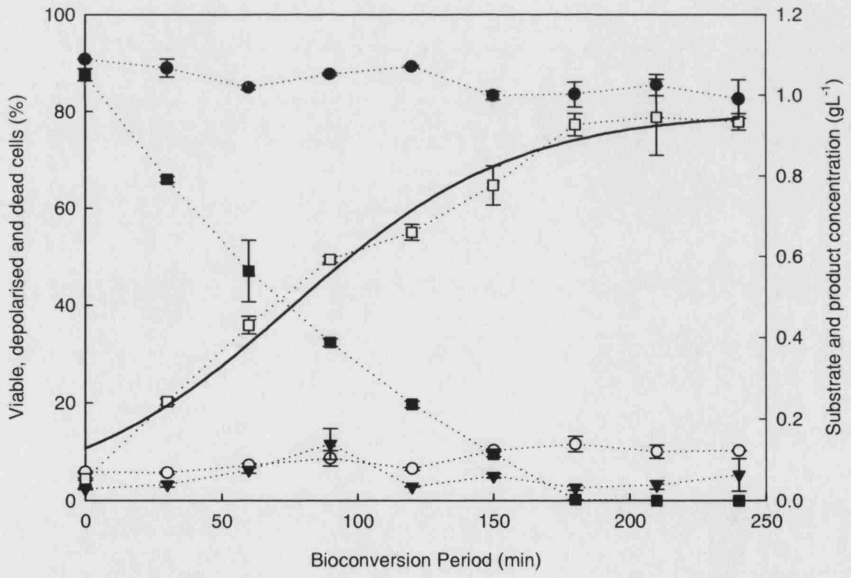

Figure 4.23. Product accumulation (□), substrate depletion (■) and cellular status (viable cells (●), dead cells (○), depolarised cells (▼))of *E.coli* TOP10 pQR239 during the bioconversion of bicyclo (3.2.0.) hept-2-en-6-one into (-)-1(S) 5(R)-2-oxabicyclo (3.3.0) oct-6-en-3-one and (-) 1(R) 5(S)-3-oxabicyclo (3.3.0) oct-6-en-2-one at pH 6.5.

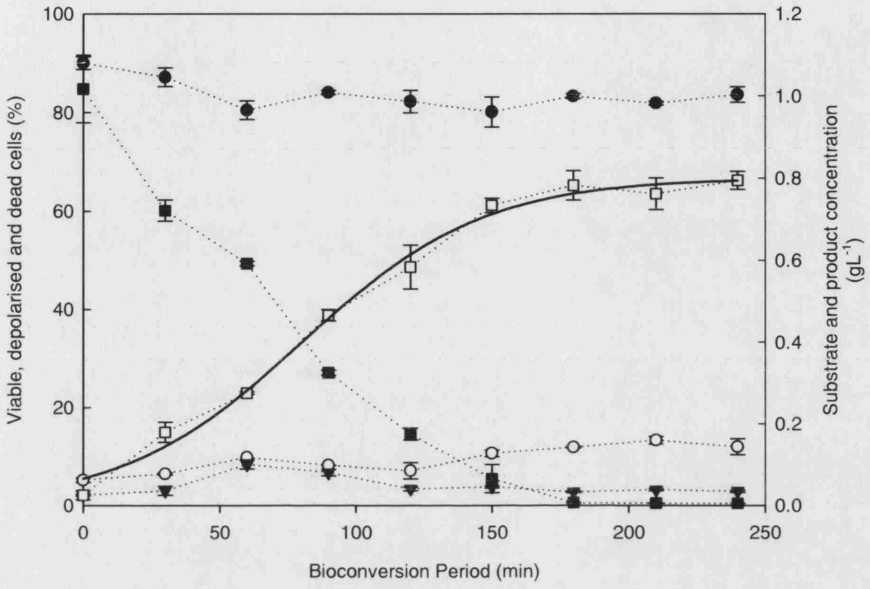

Figure 4.24. Product accumulation (□), substrate depletion (■) and cellular status (viable cells (●), dead cells (○), depolarised cells (▼)) of *E.coli* TOP10 pQR239 during the bioconversion of bicyclo (3.2.0.) hept-2-en-6-one into (-)-1(S) 5(R)-2-oxabicyclo (3.3.0) oct-6-en-3-one and (-) 1(R) 5(S)-3-oxabicyclo (3.3.0) oct-6-en-2-one at pH 7.0.

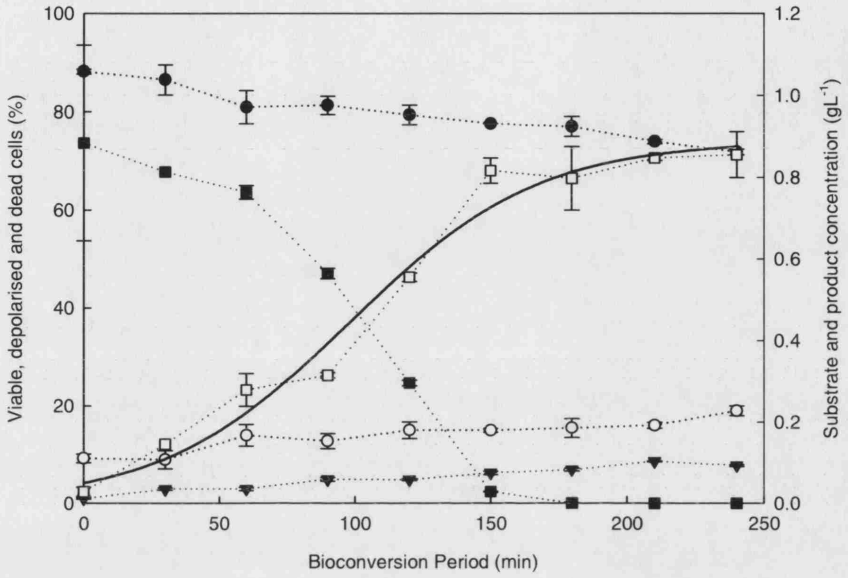

Figure 4.25. Product accumulation (□), substrate depletion (■) and cellular status (viable cells (●), dead cells (○), depolarised cells (▼)) of *E.coli* TOP10pQR239 during the bioconversion of bicyclo (3.2.0.) hept-2-en-6-one into (-)-1(S) 5(R)-2-oxabicyclo (3.3.0) oct-6-en-3-one and (-) 1(R) 5(S)-3-oxabicyclo (3.3.0) oct-6-en-2-one at pH 7.5.

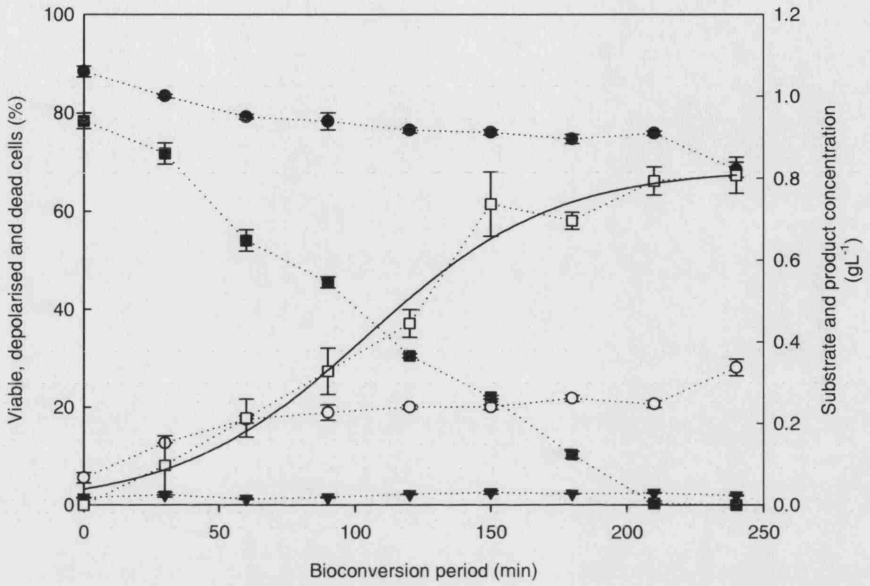

Figure 4.26. Product accumulation (□), substrate depletion (■) and cellular status (viable cells (●), dead cells (○), depolarised cells (▼)) of *E.coli* TOP10 pQR239 during the bioconversion of bicyclo (3.2.0.) hept-2-en-6-one into (-)-1(S) 5(R)-2-oxabicyclo (3.3.0) oct-6-en-3-one and (-) 1(R) 5(S)-3-oxabicyclo (3.3.0) oct-6-en-2-one at pH 8.0.

4.3. Discussion

Bacterial cells are known to inhabit a range of habitats of different temperature ranges which in turn influence their metabolic functions, such as biocatalytic capacity. Unfavourable temperature conditions may result in cell damage or death via cell lysis or in-activation of metabolic processes vital to normal cellular activity. *E.coli* TOP10 pQR239 cells were stored at different temperatures and flow cytometric analysis was used to show how cellular metabolism and physiology were impaired under the said conditions.

As expected cell quality deterioration was recorded at all temperatures (Figures 4.6 to 4.8). Storage at 4°C was the most favourable as the least cellular deterioration was recorded. This was expected since bacterial cultures are commonly stored at 4°C, for short periods of time without significant loss of cell viability.

In spite of the lower temperature of -80°C, the extent of cellular damage was not as extensive as at 25°C but was higher than at 4°C over the 168 h period. This was possibly due to the cells being suspended in a mixture of spent fermentation broth and 70% glycerol, in a 1:1 ratio. The use of glycerol as a cryoprotectant for biological systems is well known and is commonly used at concentrations of between 2 and 42% (El-Kest and Marth, 1991; Koening 2003.) Glycerol has been demonstrated to be beneficial for improving viability of a number of bacteria during frozen storage, among which are *E. coli, Staphylococcus aureus* and *Pseudomonas aereuginosa.* This supports the flow cytometry findings of stable levels of cell viability following storage at -80°C. The population of depolarized cells observed suggested a level of metabolic stress in some of the cells as a consequence of storage at -80°C.

Storage at 25°C caused the greatest cell quality degeneration indicated by the high percentage of dead cells (Figure 4.8). The fact that the cell samples were not agitated during the storage period could also be a significant factor in the cell deterioration recorded. Agitation may have increased aeration and encouraged cell proliferation.

However, any new cells would lack an active plasmid as no additional ampicillin was added for plasmid selection. Also at 25°C there was nothing to prevent the release of lytic enzymes, as was the case at 4°C and -80°C where the low temperatures would discourage lytic enzyme release, via cold shock induced proteins which may be involved in maintaining viability and possibly act as antifreeze proteins in *E.coli* (Willimsky *et al* 1992). The two populations of dead cells seen following these conditions may be attributed to different levels of fluorescence between sub-populations within the population.

Enzymes are sensitive to fluctuations in external parameters such as pH, ionic strength and temperature all of which may influence the enzyme's ability to attain maximum rates of activity (Voet and Voet 1995). CHMO enzyme activity and stability was examined via the measurement of product formation. Work by Doig *et al* (2003) has shown that the CHMO enzyme works best within the temperature range of 30-40°C, with peak activity observed at 37°C; however the effects of storage temperature on CHMO activity or the whole cell biocatalyst had not been previously examined. Enzyme activity was observed following storage at every temperature; however, there were differences in the extent to which this occurred (Figures 4.6 to 4.8). CHMO stability was highest during whole cell storage at -80°C, indicating that the enzyme was undamaged by this storage condition. This observation is not surprising in light of the fact that whole cell biocatalyst intactness was relatively stable throughout the duration of storage at this temperature; 58% viability was recorded after 168 hours. The rate of enzyme activity also remained consistent over the same period. Being an oxygenase CHMO is most likely situated in the bacterial cell membrane (Held *et al* 2000) thus, an intact, properly functioning cell membrane would suggest an intact fully functioning enzyme. Membrane integrity and enzyme quality would also be maintained by the glycerol used to store the samples (Hubalek 2003). It could also be supposed that any free enzyme released as a result of the loss of membrane integrity observed in the initial 24 hours post storage, was preserved at -80°C and remained capable of normal activity.

Enzyme activity when the whole cell biocatalyst was stored at 4°C was also consistent, with product formation rates similar to those observed at -80°C. This enzyme activity pattern appeared to mimic cell deterioration. As cell quality decreased, albeit minutely, at this temperature, 4°C appeared to be low enough to maintain the stability of the now free enzyme, thus ensuring its availability and capacity to carry out the bioconversion reaction; hence the observed enzyme activity.

The theory that the free enzyme was stable at 4°C was further supported by the enzyme activity profile of the whole cell biocatalyst stored at 25°C (Figure 4.8) where cell quality deterioration, manifest as a decrease in the percentage of viable, intact cells over time, closely mimicked the decline in enzyme activity. Cell lysis would have resulted in the release of the enzyme, which is assumed to have deteriorated at that temperature. This strongly suggests that the metabolic and physiological status of the whole cell biocatalyst are intricately linked to enzyme activity; this is illustrated in Figure 4.27, which shows the relationship between percentage enzyme activity and cell viability at all storage temperatures.

Maximum enzyme activity occurs when the bioconversion is carried out immediately after the fermentation. Following storage both enzyme activity and cell viability declined (Figure 4.27). Enzyme activity decreased by ~ 50% following storage at 4°C despite cell viability of >80%, a pattern mimicked at -80°C. At 25°C enzyme activity peaked at ~40% and then decreased as cell quality declined. The clusters of data points reflect consistency in enzyme activity. Storage temperature appears to be more detrimental to enzyme activity at 4°C and -80°C than to cell viability.

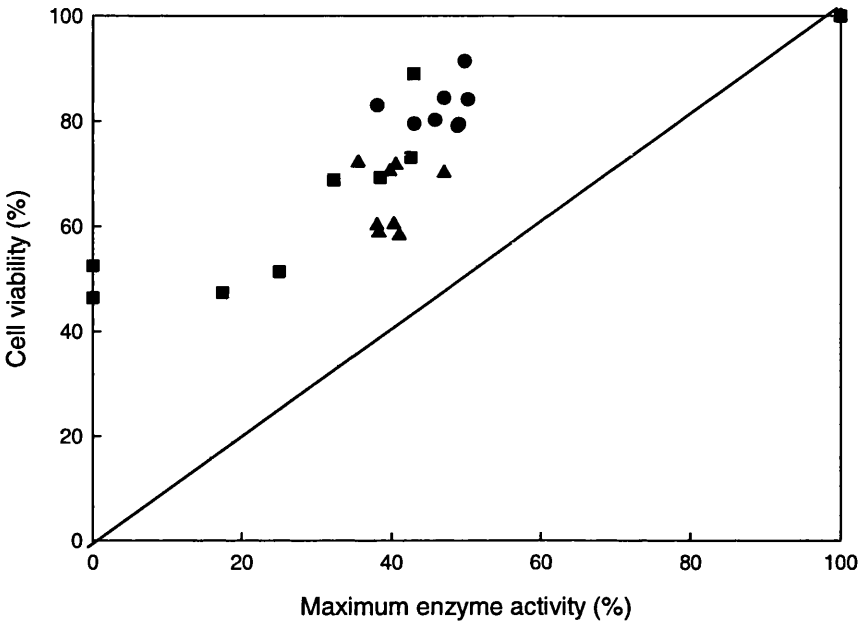

Figure 4.27. The correlation between cell viability of *E.coli* TOP10 pQR239 and enzyme activity following storage at different temperatures. -80°C (▲), 4°C (●), and 25°C (■).

Oxygenases, such as the cyclohexanone monooxygenase used in this bioconversion, are multi subunit proteins frequently located in the cell membrane (Held *et al* 2000). Therefore a high quality biocatalyst cell membrane is essential i.e. it should be intact and functioning efficiently for the duration of the bioconversion reaction to ensure maximum biocatalytic capacity. Cells with permeabilised membranes exhibit decreased or no metabolic activity (Amanullah *et al* 2002a) and as such would be incapable of efficient biocatalytic activity.

The levels of metabolic stress recorded indicated that all the aqueous media tested had minimal adverse effects on the quality of the whole cell biocatalyst in terms of metabolic status and physiological alterations. This is an advantage for the bioconversion and subsequent downstream processing steps. Since whole cell quality has an impact on

enzyme activity and hence product formation, cell stability in a more defined and less complex media could facilitate easier and less expensive down stream processing.

The removal of many if not most of the products of cellular metabolism, such as citric acid and acetate prior to the bioconversion step, when the cells are harvested and washed means that they are unavailable to adversely influence biocatalyst status and product purity. Neither would these metabolites require removal during the product recovery and purification steps. The stability of the cells in non-culture media may also allow the biocatalytic reaction to proceed for longer, as potentially toxic fermentation metabolites, such as organic acids produced as a result of carbohydrate metabolism (Prescott *et al*; 1996), are removed prior to the initiation of the bioconversion; this could be further enhanced by in-situ product removal to minimise or prevent the build up of the lactone products (Lye and Woodley 1999; Simpson 2001).

Inactivation of microorganisms is caused mainly by an increase in their membrane permeability due to compression and poration. Reducing the ionic strength can result in up to 2.2 log reductions in plate counts (Vega-Mercado *et al* 1996). Ionic strength variations are likely to result in physical damage of the cell membranes and thus may account for the lower cell viability recorded in low ionic strength phosphate buffer and NaCl solutions.

Enzyme activity was observed in all aqueous media, with the highest rates being in phosphate buffer at 50 mM and 100 mM (Figure 4.16). Surprisingly, very low initial product formation rates were recorded for spent and fresh fermentation broth, despite a relatively high cell quality in the initial 30 min of the bioconversion. The presence of spent metabolites and fermentation by products in the fermentation broth could account for this, as they could compromise cell quality. Obstruction of oxygen and mass transfer capacities of the substrate and product from the surrounding media into and out of the biocatalyst may also be a factor. The spent fermentation broth is denser than any of the aqueous non-growth media and this could adversely affect substrate transfer into and out of the whole cell biocatalyst. However the reason for low activity in fresh media may be

due to the cells attempting to proliferate in their suddenly nutrient rich environment, thus diverting metabolic energy away from the bioconversion to cell proliferation related activities.

One of the most important environmental conditions that can affect microbial cell quality is pH, with all microorganisms having a range of pHs where they can maintain metabolic capacity and physiology and exhibit optimum cell proliferation and cellular enzymatic activity. Cell damage was recorded at all pHs investigated. The best levels of cell viability were observed at pH 7.0. Being neutral pH and the pH at which the cells are routinely cultivated and perform the bioconversion (Doig *et al* 2001; 2002), this was expected. An interesting observation was the distribution of the various cell populations, at pH 6.5, 7.0 and 8.0 two main populations: viable (LL quadrant) and dead cells (UR quadrant) were present (Figures 4.19, 4.21 and 4.22). However at pH.7.5 a third population was observed, this population, located in the UL quadrant (Figure 4.20), indicated a metabolically stressed sub-population within the population. This population was seen to increase with time. The basis for this metabolic stress could be the whole cell biocatalyst's struggle to compensate for the sub-optimal pH of its environment. More of the cells appeared to gradually become depolarised but were still able to retain membrane integrity. This proposition is strengthened by the fact that at pH 8.0 this population was absent and a higher number of dead cells were present, demonstrating the cells' inability to compensate for the higher pH and a consequential loss of membrane integrity.

One of the most influential parameters affecting enzymatic activity is pH (Klibanov 2001); however enzyme activity was recorded at all pH. Generally most enzymes are active between pH 5 and 9, with a number working most efficiently at neutral pH and exhibiting Michaelis-Menten kinetics (Voet and Voet, 1995). It was expected that this would be the case with the CHMO enzyme, which drives the BVMO reaction. While the highest initial bioconversion rate was recorded at pH 7.0 and the lowest at pH 8.0, greater than 85% conversion was recorded at all pHs. The bioconversion at pH 7.0 supported the highest cell viability and enzyme activity. pH 8.0 supported the lowest cell viability and enzyme activity.

Figure 4.28 shows the relationship between enzyme activity and cell viability during the bioconversion at different pHs. Initial enzyme activity at pH 7.0 was taken to be the maximum activity. At 30, 120 and 240 min post bioconversion initiation, the enzyme activity was <60% of the maximum activity. Enzyme activity declined as the bioconversion progressed at all pHs.

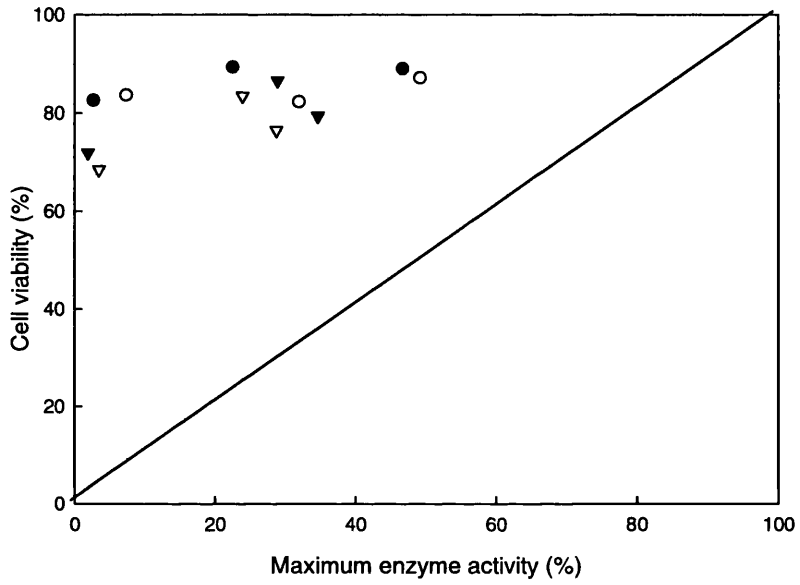

Figure 4.28. The correlation between cell viability of *E.coli* TOP10 pQR239 and enzyme activity following the bioconversion of bicyclo (3.2.0.) hept-2-en-6-one into (-)-1(S) 5(R)-2-oxabicyclo (3.3.0) oct-6-en-3-one and (-) 1(R) 5(S)-3-oxabicyclo (3.3.0) oct-6-en-2-one in phosphate buffer pH 6.5 to 8.0. pH 6 (●); pH 7.0 (○); pH 7.5 (▼) and pH 8.0 (Δ)

4.4. Summary

The results obtained indicated, using multiparameter flow cytometry, that whole cell biocatalyst and enzyme stability are separate entities. This is illustrated by the decrease in enzyme activity observed following storage despite good levels of cell viability. 50 mM phosphate buffer was found to support the highest levels of enzyme activity and cell

viability during the 4 h bioconversion period of all the bioconversion media tested. Storage at 4°C supported the highest levels of cell viability and enzyme activity over the 168 h storage duration, indicating that cells can be stored at these conditions for this period of time. The most favourable bioconversion pH was determined to be pH 7.0 as cell viability and enzyme activity were highest here in comparison to the other pHs assessed. Therefore, ideal conditions for the bioconversion are at pH 7.0 in 50 mM phosphate buffer. While bioconversion initiation immediately post fermentation would be optimal, overnight storage at 4°C is also acceptable, with respect to enzyme and whole cell biocatalyst stability.

Chapter 5

The Impact of Substrate, Product and Co-substrate Availability during the Bioconversion Reaction on the Whole Cell Biocatalyst

5.0. Introduction

The BVMO mediated stereo-selective oxidation of bicyclo (3.2.0.) hept-2-en-6-one to yield (-)-1(S) 5(R)-2-oxabicyclo (3.3.0) oct-6-en-3-one and (-) 1 (R) 5(S)-3-oxabicyclo (3.3.0) oct-6-en-2-one is an example of an industrially significant biocatalytic reaction, involving the use of whole bacteria cells to provide enzymatic activity and facilitate co-factor recycle. The whole cell biocatalyst used was *Escherichia coli* TOP10 pQR239. Figure 5.1 shows the currently accepted route for this reaction; with modifications to include the co-factor recycle aspect (Doig *et al* 2002 and 2003). In conjunction with whole cell biocatalyst stability, substrate concentration and co-factor availability could be instrumental in determining the efficiency and productivity of the bioconversion; all three are investigated in this section.

Substrate and product inhibition during the CHMO mediated bioconversion of bicyclo (3.2.0.) hept-2-en-6-one to yield (-)-1(S) 5(R)-2-oxabicyclo (3.3.0) oct-6-en-3-one and (-) 1 (R) 5(S)-3-oxabicyclo (3.3.0) oct-6-en-2-one have been identified as key limitations to biocatalyst activity and productivity (Doig *et al* 2002 and 2003; Zambianchi *et al* 2002). Other documented limitations are enzyme stability and reuse and co-factor availability. How substrate and product concentrations during the bioconversion affect the whole cell biocatalyst's metabolic and physiological status has not been previously investigated. Neither had distinguishing whether the decline in enzyme activity is related to enzyme-substrate or product interactions or whole cell biocatalyst-substrate or product

interactions. Assessing these interactions was one of the aims of this study. Both product and substrate are expected to cause loss of membrane integrity, with the percentage of intact viable cells decreasing, as would CHMO activity as concentrations increase.

In terms of process definition (improvement), the objective was to establish with regard to the quality of the whole cell biocatalyst; how much of both the substrate, racemic bicyclo (3.2.0.) hept-2-en-6-one and the co-substrate, glycerol, was required for optimum bioconversion rates. The substrate is an organic compound, which could be potentially toxic in high enough concentrations to the whole cell biocatalyst. This potential toxicity was investigated using multiparameter flow cytometry.

One of the principal driving forces behind the use of whole cell biocatalysts in industrial processes is the ease of meeting co-factor requirements. The introduction of oxygen by biocatalysts is co-factor dependent and while *in vitro* cofactor regeneration is feasible it is expensive (Held *et al* 2000). In the BVMO mediated oxidation of bicyclo (3.2.0.) hept-2-en-6-one to yield (-)-1(S) 5(R)-2-oxabicyclo (3.3.0) oct-6-en-3-on and (-)1(R) 5(S)-3-oxabicyclo (3.3.0) oct-6-en-2-one glycerol was used as the co-substrate to drive the reaction, via facilitating regeneration of the cofactor, NADPH. Work by Doig *et al* 2003, determined that glycerol worked best as a co-substrate for this reaction. They also established that glycerol concentration affected specific activity, with concentrations above $5gL^{-1}$ being sufficient for maximum enzyme activity.

Glycerol concentration was also expected to affect the quality of the whole cell biocatalyst independently of enzyme activity. Sub-optimal co-substrate concentrations were expected to result in a loss in cell viability and a decrease in enzyme activity. The extent and potential limitations of co-substrate availability on the whole cell biocatalyst was investigated by multiparameter flow cytometry.

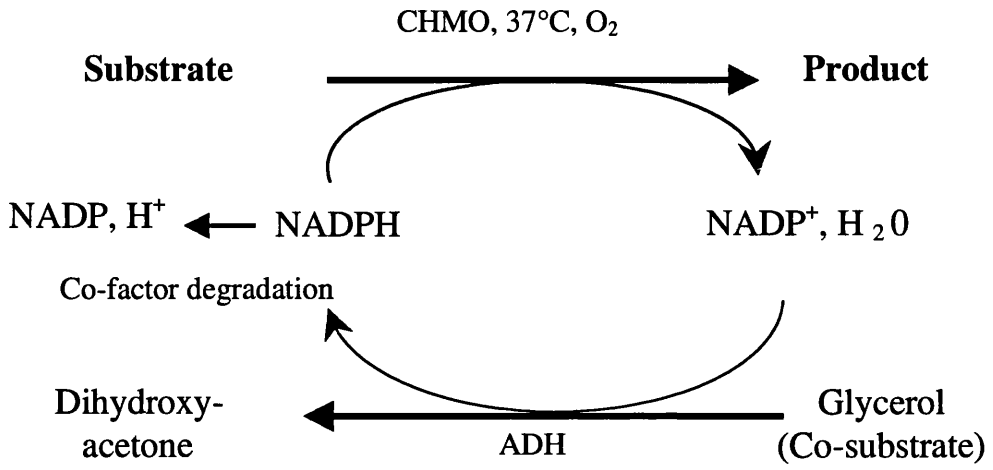

Figure 5.1. Reaction scheme of the oxidation of the substrate to the products, showing the co-factor utilization and regeneration and co substrate utilization routes. (Modified from Doig *et al* 2002 and 2003).

5.1. Materials and methods

5.1.1. Biocatalyst

The strain used was a modified *Escherichia coli* strain containing a plasmid, pQR239 into which had been cloned the cyclohexanone monooxygenase (CHMO) gene bearing the araBAD promoter, from *Acinetobacter calcoacetius* NCIMB 9871 (Doig *et al* 2001). The expression of the CHMO gene was induced by L (+) arabinose. This strain, *E. coli* TOP10 pQR239 was kindly donated by Dr. John Ward, Biochemistry Department UCL.

5.1.2. Culture media

E. coli TOP10 pQR239 was cultured in modified Luria Bertani (LB) media; composed of 10 gL^{-1} NaCl, soya-peptone (enzymatic digest), glycerol; 25 gL^{-1} yeast extract (Fluka Chemie Buches Switzerland) and 400 mgL^{-1} ampicillin (Sigma, Poole, Dorset, U.K). All

media components except ampicillin were sterilized in-situ by autoclaving at 121°C for 20 min. Ampicillin was filter sterilized using a sterile 0.2 μm filter and added to the media immediately prior to inoculation. 0.5 mlL^{-1} antifoam, polypropylene glycol '2000 (Fluka Chemie Buches Switzerland) was added to the bioreactor prior to media sterilisation.

5.1.3. Fermentation

Fermentations took place in a 20L LH 210 stirred tank reactor, working volume 15L (Bioprocessing Engineering Services, Charring, Kent, U.K). The bioreactor was inoculated with three 500 ml overnight (16 h) (10% of the total working volume) shake flask cultures cultivated from a 1ml frozen glycerol stock aliquot. The reactor was operated with an agitation speed of 1000 rpm at 37°C and aeration was maintained at 0.66vvm via a submerged sparger. Culture pH was monitored using a pH probe (Ingold, Messtechnick, Urdorf, Switzerland) and culture was maintained at 7.0 by the controlled addition of 3M H_3PO_4 and 3M NaOH. DOT was measured via a polagraphic probe (Ingold Messtechnick, Urdorf, Switzerland). CER and OUR measurements were taken using online mass spectrophotometric analysis of exit gases using the BioView Fermenter Control Software (Adaptive Biosystems, Luton, U.K). CHMO production was induced by the addition of 2.5 gL^{-1} L-arabinose, approximately 3 hours after inoculation, during the exponential phase when an optical density (OD_{670nm}) of 7-8 had been attained. After 6 h growth when a cell density of 10 gL^{-1} (Appendix IV) had been obtained and the cells were in the stationary phase, the cells were aseptically transferred into a harvest vessel and stored at 4°C overnight prior to being used in the bioconversion.

5.1.4. Biomass separation

Cells were separated from the culture medium by centrifugation in a laboratory scale centrifuge (J21 M1 Beckman, USA) at 7000 rpm for 20 min at 4°C. The pellet was re-

suspended in 50 mM phosphate buffer, pH 7.0 to a cell concentration of 10 gL^{-1} before the bioconversion was initiated.

5.1.5. Substrate and product toxicity: shake flask scale bioconversions

The influences of substrate and product concentrations on the whole cell biocatalyst were examined in shake flask scale bioconversions in order to study the impact of different concentrations of the substrate and product while minimizing the amounts used. The whole cell biocatalyst was cultured as in section 5.13 and separated from the fermentation broth as in section 5.1.4. The cell mass was suspended in 50 ml 50 mM phosphate buffer pH 7.0, to a final concentration of 10 gL^{-1} in a 500 ml baffled shake flask. Before the bioconversion was initiated the cell suspension was allowed to reach the bioconversion temperature of 37°C by agitating at 200 rpm in a rotary shaker at 37°C for 10 min. The bioconversion was initiated by the addition of glycerol at a final concentration of 10 gL^{-1} and the appropriate concentrations of substrate and / or product (Table 5.1).
The substrate bicyclo (3.2.0.) hept-2-en-6-one was kindly donated by Dr. Roland Wohlgemuth, Fluka Chemie Buches Switzerland. The product used was the chemical lactone, 1S 5R 2-oxabicyclo [3.3.0] oct- 6-en-3-one (Fluka Chemie Buches Switzerland). A 50 gL^{-1} stock solution was made up in 50 mM phosphate buffer, pH 7.0 and dispensed in the correct quantities to make up the required concentrations in a 50 ml bioconversion to investigate the influence of product concentrations.

Substrate Concentration (gL^{-1})	Product Concentration (gL^{-1})	Substrate in Product flasks (gL^{-1})
0	0	0.5
0.2	0.2	0.5
0.5	0.5	0.5
1	1	0.5
2	2	0.5
4	4	0.5
5	5	0.5
10	-	-

Table 5.1. Substrate and Product concentrations

5.1.6. Bioconversion reaction: Substrate toxicity, 5L bioreactor scale

Large-scale substrate toxicity investigations were conducted in a 7L fermenter (5L working volume (Bioprocessing Engineering Services, Charring, Kent, U.K), under conditions identical to fermentation conditions. 5L of fermentation broth from the fermentation step (section 5.1.3) was transferred aseptically into this vessel and allowed to reach 37°C before bioconversion initiation. The reactor was operated with an agitation speed of 800 rpm at 37°C and aeration was maintained at 0.66vvm via a submerged sparger. A bioconversion pH of 7.0 was maintained by the controlled addition of 3M H_3PO_4 and 3M NaOH. DOT was measured via a polagraphic probe (Ingold Messtechnick, Urdorf, Switzerland); CER and OUR measurements were taken using online mass spectrophotometric analysis of exit gases of using the BioView Fermenter Control Software, Adaptive Biosystems (Luton, UK). The bioconversion was initiated by the batch addition of 10 gL^{-1} glycerol, followed by a continuous substrate feed at 0, 0.5, 1.0, 5.0 and 10 $gL^{-1}h^{-1}$ (101 U/R pump, Watson-Marlow Ltd, Cornwall UK). At initiation enough substrate to attain the set substrate concentration was added, followed by a

gradual feed to maintain the required concentrations. These bioconversions were run for 4 hours.

5.1.7. Bioconversion reaction: Co-substrate requirement investigations, 5L bioreactor scale

Large scale co-substrate requirement investigations were conducted under conditions identical to fermentation conditions in a 7L fermenter, (5L working volume) (Bioprocessing Engineering Services, Charring, Kent, and U.K.), 5L of fermentation broth from the fermentation step (section 5.1.3) was transferred aseptically into this vessel. The reactor was operated with an agitation speed of 800rpm at 37°C and aeration was maintained at 0.66vvm (equivalent 1.5 Lml^{-1}) via a submerged sparger. A bioconversion pH of 7.0 was maintained by the controlled addition of 3M H_2PO_4 and 3M NaOH. DOT was measured via a polographic probe (Ingold Messtechnick, Urdorf, Switzerland); CER and OUR measurements were taken using online mass spectrophotometric analysis of exit gases using the BioView Fermenter Control Software, Adaptive Biosystems (Luton, UK). The bioconversion was initiated by the batch addition of the substrate at a concentration of 0.4 gL^{-1} followed by a controlled continuous substrate feed at 0.4 $gL^{-1}h^{-1}$ (101 U/R pump, Watson-Marlow Ltd, Cornwall UK), co-substrate was fed at concentrations, corresponding to 0, below, excess, at, and batch glycerol utilization rates, (505 Du digital pump, Watson-Marlow Ltd, Cornwall UK) Table 5.2. These bioconversions were run for 4 hours.

Substrate concentration ($gL^{-1}h^{-1}$)	Co-substrate concentration ($gL^{-1}h^{-1}$)	Co-substrate addition method
0.4	0	-
0.4	1.32	Feed
0.4	2.64	Feed
0.4	30	Feed
0.4	10 (gL^{-1})	Batch*

Table 5.2. Co-substrate addition

* Usual method of glycerol addition (Doig *et al* 2002 and 2003)

5.1.8. Analysis

5.1.8.1. Flow cytometry

Flow cytometric analysis was conducted using an EPICS XL-MCL (autoloader) 4 Colour Bench Top Flow Cytometer with Flow Centre II Acquisition Workstation, with 488 nm excitation from an argon-ion laser at 15mW (Beckman Coulter, High Wycombe, Bucks, U.K.). FL1 and FL3 detectors, which measured bis-(1,3-dibutylbarbituric acid) trimethine oxonol (BOX) and propidium iodide (PI) fluorescence respectively, were set at 585 and 807 volts respectively, with a corresponding compensation of 24 and 16% to minimize spectral overlap during analysis.

Stock solutions of each dye were prepared as follows: PI was made up at 200 μgml^{-1} in 1x Dulbecco's Phosphate buffered saline, pH 7.2 (DBS) (Sigma-Aldrich, Poole, Dorset, U.K). BOX was made up at 10mg ml^{-1} in dimethyl sulphoxide (DMSO). The DMSO stock was maintained at -20°C. The DBS stocks were maintained at -4°C.

All solutions were filtered prior to use using a 0.2µm filter to remove any particulate matter that could interfere with analysis. Culture samples were diluted in 1x DBS to a

final concentration of 1 x 10^{-5} cells ml^{-1} (Appendix I) and stained with PI and BOX at a final concentration of 5 and 10 μg ml^{-1} respectively. Ethylenediaminetetraacetic acid (EDTA) was added to the working solution at a final concentration of 4mM to facilitate BOX straining. The system's colour compensation was set up in such a way as to minimize the spectral overlap between the PI and BOX emitted fluorescence. PI and BOX fluorescence were measured at 630 and 525 nm respectively following a 10 min incubation period at room temperature (25°C). A total of 50,000 events were analyzed per sample. Density plots were used to illustrate flow cytometric results.

5.1.8.2. Gas Chromatography

Bicyclo (3.2.0.) hept-2-en-6-one (substrate) depletion and the accumulation of the products (-)-1(S) 5(R)-2-oxabicyclo (3.3.0) oct-6-en-3-one and (-) 1(R) 5(S)-3-oxabicyclo (3.3.0) oct-6-en-2-one was measured using an XL-2 gas chromatograph (GC) with flame ionisation detector (FID) (Perkin-Elmer, Norwalk, CT, USA) with an AT-1 column 30m x 0.2mm x 0.25μm (Alltech, Deerfield, IL, USA) with helium as the mobile phase.

A 2 ml sample was removed from the bioconversion vessel and centrifuged in at bench top centrifuge (Biofuge, Hanau, Germany) at 1300 rpm for 2 min to separate the cell biomass from the supernatant. 1 ml of the supernatant added to an equal volume of ethyl acetate containing naphthalene (1$mgml^{-1}$) as an internal standard and centrifuged for a further 2 min. The supernatant was analyzed.

The GC was operated with an injector and column temperature of 250°C and an oven temperature of 110°C. Retention times for bicyclo (3.2.0.) hept-2-en-6-one, (-)-1(S) 5(R)-2-oxabicyclo (3.3.0) oct-6-en-3-one, (-) 1(R) 5(S)-3-oxabicyclo (3.3.0) oct-6-en-2-one and the internal standard were at 1.8, 3.5, 3.55 and 3.9 minutes, respectively.

5.1.8.3. Measurement of glycerol concentration

A 1 ml sample was removed from the bioconversion vessel into a 1.5 ml eppendorf tube and centrifuged in at bench top centrifuge (Biofuge, Hanau, Germany) at 1300 rpm for 2 min to separate the cell biomass from the supernatant, the cell pellet was discarded. The supernatant was assayed to determine the glycerol concentration using a glycerol enzymatic test kit (Boehringer-Mannheim Roche, R-Biopharm GmbH, Darmstardt, Germany). In this assay the amount of glycerol present is stoichiometrically linked to the amount of NADH oxidised during a series of three enzyme mediated reactions. Glycerol is first phosphorylated by adenosine-5'-phosphate (ATP) to L-glycerol-3-phosphate in a reaction catalysed by glycerolkinase. Adenosine-5'- diphosphate (ADP) generated in this reaction is reconverted back into ATP by phosphoenolpyruvate with the aid of pyruvate kinase to form pyruvate. NADH reduces the pyruvate to L-lactate with the oxidation of NADH to NAD, in the presence of L-lactate dehydrogenase. NADH oxidation is followed spectrophotometrically by measuring the difference in absorbance at 340 nm on completion of the above reactions using a variable wavelength spectrophotometer (Unicam, Cambridge, UK).

5.1.8.4. Fermentation profiling

Off gas measurements of dissolved oxygen tension (DOT), carbon dioxide evolution rate (CER) and oxygen uptake rate (OUR) were measured using mass spectroscopy and the data logged using the BioView Fermenter Control Software, Adaptive Biosystems (Luton, UK).

5.2. Results

5.2.1. Substrate and product toxicity: shake flask scale bioconversions

Shake flask experiments were carried out to determine the system's limitations with respect to the concentrations of substrate and product the whole cell biocatalyst was able to withstand without losing viability and/or enzyme activity under bioconversion conditions. These reactions were carried out at shake flask scale maximise the number of bioconversions carried out, to examine the feasibility of a larger scale reaction and to minimize the amount of substrate and product used. The product used in these experiments was the chemical lactone, 1S 5R 2-oxabicyclo [3.3.0] oct- 6-en-3-one. It was expected that substrate and product associated loss of cell viability and stability would be concentration dependent and irreversible. Product and concentration dependent enzyme inhibition was also expected to occur. The results presented in this section do not completely validate these theories. Substrate concentration was found to cause irreversible, concentration dependent damage. However, product associated damage was found to be time rather than concentration dependent and reversible. Loss of enzyme activity was found to be affected by both substrate and product concentration.

5.2.1.1. Substrate toxicity

Flow cytometric analysis of samples taken from the shake flask reactions 30 min after the initiation of the bioconversion indicated that there were alterations to cellular physiology and metabolism in response to variations in the concentration of the substrate, bicyclo (3.2.0.) hept-2-en-6-one. Figure 5.2 shows this data. The control reaction (no substrate) showed that after 30 min 94.60% of the cells were intact and viable, 1.10% were metabolically stressed showing signs of membrane depolarization and 3.40% were dead. When substrate concentrations were between 0.2 and 2.0 gL^{-1} the percentage of viable cells dropped to between 83 and 89.0%, subsequent declines in cell viability were more

pronounced, at 73 to 36.0% for concentrations between 3.0 and 10 gL^{-1}. The percentage of depolarized and dead cells within the population increased exponentially with increasing substrate concentration.

Enzyme activity characterized by the bioconversion of bicyclo (3.2.0.) hept-2-en-6-one to yield (-)-1(S) 5(R)-2-oxabicyclo (3.3.0) oct-6-en-3-one and (-) 1 (R) 5(S)-3-oxabicyclo (3.3.0) oct-6-en-2-one, was observed at all substrate concentrations albeit to varying degrees (Figure 5.2). Product formation peaked at 1.0 gL^{-1} (when the substrate concentration was at 0.5 gL^{-1}) an initial product formation rate of 5.70 gL^{-1} h^{-1} was recorded, subsequently the rate of product formation declined. At 4.0, 5.0 and 10.0 gL^{-1} substrate concentration, the rate of product formation recorded was extremely low at $\leq$ 0.024 $gL^{-1}h^{-1}$, indicating that high substrate concentrations inhibit CHMO activity.

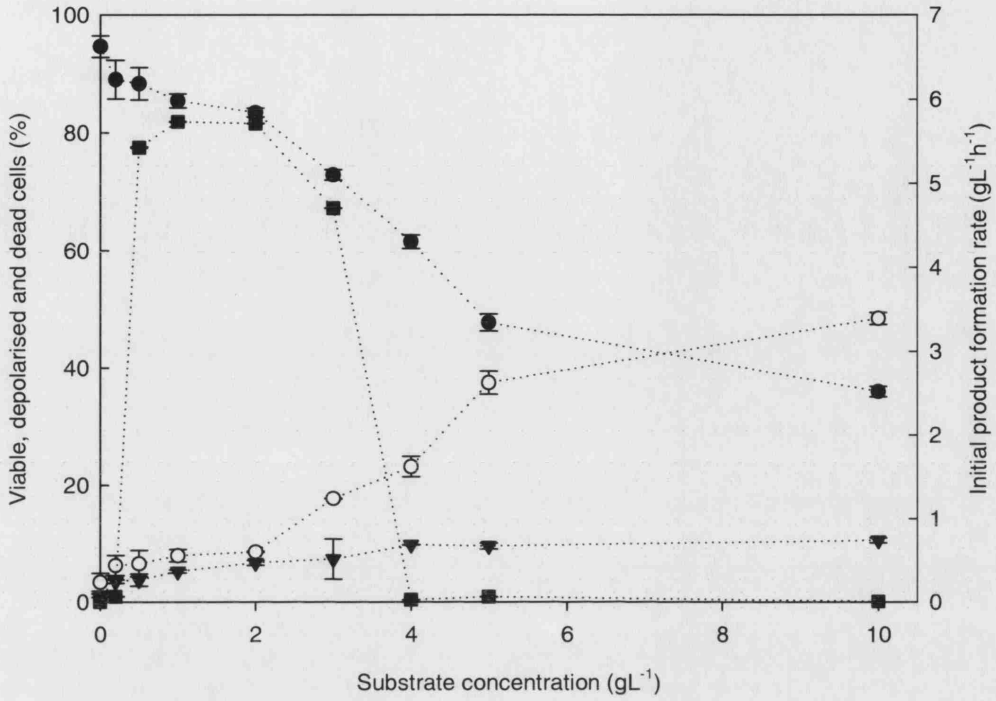

Figure 5.2. Cellular status (viable•, depolarized▼ and dead ○) and initial product formation rate (■) profiles of *E.coli* TOP10 pQR239 at different substrate concentrations during shake flask bioconversions of bicyclo (3.2.0.) hept-2-en-6-one to yield (-)-1(S) 5(R)-2-oxabicyclo (3.3.0) oct-6-en-3-one and (-) 1 (R) 5(S)-3-oxabicyclo (3.3.0) oct-6-en-2-one. Flow cytometry samples were taken 30 min after the bioconversion was initiated and 50,000 events were analyzed.

5.2.1.2. Product toxicity

Flow cytometric analysis of samples taken from the shake flask reactions 30 min after the initiation of the bioconversion with 0.5 gL^{-1} substrate and 10 gL^{-1} glycerol in the presence of different concentrations of the product, the chemical lactone, 1S 5R 2-oxabicyclo [3.3.0] oct- 6-en-3-one, showed that there was a change in cellular physiology and

metabolic status in response to exposure to the product (Figure 5.3). Flow cytometric analysis of the control reaction (no product) showed that after 30 min 89.0% of the cells were intact and viable, 3.50% were metabolically stressed showing signs of membrane depolarization and 6.30% were dead. Cell viability 30 min post bioconversion initiation remained greater than 85.0% at all product concentrations, depolarized cells peaked at 9.70% and dead cells reached a maximum of 5.12%. Increasing levels of metabolic stress, indicated by an increasing population of depolarised cells, was observed (Figure 5.3 B, D, F, H, J & I). This decrease in cell viability was found to be time dependent and not observed until 2h post bioconversion initiation at all product concentrations. This trend conforms to the opinion that even minute amounts of bioconversion products may lead to whole cell biocatalyst quality being compromised.

Enzyme activity characterized by the rate of substrate depletion in the presence of increasing concentrations of the product, the chemical lactone, 1S 5R 2-oxabicyclo [3.3.0] oct- 6-en-3-one was observed at all product concentrations albeit to varying degrees (Figure 5.4). Product formation rates peaked in the presence of 0.5 gL^{-1} product at 1.49 $gL^{-1}h^{-1}$, enzyme activity was at its best between 0.2 gL^{-1} and 0.5 gL^{-1} product concentration, after which it declined steadily, reaching a low of 0.09 gL^{-1} h^{-1} when product concentration was at 10 gL^{-1}. Thus CHMO activity was demonstrated to be susceptible to product concentration associated inhibition.

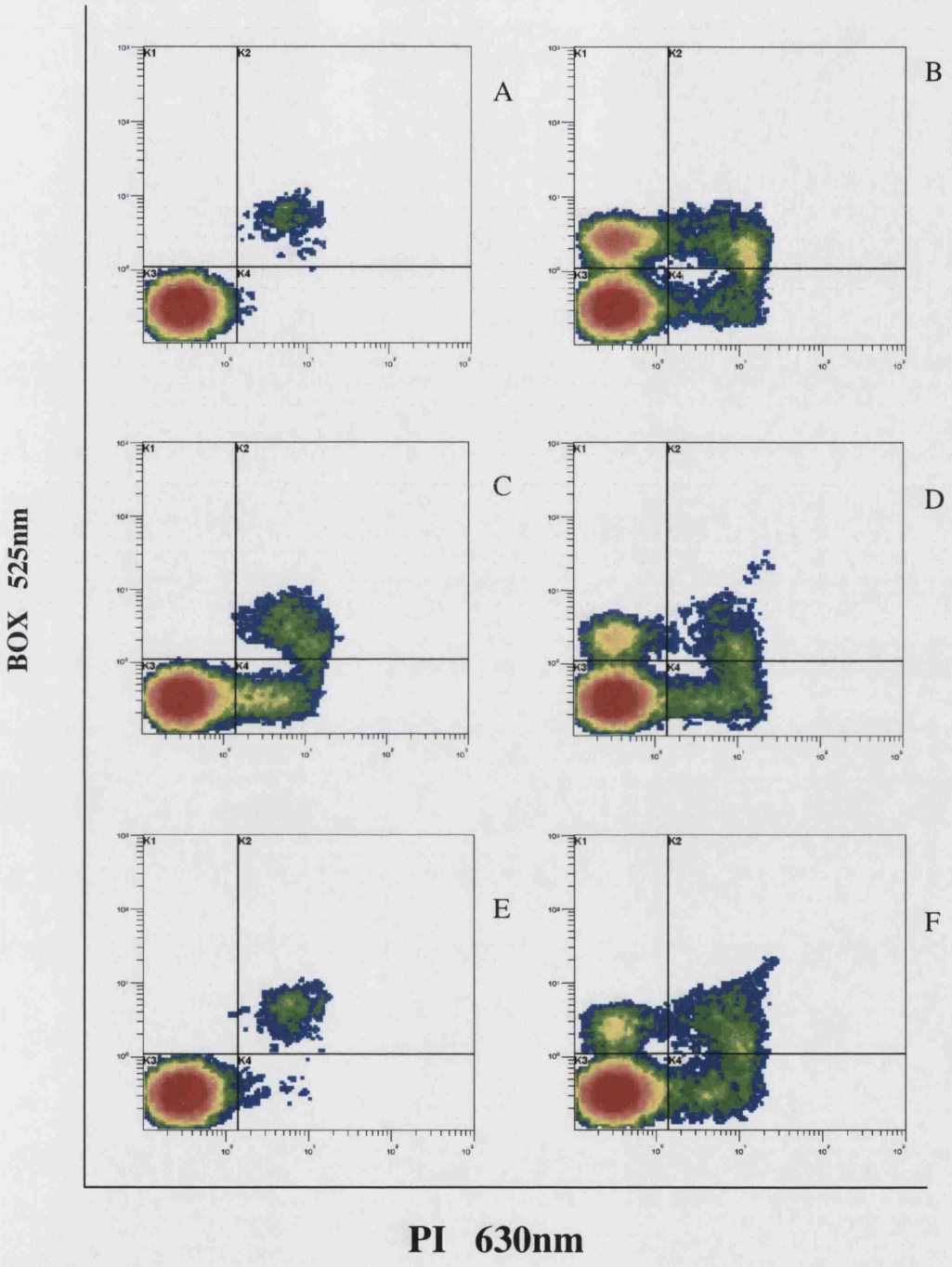

Figure 5.3. Flow cytometric density plots of *E.coli* TOP10 pQR239 in the presence of different concentrations of the chemical lactone, 1S 5R 2-oxabicyclo [3.3.0] oct- 6-en-3-one. 0.2 gL^{-1} at 30 (A) and 240 (B) min post exposure. 0.5 gL^{-1} at 30 (C) and 240 (D) min post exposure. 1.0 gL^{-1} at 30 (E) and 240 (F) min post exposure. 50,000 events were analyzed.

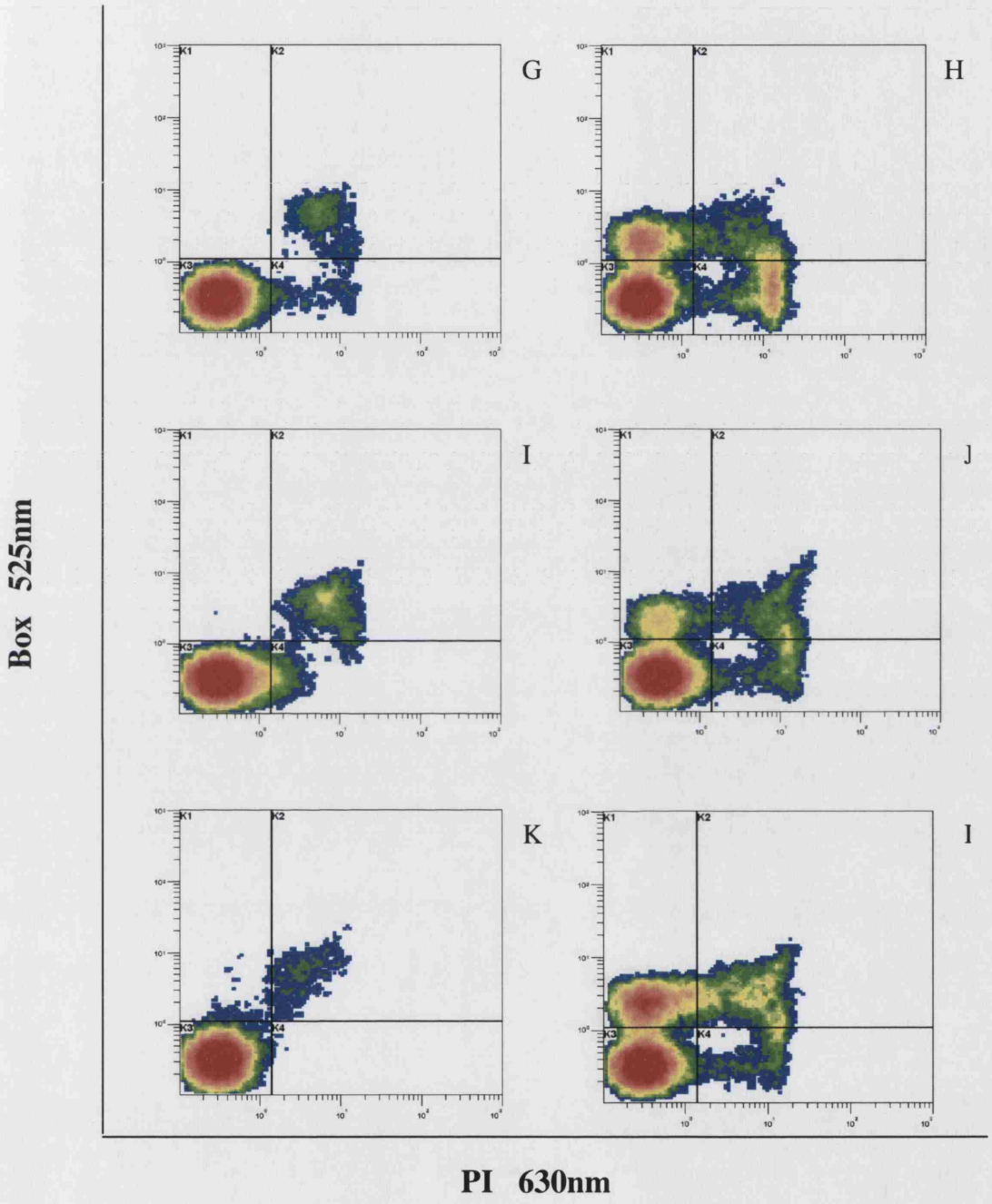

Figure 5.3 continued. Flow cytometric density plots of *E.coli* TOP10 pQR239 in the presence of different concentrations of the chemical lactone, 1S 5R 2-oxabicyclo [3.3.0] oct- 6-en-3-one. 2.0 gL^{-1} at 30 (G) and 240 (H) min post exposure, 3.0 gL^{-1} at 30 (I) and 240 (J) min post exposure, 4.0 gL^{-1} at 30 (K) and 240 (L) min post exposure. 50,000 events were analyzed.

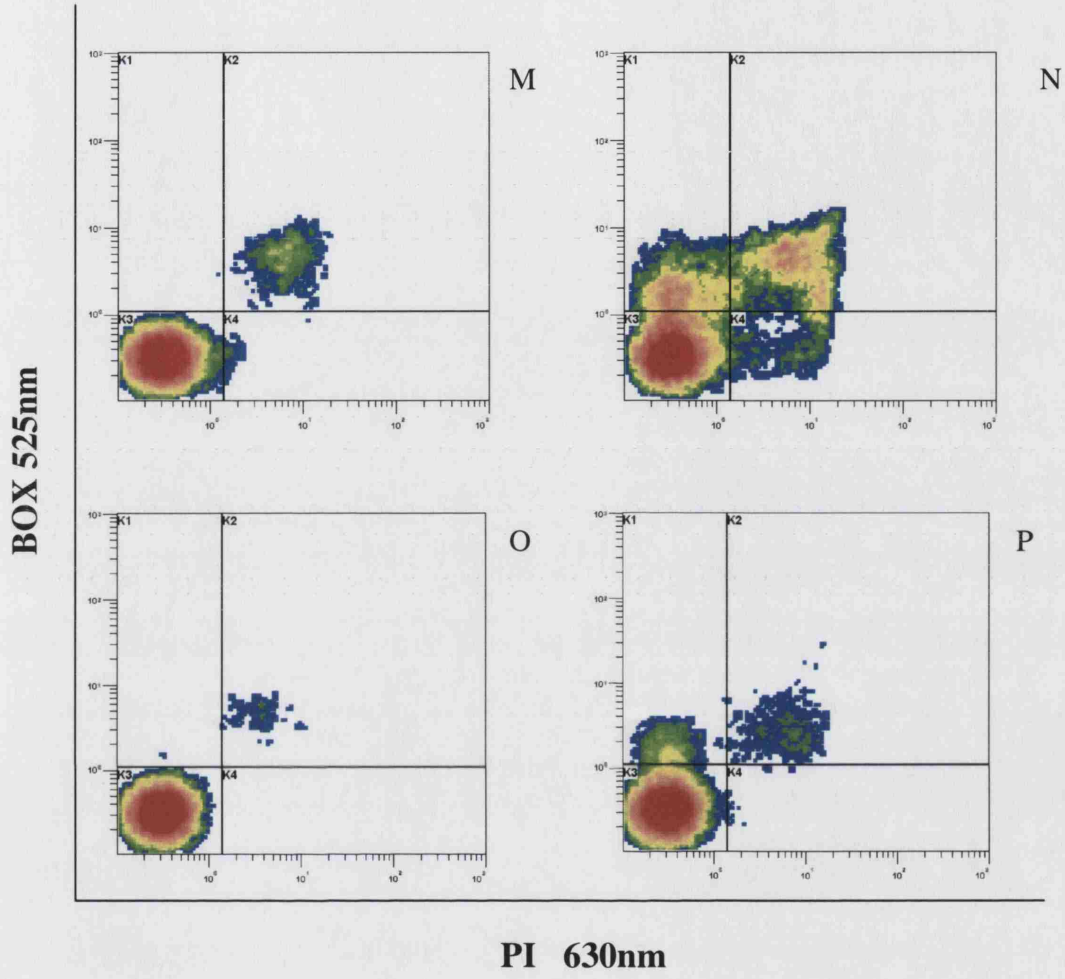

Figure 5.3 continued. Flow cytometric density plots of *E.coli* TOP10 pQR239 in the presence of different concentrations of the chemical lactone, 1S 5R 2-oxabicyclo [3.3.0] oct- 6-en-3-one. 5.0 gL^{-1} at 30 (M) and 240 (N) min post exposure, 0.2 gL^{-1} substrate and no product at 30 (O) and 240 (P) min post exposure. 50,000 events were analyzed.

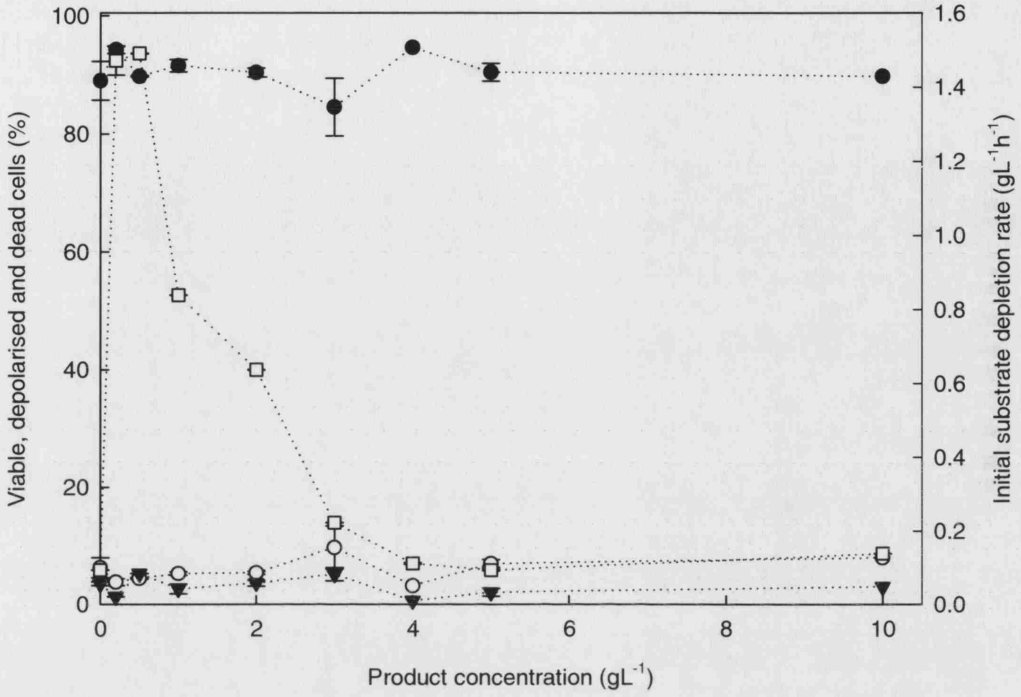

Figure 5.4. Cellular status (viable●, depolarized▼ and dead ○) and initial substrate depletion rate (□), profiles of *E.coli* TOP10 pQR239 at different product concentrations during shake flask bioconversions with 0.2 gL^{-1} of bicyclo (3.2.0.) hept-2-en-6-one. Flow cytometry samples were taken 30 min after the bioconversion was initiated. 50,000 events were analyzed via flow cytometry.

5.2.2. Control fermentations, 5L bioreactor scale

The whole cell biocatalyst *E.coli* TOP10 pQR239 was cultured in a 20L fermenter, 15L working volume, and the status of the whole cell biocatalyst in terms of cellular physiology and metabolism, enzyme activity and cellular respiration monitored over a 10 h period which constituted the 6 h fermentation and 4 h bioconversion periods. Cell viability was monitored using multi-parameter flow cytometry. Cell respiration during the fermentation and bioconversion period was charted by recording the DOT, CER and OUR, to establish the typical cell respiration profile. Whole cell biocatalyst working

biomass was normalised at $10gL^{-1}$ (Appendix IV). Enzyme activity under non-reacting conditions was assessed via GC analysis of initial product formation in small scale bioconversion reactions.

5.2.2.1. Flow cytometric analysis

Flow cytometric analysis of the whole cell biocatalyst during the fermentation was carried out to investigate the cellular quality over the 10 h period. The cells were stained with a combination of PI and BOX prior to analysis. This enabled the cells to be separated on the basis of viability and membrane integrity. The flow cytometric density plots can be seen in Figure 5.5.

At inoculation (t = 0) 96% of the cell population were viable, these cells had been incubated over night in modified LB with 400 mgL^{-1} ampicillin, at 37°C; 0.5% were depolarized and the remaining dead (Figure 5.5A). However 1h later the percentage of viable cells had decreased to 76.5% and the depolarized population had also increased significantly to 4%. Following a peak in cell viability 3 hours after growth of 90%, cell viability remained relatively stable for the remaining 7 hours at 90% ±5. The percentage of dead cells was lowest at just prior to induction (3%) this increased steadily to account for 8% of the population at the end of the fermentation. The percentage of depolarized cells within the population remained relatively low and constant post induction at 2%± 0.6, suggesting a low incidence of metabolic stress within the cell population. Cellular debris accounted for the remaining 3.5% of the events recorded from the flow cytometric analysis. Figure 5.6 shows the distribution of viable, depolarized and dead cells over the 10 h period.

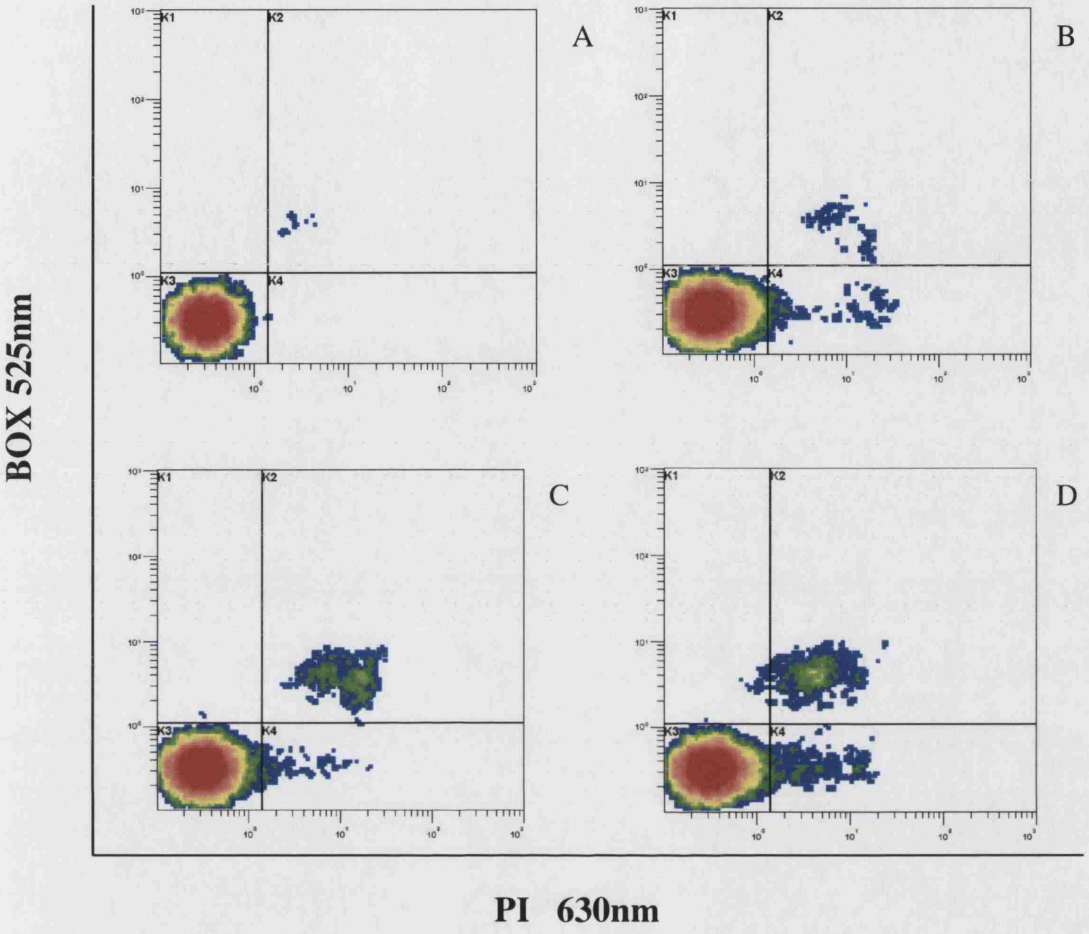

Figure 5.5. Flow cytometric density plots of flow cytometric analysis of *E.coli* TOP10 pQR239 during 10 h fermentation under standard culture conditions. Cells were stained with a combination of PI and BOX. Inoculum (A); pre-induction (B) (3h culture age); 3h post induction (C) (6h culture age); 10h culture age (D). 50,000 events were analyzed. No substrate or co-substrate was added to the system.

5.2.2.2. Enzyme activity assay

50 ml shake flask bioconversions were carried out with 1.0 gL^{-1} substrate and 10 gL^{-1} glycerol to investigate the presence and efficiency of the CHMO enzyme during the fermentation; the findings are shown in Figure 5.6. Pre induction the rate of enzyme

activity was found to be 4.9 gL^{-1} h^{-1}; this activity suggests that there is some basal expression of the CHMO gene in plasmid pQR239. Following induction enzyme activity increased exponentially for 2 hours, after which enzyme activity remained relatively stable at 7.2 ± 0.5 gL^{-1} h^{-1} until an hour before the fermentation was terminated, when enzyme activity dipped to a low of 6.2 $gL^{-1}h^{-1}$. CHMO was found to be still active 7 hours post induction, when the bioconversion would normally be terminated, at a reasonably consistent rate. This corresponded to the relative stability in cell quality recorded for non-reacting cells (Figure 5.6).

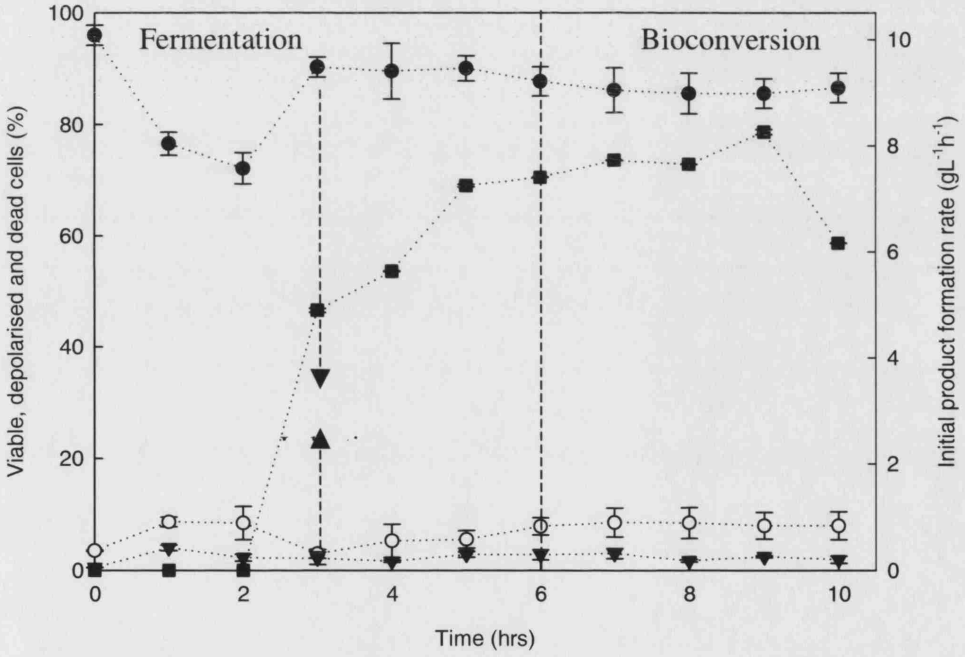

Figure 5.6. Cellular status (viable●, depolarized▼ and dead ○) and enzyme activity (■) profiles of *E.coli* TOP10 pQR239 during a 10 h fermentation. 50,000 events were analyzed via flow cytometry. No substrate or co-substrate was added to the system.

5.2.2.3. Cell respiration profiles

Following inoculation of the fermenter with a 10% of the final volume overnight seed culture, the DOT within the vessel began to slowly decrease as cell proliferation began to occur, finally reaching zero after approximately 3 hours growth (late exponential phase). (Figure 5.7) At this point CHMO production by the whole cell biocatalyst was induced by the addition of L-arabinose, subsequently the DOT remained at zero for a further 3.5 h suggesting that during this time all the oxygen within the vessel was being utilized by the cells, which had entered the stationary phase. Typically the cells would be harvested at the end of the fermentation step and/or the bioconversion initiated with the DOT at zero after approximately 6 hours growth when a cell density of 10 gL^{-1} (Appendix IV) had been achieved and the cells were in the stationary phase. Over the course of the next four hours the DOT within the vessel slowly increased demonstrating a slow down in cellular respiration.

The oxygen uptake and carbon-dioxide evolution rates (OUR and CER), both show a steady exponential increase during the first 3 hours of the fermentation after which they both stabilized at ~50 $mmolL^{-1}h^{-1}$ for the next 5 hours (Figure 5.7). OUR and CER rates were almost identical.

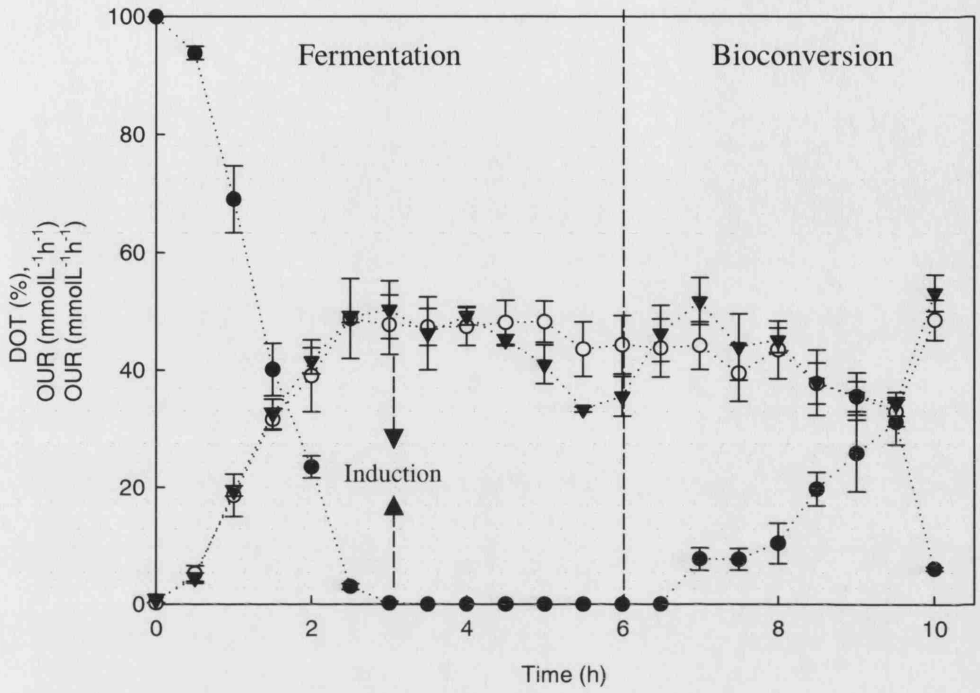

Figure 5.7. Cell respiration profile of *E.coli* TOP10 pQR239 showing the DOT (●), OUR (○), and CER (▼) over a 10 h period; corresponding to the combined fermentation and bioconversion period. No substrate or co-substrate was added to the system.

5.2.3. Bioconversion reaction: Substrate toxicity, 5L bioreactor scale

The shake flask experiments were used primarily to determine the concentrations at which the whole cell biocatalyst was least susceptible to physiological damage and possible inhibitory effects on CHMO. Substrate toxicity studies were carried out a larger scale in order to further investigate these conditions under fed-batch conditions which would allow substrate levels to be kept constant i.e. any substrate used would be replenished and also permit monitoring of cell respiration during the bioconversion. This set of experiments were carried out to investigate the effects of different substrate concentrations on whole cell viability and enzyme activity. Previous studies by Doig *et al*

2003, 2003 and Zambianchi *et al* 2002 have identified substrate inhibition as one of the key limitations of this bioconversion.

The whole cell biocatalyst was expected to show a decrease in cell viability as substrate concentration increases. This in turn was expected to result in a decrease in enzyme activity. Bioconversion reactions where substrate concentrations were varied, while maintaining set reaction parameters (e.g temperature, pH and co-substrate concentration) were used to investigate substrate-whole cell and enzyme- substrate interactiona, via multiparameter flow cytometry and GC analysis respectively. Substrate was fed into the bioreactor at the rates of 0.5, 1.0, 5 and 10 $gL^{-1}h^{-1}$. The results presented in this section support the hypothesis that cell viability is compromised by increasing substrate concentrations, the manner of which is illustrated by multiparameter flow cytometry (see Figures 5.8-5.12). This indicates that whole cell biocatalyst viability is also a key limitation to the reaction.

5.2.3.1. Flow cytometric analysis

The first experiment was with 10 gL^{-1} glycerol and no substrate. This experiment was used to determine how the whole cell biocatalyst behaved in the absence of the substrate but with the co-substrate present. Flow cytometric analysis, following staining with PI and BOX show the status of the cells during the bioconversion period. The density plots for this can be seen in Figure 5.8. At initiation of the bioconversion 85.6% of the cell population was found to be viable, half way through the bioconversion period this figure had decreased slightly to 84.1% and had dropped to 79.5% by the end of the bioconversion. However, the density plots show a significant proportion of the events analyzed to be cellular debris and free nucleic material, this can be seen in the LL quadrant of the density plots in Figure 5.8.

The substrate was then added into the bioreactor at the rate of 0.5 gL^{-1} h^{-1}. This concentration had previously been established as sub-inhibitory from batch shake flask

bioconversions. Flow cytometric analysis showed that the whole cell biocatalyst exhibited minimal levels of cellular damage under these conditions; this is shown in Figure 5.9. A 10% total decrease in cell viability was recorded during the bioconversion.

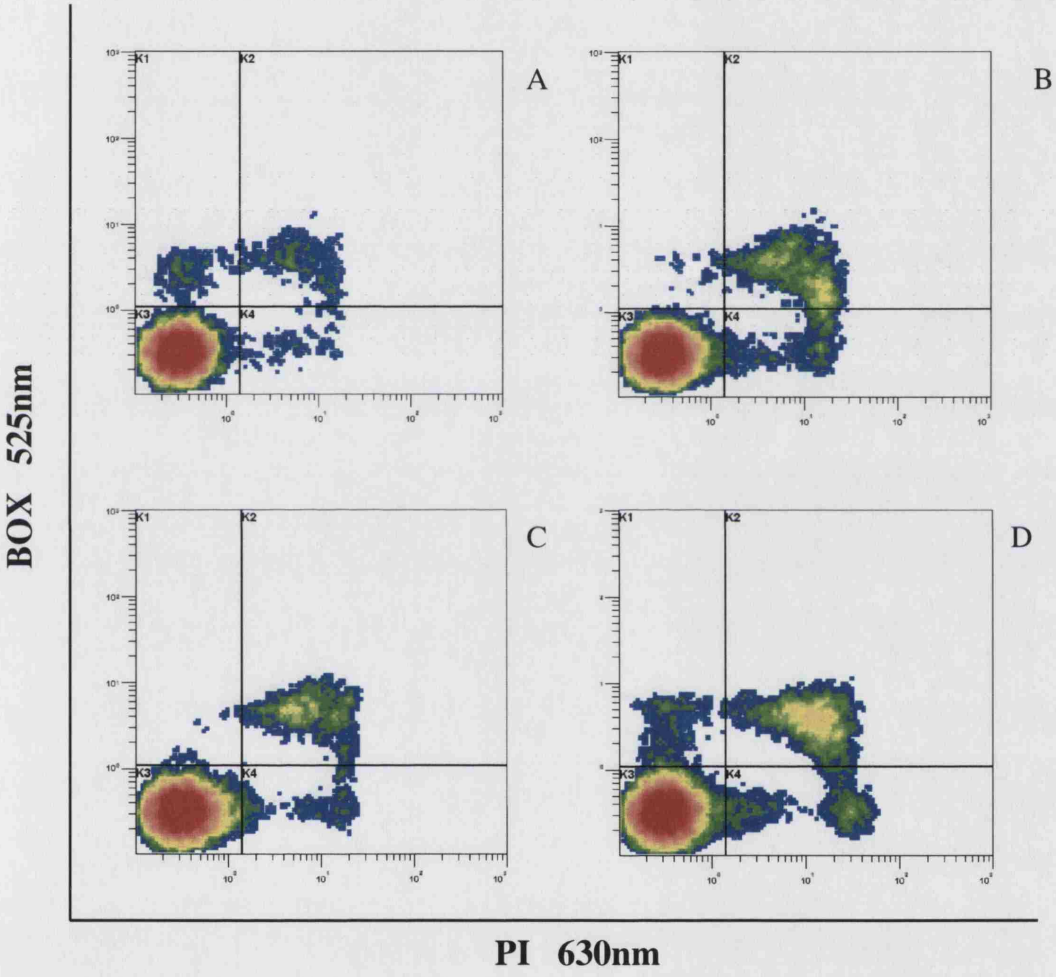

Figure 5.8. Flow cytometric density plots of *E.coli* TOP10 pQR239 under bioconversion conditions in the absence of substrate. 0 min (A), 30 min (B), 120 min (C), 240 min (D). 50,000 events were analyzed.

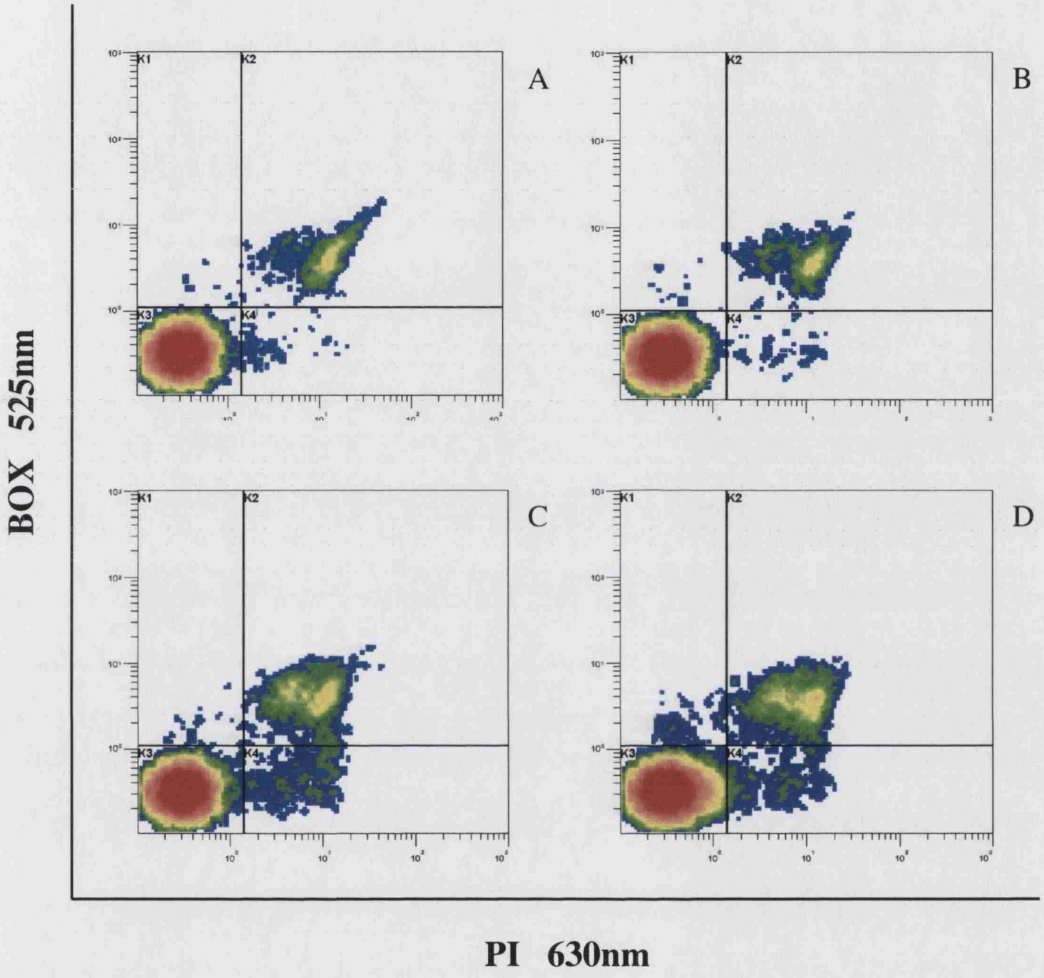

Figure 5.9. Flow cytometric density plots of *E.coli* TOP10 pQR239 under bioconversion conditions, with 0.5 gL^{-1} h^{-1} substrate feed and 10 gL^{-1} glycerol. 0 min (A), 30 min (B), 120 min (C), 240 min (D). 50,000 events were analyzed.

Flow cytometric analysis, depicted in Figure 5.10, shows the pattern of cell deterioration during the bioconversion with 1gL^{-1} h^{-1} substrate. When the bioconversion was initiated

90% of the cells were viable, this dropped by ~8% halfway through the bioconversion and finally reached 74.5% at the end. Halfway through the bioconversion a percentage of the cells showed signs of metabolic stress and stained positively for BOX only, possibly as a consequence of product accumulation. This sub-population is located in the UL quadrant of density plots C and D (120 and 240 min post bioconversion initiation). The percentage of cellular debris and free nucleic acids also increases over the bioconversion period.

When higher concentrations of substrate were fed into the bioconversion vessel the whole cell biocatalyst behaved in a completely different manner. At a substrate feed of 5 gL^{-1} h^{-1} cell viability became severely compromised almost as soon as the bioconversion was initiated; this is shown in Figure 5.11. After the first half hour it became apparent that a significant proportion of the cells were experiencing metabolic stress; this population increased exponentially after the first 2 h of the bioconversion. This was indicated by the steady increase in the percentage of the population which stained positively for BOX only, UL quadrant of density plots C and D in Figure 5.11. The percentage of viable intact cells decreased steadily until 150 min post bioconversion initiation and then stabilized at 27.9%. For dead cells the reverse occurred, with the percentage of dead cells within the population peaking at 38.1% at the same time point.

Flow cytometric analysis of *E.coli* TOP10 pQR239 subjected to a 10 $gL^{-1}h^{-1}$ substrate feed also showed severe damage to the whole cell biocatalyst in comparison to the bioconversion in the absence of substrate and those with lower substrate concentrations. Figure 5.12, of the flow cytometric analysis, shows that cell mortality was rapid and occurred at very high percentages, being >75% in the first 30 min of the bioconversion and reaching a high of almost 90% by the end of the conversion. At this substrate concentration metabolic stress was not apparent, suggesting that cell death was close to instantaneous.

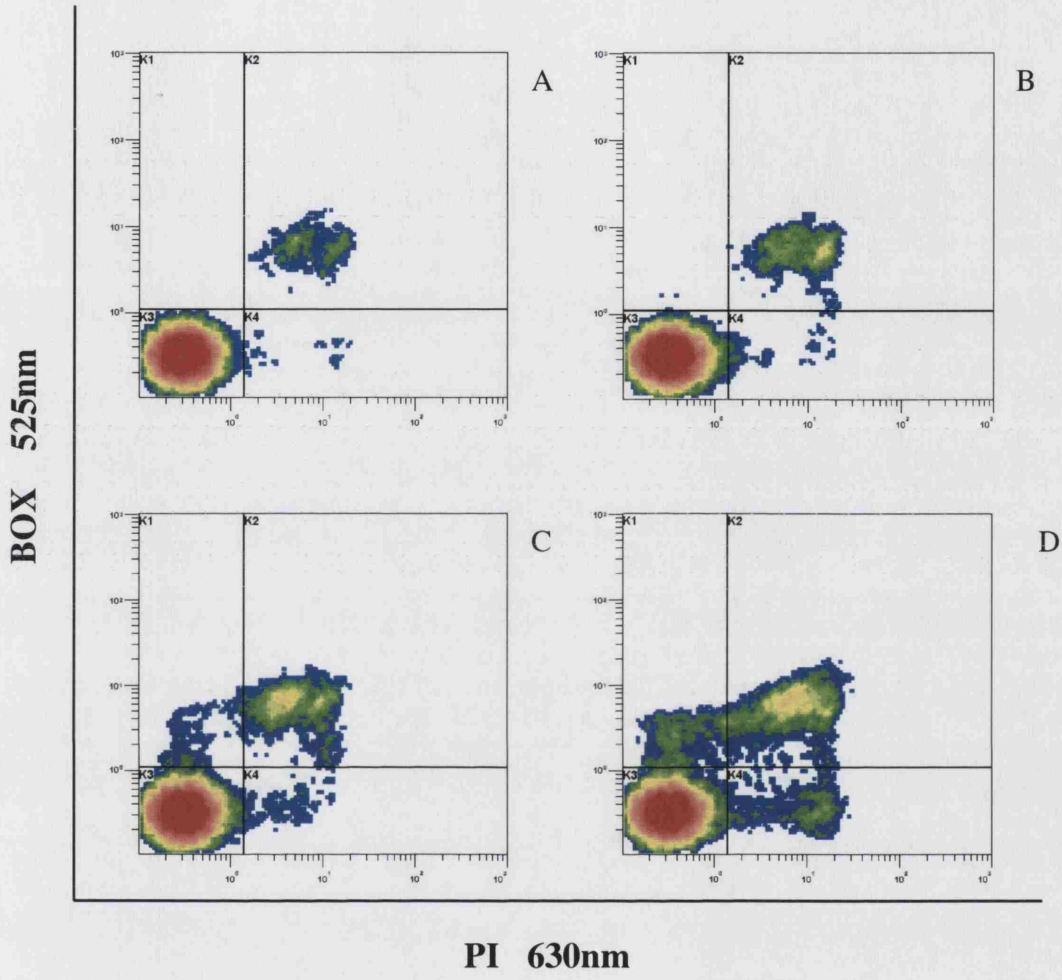

Figure 5.10. Flow cytometric density plots of *E.coli* TOP10 pQR239 under bioconversion conditions, with 1.0 gL^{-1} h^{-1} substrate feed and 10 gL^{-1} glycerol. 0 min (A), 30 min (B), 120 min (C), 240 min (D). 50,000 events were analyzed.

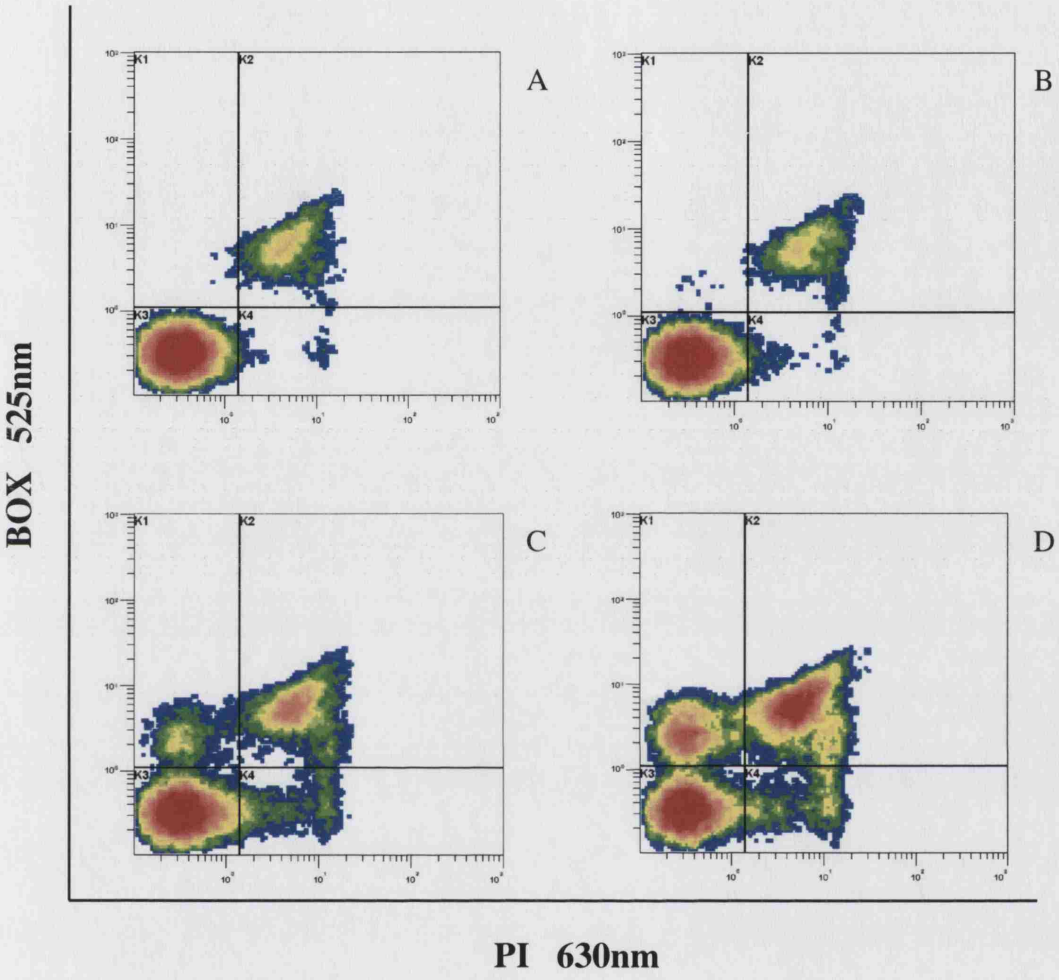

Figure 5.11. Flow cytometric density plots of *E.coli* TOP10 pQR239 under bioconversion conditions, with 5.0 gL^{-1} h^{-1} substrate feed and 10 gL^{-1} glycerol. 0 min (A), 30 min (B), 120 min (C), 240 min (D). 50,000 events were analyzed.

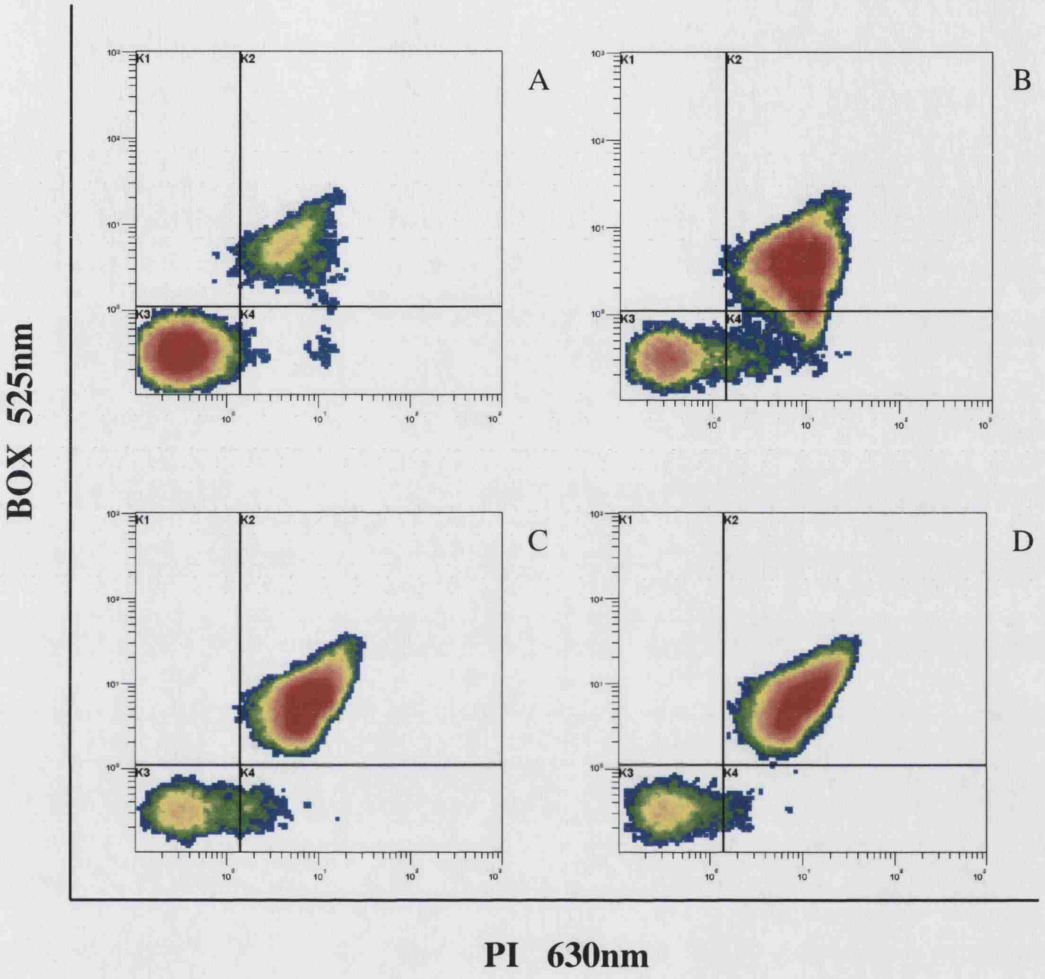

Figure 5.12. Flow cytometric density plots of *E.coli* TOP10 pQR239 under bioconversion conditions, with 10.0 gL^{-1} h^{-1} substrate feed and 10 gL^{-1} glycerol. 0 min (A), 30 min (B), 120 min (C), 240 min (D). 50,000 events were analyzed.

5.2.3.2. Enzyme activity assay

Elevated substrate concentrations can significantly affect enzyme activity. However, enzyme activity was recorded at all substrate concentrations but varied with respect to the substrate concentrations being investigated. During the course of each experiment enzyme activity was measured by GC analysis of samples taken from the bioconversion vessel at regular intervals. The enzyme activity profiles chart the increase in accumulated product concentration with the corresponding levels of substrate present in the system and can be seen in Figures 5.13 to 5.17. These figures also show cellular status profiles under the said conditions.

Figure 5.13 depicts the cellular status of *E.coli* TOP10 pQR239 in the absence of the substrate. No enzymatic activity was screened for, on account of the substrate being excluded. Product formation was recorded when the substrate was fed into the bioreactor at 0.5 $gL^{-1}h^{-1}$. This is shown in Figure 5.14. This concentration was assumed to be sub-inhibitory to enzyme activity. Substrate accumulation occurred slowly, suggesting a rapid conversion rate. The total accumulated product was very high at 4.4 gL^{-1}, this further supports the theory that this substrate feed rate is non inhibitory to enzyme activity.

At 1.0 $gL^{-1}h^{-1}$ substrate feed the enzyme activity was rapid with product accumulation occurring exponentially; however the accumulated product concentration was significantly lower than the value recorded at 0.5 $gL^{-1}h^{-1}$ at ~2gL^{-1}. This data is shown in Figure 5.15. 5 and 10 $gL^{-1}h^{-1}$ substrate feeds showed very little enzyme activity. Accumulated product concentrations in both cases reached a maximum of just 0.09 gL^{-1} and 0.03 gL^{-1} respectively. This suggests a severe disruption of enzyme activity as a consequence of substrate inhibition and decreased cell quality (section 5.2.3.1)

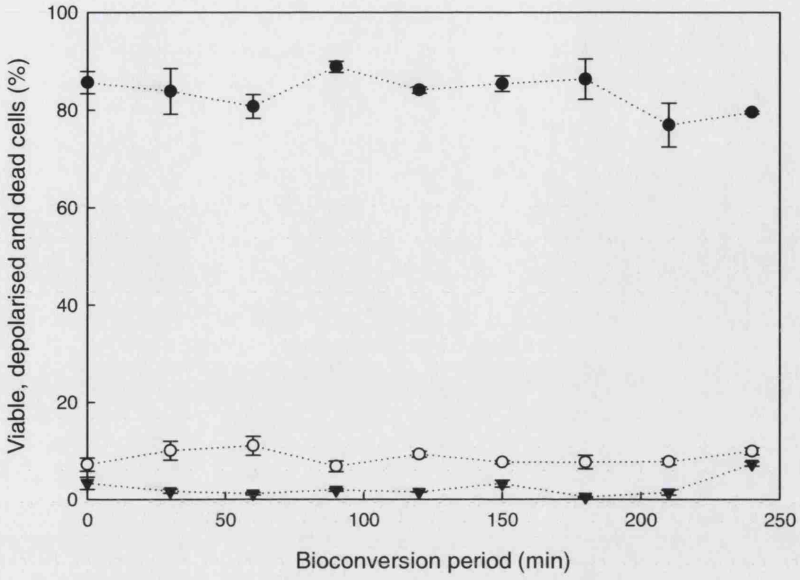

Figure 5.13. Cellular status of *E.coli* TOP10 pQR239 (● viable cells, ○ dead cells, ▼ depolarized cells), during the bioconversion period in the absence of substrate. Glycerol was added at a concentration of 10 gL^{-1}.

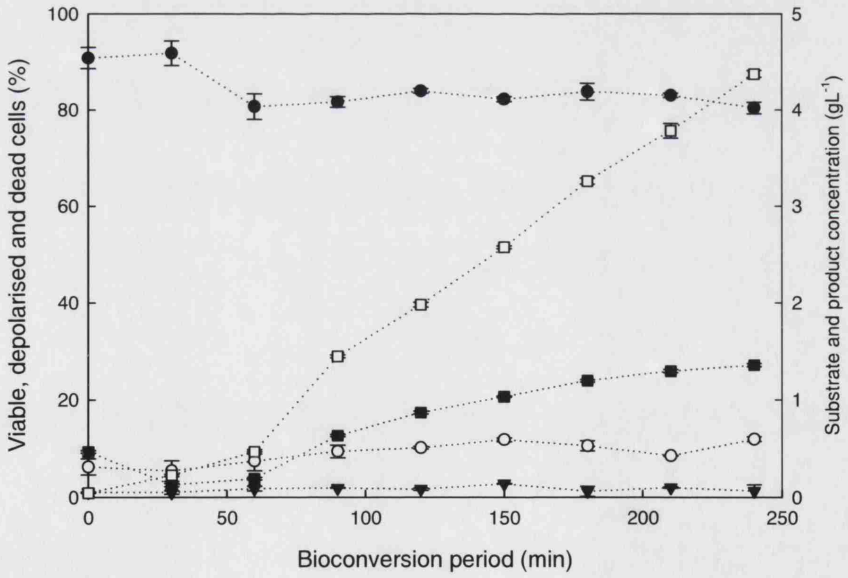

Figure 5.14. Product accumulation (□), substrate concentration (■) and cellular status of *E.coli* TOP10 pQR239 (● viable cells, ○ dead cells, ▼ depolarized cells), during a bioconversion with 0.5 gL^{-1} h^{-1} substrate feed. Glycerol was added at a concentration of 10 gL^{-1}.

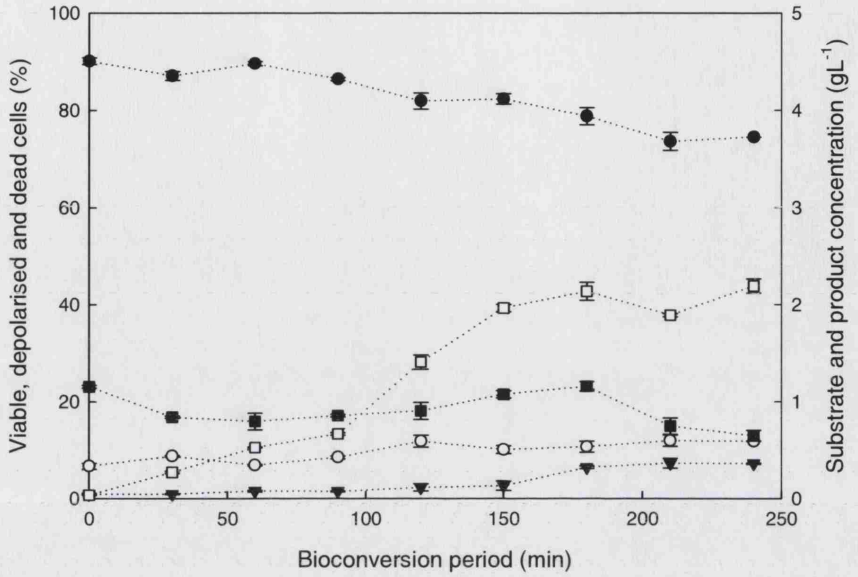

Figure 5.15. Product accumulation (□), substrate concentration (■) and cellular status of *E.coli* TOP10 pQR239 (● viable cells, ○ dead cells, ▼ depolarized cells), during a bioconversion with 1.0 gL^{-1} h^{-1} substrate feed. Glycerol was added at a concentration of 10 gL^{-1}.

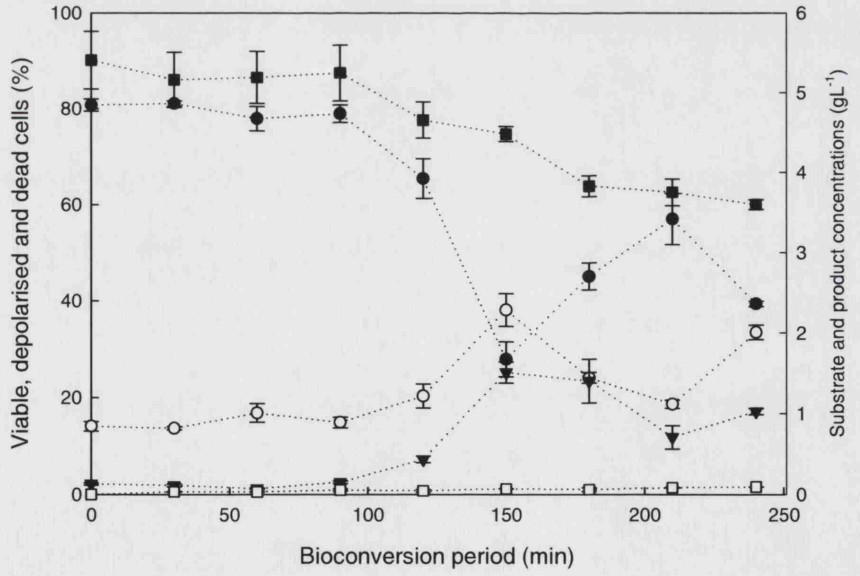

Figure 5.16. Product accumulation (□), substrate concentration (■) and cellular status of *E.coli* TOP10 pQR239 (● viable cells, ○ dead cells, ▼ depolarized cells), during a bioconversion with 5.0 gL^{-1} h^{-1} substrate feed. Glycerol was added at a concentration of 10 gL^{-1}.

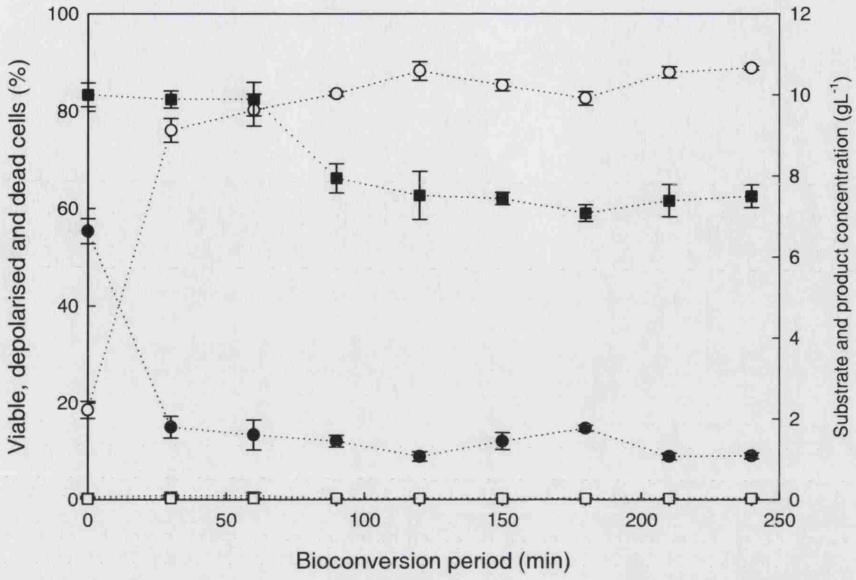

Figure 5.17. Product accumulation (□), substrate concentration (■) and cellular status of *E.coli* TOP10 pQR239 (● viable cells, ○ dead cells, ▼ depolarized cells), during a bioconversion with 10.0 gL^{-1} h^{-1} substrate feed. Glycerol was added at a concentration of 10 gL^{-1}.

5.2.3.3. Cellular respiration profiles

Microbial respiratory patterns during the fermentation or biocatalytic process can provide some insight into how viable the cells are within the said environment. Dissolved oxygen tension (DOT) measurements provided a measure of the percentage of available oxygen dissolved in the process media during the bioconversion (or fermentation process). Oxygen uptake and carbon dioxide evolution rates (OUR and CER) measurements taken from the exit gases from the bioconversion vessel gave an indication of cellular respiration. Resting cells would be characterized by no or extremely low CER and OUR levels as cell respiration would be minimal. If cells are in the stationary phase the amount of oxygen taken up would equal the amount of carbon dioxide being produced by the cells. The respiration patterns of *E.coli* TOP10 pQR239 during the bioconversion when

different rates of substrate were fed into the system are shown in the graphs in Figure 5.18 to 5.22.

In the absence of any substrate, the DOT remained relatively low, less than 5% over the 4 h bioconversion duration. The increase in CER observed at ~180min into the bioconversion may be attributed to depleting glycerol concentrations in the media. This is portrayed in Figure 5.18.

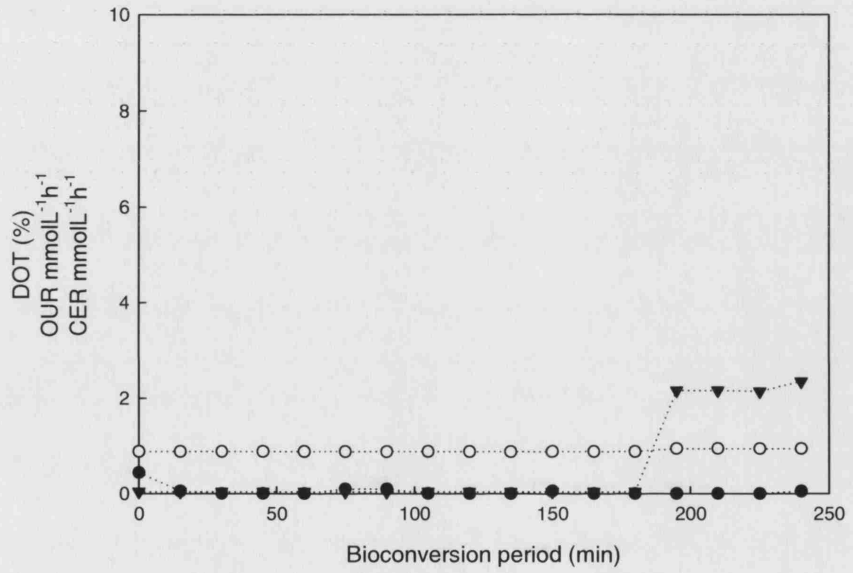

Figure 5.18. Cell respiration profile of *E.coli* TOP10 pQR239 showing the DOT (•), OUR (○), and CER (▼) during the bioconversion period in the absence of substrate. Glycerol was added at a concentration of 10 gL^{-1}.

The addition of the substrate at a rate of 0.5 gL^{-1} h^{-1} resulted in higher OUR and CER measurements. These are illustrated in Figure 5.19. OUR was found to range between 31 and 50 $mmolL^{-1}h^{-1}$ and CER between 21 and 40 $mmolL^{-1}$ h^{-1} this was significantly higher than the OUR of <1 and CER of <1.5 $mmolL^{-1}$ h^{-1} recorded in the absence of substrate.

The DOT remained at zero for the duration of the bioconversion. The profile suggests that the cells were still undergoing active respiration despite also carrying out the bioconversion. It may be that the substrate levels were too low to significantly impact normal cellular respiration.

When the substrate feed rate was doubled the cell respiration profile was very different; DOT remained less than 1 and OUR and CER were ~ 1 $mmolL^{-1}$ h^{-1} for the entire duration of the bioconversion. This is illustrated in Figure 5.20.

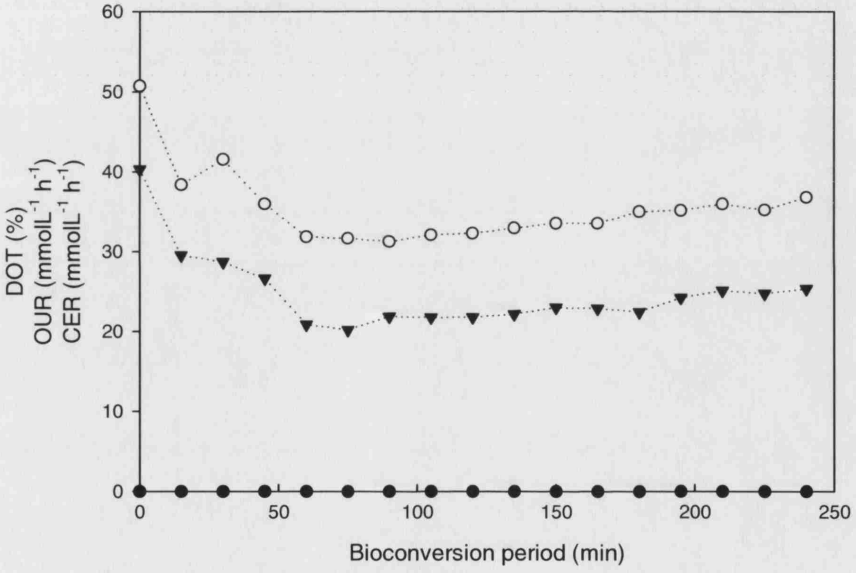

Figure 5.19. Cell respiration profile of *E.coli* TOP10 pQR239 showing the DOT (•), OUR (○), and CER (▼) during the bioconversion period, when substrate is fed at a rate of 0.5 gL^{-1} h^{-1} and glycerol was added batch-wise at a concentration of 10gL^{-1}.

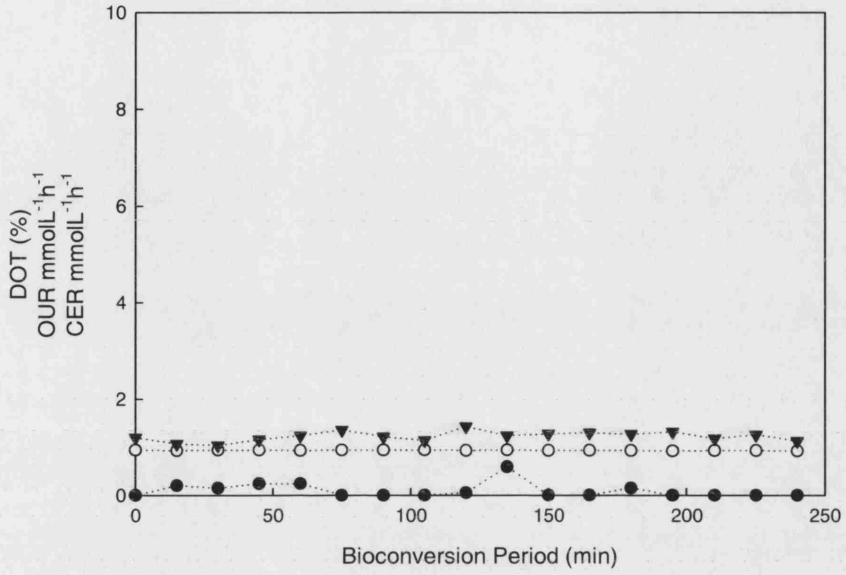

Figure 5.20. Cell respiration profile of *E.coli* TOP10 pQR239 showing the DOT (•), OUR (○), and CER (▼) during the bioconversion period, when substrate is fed at a rate of 1.0 gL^{-1} h^{-1} and glycerol was added at a concentration of $10gL^{-1}$.

Figure 5.21 shows the respiratory profile obtained when a five-fold increase in the rate of substrate feed, 5.0 gL^{-1} h^{-1}, was used. It shows a relatively high DOT level during the bioconversion, with the DOT remaining at ~ 60% for the entire duration. This is indicative of a slow down in cellular respiration, which results in high DOT levels within vessel, as the supplied oxygen is not being utilized. This slow down in respiration is further supported by the low OUR and CER recorded. It is also indicative of a severe retardation of biocatalytic activity; oxygen is required for enzyme activity.

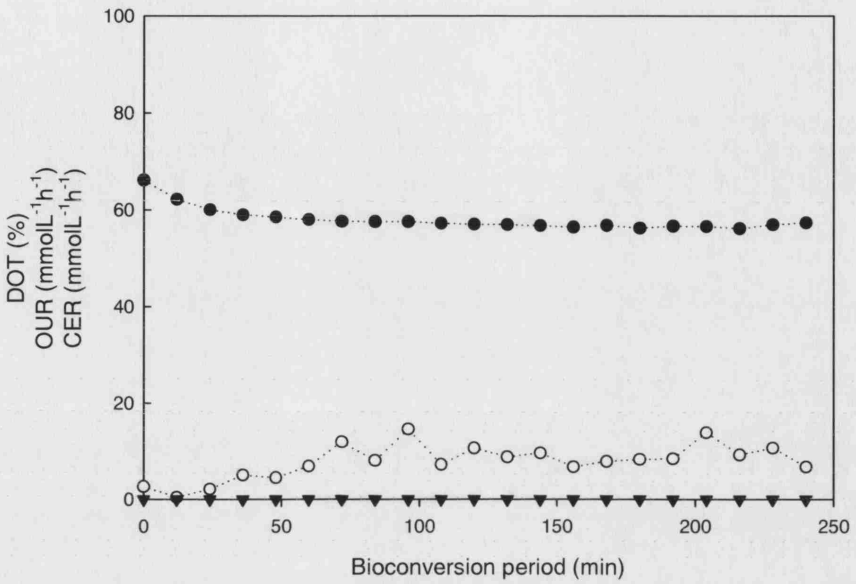

Figure 5.21. Cell respiration profile of *E.coli* TOP10 pQR239 showing the DOT (•), OUR (○), and CER (▼) during the bioconversion period, when substrate is fed at a rate of 5.0 gL^{-1} h^{-1} and glycerol was added at a concentration of 10gL^{-1}.

At 10 gL^{-1} h^{-1} substrate feed, the respiratory profile showed a low OUR and CER for the entire duration of the bioconversion. CER remained at zero and OUR fluctuated between 0.5 and 9 $mmolL^{-1}$ h^{-1}. This is illustrated in Figure 5.22. DOT began to increase exponentially 2 hours into the bioconversion, this continued until the end of the reaction and may be due to decreasing availability of a carbon source, possibly as a result of damage to transportation systems present in the cell membrane due to the high substrate concentrations.

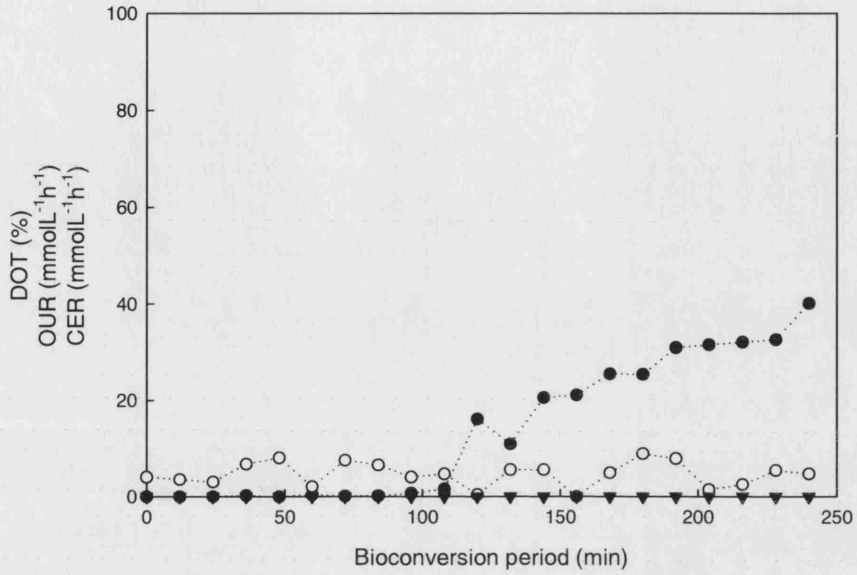

Figure 5.22. Cell respiration profile of *E.coli* TOP10 pQR239 showing the DOT (•), OUR (○), and CER (▼) during the bioconversion period, when substrate is fed at a rate of 10.0 gL^{-1} h^{-1} and glycerol was added at a concentration of 10gL^{-1}.

5.2.4. Co-substrate requirement investigations, 5L bioreactor scale

The co-substrate used in the BVMO mediated oxidation of bicyclo (3.2.0.) hept-2-en-6-one to yield (-)-1(S) 5(R)-2-oxabicyclo (3.3.0) oct-6-en-3-one and (-)1 (R)5(S)-3-oxabicyclo (3.3.0) oct-6-en-2-one was glycerol. This was used to drive the reaction via facilitating the regeneration of the co-factor, NADPH. A number of different concentrations of glycerol were investigated. These investigations were directed at: (a) the effects of glycerol concentrations on the metabolic and physiological status of the whole cell biocatalyst analyzed with flow cytometry and (b) the effects of glycerol concentrations on the activity of the CHMO enzyme, analyzed by measuring product accumulation by GC analysis. In 2003, Doig *et al* established that 5gL^{-1} glycerol was

sufficient for maximum enzyme activity. However the impact of the co-substrate on the viability and stability of the whole cell biocatalyst had not been previously examined. Sub-optimal co-substrate concentrations were not expected to hugely affect cell viability but were expected to impact enzyme activity. The results illustrated in this section show that this hypothesis was upheld, all investigated co-substrate concentrations resulted in similar low levels of cell viability and stability. Co-substrate availability was also shown to affect enzyme activity, the supply of glycerol at the utilisation rate was found to promote a high accumulated product concentration.

5.2.4.1. Flow cytometric analysis

Flow cytometric analysis, following dual staining with a combination of PI and BOX was used to visualize the effects of the different glycerol concentrations, and the absence of any additional glycerol, on *E.coli* TOP10 pQR239 during the BVMO mediated oxidation of bicyclo (3.2.0.) hept-2-en-6-one to yield (-)-1(S) 5(R)-2-oxabicyclo (3.3.0) oct-6-en-3-one and (-) 1 (R) 5(S)-3-oxabicyclo (3.3.0) oct-6-en-2-one. The absence of and different concentrations of glycerol all had an influence on the cells' metabolic and physiological status. Figures 5.23 to 5.27 illustrate the effects of these influences.

In Figure 5.23 the density plots are of *E.coli* TOP10 pQR239 in the absence of any additional glycerol undergoing the bioconversion reaction. The only glycerol present here is that which remained at the end of the fermentation step, approximately 6.7 gL^{-1}. The percentage of intact viable cells during this period was relatively high and remained stable at >85%, only a 5% drop in cell viability was recorded over the 4 h bioconversion period. Dead cells which stained positively for both stains (UR quadrants) remained constant at >10%. Membrane depolarization within the population was low, at >2.5% for the duration of the bioconversion.

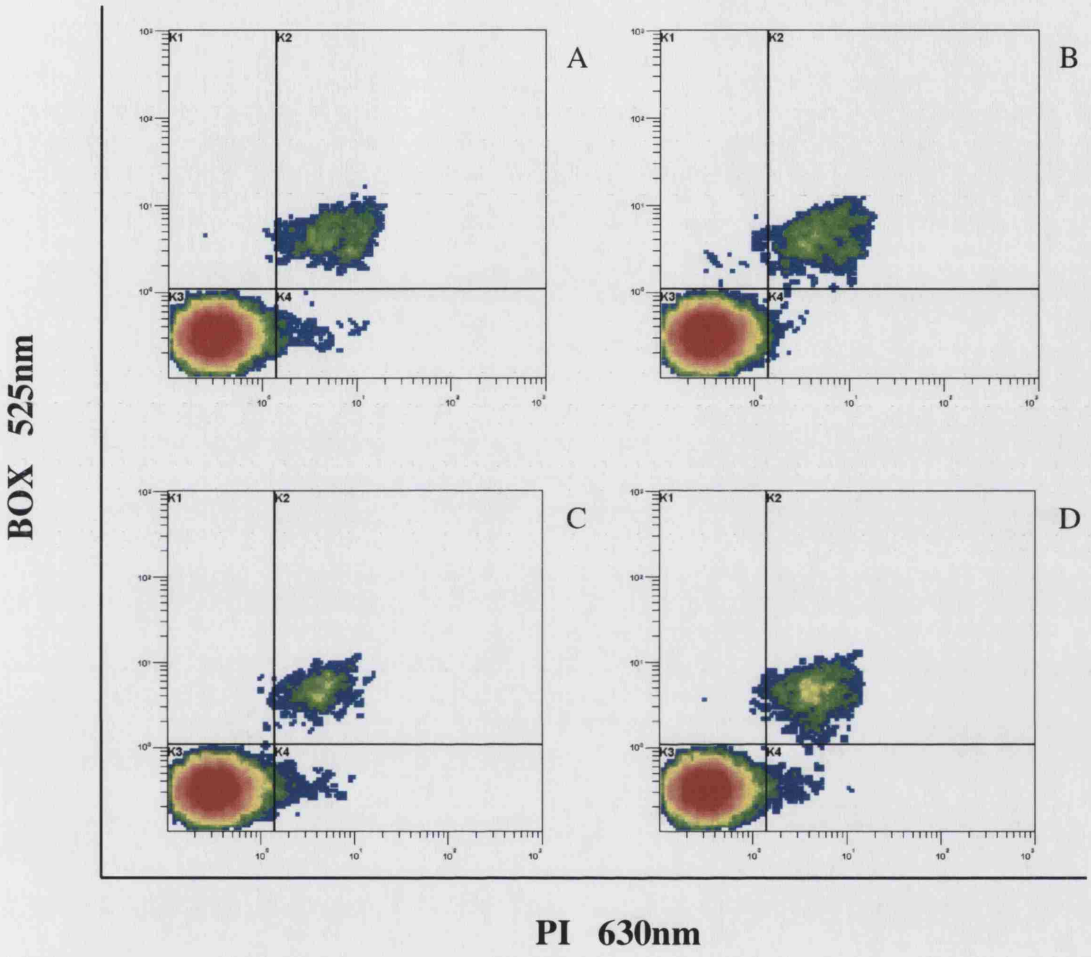

Figure 5.23. Flow cytometric density plots, 0 min (A), 30 min (B), 120 min (C), 240 min (D) of *E.coli* TOP10 pQR239 under bioconversion conditions, with 0.4 gL^{-1} h^{-1} substrate feed and no additional glycerol. 50,000 events were analyzed.

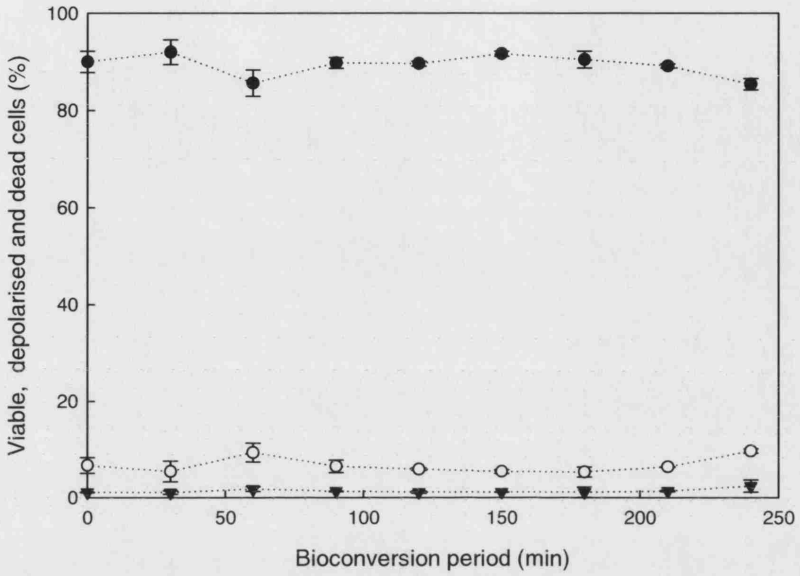

Figure 5.23 continued. Viable cells (●), dead cells (○), depolarized cells (▼), of *E.coli* TOP10 pQR239 under bioconversion conditions, with 0.4 gL^{-1} h^{-1} substrate feed and no additional glycerol. 50,000 events were analyzed.

When glycerol was added in batch into the system at a concentration of 10 gL^{-1} cell viability was comparable and slightly better than when glycerol was precluded, this is shown in Figure 5.24. The presence of glycerol at this concentration (10gL^{-1}) had no outstandingly adverse effects on the metabolic and physiological status of the whole cell biocatalyst. Cell viability was recorded at between 86 and 88% for the entire 4 h period and dead cells accounted for <7.5% of the population. Cells with depolarized membranes accounted for <2% of the population.

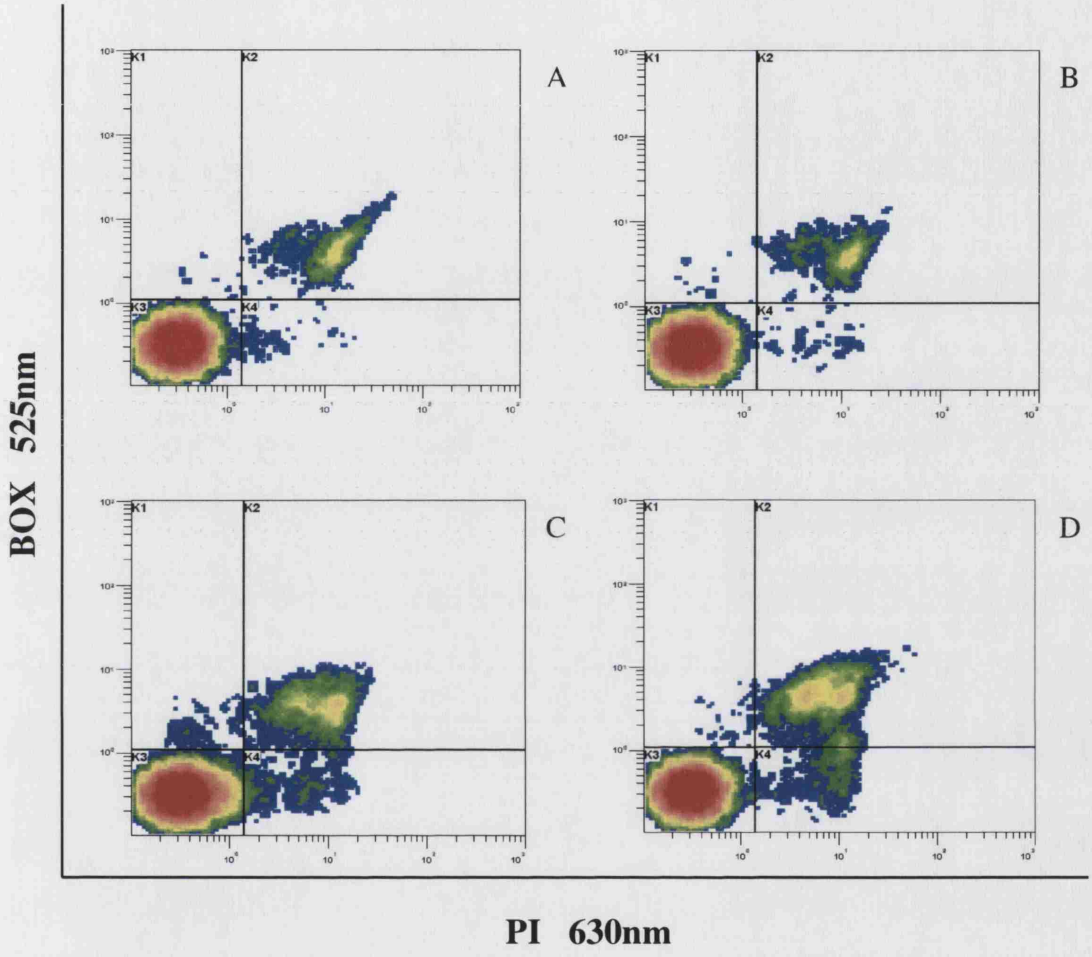

Figure 5.24. Flow cytometric density plots, 0 min (A), 30 min (B), 120 min (C), 240 min (D) of *E.coli* TOP10 pQR239 under bioconversion conditions, with 0.4 gL^{-1} h^{-1} substrate feed and 10 gL^{-1} glycerol batched in at initiation. 50,000 events were analyzed.

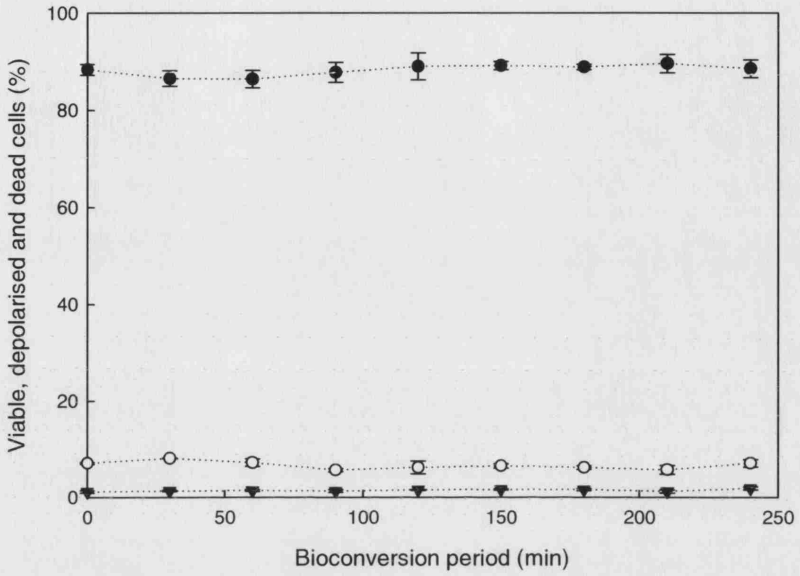

Figure 5.24 continued. Viable cells (●), dead cells (○), depolarized cells (▼), of *E.coli* TOP10 pQR239 under bioconversion conditions, with 0.4 gL^{-1} h^{-1} substrate feed and 10 gL^{-1} glycerol batched in at initiation. 50,000 events were analyzed.

Figure 5.25 shows the distribution of cells following flow cytometric analysis of cells when the co-substrate was fed into the reaction at a rate of 2.64 gL^{-1} h^{-1}, this correspond to the experimentally determined rate of glycerol consumption. A 12.7% decrease in cell viability along with an exponential increase in the percentage of dead cells to < 22% was recorded over the 4 h bioconversion period. Cells with depolarised cells made up ~2.9% of the cell population.

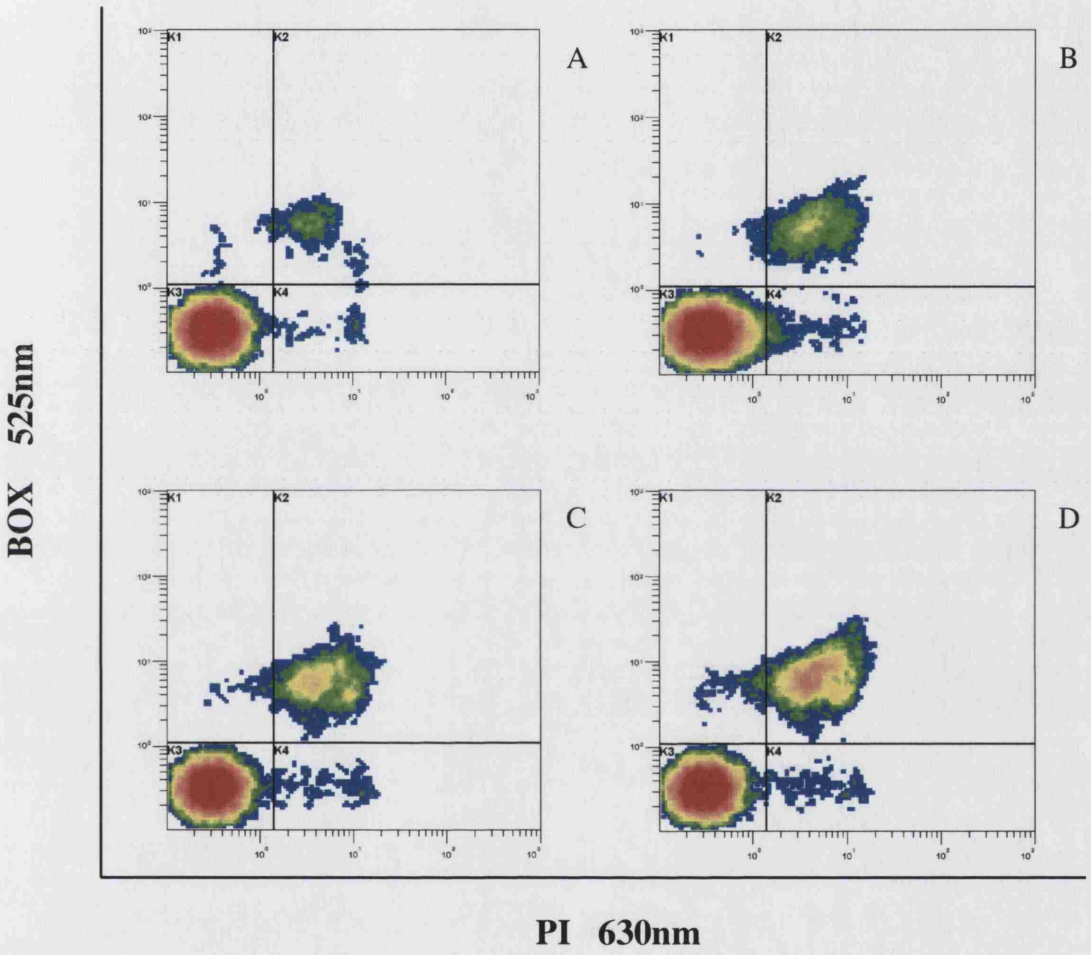

Figure 5.25. Flow cytometric density plots, 0 min (A), 30 min (B), 120 min (C), 240 min (D) of *E.coli* TOP10 pQR239 under bioconversion conditions, with 0.4 gL^{-1} h^{-1} substrate feed and a glycerol feed at the utilization rate of 2.64 gL^{-1} h^{-1}. 50,000 events were analyzed.

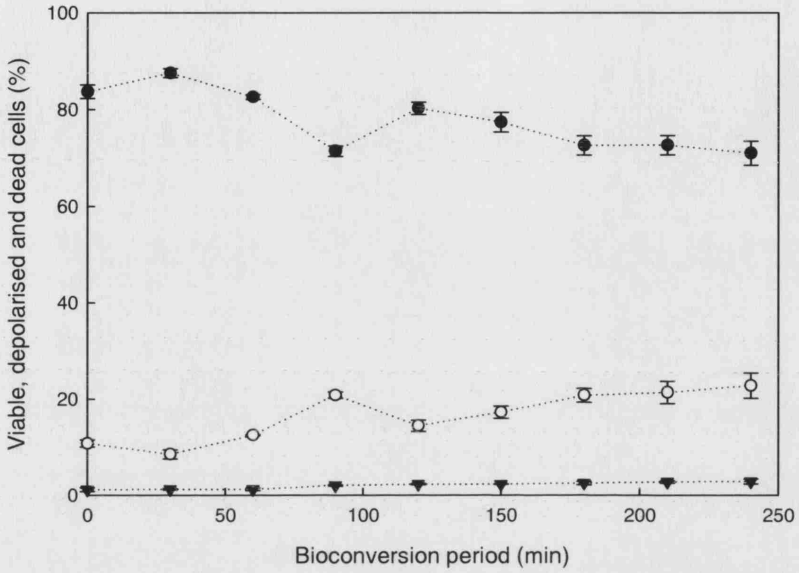

Figure 5.25 continued. Viable cells (●), dead cells (○), depolarized cells (▼), of *E.coli* TOP10 pQR239 under bioconversion conditions, with a 0.4 gL^{-1} h^{-1} substrate feed and a glycerol feed at the utilization rate of 2.64 gL^{-1} h^{-1} . 50,000 events were analyzed.

Introducing the co-substrate below the utilization rate, at 1.32 gL^{-1} h^{-1}, induced an even greater decrease in cell viability, with the percentage of intact cells decreasing by nearly 20% during the bioconversion. Figure 5.26 illustrates these findings. The percentage of dead cells was comparable to that recorded from the experiment where glycerol was fed at the utilization rate, at 23% after 4 hours. Metabolic stress levels, indicated by the loss of membrane polarization and the subsequent uptake of BOX only, were slightly higher and peaked at 3.6 % by the end of the bioconversion.

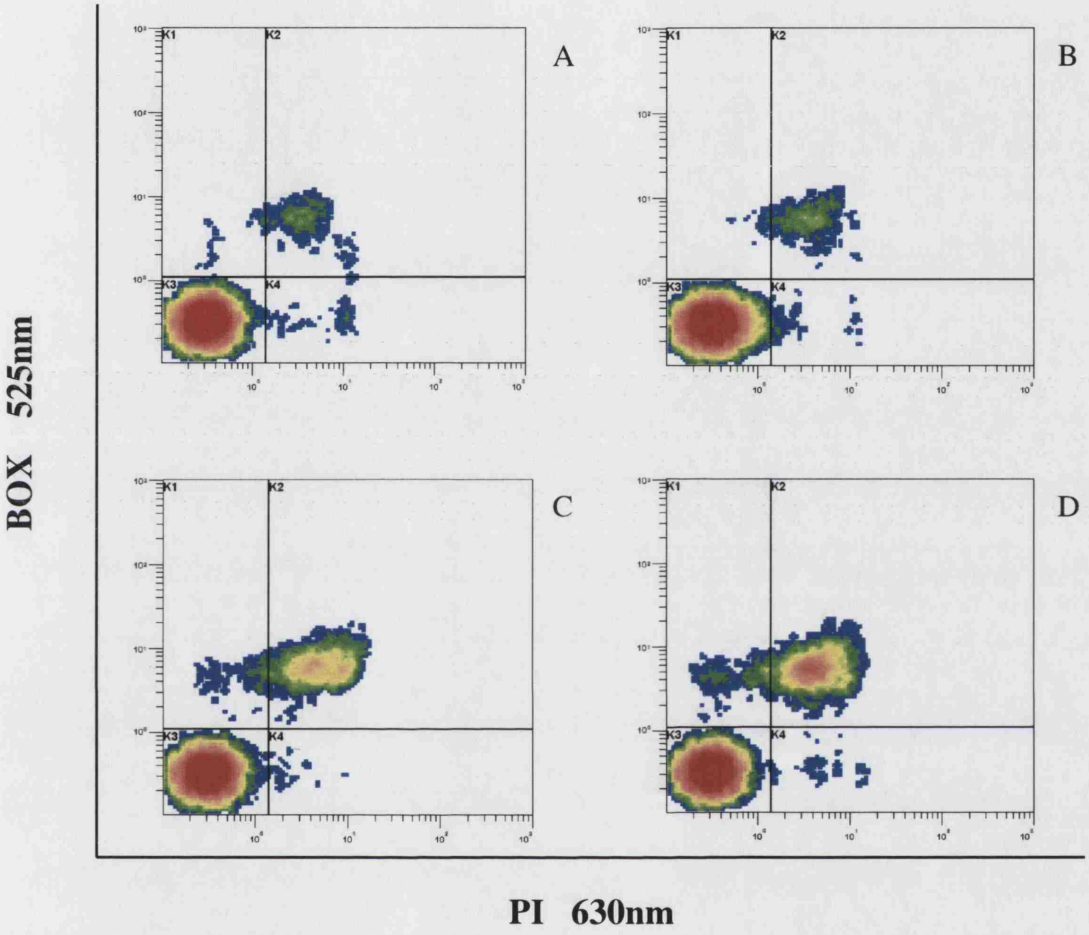

Figure 5.26. Flow cytometric density plots, 0 min (A), 30 min (B), 120 min (C), 240 min (D) of *E.coli* TOP10 pQR239 under bioconversion conditions, with a 0.4 gL^{-1} h^{-1} substrate feed and a glycerol feed at below the utilization rate at 1.32 gL^{-1} h^{-1} .50,000 events were analyzed.

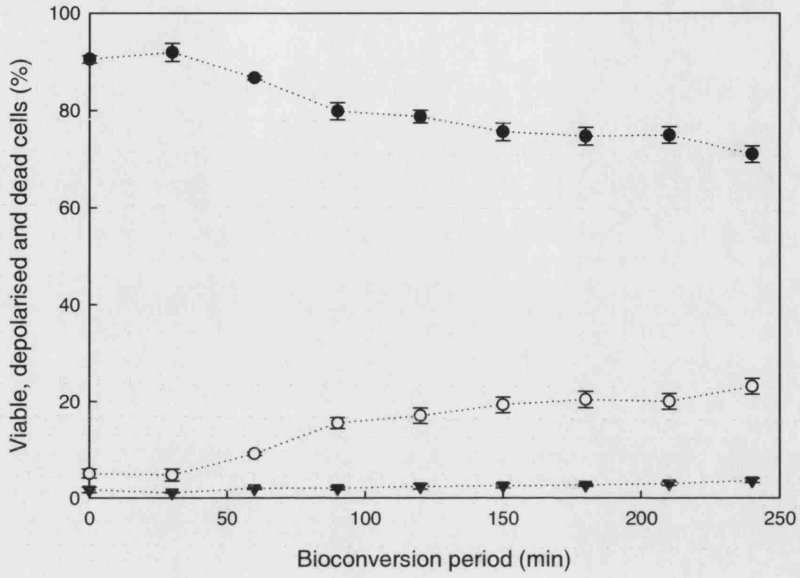

Figure 5.26 continued. Viable cells (●), dead cells (○), depolarized cells (▼), of *E.coli* TOP10 pQR239 under bioconversion conditions, with a 0.4 gL^{-1} h^{-1} substrate feed and a glycerol feed at below the utilization rate at 1.32 gL^{-1} h^{-1}. 50,000 events were analyzed.

An excess amount of co-substrate, 30 gL^{-1} h^{-1}, was found to be significantly detrimental to cell quality, this is depicted in Figure 5.27. Once again the percentage of viable cells decreased during the course of the bioconversion. A >24% decrease in cell viability was recorded over the 4 h period. The highest levels of dead cells, < 30%, were recorded at this glycerol concentration by the end of the bioconversion. However, the percentage of the cell population which had lost membrane polarity remained quite low at ~2%. This implies that high concentrations of glycerol within the bioreactor may be lethal to *E.coli* TOP 10 pQR239; presumably as a result of inducing a decrease in the cells' respiratory capacity.

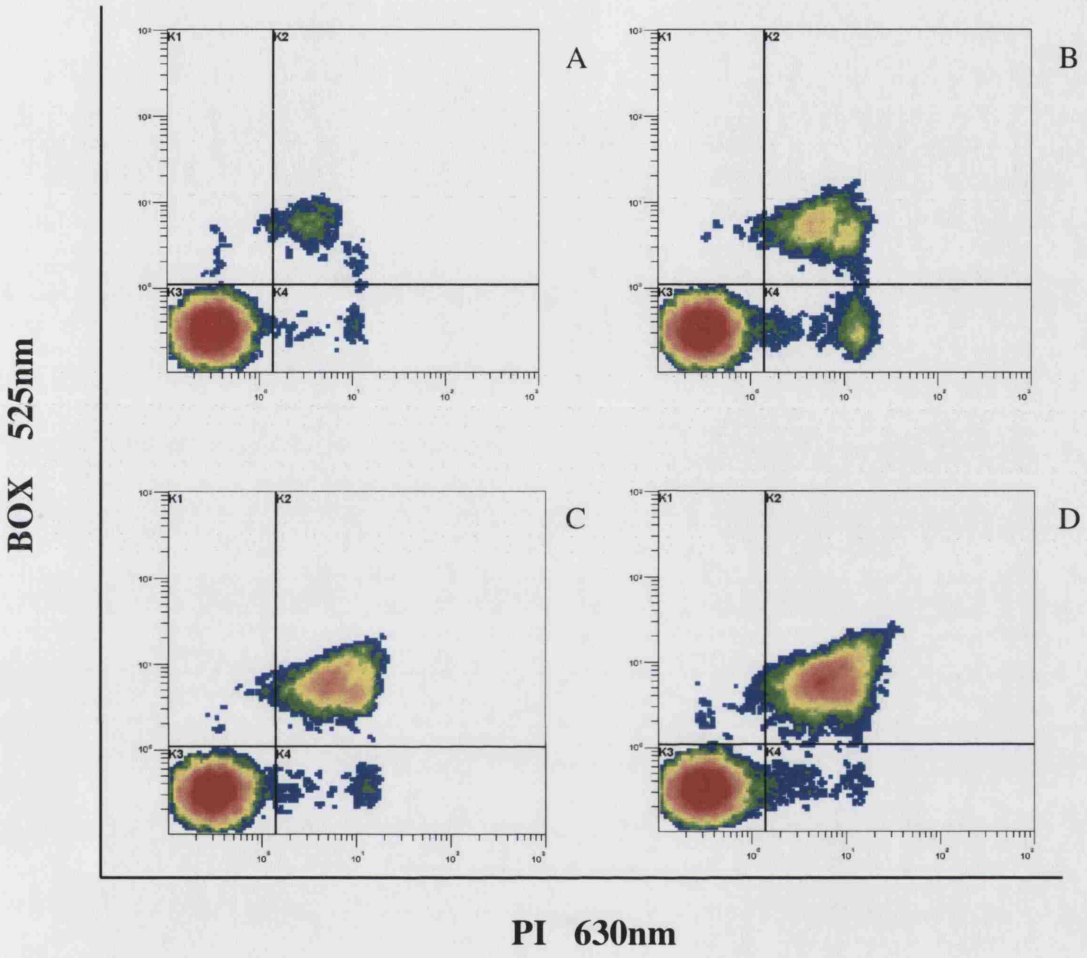

Figure 5.27. Flow cytometric density plots, 0 min (A), 30 min (B), 120 min (C), 240 min (D) of *E.coli* TOP10 pQR239 under bioconversion conditions, with a 0.4 gL^{-1} h^{-1} substrate feed and a glycerol feed in excess of the utilization rate, at 30 gL^{-1} h^{-1} .50,000 events were analyzed.

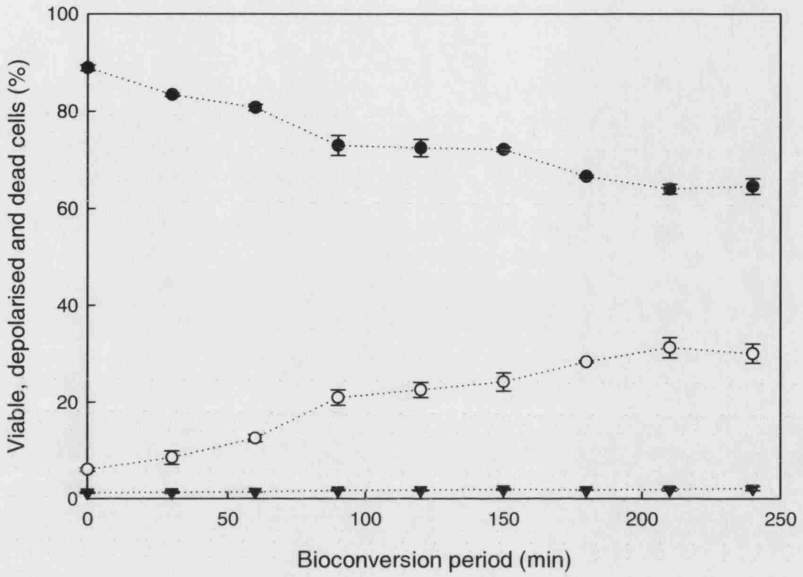

Figure 5.27 continued. Viable cells (●), dead cells (○), depolarized cells (▼), of *E.coli* TOP10 pQR239 under bioconversion conditions, with a 0.4 gL^{-1} h^{-1} substrate feed and a glycerol and a glycerol feed in excess of the utilization rate, at 30 gL^{-1} h^{-1} .50,000 events were analyzed.

5.2.4.2. Enzyme activity and co-substrate consumption

Enzyme activity was recorded under all of the conditions, which were investigated. The enzyme activity rate and final concentration of accumulated product following each reaction varied with co-substrate supply concentrations.

The rate of co-substrate consumption in the presence of 0.4 $gL^{-1}h^{-1}$ substrate was determined to be 2.64 $gL^{-1}h^{-1}$. The graph from which this was calculated can be seen in Figure 5.28. 2.64 $gL^{-1}h^{-1}$ was the calculated slope of the line and a R^2 value of 0.92 was obtained. A glycerol concentration of 6.7 gL^{-1} was present at the end of the fermentation step.

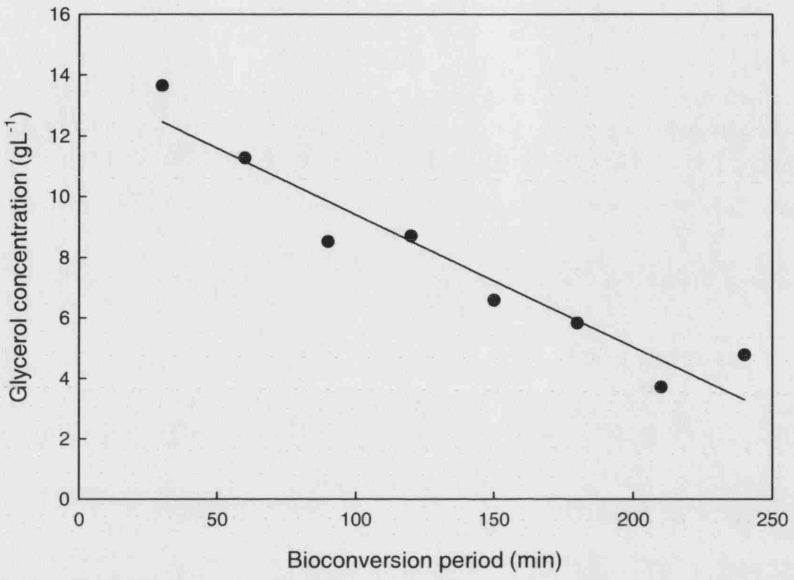

Figure 5.28. Graph of co-substrate (glycerol) consumption during a bioconversion with 0.4 $gL^{-1}h^{-1}$ substrate feed, under standard conditions. Consumption rate 2.64 $gL^{-1}h^{-1}$, R^2 value = 0.9.

The first experiment followed the standard bioconversion conditions (Doig *et al* 2001, 2003), with the batch addition of glycerol to the bioconversion vessel at a concentration of 10 gL^{-1}, at the start of the bioconversion. Product formation was rapid and titre increased as the reaction proceeded, such that substrate accumulation did not occur. The highest recorded amount of accumulated product, 2.5 gL^{-1} after 4 h, under all conditions, was obtained at this glycerol concentration, Figure 5.29.

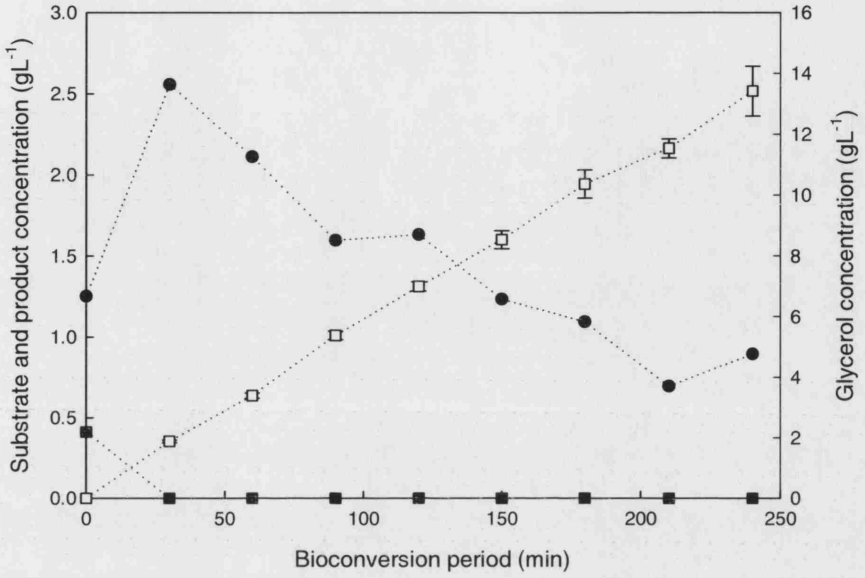

Figure 5.29. Product accumulation (□), substrate concentration (■) and glycerol concentration (●) by *E.coli* TOP10 pQR239 during the oxidation of bicyclo (3.2.0.) hept-2-en-6-one to yield (-)-1(S) 5(R)-2-oxabicyclo (3.3.0) oct-6-en-3-one and (-) 1 (R) 5(S)-3-oxabicyclo (3.3.0) oct-6-en-2-one, with 0.4 $gL^{-1}h^{-1}$ substrate feed rate and glycerol batched in at the start of the bioconversion at a concentration of 10 gL^{-1}.

The absence of additional glycerol during the bioconversion resulted in an almost 3-fold decrease in accumulated product concentration in comparison to when glycerol was added via a batch addition, this is shown in Figure 5.30. Despite the lower final product titre recorded, it was observed that the levels of substrate within the vessel decreased to near zero in the first 150 min of the bioconversion after which it began to accumulate. This could be as a result of the substrate being taken into the cell or binding the active sites but being unable to exit or perform the conversion possibly as a result of co-factor re-cycle limitations.

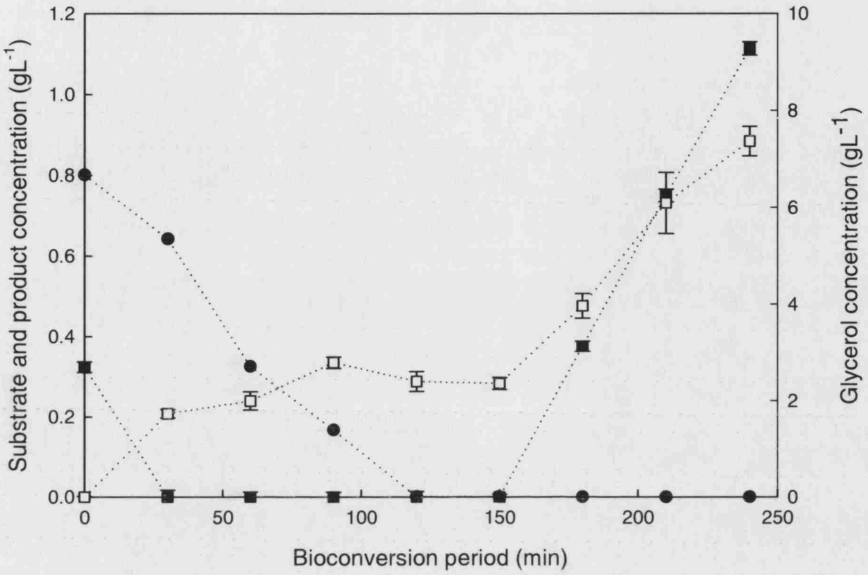

Figure 5.30. Product accumulation (□), substrate concentration (■) and glycerol concentration (●) by *E.coli* TOP10 pQR239 during the oxidation of bicyclo (3.2.0.) hept-2-en-6-one to yield (-)-1(S) 5(R)-2-oxabicyclo (3.3.0) oct-6-en-3-one and (-) 1 (R) 5(S)-3-oxabicyclo (3.3.0) oct-6-en-2-one, with 0.4 $gL^{-1}h^{-1}$ substrate feed rate and no additional glycerol.

When glycerol was added to the reaction at the utilization rate of 2.64 $gL^{-1}h^{-1}$ product formation was also observed. It reached a final concentration of 1.02 gL^{-1}. However as illustrated in Figure 5.31, the substrate concentration remained fairly constant, remaining between 0.2 and 0.4 gL^{-1}. Glycerol concentration remained below 0.2 gL^{-1} at all times, suggesting rapid and near total consumption.

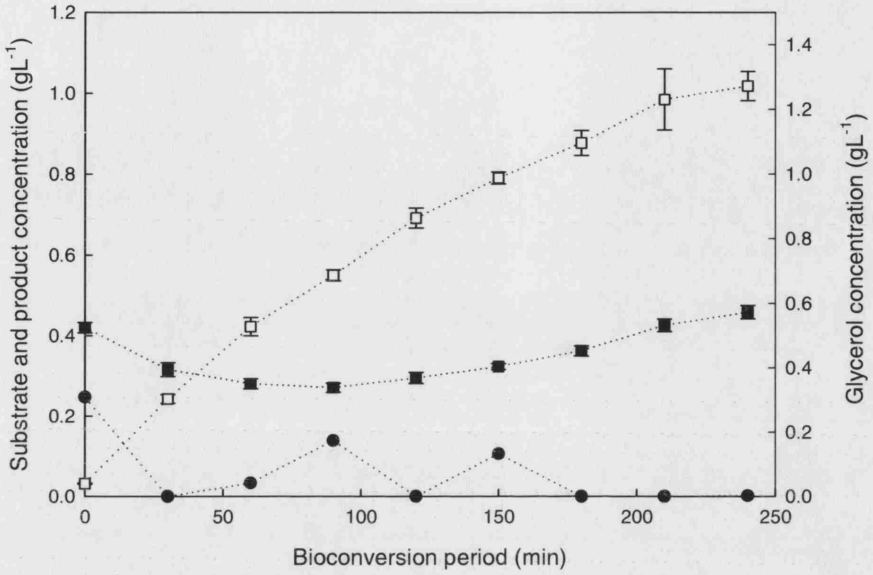

Figure 5.31. Product accumulation (□), substrate concentration (■) and glycerol concentration (●) by *E.coli* TOP10 pQR239 during the oxidation of bicyclo (3.2.0.) hept-2-en-6-one to yield (-)-1(S) 5(R)-2-oxabicyclo (3.3.0) oct-6-en-3-one and (-) 1 (R) 5(S)-3-oxabicyclo (3.3.0) oct-6-en-2-one, with 0.4 $gL^{-1}h^{-1}$ substrate feed rate and glycerol added at the consumption rate of 2.64 $gL^{-1}h^{-1}$.

Introducing the co-substrate into the system at a concentration below the utilization rate, at 1.32 $gL^{-1}h^{-1}$, resulted in an initial exponential increase in product accumulation in the first 60 min of the bioconversion after which product accumulation plateaued, despite records of low substrate concentrations in the bioconversion media. The near zero quantities of glycerol recorded suggest that the system was consuming it effectively and rapidly.

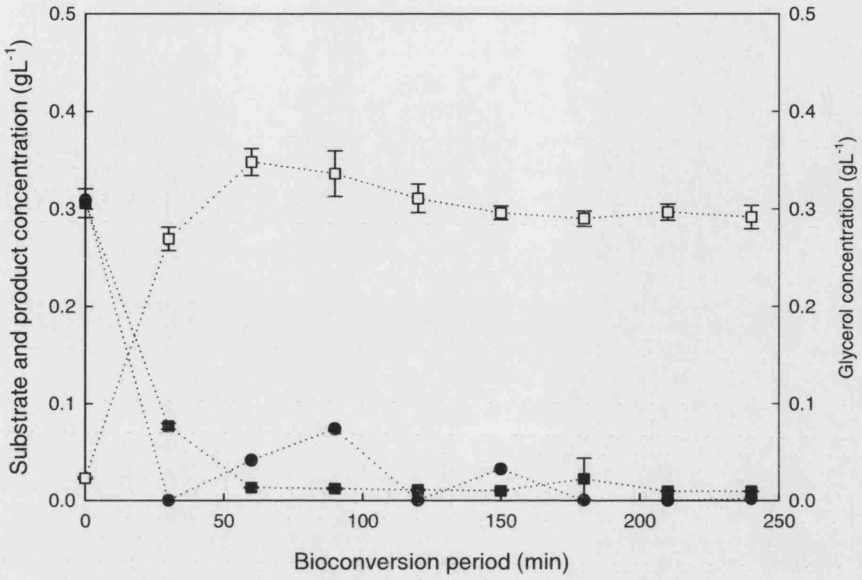

Figure 5.32. Product accumulation (□), substrate concentration (■) and glycerol concentration (●) by *E.coli* TOP10 pQR239 during the oxidation of bicyclo (3.2.0.) hept-2-en-6-one to yield (-)-1(S) 5(R)-2-oxabicyclo (3.3.0) oct-6-en-3-one and (-) 1 (R) 5(S)-3-oxabicyclo (3.3.0) oct-6-en-2-one, with 0.4 gL^{-1} h^{-1} substrate feed rate and glycerol added below the consumption rate at 1.32 $gL^{-1}h^{-1}$.

When glycerol was fed into the system at the rate of 30 gL^{-1} h^{-1}, a concentration 11 times greater than the consumption rate in the presence of a 0.4 $gL^{-1}h^{-1}$ substrate feed, product accumulation also occurred. This is shown in Figure 5.33. However, the final product concentration, 1.06 gL^{-1} was comparable to what was recorded when glycerol was fed at the consumption rate of 2.64 $gL^{-1}h^{-1}$. This suggested that the excess glycerol was not utilized i.e. glycerol was still used at the consumption rate. Substrate concentration also remained close to the introduction concentration for the duration of the bioconversion. The concentration of glycerol within the system on the other hand slowly decreased, finally stabilizing at ~30 $gL^{-1}h^{-1}$ by the end of the bioconversion.

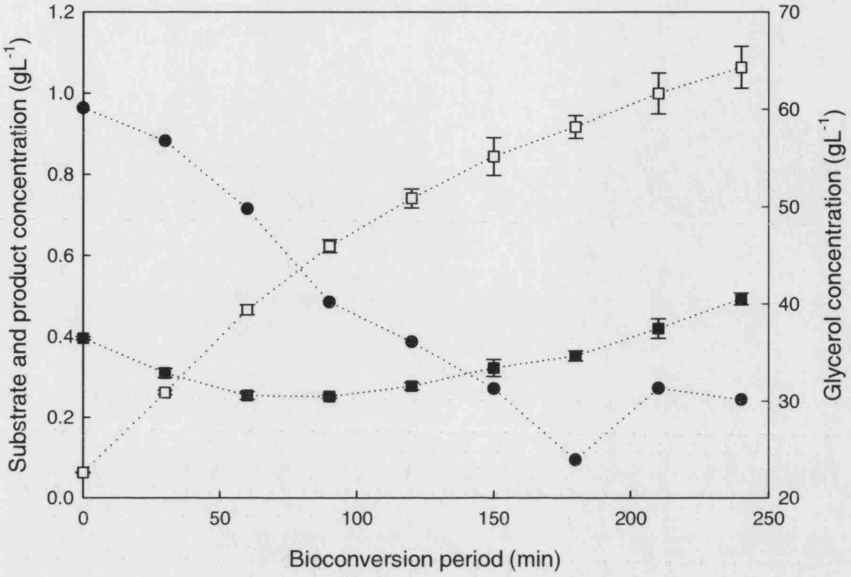

Figure 5.33. Product accumulation (□), substrate concentration (■) and glycerol concentration (●) by *E.coli* TOP10 pQR239 during the oxidation of bicyclo (3.2.0.) hept-2-en-6-one to yield (-)-1(S) 5(R)-2-oxabicyclo (3.3.0) oct-6-en-3-one and (-) 1 (R) 5(S)-3-oxabicyclo (3.3.0) oct-6-en-2-one, with 0.4 gL^{-1} h^{-1} substrate feed rate and glycerol added in excess of the consumption rate at 30 $gL^{-1}h^{-1}$.

5.2.4.3. Cell respiration profiles

During the course of the bioconversions at different co-substrate feed rates, cell respiration was monitored. The data collected indicated significant variations with respect to the uptake of oxygen, the dissolved oxygen tension within the bioconversion vessel and the carbon dioxide produced. This implied that the concentration of glycerol within the system had some impact on cellular respiration.

When glycerol was added batch-wise at a final concentration of 10 gL^{-1}, DOT within the vessel was at zero, despite a constant supply of oxygen into the vessel at the rate of 0.66vvm, suggesting enzyme activity. CER and OUR levels remained relatively low; the latter of which fluctuated during the bioconversion period. CER values were constant at ~1.5mmol$L^{-1}h^{-1}$. This data illustrated in Figure 5.34.

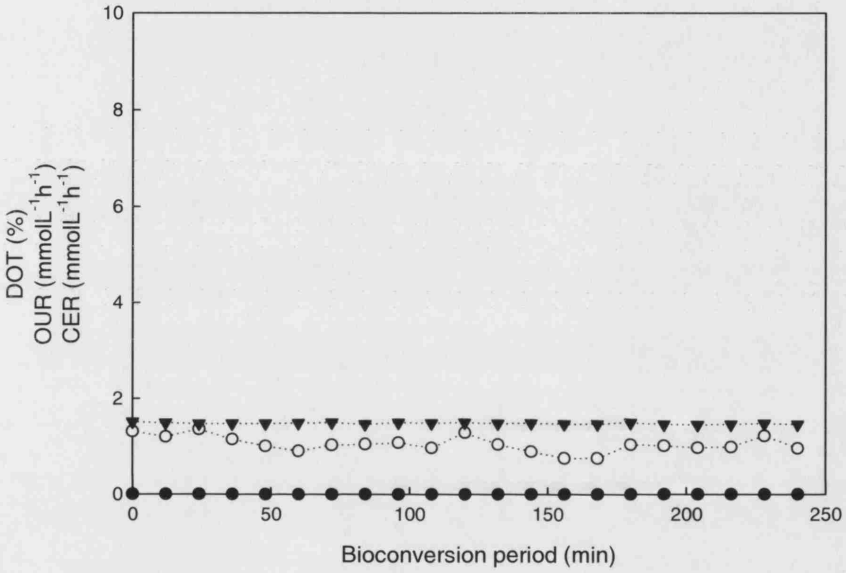

Figure 5.34. Cell respiration profile of *E.coli* TOP10 pQR239, DOT (•), OUR (○), and CER (▼), during the oxidation of bicyclo (3.2.0.) hept-2-en-6-one to yield (-)-1(S) 5(R)-2-oxabicyclo (3.3.0) oct-6-en-3-one and (-) 1 (R) 5(S)-3-oxabicyclo (3.3.0) oct-6-en-2-one, with 0.4 $gL^{-1}h^{-1}$ substrate feed rate and 10 gL^{-1} glycerol batched in at the start of the bioconversion.

In the absence of additional glycerol the respiratory pattern was very different, this is depicted in Figure 5.35, which shows the DOT, OUR and CER patterns observed. Dissolved oxygen levels remained low ~0 % until the last hour of the bioconversion during which it began to rise, this suggest that a vital carbon source was becoming depleted at this point and enzyme activity was declining. This was accompanied by a

corresponding decrease in OUR and CER, which began an hour prior to the increasing DOT. This implied that some cellular respiration occurred during this time period.

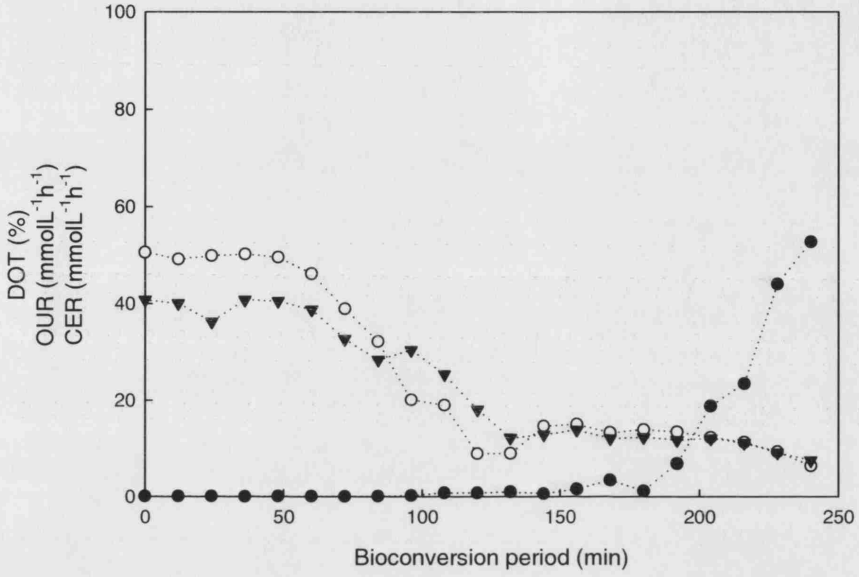

Figure 5.35. Cell respiration profile of *E.coli* TOP10 pQR239, DOT (•), OUR (○), and CER (▼), during the oxidation of bicyclo (3.2.0.) hept-2-en-6-one to yield (-)-1(S) 5(R)-2-oxabicyclo (3.3.0) oct-6-en-3-one and (-) 1 (R)5(S)-3-oxabicyclo (3.3.0) oct-6-en-2-one, with 0.4 $gL^{-1}h^{-1}$ substrate feed rate and no additional glycerol.

It had been previously determined that glycerol was consumed at the rate of 2.64 $gL^{-1}h^{-1}$ in the presence of a 0.4 $gL^{-1}h^{-1}$ substrate feed. Here the respiratory profile, seen in Figure 5.36, shows a steady DOT and CER at approximately 2.0% and 0.05mmol$L^{-1}h^{-1}$ respectively for the four hour duration of the bioconversion. The DOT on the other hand fluctuated during that time period.

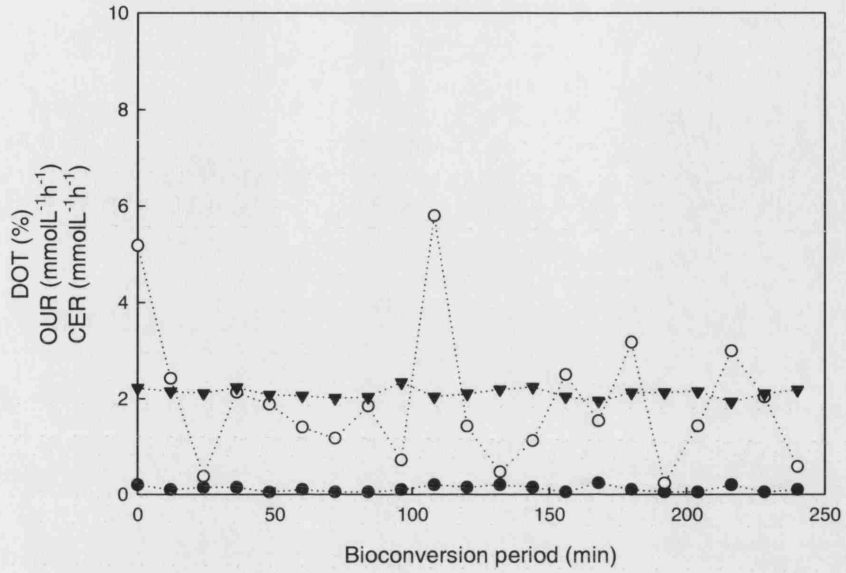

Figure 5.36. Cell respiration profile of *E.coli* TOP10 pQR239, DOT (•), OUR (○), and CER (▼), during the oxidation of bicyclo (3.2.0.) hept-2-en-6-one to yield (-)-1(S) 5(R)-2-oxabicyclo (3.3.0) oct-6-en-3-one and (-) 1 (R) 5(S)-3-oxabicyclo (3.3.0) oct-6-en-2-one, with 0.4 $gL^{-1}h^{-1}$ substrate feed rate and glycerol added at the consumption rate of 2.64 $gL^{-1}h^{-1}$.

Feeding glycerol into the bioconversion at the rate of 1.32 $gL^{-1}h^{-1}$, which was below the utilization rate when the bioconversion was run with a 0.4 $gL^{-1}h^{-1}$ substrate feed rate, resulted in a cell respiration profile that closely mimicked the profile obtained when glycerol was added at the utilization rate. This is shown in Figure 5.37.

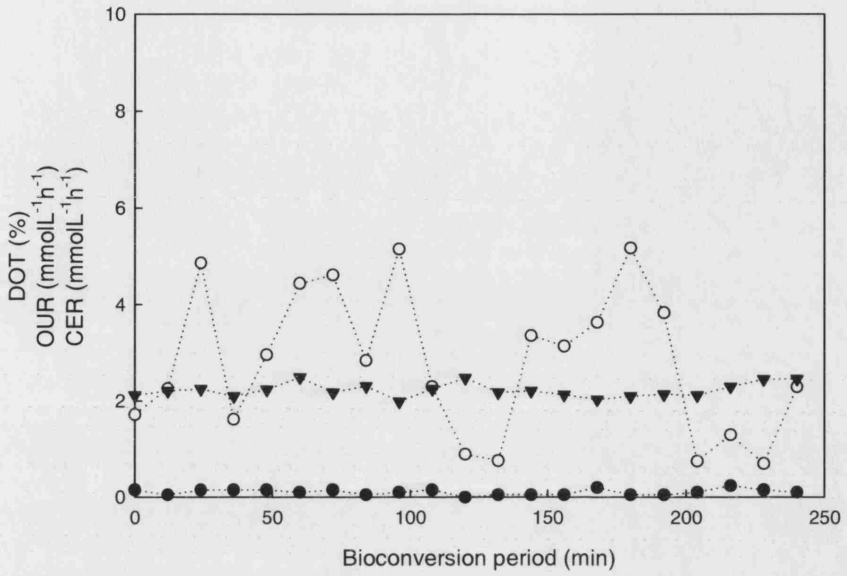

Figure 5.37. Cell respiration profile of *E.coli* TOP10 pQR239, DOT (•), OUR (○), and CER (▼), during the oxidation of bicyclo (3.2.0.) hept-2-en-6-one to yield (-)-1(S) 5(R)-2-oxabicyclo (3.3.0) oct-6-en-3-one and (-) 1 (R) 5(S)-3-oxabicyclo (3.3.0) oct-6-en-2-one, with 0.4 $gL^{-1}h^{-1}$ substrate feed rate and glycerol below the consumption rate, at 1.32 $gL^{-1}h^{-1}$.

The introduction of the glycerol at a rate in excess of the utilization rate, at 30 $gL^{-1}h^{-1}$, resulted in a DOT of ~ 0%, for the duration of the bioconversion, the oxygen uptake rate fluctuated and once again attained a maximum of 6 $mmolL^{-1}h^{-1}$; carbon-dioxide evolution also remained constant at a rate of 2 $mmolL^{-1}h^{-1}$ during this period. These are the same values as those observed when glycerol was fed into the system at the utilization rate. This data is shown in Figure 5.38.

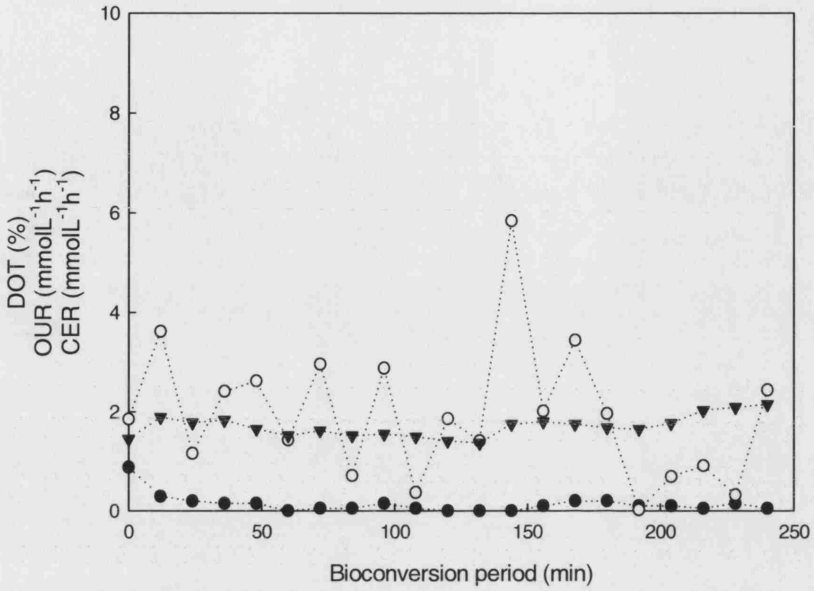

Figure 5.38. Cell respiration profile of *E.coli* TOP10 pQR239, DOT (•), OUR (○), and CER (▼), during the oxidation of bicyclo (3.2.0.) hept-2-en-6-one to yield (-)-1(S) 5(R)-2-oxabicyclo (3.3.0) oct-6-en-3-one and (-) 1 (R) 5(S)-3-oxabicyclo (3.3.0) oct-6-en-2-one, with 0.4 $gL^{-1}h^{-1}$ substrate feed rate and glycerol added in excess of the consumption rate, at 30 $gL^{-1}h^{-1}$.

5.3. Discussion

5.3.1. Substrate and product associated cell damage

In the development of whole cell biocatalytic processes the effects of culture and reaction media, process conditions, substrate and products on cell physiology, enzyme activity and co-factor regeneration need to be investigated and optimized. This section investigated the effects of substrate, co-substrate and product(s) on the physiology, respiration, enzyme activity and co-factor regeneration in *E.coli* TOP10 pQR239. *E.coli* TOP10 pQR239 is the whole cell biocatalyst involved in the BVMO mediated stereo-selective oxidation of bicyclo (3.2.0.) hept-2-en-6-one to yield (-)-1(S) 5(R)-2-oxabicyclo (3.3.0) oct-6-en-3-one and (-) 1 (R) 5(S)-3-oxabicyclo (3.3.0) oct-6-en-2-one.

The concentrations of substrate and/or product that a given whole cell biocatalyst can withstand without compromising cell quality and productivity is one of the essential parameters which requires optimization during process development. In this case the substrate and product(s) are xenobiotic compounds, which could be potentially harmful to *E.coli* TOP10 pQR239, even at low concentrations. Sikkema *et al* (1992) have demonstrated that tetralin is toxic to bacterial cells at concentrations below $100\mu molL^{-1}$. Studies of the substrate and product effects on the whole cell biocatalyst confirm that there are toxic and non-lethal effects on the cells. Toxic effects are characterised by cell death and non-lethal effects by metabolic stress, indicated by membrane depolarisation.

Bacteria are not able to accommodate the high concentrations of non-natural substrates and products that may be required in industrial biocatalyst processes, in spite of the mechanisms they have in place to compensate for unfavourable environmental conditions (Held *et al* 2000). Cyclic hydrocarbon transformations in micro-organisms are often characterised by low stability of the desired enzymatic activity. This is primarily due to the inactivation of the cells (Sikkema *et al* 1995). In solvent toxicity studies using bacteria and yeast the cytoplasmic membrane has been identified as a possible target.

However, the exact method of action of these solvents is not well defined (Sikkema *et al* 1992; Amanullah *et al* 2002b). Nevertheless, the Gram-negative cell membrane has been demonstrated to be more resistant to solvent associated cell damage than the Gram-positive cell membrane (Harrop *et al* 1989).

This study has demonstrated that the accumulation of bicyclo (3.2.0.) hept-2-en-6-one and its associated products (-)-1(S) 5(R)-2-oxabicyclo (3.3.0) oct-6-en-3-one and (-) 1 (R) 5(S)-3-oxabicyclo (3.3.0) oct-6-en-2-one, in the cytoplasmic membrane of *E. coli* TOP10 pQR239 can significantly affect its structure and function. Flow cytometric analysis following dual staining with PI and BOX indicated that the percentage of viable cells decreased with increasing substrate concentrations and with increased exposure to the product at all concentrations.

Very low concentrations of reaction products may poison the biocatalyst (Held *et al* 2000). This study demonstrated that this poisoning does not necessarily result in irreversible damage or death. Instead of the exponential cell death recorded for the substrate reactions, the presence of the added lactone product, 1S 5R 2-oxabicyclo [3.3.0] oct- 6-en-3-one (in the presence of a non-lethal substrate concentration of $0.5gL^{-1}$) caused a slow time-dependent decline into metabolic stress (Figure 5.39), indicated by the increasing population of BOX positive cells observed from 120 min post bioconversion initiation, at all product concentrations investigated. This population of depolarised cells peaked at 180min into the reaction before declining, implying that the cells built up a tolerance to the presence of the lactone product or developed the capacity to be able to remove it from the intracellular environment. However, this recovery trend was not observed at $5gL^{-1}$ product concentration, due to the higher concentration making cell recovery difficult. It appeared that while cell membrane depolarisation occurred in response to increased exposure time at all product concentrations, total loss of membrane integrity was not widespread within the population. Hence, this observed loss of membrane potential may be an early indicator of cell damage that could ultimately compromise cell viability (Reiseberg *et al* 2001); and therefore a greater percentage of cell death may occur if the reaction was allowed to proceed for longer. These findings

indicate that substrate concentration associated cell damage occurs rapidly and as such is significantly more detrimental to whole cell biocatalyst viability than product associated cell damage. However, increasing product concentrations can cause a decrease in enzyme activity. Thus product associated enzyme inhibition also appears to be a factor affecting bioconversion productivity.

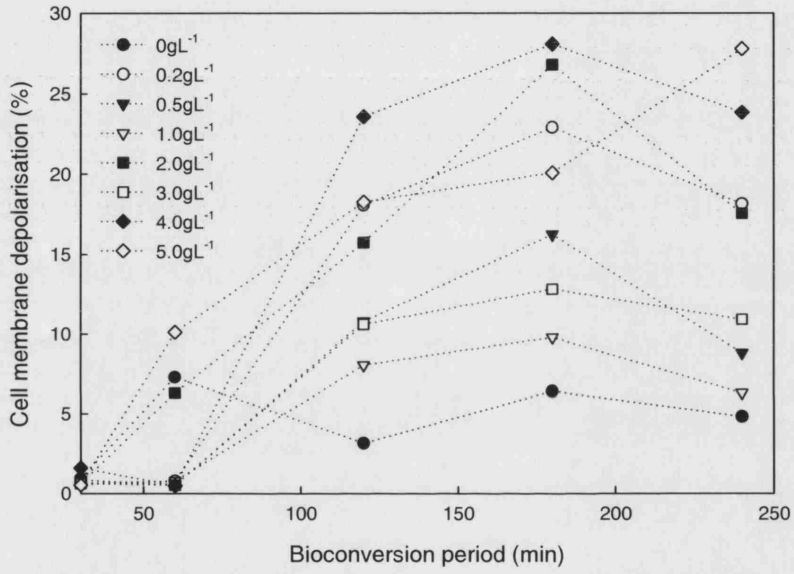

Figure 5.39. Product associated time- dependent cell membrane depolarisation.

Fed-batch bioconversions with air sparged into the reactor to provide the oxygen required for CHMO enzyme activity were used to further characterize the impact of substrate concentrations on the whole cell biocatalyst. Cell respiratory profiles and enzyme activity under these conditions were also examined. All concentrations of substrate caused cell damage, which increased with increasing concentration. At 1.0 and 5.0 $gL^{-1}h^{-1}$ substrate feed a significant population of depolarised cells became apparent 2 hours post bioconversion initiation, doubling the substrate feed rate to 10.0 $gL^{-1}h^{-1}$ caused a virtually instantaneous decline in cell viability; the depolarised population was not observed

(Figures 5.11 and 5.12). Substrate associated cell damage was measured over the entire duration of the bioconversion, allowing the effect of primary (e.g. efflux pumps) and secondary (e.g. lipopolysacharide modification) protective mechanisms to be analyzed. It may be argued that the depolarization observed at 120 and 240 min post initiation at 1.0 and 5.0 $gL^{-1}h^{-1}$ substrate feeds are as a result of the secondary protective mechanisms trying to overcome the dehabilitating effects of the substrate and actively working to exclude it from the internal cell compartment. Boucabeille *et al* (1998) reported an immediate perturbation of the permeability properties of the cytoplasmic membrane of the Gram-positive *Listeria innocua* due to the formation of pore like structures, which facilitated the loss of potassium ions (essential for maintaining membrane polarization) and hydrolysis of internal ATP in response to low doses of linenscin OC2. It may therefore follow that at the higher substrate feed concentrations (10 $gL^{-1}h^{-1}$) any pores formed in the membrane would be large enough to result in a complete loss in membrane integrity ultimately resulting in cell death. Lower substrate feed concentrations (1.0 and 5.0 $gL^{-1}h^{-1}$) would simply result in a leakage of ions such as potassium and phosphate thus only resulting in depolarization.

The accumulation of lipophillic compounds in lipid membranes causes loss of membrane integrity (Uribe *et al* 1995; Sikkema *et al* 1992), thus compromising cell viability. This may also be accompanied by changes in enzyme activity (Osborne *et al* 1990). Enzyme activity was recorded at all substrate concentrations but was significantly impacted by the levels of substrate present in the cellular environment. It was found that accumulated product concentration peaked at 4.4 gL^{-1} with 0.5 $gL^{-1}h^{-1}$ substrate feed and declined after this feed concentration. Substrate feeds of 5.0 and 10 $gL^{-1}h^{-1}$ produced almost undetectable amounts of product. This decrease in activity can be attributed to a combination of factors. Firstly, substrate inhibition as a result of excess substrate availability resulting in the enzyme's active site becoming overwhelmed by substrate molecules. The second factor, is a potential hindering of effective co-factor regeneration; a non-fully functioning cell membrane may also be responsible as oxygenases and transport proteins are commonly located in the cytoplasmic membrane (Held *et al* 2000; Amanullah *et al* 2002b). Thus once membrane polarization has been lost the cells'

capacity to regenerate the co-factor – NADPH becomes severely compromised. Cell death, characterized by a complete breakdown in membrane integrity at higher concentrations, releases the enzyme into the bioconversion media where it is available for the reaction allowing enzyme activity to be observed early in the reaction. However, owing to a combination of substrate inhibition and the lack of intact co-factor regeneration machinery, further enzyme activity does not occur (see Figure 5.5).

Enzyme activity decreases with increasing substrate concentration, as does cell viability. However, cell viability remains above 40% in the in the first half hour of the bioconversion, when initial enzyme activity measurements were taken. Substrate concentration associated inhibition was determined to be the main reason for loss of enzyme activity. Substrate associated loss of cell viability is irreversible as it was mainly characterised by cell lysis (PI and BOX positive cells). Consequently it may be inferred that the loss of enzyme activity is predominantly a result of cell death.

Enzyme activity is also shown to decrease with increasing product concentration, Figure 5.40. Cell viability remains relatively high (>80%) in the first half hour of the bioconversion. This indicates that increasing product concentrations and not whole cell biocatalyst quality is the primary impediment to optimal enzyme activity. For the total bioconversion period at all product concentrations cell viability remained above 45%, further supporting the finding that whole cell biocatalyst viability is not the primary impediment to optimal enzyme activity. However a subsequent trend of time-dependent membrane depolarisation was observed. This product-induced depolarisation is reversible, and was shown to be the case at product concentrations below $5gL^{-1}$ (Figure 5.39). As the reaction proceeds and the depolarised population increases, cell quality may begin to affect enzyme activity in a more significant manner due to a poorly functioning cell membrane, which would hinder effective co-factor supply. This may be prevented by implementing *in-situ* product removal strategies (Lye and Woodley 1999), which could serve the dual function of optimising enzyme activity and whole cell biocatalyst viability.

A schematic of the proposed effects of product concentration on enzyme activity and whole cell biocatalyst viability and of product concentration on cell viability as a function of time is illustrated in Figure 5.40.

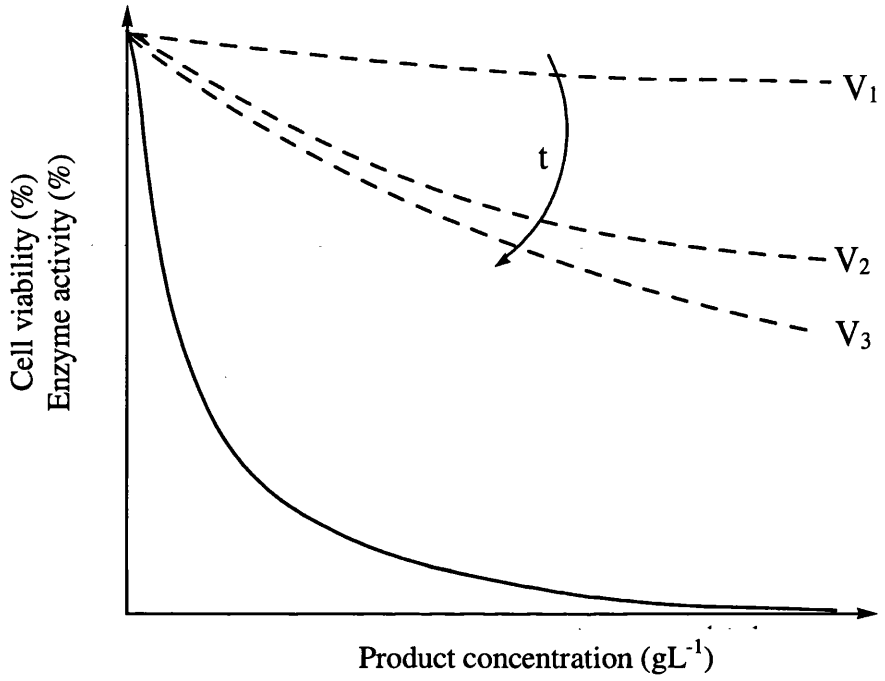

Figure 5.40. Proposed effects of product concentration on enzyme activity (–) and whole cell biocatalyst viability and of product concentration on cell viability (V_1, V_2, V_3) as a function of time, (t).

In order to circumvent the above mentioned events, controlled substrate addition, via in-situ substrate supply may be implemented to reduce irreversible substrate associated cell damage. Control of product accumulation and operating at a sufficiently high substrate concentration to facilitate a rapid reaction will avoid the observed time-dependent product concentration associated loss of cell viability.

Bacterial respiratory systems are commonly located in the cytoplasmic membrane, along with associated enzymes such as ATPases, transport proteins and a number of oxidoreductases (Sikkema *et al* 1995; Amanullah *et al* 2002b). Consequently it was expected that anything that would disruption normal cellular function, such as substrate or product toxicity, would in turn affect cell respiration. This was found to be the case with decreasing cell viability mirroring a decline in cell respiration, as previously demonstrated by Osborne *et al* (1990).

5.3.2. Co-substrate requirement investigations

The primary objective of this part of the study was to investigate the behaviour of the whole cell biocatalyst in the presence of different co-substrate concentrations during the bioconversion reaction. The secondary objectives were to assess the significance of the co-factor in the bioconversion and to examine the effect of glycerol feeding into the system as this could potentially affect productivity. Fed-batch bioconversions with air sparged into the reactor to provide the oxygen required for CHMO enzyme activity were used to characterize the impact of glycerol concentrations on the whole cell biocatalyst. Cell respiratory profiles and enzyme activity under these conditions were also examined.

A sub-lethal and sub-inhibitory substrate concentration was fed into the system along with co-substrate at different feed rates. This concentration is not inhibitory to the enzyme activity; neither does it significantly compromise cell viability. Flow cytometric analysis of cells undergoing the bioconversion under said conditions showed that cell death occurred at all glycerol concentrations, with this percentage of the population increasing with increasing glycerol concentration. This may be as a consequence of oxygen transfer limitations. Higher concentrations of the co-substrate could make it difficult for oxygen to reach the cells thus disrupting normal cellular respiration as well as hindering enzyme activity, oxygen is essential for normal CHMO activity.

While the presence of glycerol in the bioconversion media at a concentration of $10gL^{-1}$ marginally appeared to enhance cell viability (by 3% in comparison to when no additional glycerol was added), it was shown to be vital for the bioconversion to proceed, (compare Figures 5.29 and 5.30) and in fact supported the highest concentration of accumulated product, 2.5 gL^{-1}. This was more than 3 times higher than the final product concentration observed when additional glycerol was not added to the system and more than seven times greater than when sub-optimal glycerol was added. Identical final product concentrations were observed when glycerol was supplied in excess and at the utilization rate. The lower enzyme activity observed when the co-substrate fed into the bioconversion at 30 gL^{-1} h^{-1}, could be as a result of the high concentrations inhibiting the transport of the substrate into the cell. A similar pattern was observed in the xylose bioconversion with glucose, fructose, mannose, galactose and ethanol as co-substrates (Meinander and Hahn-Hägerdal 1997). Figure 5.41 shows how enzyme activity (indicated by the accumulated product concentration), whole cell viability and co-substrate concentration are intertwined.

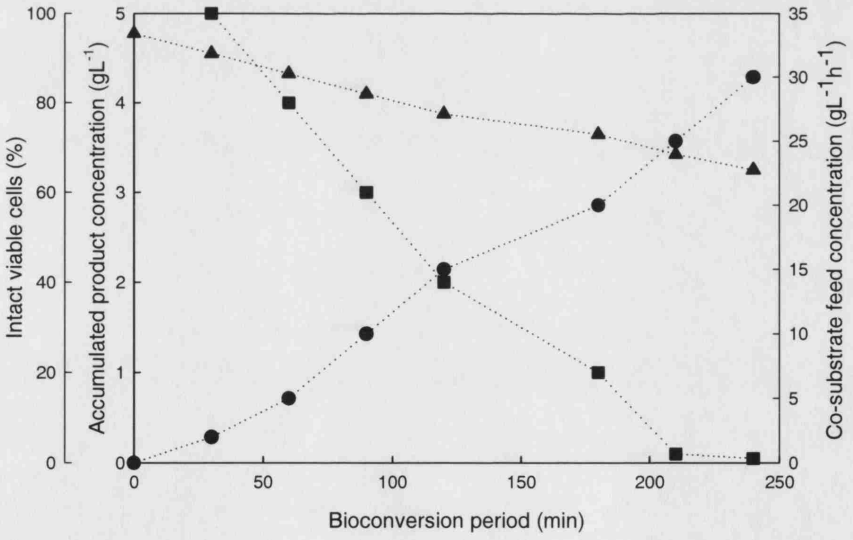

Figure 5.41. The relationship between the viability of the whole cell biocatalyst (▲), co-substrate concentration (■) and accumulated product concentration (●) during the 4 h bioconversion with 0.4 gL^{-1} substrate feed.

In spite of the high accumulated product concentration recorded when glycerol was added batch-wise at the start of the bioconversion, it may be more feasible to feed glycerol into the system. Figure 5.41 implies that if glycerol is supplied at a feed rate of below $5gL^{-1}h^{-1}$ high product titres and cell viability can be achieved. Excess glycerol would result in oxygen limitation to the biocatalyst, in a reaction which is already oxygen limited. A high percentage of the available oxygen is directed toward maintaining enzyme activity. High glucose availability would result in the diversion of valuable oxygen to glycerol breakdown at the expense of the bioconversion. Lower glycerol concentrations may also promote maintenance of cell quality during the bioconversion.

5.4. Summary

Multiparameter flow cytometry has been used to successfully illustrate that the accumulation of bicyclo (3.2.0.) hept-2-en-6-one to and its associated products (-)-1(S) 5(R)-2-oxabicyclo (3.3.0) oct-6-en-3-one and (-) 1 (R) 5(S)-3-oxabicyclo (3.3.0) oct-6-en-2-one in *E. coli* TOP10 PQR239 during the bioconversion can lead to severe impairment of normal metabolic activity and cell physiology. The stress responses elicited are characterised by loss of membrane polarisation and often a total loss of cell viability via the physical disruption of the cytoplasmic membrane. The decrease in physical membrane integrity and polarisation, cell respiratory output and enzyme activity all occurred in a concentration dependent manner for the substrate. A low substrate feed rate was established as resulting in the highest product yield and cell quality. Cell damage attributed to product toxicity was found to be time dependent. High concentrations of the substrate and product were found to cause a decrease in enzyme activity. It was established that increasing substrate and product concentrations and not whole cell biocatalyst viability is the primary impediment to optimal enzyme activity.

Availability of the co-substrate, glycerol, was established to be intrinsic to the bioconversion of bicyclo (3.2.0.) hept-2-en-6-one to yield (-)-1(S) 5(R)-2-oxabicyclo (3.3.0) oct-6-en-3-one and (-) 1 (R) 5(S)-3-oxabicyclo (3.3.0) oct-6-en-2-one, it provided

the means for the regeneration of the co-factor, NADPH. However glycerol availability was also found to impact the quality of the whole cell biocatalyst, causing damage at high concentrations.

Chapter 6

General discussion

6.0. Introduction

This project has applied multiparameter flow cytometry to two *E.coli* processes: The first where the organism, *E.coli* IL-13, is used for the expression of a therapeutically significant protein, human interleukin 13, following recombinant gene expression induction during the fermentation stage. The second process is a biocatalytic reaction, the BVMO mediated stereo-selective oxidation of bicyclo (3.2.0.) hept-2-en-6-one to yield (-)-1(S) 5(R)-2-oxabicyclo (3.3.0) oct-6-en-3-one and (-) 1 (R) 5(S)-3-oxabicyclo (3.3.0) oct-6-en-2-one. This process used *E.coli* TOP10 pQR239 as the whole cell biocatalyst to facilitate the reaction via the supply of the CHMO enzyme. This study demonstrates valuable insights into the use of multiparameter flow cytometry in the process environment, which could have more general implications.

6.1. Flow cytometry in induction studies

The control of induction conditions during recombinant bacterial processes requires the careful consideration and optimisation of a number of factors, including when during the growth cycle to induce and what concentration of the inducer to use (where a chemical inducing agent is being used). This is so that recombinant protein expression may be maximised for as long as possible with as high as possible cell quality; both of which would work in concert to improve product titres and possibly product quality also. In many instances this is significantly influenced by the physiological quality and metabolic status of the host cell.

This study investigated the consequences of induction *E.coli* IL-13 when protein expression was induced early, midway and late in the exponential growth phase and the effects of fermentation conditions (dissolved oxygen and pH changes). Induction with IPTG is known to cause a steady decrease in active cell proliferation and growth, resulting in a decreased cell growth rate and increasing metabolic stress (Bentley *et al* 1990; Andersson *et al* 1996; Soriano *et al* 2002). This study demonstrated that metabolic stress presented in *E.coli* IL-13 as depolarisation of the cell membrane. Using multiparameter flow cytometry also established the optimal induction conditions required for the expression of the IL-13 protein in *E.coli* IL-13; thus signifying its value as a process optimisation tool for this and other such processes.

6.2. Flow cytometry in Baeyer-Villiger studies

The BVMO reaction is commonly achieved by the use of whole cells, which serve as both the enzyme and the co-factor supplier; primarily to prevent co-factor availability limitations to the biocatalysts (Van Der Werf 2000; Mihovilovic *et al* 2000; Doig *et al* 2002; 2003). The physiological status and metabolic capacity of the whole cell biocatalyst must therefore be kept at optimal levels to facilitate maximum enzyme activity and product formation.

Flow cytometry has been used to assess the stability of the whole cell biocatalyst. Bioconversion media, storage temperatures and reaction pH all impact the metabolic and physiological status of *E.coli* TOP10 pQR239 as well as enzyme activity. A clear link between whole cell viability, the status of the biocatalyst cytoplasmic membrane, substrate and product concentration, and enzyme activity has been shown. The nature of the concentration-associated cell damage resulting from the exposure to the substrate and product(s) as established in this study has not been previously established.

The results obtained have indicated a time dependent decrease in metabolic activity in the presence of the product. While previous studies have suggested that accumulation of the lactone product(s) may hinder CHMO activity (Hilker *et al* 2004), the exact nature of the

effect on the whole cell biocatalyst has not been previously elucidated. To overcome product accumulation and its associated cell damage and enzyme inhibition, in-situ product removal (Lye and Woodley 1999; Simpson *et al* 2001; Hilker *et al* 2004) may be implemented. In some cases an adsorbent resin has been added to the bioconversion vessel. In situ product removal would facilitate the bioconversion proceeding for longer and with greater productivity if cell quality is not compromised

Flow cytometry can play a significant role in bioprocesses, such as the BVMO reaction, that rely heavily on co-factor availability, provided by resting or metabolically active whole cells. It can be used to visualise the physiological effects of substrates, reaction media, fermentation and bioconversion conditions etc on the whole cell biocatalyst and aid in its subsequent improvement when cell sorting is implemented, via the selection of cells capable of withstanding certain conditions

6.3. Flow cytometry in bioprocessing

6.3.1. Research

Flow cytometry is a realistic research tool for processes involving the use of bacterial cells. The broad scope of parameters that can be investigated and the relative ease of its application, coupled with rapid analytical times; means that multiparameter flow cytometry can be easily applied to many situations.

Mammalian cells are screened and selected following flow cytometric analysis and cell sorting (Borth *et al* 2000) and this principle can be applied to bacterial systems. Screening and selection of bacterial cells during the development of biotechnologically valuable strains is an area where flow cytometry can be an advantage. The use of single fluorescent stains may be used to detect specific microbial cells and rare cells using multiple labels both without the use of cell sorting (Veal *et al* 2000). Coupling flow cytometry with cell sorting may be used to physically isolate these rare or specific microbial cells (Nebe-von Caron *et al* 1998 and 2000; Ibrahim and van der Engh 2003).

Another way in which flow cytometry may be utilised for biotechnological research is in bacteria genome fingerprinting (Huang *et al* 1999; Kim *et al* 1999). This would be advantageous during the characterisation of novel wild-type and modified bacterial strains of interest.

6.3.2. Development

Flow cytometry has been demonstrated to be an important tool in the study of single cell microbial physiology (Comas-Riu and Vives-Rego 1999; Bragga *et al* 2003; Hewitt *et al* 1999a, b; Amanullah *et al* 2002a, b and 2003). It can also provide valuable information for process development via the study of continuous and batch processes (Fouchet *et al* 1994; Hewitt and Nebe-von Caron 2001; Lú Chau *et al* 2001; Lewis *et al* 2004); where the analysis and selection of different parameters is primarily due to the genetic, physiological and metabolic characteristics of the microorganisms.

In many bioprocesses bacteria are often cultivated in the presence of antibiotics which aid selectivity for a given plasmid. During the development stage it is necessary to determine and optimise the antibiotic susceptibility threshold of the microorganism whilst still maintaining plasmid stability and copy number. Flow cytometry can be used to measure such antibiotic induced bacterial damage (Suller and Lloyd 1999; Novo *et al* 2000; Mortimer *et al* 2000; Braga *et al* 2003).

6.4. Conclusions

Multiparameter flow cytometry has illustrated that microbial populations within a process consists of a variety of sub-populations, some of which are transient. These populations are of cells which have responded differently to a number of process conditions. It has also allowed the visualisation and quantification of these different populations. This study has provided a fascinating insight into process development and characterisation strategy via the use of multiparameter flow cytometry. This tool allowed the assessment of the

effects of the process environment, induction conditions, substrate and product concentrations on the microorganisms utilised in the bioprocess.

The physiological status of the microorganism is one of the most important parameters in a bioprocess, whether it is a biocatalytic reaction or fermentation. The information obtained from flow cytometry can be applied to better culture characterisation and hence be used to improve it. Process efficiency can also be improved. For instance the early identification of a significant percentage of compromised cells allows termination with a reduced loss of resources.

While flow cytometry offers relatively rapid qualitative and quantitative analysis and provides information on what it taking place within a microbial population, its use in large-scale processes may be limited. This is in light of the fact that online measurements are not practical. Cells require staining and incubation periods; and may require washing, fixing or treatment with chelating agents to facilitate staining, all of which are difficult to incorporate into online measuring. And there are other established online measurements which can provide adequate bioprocess monitoring and profiling, though without the level of detail afforded by multiparameter flow cytometry. However, it can be a powerful tool in the research and development stages of any given process (see section 6.3).

The relative ease of using the equipment, sample analysis and the wealth of information that may be accrued means that flow cytometry will lend itself easily to routine microbial system investigation (especially in the research and academic environments) once the correct protocols have been established. This technique can be applied to pre-pilot plant or early pilot plant stages, media development, long and short-term cell stability studies and process development in academic and industrial applications.

Chapter 7

Conclusions

Multiparameter flow cytometry has been applied to two *E.coli* processes. The optimisation of induction conditions for the expression of recombinant human interleukin 13 in *E.coli* IL-13, which is representative of a fermentation process (Figure 1.1A). The second process was the Baeyer-Villiger monooxygenase mediated stereo-selective oxidation of a cyclic ketone, bicyclo (3.2.0.) hept-2-en-6-one to yield two chiral lactone products, (-)-1(S) 5(R)-2-oxabicyclo (3.3.0) oct-6-en-3-one and (-) 1 (R) 5(S)-3-oxabicyclo (3.3.0) oct-6-en-2-one, using *E.coli* TOP10 pQR239 (Figure 1.4). This process is representative of a two- and three- step upstream process (Figure 1.1 B and C). The following conclusions were made:

- Induction with 1mM IPTG has an adverse effect on cell viability and cellular stress levels as indicated by alterations to normal cell membrane polarisation following flow cytometric analysis. Induction also caused a decrease in cellular respiration and proliferation.

- Induction with 1mM IPTG early in the exponential growth phase of *E.coli* IL-13 is most physiologically favourable for inducing the expression of recombinant IL-13. This is further supported by optimum fermentation conditions of pH 7 and maintaining dissolved oxygen tension at 30% above air saturation.

- The metabolic and physiological status of the whole cell biocatalyst *E.coli* TOP10 pQR239 is affected by the environmental conditions of storage temperature, bioconversion media and bioconversion pH. As is CHMO activity.

- 4°C was found to be the most favourable temperature to store *E.coli* TOP10 pQR239 with respect to the stability of cell quality and enzyme activity.

- Carrying out the bioconversion in 50mM phosphate buffer at pH 7 supports the highest rates of enzyme activity (14.7 gL^{-1} h^{-1}, shake flask reaction and 24.4 gL^{-1} h^{-1}, bioreactor reaction per 10g DCW) and cell quality (>80%).

- Substrate and product accumulation in the cytoplasmic membrane of the whole cell biocatalyst *E.coli* TOP10 pQR239 significantly affects its integrity and function.

- Irreversible cell damage increases with increasing substrate concentration.

- Product associated cell damage is time dependent but not concentration dependent. This impairment, manifested as a loss in membrane polarisation could therefore be potentially reversible.

- Increasing substrate concentration and exposure to product and not loss of whole cell biocatalyst viability is the primary impediment to optimal enzyme activity during the 4 h bioconversion.

- Co-substrate availability is essential for enzyme activity. However the quantities present can have detrimental effects on productivity.

- High levels of co-substrate in the system (11x more than the utilisation rate) causes severe physiological and metabolic damage to *E.coli* TOP10pQR239 whilst facilitating a similar level of enzyme activity as when the co-substrate is present at the utilisation rate

- Enzyme activity is dependent on a combination of the physiological and metabolic status of the whole cell biocatalyst, substrate and product concentration and co-substrate availability.

- Multiparameter flow cytometry is an invaluable tool for the characterisation of microbial bioprocesses, with respect to process development and optimisation.

Appendices

Appendix I: Cell dilution assumptions for flow cytometry

Samples of cells taken from the fermentation vessel were diluted in 1X Dulbeco's buffered saline, pH 7.0 to a final concentration of 10^5 ml $^{-1}$.

OD Value	N° of cells	Volume per 10ml to give 1 x 10^9 cells
0.25	0.025 x 10^9	400 µl
2.5	0.25 x 10^9	40 µl
4	0.4 x 10^9	25µl
5	0.5 x 10^9	20µl
10	1.0 x 10^9	10µl
20	1.75 x 10^9	5µl

Appendix II: SDS PAGE size marker calibration curve

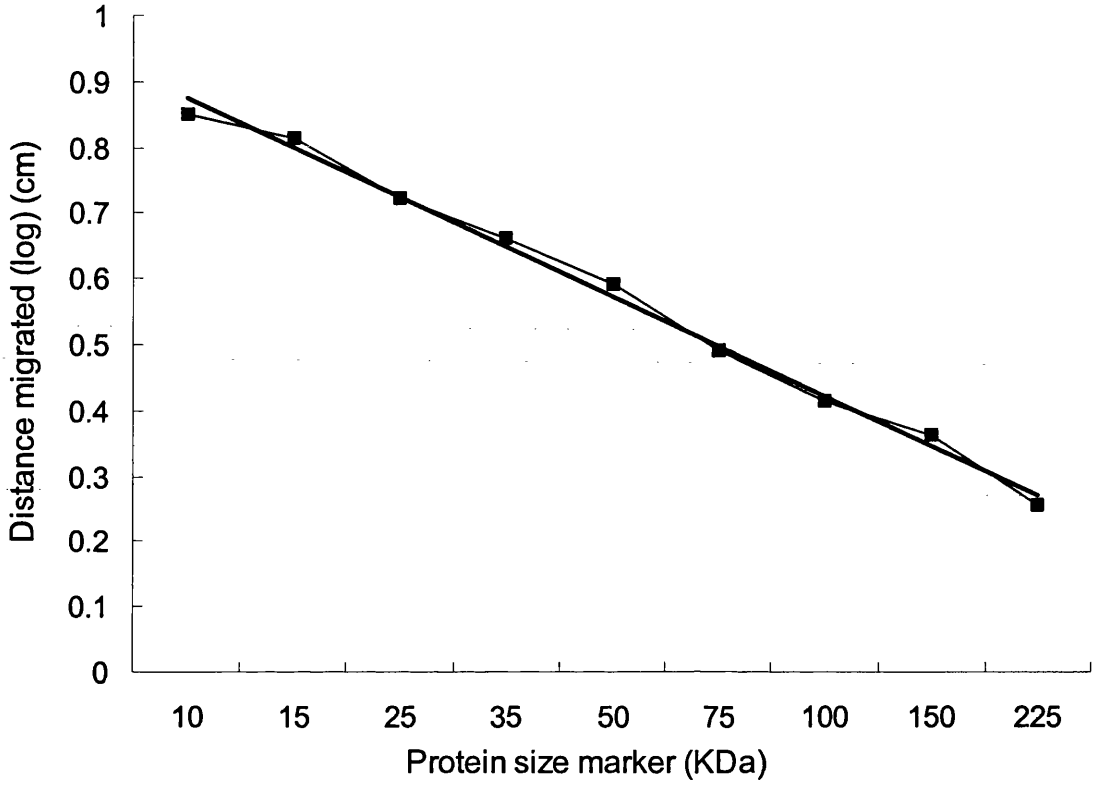

Appendix II. SDS PAGE molecular weight marker calibration curve. The linear squares fitted line had an R2 value of 0.99.

Appendix III: Growth curve of *E.coli* IL-13

OD measurements were taken to measure biomass increases and identify growth phases during the fermentation of *E.coli* IL-13. OD was measured according to the method described in chapters 3. The plot below shows the biomass increase in and un-induced fermentation. The error bars shown on the graph are the standard deviations from the mean of three independent measurements.

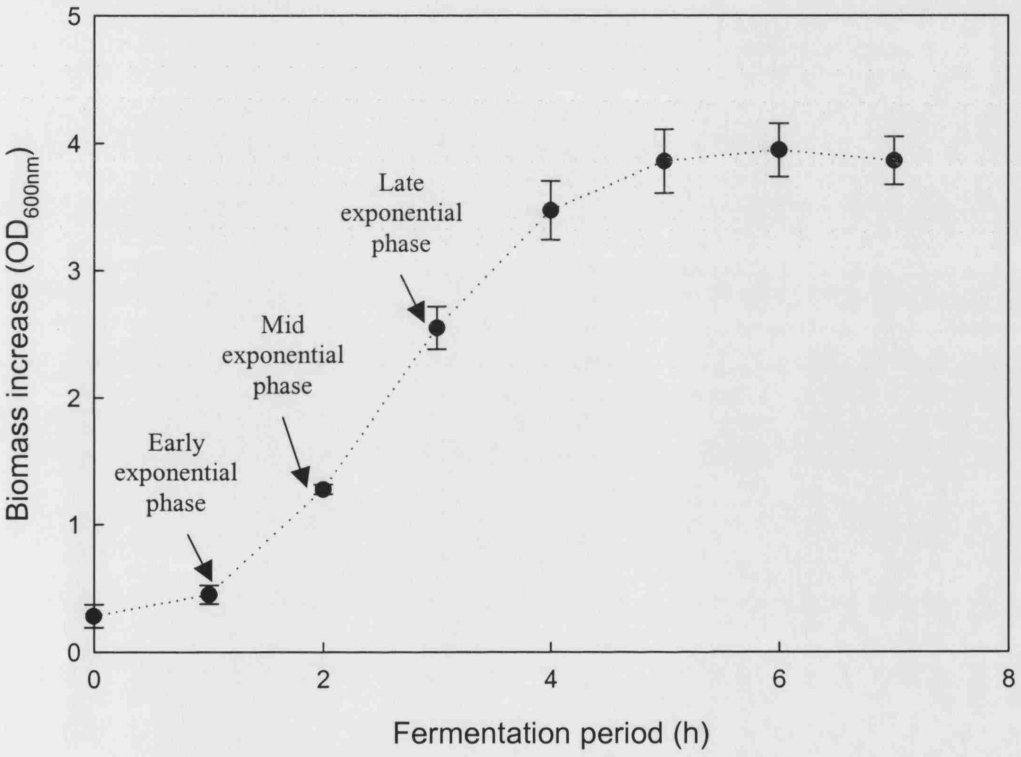

Appendix III. Growth curve of un-induced *E.coli* IL-13

Appendix IV: Calibration curve of optical density against dry cell weight for *E.coli* TOP10 pQR239

Calibrations of the dry cell weight (DCW) against optical density (OD_{670nm}) measurements were used to determine the DCW of *E.coli* TOP10 pQR239 during culture. DCW and OD were measured according to the methods described in chapters 4 and 5. The plot below shows the calibration curve correlating DCW and OD. The error bars shown on the graph are the standard deviations from the mean of three independent measurements.

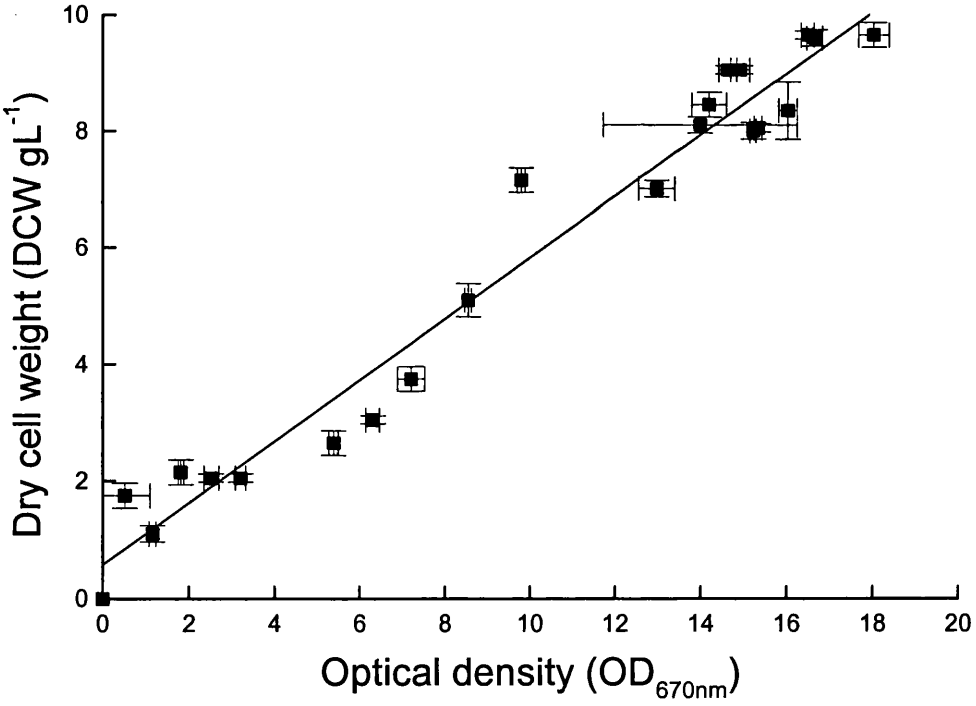

Appendix IV. Calibration of OD_{670nm} with DCW measurements for *E.coli* TOP10 pQR239 fermentations. The linear squares fitted line had an R2 value of 0.99.

Appendix V: Gas chromatography calibration curve of bicyclo (3.2.0.) hept-2-en-6-one (substrate)

Known concentrations of substrate in ethyl acetate with naphthalene at a concentration of 1mg ml^{-1}, as an internal standard, were used as GC calibration standards, to measure the amounts of substrate present in samples taken from the bioconversion vessel.

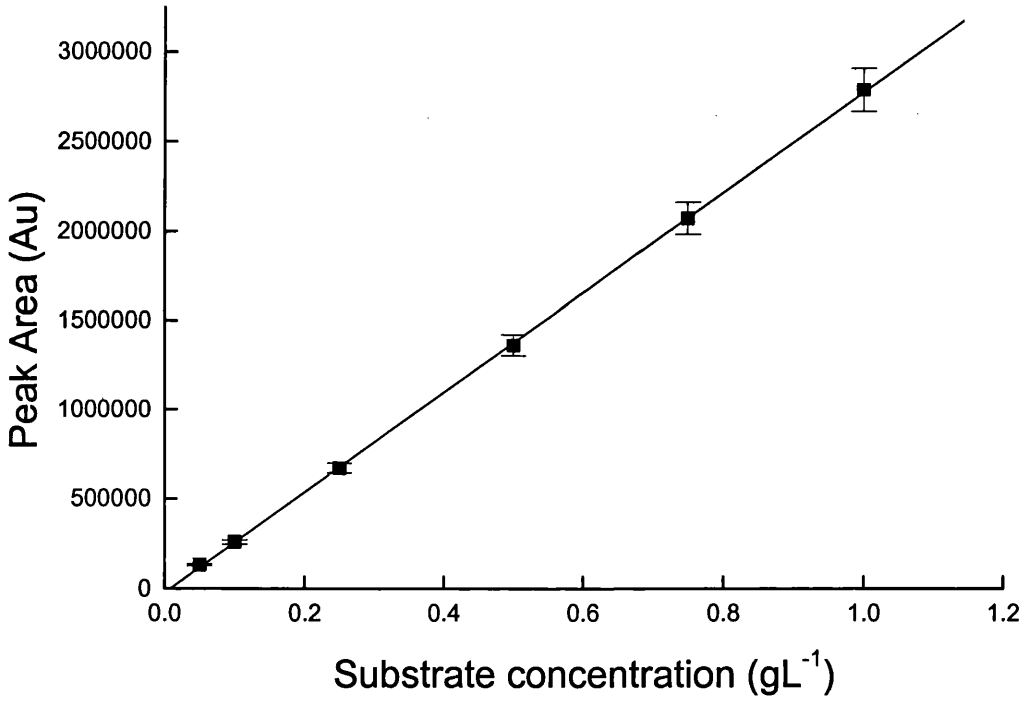

Appendix V: Bicyclo (3.2.0.) hept-2-en-6-one (substrate) calibration curve.
The linear squares fitted line had an R2 value of 0.99.

Appendix VI: Gas chromatography calibration curve of the chemical lactone, 1S 5R 2-oxabicyclo [3.3.0] oct- 6-en-3-one (product)

Known concentrations of product in ethyl acetate with naphthalene at a concentration of 1mg ml^{-1}, as an internal standard, were used as GC calibration standards, to measure the amounts of substrate present in samples taken from the bioconversion vessel. The chemical lactone was used because purity was consistent. This was used for both chemical and enzymatic lactone identification.

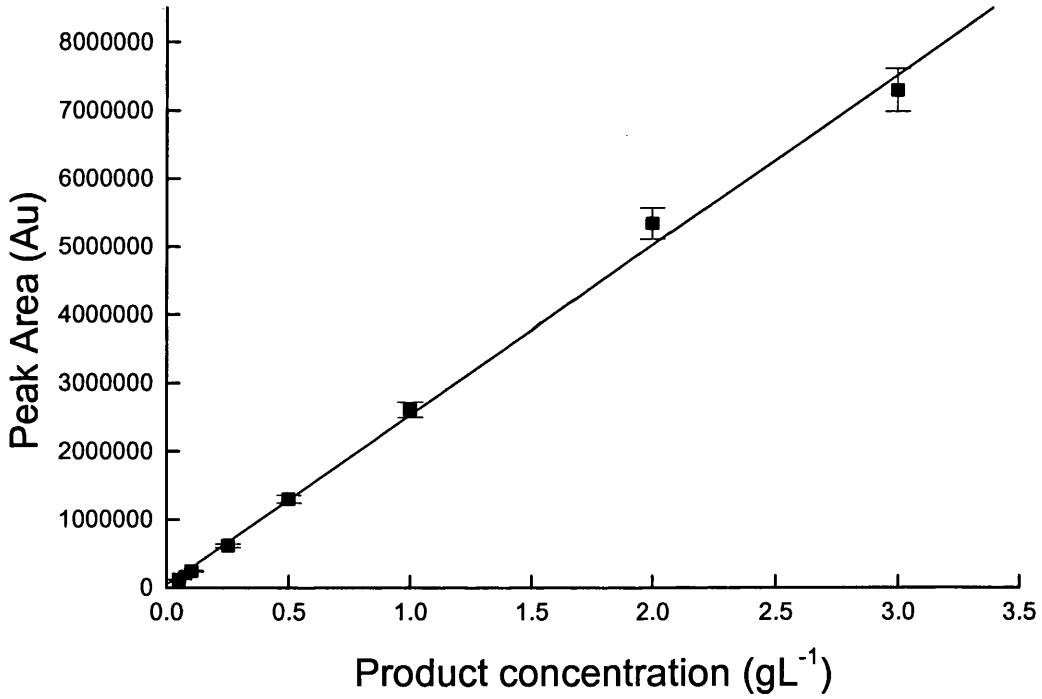

Appendix VI. Chemical lactone, 1S 5R 2-oxabicyclo [3.3.0] oct- 6-en-3-one (Product) calibration curve. The linear squares fitted line had an R2 value of 0.99.

Appendix VII: Example gas chromatography showing peaks corresponding to the substrate, product, ethyl acetate and the internal standard.

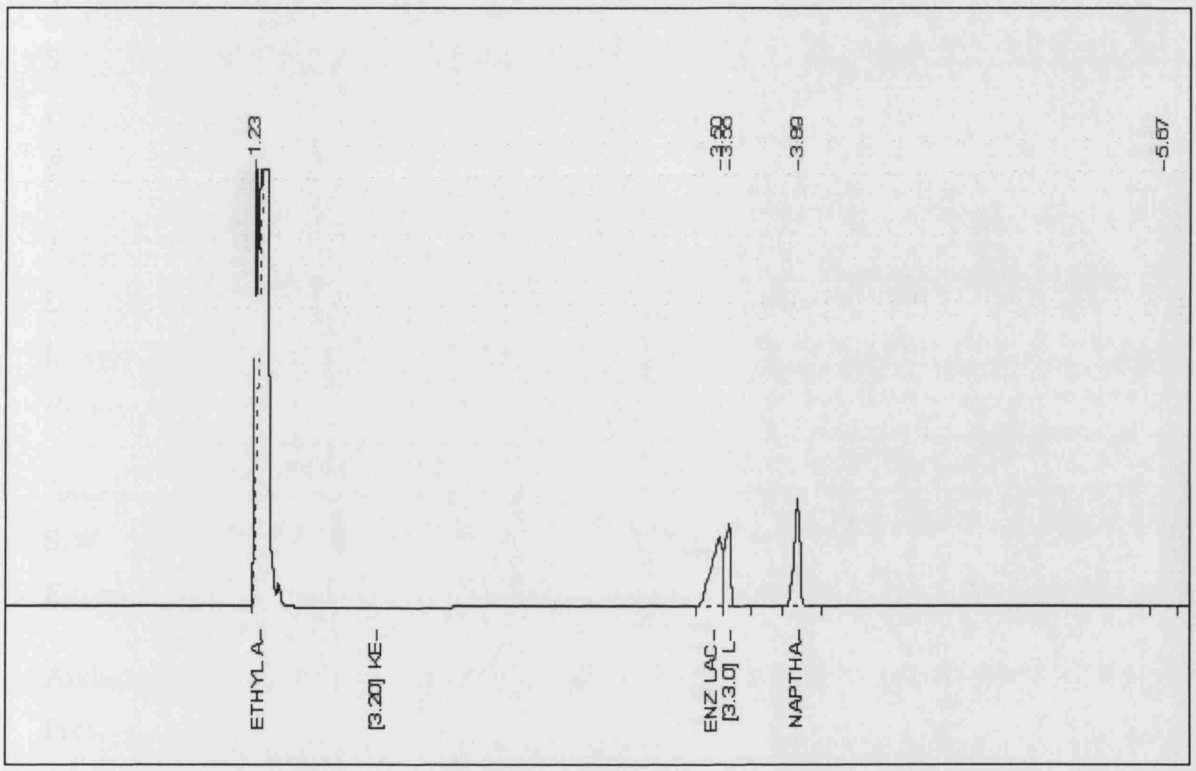

References

Alphand, A., Carrea, G., Wohlgemuth, R., and Woodley J.M. (2003) Towards Large-Scale Synthetic Applications of Baeyer-Villiger Monoxygenases. *Trends in Biotechnology,* **21**(7), 318-323.

Amanullah, A., Hewitt, C. J., Nienow A.W., Lee C., Chartrain M., Buckland B.C., Drew S.W., and Woodley J. M. (2002a) Application of Multiparameter Flow Cytometry Using Fluorescent Probes to Study Substrate Toxicity in the Indene Bioconversion. *Biotechnology and Bioengineering*, **80**(3), 239-249.

Amanullah, A., Hewitt, C. J., Nienow, A. W., Lee, C., Chartrain, M., Buckland, B. C., Drew S.W. and Woodley J. M. (2002b) Measurement of Strain-Dependent Toxicity in the Indene Bioconversion Using Multiparameter Flow Cytometry. *Biotechnology and Bioengineering*, **81**(4), 405-420.

Amanullah, A., Hewitt, C. J., Nienow A.W., Lee C., Chartrain M., Buckland B.C., Drew S.W., and Woodley J. M. (2003a) Fed-batch Bioconversion of Indene to Cis-Indandiol. *Enzyme Microbial Technology,* **3**(7), 954-967.

Andersson, L., Yang, S., Neubauer, P., and Enfors, S. (1996). Impact of Plasmid Presence and Induction on Cellular Responses in Fed Batch Cultures of *Escherichia coli*. *Journal of Biotechnology,* **46**, 255-263.

Bagwell, C. B., and Adams, E. G. (1993). Fluorescence Spectral Overlap Compensation for Any Number of Flow Cytometry Parameters. *Annals of the New York Academy of Science*, **677**, 167-184.

Barclay, S. S., Woodley, J. M., Lilly, M. D., Spargo, P. L., Pettman, A. J. (2001). Production of Cyclohexanone Monooxygenase from *Acinetobacter calcoaceticus* for Large Scale Baeyer-Villiger Monooxygenase Reactions. *Biotechnology Letters,* **23**, 385-388.

Bearson, S., Bearson, B., and Foster, J. W. (1997) Acid Stress Responses in Enterobacteria. *FEMS Microbiology Letters* **147**(2), 173-180.

Beecher, J., and Willetts, A. (1998) Biotransformation of Organic Sulfides. Predictive Active Site Models for Sulfoxidation Catalysed by 2,5-diketocamphane 1,2-monooxygenase and 3,6-diketocamphane 1,6-monooxygenase, Enantio-complementary Enzymes from *Pseudomonas putida* NCIMB 10007. *Tetrahedron: Asymmetry,* **9**(11), 1899-1916.

Bentley, W. E., Mirjalili, N., Andersen, D. C., Davis, R. H, and Kompala, D. S. (1990) Plasmid-Encoded Protein: The Principal Factor in the "Metabolic Burden" Associated with Recombinant Bacteria. *Biotechnology and Bioengineering,* **35**, 668-681.

Bhattacharya, S. K., and Dubey, A. K. (1997). Effects of Dissolved Oxygen and Oxygen Mass Transfer on Over Expression of Target Gene in Recombinant *E.coli. Enzyme Microbial Technology*, **20**, 355-360.

Bigos, N., Baumgarth, N., Jager, G. C., Herman, O. C., Nozaki, T., Stovel, R. T., Parks, D. R. and Herzenberg, L. A. (1999) Nine Color Eleven Parameter Immunophenotyping Using Three Laser Flow Cytometry. *Cytometry*, **36 (1),** 36-45.

Bird, P. A., Sharp, David C. A., and Woodley J. M. (2002) Near-IR Spectroscopic Monitoring of Analytes During Microbially Catalysed Baeyer-Villiger Bioconversions. *Organic Process Research & Development,* **6**, 569-576.

Borth, H., Zeyda, M., and Katinger, H. (2001) Efficient Selection of High-Producing Subclones During Gene Amplification of Recombinant Chinese Hamster Ovary Cells by Flow Cytometry and Cell Sorting. *Biotechnology and Bioengineering,* **71**, 266-273.

Boucabeille, C., Letellier, L., Simonet, J. Henckes, G. (1998) Mode of Action of Linenscin OC2 against *Listeria innocua. Applied Environmental Microbiology.* **64**, (9). 3416-3421.

Bouchez, J. C., Cornu, M., Danzart, M, Leveau, J. Y., and Bouix, M. (2004) Physiological Significance of the Cytometric Distribution of Fluorescent Yeasts After Viability Staining. *Biotechnology and Bioengineering,* **86** (5), 520-530.

Bragga, P. C., Bovio, C, Culici, M, and Dal Sassa M. (2003) Flow Cytometric Assessment of Susceptibilities of *Streptococcus pyogenes* to Erythromycin and rokitamycin. *Antimicrobial Agents and Chemotherapy* **47** (1), 408-412.

Breese, M. D., and Sharp, R. J. (1980). Storage of *Escherichia coli* strains Containing Plasmid DNA in Liquid Nitrogen. *Journal of Applied Bacteriology*, **48**, 63-68.

Breeuwer, P., and Abee, T. (2000) Assessment of Viability of Microorganisms Employing Fluorescence Techniques. *International Journal of Food Microbiology* (55), 193-200.

Breeuwer, P., Drocourt, J., Bunschoten, N., Zwietering, M. H., Rombouts, F. M., and Abee, T. (1995) Characterisation of Uptake and Hydrolysis of Fluorescein Diacetate and Carboxyfluorescein Diacetate by Intracellular Esterases in Saccharomyces cerevisiae, Which Result in Accumulation of Fluorescent Product. *Applied and Environmental Microbiology,* **61**(4), 1614-1619.

Bryne, K. M., Reinhart, G. A., and Hayek, M. G. (2000) Standardized flow cytometry gating in veterinary medicine. *Methods in Cell Science,* **22** (2-3), 191-198.

Buckland, B. C., .Robinson, D. K. and Chartrain, M. (2000) Biocatalysis for Pharmaceuticals- Status and Prospects for a Key Technology. *Metabolic Engineering*, **2,** 42-48.

Bunthof, C. J., van Schalawijk S., Meijer W, Abee T, and Hugenholtz J. (2001) Fluorescent Method for Monitoring Cheese starter Permeabilization and Lysis. *Applied and Environmental Microbiology* **67** (9), 4264-4271.

Chao, Y., Chiang C., Wang, Y., and Wang, Z. W. (2003) Applicability of New Expression Vectors for Both Engineering Uses and Biological Studies. *Biotechnology Progress* **19**, 1076-1080.

Chen, B., Lin, C., and Lim, H. C. (1995) Temperature Induction of Bacteriophage Lamda Mutants in *Escherichia coli*. *Journal of Biotechnology*, **40**, 87-97.

Comas-Riu, J., and Vives-Rego, J. (1999) Use of Calcein and SYTO-13 to Assess Cell Cycle Phases and Osmotic Shock Effects on *E.coli* and *Staphylococcus aureus* by Flow Cytometry. *Journal of Microbiological Methods*, **34**, 215-221.

Comas, J., and Vives-Rego, J. (1998) Enumeration, Viability and Heterogeneity in *Staphylococcus aureus* Cultures by Flow Cytometry. *Journal of Microbiological Methods*, **32**, 45-53.

Crissman, H. A., Orlicky, D. J., and Kissane, R. J. (1979) Fluorescent DNA Probes for Flow Cytometry. Considerations and Prospects. *Journal of Histochemistry and Cytochemistry*. **27**(12), 1652-1654.

Crosland-Taylor, P. J. (1953) A Device for Counting Small Particles Suspended in a Fluid Through a Tube. *Nature*, **171**, 37-38.

Cunningham, B. A. (2001) A Growing Issue: Cell Proliferation Assays. The Scientist **15** (13), 26.

Davey, H. M., and Kell, D. B. (1996) Flow Cytometry and Cell Sorting of Heterogeneous Microbial Populations: The Importance of Single-Cell Analyses. *Microbiological Reviews*, **60** (4), 641-696.

De Bont, J. A. M. (1998) Solvent-Tolerant Bacteria in Biocatalysis. *Trends in Biotechnology* **16**, 493-499.

De León, A., Hernández, V., Galindo, E., and Ramírez, O. T. (2003) Effects of Dissolved Oxygen Tension on the Production of Recombinant Penicillin Acylase in *Escherichia coli*. *Enzyme Microbial Technology*, **33**, 689-697.

Dean, G. A., Barger, A., and LaVoy, A. (2005) Cloning and Expression of Feline Interleukin 15. *Cytokine,* **29**, 77-83.

Deere, D., Shen, J., Vesey, G., Bell, P., Bissinger, P., and Veal, D. (1998) Flow Cytometry and Cell Sorting for Yeast Viability Assessment and Cell Selection. *Yeast,* **14,** 147-160.

De Santis, G., and Jones, J. B. (1999) Chemical Modification of Enzymes for Enhanced Functionality. *Current Opinions in Biotechnology*, **10**, 324-330.

Doig, S. D, O'Sullivan, L. M., Patel, S., Ward, J. M., and Woodley, J. M. (2001) Large Scale Production of Cyclohexanone Monooxygenase from *Escherichia coli* TOP10 pQR239. *Enzyme and Microbial Technology,* **28**, 265-274.

Doig, S. D., Avenell, P. J., Bird, P. A., Gallanti, P., Lander, K.S, Lye, G. J., Wohlgemuth, R., and Woodley J. M. (2002) Reactor Operation and Scale-Up of Whole Cell Baeyer-Villiger Catalyzed Lactone Synthesis. *Biotechnology and Bioengineering,* **18**, 1039-1046.

Doig, S. D., Simpson, H., Alphand, V., Furstoss, R., and Woodley, J. M. (2003) Characterization of a Recombinant *Escherichia coli* TOP10 [pQR239] Whole-cell Biocatalyst for Stereoselective Baeyer-Villiger Oxidations. *Enzyme and Microbial Technology*, **32**, 347-355,

Doran, P.M. (1999) *Bioprocess Engineering Principles*. Academic Press Limited.

Duetz, W. A., van Beilen, J. B., and Witholt, B. (2001) Using Proteins in Their Natural Environment: Potential and Limitations of Microbial Whole-Cell Hydroxylations in Applied Biocatalysis. *Current Opinion in Chemical Biology*, **12,** 419-425.

Dunlop, E. H., and Ye, S. J. (1990) Micromixing in Fermentors: Metabolic Changes in *Saccharomyces cerevisiae* and Their Relationship to Fluid Turbulence. *Biotechnology and Bioengineering*, **36**, 854-864.

Dumon-Seignovert, L., Cariot, G., and Vuillard, L. (2004) The Toxicity of Recombinant Proteins in *Escherichia coli*: A Comparison of Over-expression in BL21 (DE3), C41 (DE3), and C43 (DE3). *Protein Expression and Purification*, **37**, 203-206.

Eales, Lesley-Jane. *Immunology for Life Scientists*. Second edn. Wiley.

Ecstein, M., Daußmann, T., and Kragl, U. (2004) Recent Developments in NAD(P) Regeneration for Enzymatic Reductions in One- and Two-Phase Systems. *Biocatalysis and Biotransformations,* **22** (2), 89-96.

Eisenmesser, E. Z., Kapust, R. B., Nawroki, J. P., Mazzulla, M. J., Pannell, L. K., Waugh, D. S., and Byrd, R. A. (2000) Protein Expression, Purification, Refolding and Characterization of Recombinant Human Interleukin-13: Utilization of Intracellular Processing. *Expression and Purification*, **20**, 186-195.

El-Kest, S. E., and Marth, H. E. (1991) Injury and Death of Frozen Listeria monocytogenes as Affected by Glycerol and Milk Components. *Journal of Dairy Science* **74**,1201-1208.

Endo, T., and Koizumi S. (2001) Microbial Conversion with Cofactor Regeneration Using Genetically Engineered Bacteria. *Advanced synthesis and catalysis* **343**, 521-526.

Faber, K. (1997) Biotransformations of Non-Natural Compounds: State of the Art and Future Development. *Pure and Applied Chemistry* **69** (8) 1613-1632.

Faber, K. (2000) *Biotransformations in organic chemistry.* Springer-Verlag New York.

Fouchet, P., Manin, C., Richard, H., Frelat, G., and Barbotin, J. N. (1994) Flow Cytometry Studies of Recombinant *Escherichia coli* in Batch and Continuous Cultures: DNA and RNA Contents; Light-Scatter Parameters. *Applied Microbiology and Biotechnology*, **41**, 584-590.

Fowler, J. D., and Dunlop, E. H. (1989) Effects of Reactant Heterogeneity and Mixing on Catabolite Repression in Cultures of *Saccharomyces cerevisiae. Biotechnology and Bioengineering*, **33**, 1039-1046.

Freyer, S. A., König, M., and Kunkel, A. (2004) Validating Shaking flasks as Representative Screening Systems. *Biochemical Engineering Journal,* **17**, 169-173.

Fu, A. Y., Spence, C., Schere, A., Arnold, F. A., and Quake, S. R. (1999) A Microfabricated Fluorescence-Activated Cell Sorter. *Nature Biotechnology,* **17**, 1109-1111.

Givan, A. L. (2001) *Flow cytometry. First principles* second edn. Wiley-Liss Publishers.

Goldsby, R. A., Kindt, T. J., and Osborne, B. A. (2000) *Immunology*. Fourth edn. W. H. Freeman.

Gorvadhan, C. P. (1999) Crosslinking of Enzymes for Improved Stability and Performance. *Current Opinion in Biotechnology,* **10**, 331-335.

Green, D. W. (2002) The Bacterial Cell Wall as a Source of Antibacterial Targets. *Expert Opinions in Therapeutic Targets* **6** (1), 1-19.

Grimsley, G. R., Shaw, K. L., Fee, L. R., Alston, R. W., Huyghues-Despointes, B. M. P., Thurkill, R. L., Scholtz, J. M., and Pace, C. N. (1999) Increasing Protein Stability by Altering Long-Range Coulombic Interactions. *Protein Science,* **8**, 1843-1849.

Gucker, F. T., O'Konski, C, T., Pikard, H. B., and Pitts, J. N. (1947) A Photoelectric Counter for Colloidal Particles. *Journal of the American Chemical Society.* **69**, 2422-2431.

Harding, C. L., Lloyd, D. R., MacFarlane, C. M., and Al-Rubeai, M. (2000) Using the Microcyte Flow Cytometer To Monitor Cell Number, Viability, and Apoptosis in Mammalian Cell Culture. *Biotechnology Progress*, **16**, 800-802.

Harrop, A. J., Hocknull, M. D., and Lilly, M. D. (1989) Biotransformations in organic solvents: A difference between Gram-positive and Gram-negative bacteria. *Biotechnology Letters,* **11** (11), 807 – 810.

Haugland, R., P. (2002) Handbook of Fluorescent Probes and Research Products. 9th Ed. Molecular Probes.

Held, M., Schmid A., van Beilen J.B., and Witholt B. Biocatalysis. Biological Systems for the Production of Chemicals*. *Pure and applied chemistry,* **72** (7), 1337-1343.

Herrera, G., Martinez, A., Blanco, M., and O' Connor J. (2002) Assessment of *Escherichia coli* B with Enhanced Permeability to Fluorochromes for Flow Cytometric Assays of Bacterial Cell Function. *Cytometry*, **49**, 62-69.

Hewitt, C. J., Nebe-von Caron, G., Nienow, A.W., and McFarlane, C. M. (1999a) Use of Multi-staining Flow Cytometry to Characterise the Physiological State of *Escherichia coli* W3110 in High Cell Density Fed-Batch Cultures. *Biotechnology and Bioengineering*, **64,** 1-7.

Hewitt, C. J., Nebe -von Caron, G., Nienow, A. W., and McFarlane, C. M. (1999b) The Use of Multi-Parameter Flow Cytometry to Compare the Physiological Response of *Escherichia coli* W3110 to Glucose Limitation During Batch, Fed-Batch and Continuous Culture Cultivations. *Journal of Biotechnology,* **75,** 251-264.

Hewitt, C. J., and Nebe-von Caron, G. (2001) An industrial Application of Multiparameter Flow Cytometry: Assessment of Cell Physiological State and Its Application to the Study of Microbial Fermentations. *Cytometry,* **44** (3) 179-187.

Hilker, I., Gutiérrez, M. C., Alpand, V., Wohlgemuth, R., and Furstoss, R. (2004) Microbiological Transformations 57. Facile and Efficient Resin-Based in Situ SFPR Preparative-Scale Synthesis of an Enantiopure "Unexpected" Lactone Regioisomer via a Baeyer-Villiger Oxidation Process. *Organic Letters,* **6**, (12), 1955-1958.

Hogan, M. C., and Woodley, J. M. (2000) Modelling of Two Enzyme Reactions in a Linked Cofactor Recycle System for Chiral Lactone Synthesis. *Chemical Engineering Science*, **55** (2), 2001-2008.

Hohenblum, H., Borth, N. and Mattanovich, D. (2003) Assessing viability and cell-associated production of recombinant protein producing *Pichia pastoris* with flow cytometry. *Journal of Biotechnology,* **102**, 281-290.

Horan, P. K., and Wheeless Jr, L. L. (1977) Quantitative Single Cell Analysis and Sorting. *Science,* **198,** 149-157.

Huang, Z., Jett, J. H., and Keller, R. A. Bacteria Genome Fingerprinting by Flow Cytometry. *Cytometry*, **35**, 169-175.

Hubalek, Z. (2003). Protectants Used in the Cryopreservation of Microorganisms. *Cryobiology*, **46**(3), 2005-229.

Hutter, K. J., and Eipel, H. E., (1979) Microbial determinations by flow cytometry. *Journal of General Microbiology*, **113**(2), 369-75.

Ibrahim, S. F., and van der Engh, G. (2003) High-Speed Cell Sorting: Fundamentals and Recent Advances. *Current opinion in Biotechnology*, **14**, 5-12.

Illanes, A. (1999) Stability of biocatalysts. *European Journal of Biochemistry,* **2**, (1), 1-9.

Itagaki, E., (1986) Studies on Steroid Monooxygenase from *Cylindrocarpon radicicola* ATCC 11011. Purification and characterisation. *Journal of Biochemistry* (Tokyo), **99** (3), 815-824.

Jaroszeski, M. J., and Radcliff, G. (1999) Fundamentals of Flow Cytometry. *Molecular Biotechnology*, **11,** 37-53.

Jepras, R. I., Paul, F. E., Pearson, S. C., and Wilkinson, M. J. (1997) Rapid Assessment of Antibiotic Effects on *Escherichia coli* by bis-(1,3-Dibutylbarbituric Acid) Trimethine Oxonol and Flow Cytometry. *Antimicrobial Agents and Chemotherapy* **41**, (9), 2001-2005.

Joshi, B. H., Puri, R. K., (2005) Optimization, Expression and Purification of Two Biologically Active Chimeric Fusion Proteins that Consist of Human Interleukin-13 and *Pseudomonas* exotoxin in *Escherichia coli. Protein Expression and Purification,* **39**, 189-198.

Kell, D. B., Ryder, H. M., Kaprelyants, A. S., and Westerhoff HV. (1991) Quantifying Heterogeneity: Flow Cytometry of Bacterial Cultures. *Antonie Van Leeuwenhoek*, **60(3-4),** 145-158.

Kelly, D. R. (1996) A Proposal for the Origin of the Stereoselectivity in Enzyme Catalysed Baeyer-Villiger Reactions. *Tetrahedron: Asymmetry,* **7** (4), 1149-1152.

Keyes, W. M., and Mills, A. A. (2003) Inducible Systems see the Light. *Trends in Biotechnology*, **21**(2), 53-55.

Kim, Y., Jett, J. H., Larson, E. J., Penttila, J. R., Marrone, B. L., and Keller, R. A. (1999). Bacterial Fingerprinting by Flow Cytometry: Bacteria Species Discrimination. *Cytometry*, **36**, 324-332.

Klibanov, A. M. (2001) Improving Enzymes by Using Them in Organic Solvents. *Nature* **409**, 241-246.

Koenig, G. L. (2003) Viability of and Plasmid retention in Frozen Recombinant Escherichia coli over Time: A Ten-Year Prospective Study. *Applied and Environmental Microbiology*, **69**(11) 6605-6609.

Kosinski, M. J., Rinas, U., and Bailey, J. E. (1992) Isopropyl-β-D-thiogalactopyranoside Influences the Metabolism of *Escherichia coli. Applied Microbiology and Biotechnology*, **36,** 782-784.

Kurland, C. G., and Dong, H. (1996) Bacterial Growth Inhibition by Overproduction of Protein. *Molecular Microbiology,* **21**(1), 1-4.

Laemmli, U. K. (1970) Cleavage of Structural Proteins during the Assembly of the Head of Bacteriophage T4. *Nature*, **227**(5259), 680-5.

Lawry J. (1998) The Use of Flow Cytometry to Sort Cells or Particles. *Proceedings RMS* **33**(1), 27-29.

Lewis, G., Taylor, I. W., Nienow, A. W., and Hewitt, C. J. (2004) The Application of Multi-parameter Flow Cytometry to the Study of Recombinant *Escherichia coli* Batch Fermentation Processes. *Journal of Industrial Microbiology and Biotechnology,* **31**, 311-322.

Lú Chau, T., Gullián, A., Roca, E., Núñez, M. J., and Lema, J. M. (2001) Population Dynamics of a Continuous Fermentation of Recombinant *Saccharomyces cerevisiae* Using Flow Cytometry. *Biotechnology Progress,* **17**, 951-957.

Lye, G. J. and Woodley, J. M. (1999) Application of In Situ Product-Removal Techniques to Biocatalytic Processes. *Trends in Biotechnology*, **17**, 395-402.

Malabarba, G. M., Rui, H., Deutsch, H. H. J., Chung, J., Kalthoff, S. F., Farrar, W., and Kirken, R. A. (1996) Interleukin-13 is a Potent Activator of JAK3 and STAT6 in Cells Expressing Interleukin-2 Receptor-g and Interleukin-4 Receptor-a. *Biochemistry Journal.* **319,** 865-872.

Malito, E., Alfier, A., Fraaije, M. W., and Mattevi, A. (2004) Crystal Structure of a Baeyer-Villiger Monooxygenase. *Proceedings of the National Academy of Science USA,* **101**, 13157-13162.

Mason, D. J., Shanmuganathan, S., Mortimer, F. C., and Gant, V. A. (1998) A Fluorescent Gram Stain for Flow Cytometry and Epifluorescence Microscopy. *Applied and Environmental Microbiology*, **64**(7), 2681-2685.

Mason, D. J., Lopéz-Amorós, R., Allman, R., Stark, J. M., and Lloyd, D. The Ability of Membrane Potential Dyes and Calcafluor white to Distinguish between Viable and Non-Viable Bacteria. *Journal of Applied Bacteriology*, **78**,309-315.

Mattanovich, D., Lopéz-Amorós, R., Allman, R., and Lloyd D. (1995) The Ability of Membrane Potential Dyes and Calcafluor White to Distinguish Between Viable and Non-viable Bacteria. *Journal of Applied Bacteriology*, **78**, 309-315.

McCoy, M. (2001) Making Drugs With Little Bugs. *Chemical and Engineering News*, **79**(21), 37-43.

McFarland, B. L. (2003) Biodesulphurization. Current Opinions in Microbiology, **2**(3), 257-264.

Meinander, N. Q. and Han-Hägerdal, B. (1997) Influence of Co-Substrate Concentration on Xylose Conversion by Recombinant, XYL1 Expressing *Saccharomyces cerevisiae*: A Comparison of Different Sugars and Ethanol as Co-Substrates. Applied and *Environmental Microbiology*, **63**(5), 1959-64.

Mihovilovic, M. D., Muller, B., Kayser, M. M., Stewart, J. D., Frohlich, J., Stanetty, P., and Spreitzer, H. (2001) Baeyer-Villiger Oxidations of Representative Heterocyclic Ketones by Whole Cells of Engineered *Escherichia coli* Expressing Cyclohexanone Monooxygenase. *Journal of Molecular Catalysis B: Enzymatic* **11**, 349-353.

Miroux, B., and Walker, J. E. (1996) Over-Production of Proteins in *Escherichia coli*: Mutant hosts that Allow Synthesis of Some Membrane Proteins and globular Proteins at High Levels. *Journal of Molecular Biology*, **260**(3), 289-298.

Mortimer, F. C., Mason, D. J., and Gant, V. A., (2000) Flow Cytometric Monitoring of Antibiotic-Induced Injury in *Escherichia coli* Using Cell-Impermeant Fluorescent Probes. *Antimicrobial Agents and Chemotherapy* **44**(3), 676-681.

Müller, S., Bley, T., and Wolfgang, B. (1999) Adaptive Responses of *Ralstonia eutropha* to Feast and Famine Conditions Analysed by Flow Cytometry. *Journal of Biotechnology*, **75**, 81-97.

Müller, S., Ullrich, S., Lösche, A., Loffhagen, N., and Babel, W. (2000) Flow cytometric Techniques to Characterise Physiological States of *Acinetobacter calcoaceticus*. Jo*urnal of Microbiology*, **40**, 67-77.

Müller, S. Straüber, H., Lösche, A., and Wolfgang, B. (2002) Population Analysis of a Binary Bacterial Culture by Multi-parametric Flow Cytometry. *Journal of Biotechnology* 97, 163-176.

Nebe-Von Caron, G., Stephens, P., and Badley, A. R. (1999) Bacterial Detection and Differentiation by Cytometry and Fluorescent Probes. *Proceedings of the Royal Microbiological Society* RMS **34**(1), 321-327.

Nebe-von Caron, G., and Badley, R. A. (1995) Viability Assessment of Bacteria in Mixed Populations Using Flow Cytometry. ***Journal of Microscopy***, **179** (Pt.1), 55-66.

Nebe-von Caron, G., Stephens, P., and Badley R. A. (1998) Assessment of Bacterial Viability Status by Flow Cytometry and Single Cell Sorting. *Journal of Applied Microbiology*, **84,** 988-998.

Nebe-von Caron, G., Stephens, P. J., Hewitt, C. J., Powell, J. R., and Badley R. A. (2000) Analysis of Bacterial Function by Multi-colour Fluorescence Flow Cytometry and Single Cell Sorting. *Journal of Microbiological Methods*, **42**, 97-114.

Niccolai, A. (2003) Maximization of Recombinant *Helicobacter pylori* Neutrophil Activating Protein Production in *Escherichia coli*: Improvement of a Chemically Defined Medium Using Response Surface Methodology. *FEMS Microbiology Letters*, **221**, 257-262.

Nikaido, H. (1994) Prevention of Drug Access to Bacterial Targets: Permeability Barrier and Active Efflux. *Science* **264**, 382-388.

Novo, D., Perlmutter, N. G., Hunt, R. H., and Shapiro, (1999) H. M. Accurate Flow Cytometric Membrane Potential Measurement in Bacteria Using Diethyloxacarbocyanine and a Ratiometic Technique. *Cytometry* **35**, 55-63.

Novo, D. J., Perlmutter, N. G, Hunt, R. H., and Shapiro, H. M. (2000) Multiparameter Flow Cytometric Analysis of Antibiotic Effects on Membrane Potential, Membrane Permeability, and Bacterial Counts of *Staphylococcus aureus* and *Micrococcus luteus*. *Antimicrobial Agents and Chemotherapy*, **44**,(4), 827-834.

Novy, R. and Morris, B. (2001) Use of Glucose to Control Basal Expression in the pET system. *inNovations*, **13**, 8-10.

Onyeaka, H., Nienow, A. W., and Hewitt, C. J. (2003) Further Studies Related to the Scale-up of High Density *Escherichia coli* Fed-Batch Fermentations: The Additional Effect of a Changing Microenvironment when Using Aqueous Ammonia to Control pH. *Biotechnology and Bioengineering,* **84**(4), 474-484.

Ormerod, M. G. (1994) *Flow Cytometry.* ßIOS Scientific Publishers.

Ormerod, M. G. (2000) *Flow Cytometry. A practical approach.* Third edn. Oxford University Press.

Osborne, S. J., Leaver, J., Turner, M. K., and Dunnill, P. (1990). Correlation of biocatalytic activity in an organic-aqueous two-liquid phase system with solvent concentration in the cell membrane. *Enzyme Microbial Technology,* **12**(4):281-291.

Pan, S., and Malcolm, B. A. (2000) Reduced Background Expression and Improved Plasmid Stability with pET Vectors in BL21 (DE3). *BioTechniques*, **29**, 1234-1238.

Parthuisot, N., Catala, P., Lebaron, P., Clermont, D., and Bizet, C. (2003) A Sensitive and Rapid Method to Determine the Viability of Freeze-Dried Bacterial Cells. *Letters in Applied Microbiology*, **36**, 412-417.

Patkar, A., Vijayasankaran, N., Urry, D. W. and Srienc, F. (2002) Flow Cytometry as a Useful Tool for Process Development: Rapid Evaluation of Expression Systems. *Journal of Biotechnology*, **93,** 217-229.

Patra, A. K., Mukhopadhyay, R., Mukhija, R., Krishnan, A., Garg, L. C., and Panda, A. K. (2000) Optimization of Inclusion Body Solubilization and Renaturation of Recombinant Human Growth Hormone from *Escherichia coli. Protein Expression and Purification*, **18**, 182-192.

Patterson, B. K., Till, M., Otto, P., Goolsby, C., Furtado, M. R., McBride, L. J., and Wolinsky, S. M. (1993) Detection of HIV-1 DNA and Messenger RNA in Individual cells by PCR-driven in Situ Hybridization and Flow Cytometry. *Science* **260**, (5110), 976-979.

Pereira, D. A., Pinto, G. F., Oestreicher, E. G. (1994) Kinetic mechanism of the Oxidation of 2-Propanol Catalyzed by *Thermoanaerobium brokii* alcohol dehydrogenase. *Journal of Biotechnology*, **34**, 43-50.

Petry, S., Furlan, S., Crepeau, M. J., Cerning, J., and Desmazeaud, M. (2000) Factors Affecting Exocellular Polysaccharide Production by *Lactobacillus delbrueckii* subsp. *bulgaricus* grown in a Chemically Defined Medium. *Applied and Environmental Micobiology*, **66**(8), 3427-31.

Plasek, J., and Sigler, K. (1996) Slow Fluorescent Indicators of Membrane Potential: a Survey of Different Approaches to Probe Analysis. *Journal of Photochemistry and phytobiology B: Biology,* **33**, 101-124.

Porro, D. and Srienc, F. (1995) Tracking of Individual Cell Cohorts in Asynchronous *Saccharomyces cerevisiae* Populations. *Biotechnology Progress*, **11**(3), 342-7.

Prescott, L. M., Harley, J. P., and Klein, D. A., (1996) *Microbiology*. 3rd ed. Wm. C. Brown Publishers.

Radcliff, G., and Jaroszeski, M. J. (1998) Basics of Flow Cytometry. *Methods in Molecular Biology*, **91**, 1-24.

Rasor, J. P., and Voss, E. (2001) Enzyme-Catalyzed Processes in the Pharmaceutical Industry. *Applied Catalysis A: General,* **221**, 145-158.

Reiseberge, M., Kasper, C., Reardon, K. F, and Scheper, T. (2001) Flow Cytometry in Biotechnology. *Applied Microbiology and Biotechnology* **56**, 350-360.

Roberts, S. M., Turner, N. J., Willetts, A. J. and Turner, M. K. (1995) *Introduction to Biocatalysis Using Enzymes and Microorganisms*, Cambridge University Press.

Roberts, S. M., and Wan, P. W. H. (1998) Enzyme-Catalysed Baeyer-Villiger Oxidations. *Journal of Molecular Catalysis B: Enzymatic* **4**, 111-136.

Robertson, B. R., Button, D. K., and Koch, A. L., (1998) Determination of the Biomasses of Small Bacteria at Low Concentrations in a Mixture of Species with Forward Light Scatter Measurements by Flow Cytometry. *Applied and Environmental Microbiology,* **64**(10) 3900-3909.

Roszak, D. B., and Colwell, R. R., (1987) Metabolic Activity of Bacterial cell Enumerated by Direct Viable Count. *Applied and Environmental Microbiology*, **53**(12), 2889-93.

Rozzell, J. D. (1998) Commercial Scale Biocatalysis: Myths and Realities. *Bioorganic & Medical Chemistry*, **7**, 2253-2261.

Ryan, W. Collier, P., Loredo, L., Pope, J., and Sachedev, R. (1996) Growth Kinetics of *Escherichia coli* and Expression of a Recombinant Protein and Its Isoforms under Heat Shock Conditions. *Biotechnology Progress,* **12**, 596-601.

Shapiro, H. M., Natale, P. J. and Kamentsky, L. A. (1979) Estimation of Membrane Potentials of Individual Lymphocytes by Flow Cytometry. *Proceedings of the National Academy of Science USA*, **76**(11), 5728-5730.

Shapiro, H. M., (2000a) Microbial Analysis at the Single Cell Level: Tasks and Techniques. *Methods,* **42**, 3-16.

Shapiro, H. M. (2000b) Membrane Potential Estimation by Flow Cytometry. Methods, **21**, 271-279.

Shapiro, H. M., (2003) *Practical Flow Cytometry* Fourth edn. 2003. John Wiley & Sons Inc.

Shaw, A. (1999) Protein Engineering of a-amylase for Low pH Performance. *Current Opinions in Biotechnology*, **10**, 349-352.

Sikkema, J., de Bont, J. A., and Poolman, B. (1995) Mechanisms of membrane toxicity of hydrocarbons. *Microbiology Review*, **59**(2), 201-222.

Sikkema, J., Poolman, B., Konings, W. N., and de Bont, J. A. (1992). Effects of the membrane action of tetralin on the functional and structural properties of artificial and bacterial membranes. *Journal of Bacteriology,* **174**(9), 2986-92.

Simpson, H. D., Alphand, V. and Furstoss, R. (2001) Microbiological Transformations 49. Asymmetric Biocatalysed Baeyer-Villiger Oxidation: Improvement Using a Recombinant *Escherichia coli* Whole Cell Biocatalyst in the Presence of an Adsorbent Resin. *Journal of Molecular Catalysis B: Enzymatic,* 16, 101-108.

Skarstad, K., Steen H. B., and Boye, E. (1983) Cell Cycle Parameters of Slowly Growing *Escherichia coli* B/r Studied by Flow Cytometry. *Journal of Bacteriology,* **154** (2), 656-662.

Soriano, E., Borth, H. K., and Mattanovich, D. (1999) Flow Cytometric Analysis of Metabolic Stress Effects Due to Recombinant Plasmids and Proteins in *Escherichia Coli* Production Strains. *Metabolic Engineering* **1** (1), 270-274. 1999.

Soriano, E., Borth, N, Katinger, H, and Mattanovich, D. (2002) Optimization of Recombinant Protein Expression Level in *Escherichia coli* by Flow Cytometry and Cell Sorting. *Biotechnology and Bioengineering* **80** (1), 92-99.

Srienc, F., and Dien, B S., (1992) Kinetics of the Cell Cycle of *Saccharomyces cerevisiae. Annals of the New York Academy of Science,* **665**, 59-71.

Steen, H. B (2004) Flow Cytometer for Measurement of the Light Scattering of Viral and other Submiccroscopic Particles. *Cytometry Part A,* **57A**, 94-99.

Steen, H. B., and Boye, E. (1980) Bacterial Growth Studied by Flow Cytometry. *Cytometry*, **1**(1), 32-6.

Steen, H.B., and Lindmo, T. (1979) Flow Cytometry: A High -Resolution Instrument for Everyone. *Science,* **207**(4391), 403-404.

Stevens, C. V., and Vanderhoydonck, B. (2001) Use of Acylphosphonates for the Synthesis of a α-Chlorinated Carboxylic and α ,ά- Dichloro Dicarboxylic acids and their Derivatives. *Tetrahedron,* **22**, 4793-4800.

Stewart, J. D. (1998) Cyclohexanone Monooxygenase: A Useful Reagent for Asymmetric Baeyer-Villiger Reactions. *Current Organic Chemistry,* **2**, 195-216.

Suller, M. T. E., and Lloyd, D. (1999) Fluorescence Monitoring of Antibiotic-Induced Bacterial Damage Using Flow Cytometry. *Cytometry*, **35**, 235-241.

Teich, A., Lin, H. Y., Andersson, L., Meyer, S., and Neubauer, P. (1998) Amplification of ColE1 Related Plasmids in Recombinant Cultures of *Escherichia coli* After IPTG Induction. *Journal of Biotechnology,* **64**, 197-210.

Thayer, A. M. (2001) Biocatalysis: Chemical and Pharmaceutical Makers Seek More Efficient and Often Cleaner Routes to Making Old and New Products. *Chemical and Engineering News,* **79**(21), 27-34.

Thompson, J. P., and Debinski, W. (1999) Mutants of Interleukin 13 with Altered Reactivity toward Interleukin 13 Receptors. *Journal of Biological Chemistry,* **274** (42), 29944-29950.

Thusitha, S. G., Attfields, P.V., and Veal, D. A. (2000) A Flow Cytometric Method for Rapid Detection and Enumeration of Total Bacteria in Milk. *Applied and Environmental Microbiology*. **66**(3), 1228-1232.

Uribe, S., Ramirez, J., and Pena, A. (1985) Effects of Beta-pinene on Yeast Membrane Functions. *Journal of Bacteriology*, 161(3), 1195-1200.

Van den Burg, B. (1999) Characterization of a Novel Stable Biocatalyst Obtained by Protein Engineering. *Biotechnology and Applied Biochemistry,* **30**, 35-40.

Van Der Werf, M. J. (2000) Purification and Characterisation of a Baeyer-Villiger Mono-Oxygenase from *Rhodococcus erythropolis* DCL14 Involved in Three Different Monocyclic Monoterpene Degredation Pathways. *Biochemistry Journal.* **347**, 693-701.

Van Dilla, M. A., Trujillo, T. T., Mullaney, F. P, and Coulter J.R. (1969) Cell Microfluorometry: A Method for Rapid Fluorescence Measurement. *Science,* **163** (3872), 1213-1214.

Veal, D., Deere, D., Ferrari, B., Piper, J., and Attfield, P. V. (2000) Fluorescence Staining and Flow Cytometry for Monitoring Microbial Cells. *Journal of Immunological Methods*, **243**, 191-210.

Vega-Mercado, H., Pothakamury, U.R., Chang, F., Barbosa-Canovas, G.V., and Swanson, B G. (1996) Inactivation of *Escherichia coli* by Combining pH, Ionic Strength and Pulsed Electric Fields Hurdles. *Food Research International*, **29** (2), 117-121.

Voet, D., and Voet, J. (1995) *Biochemistry*, Second ed. New York J. Wiley and Sons Publishers.

Walton, A. Z., and Stewart, J. D. (2002) An Efficient Enzymatic Baeyer-Villiger Oxidation by Engineered *Escherichia coli* Cells Under Non-Growing Conditions. *Biotechnology Progress,* **18**, 262-268.

Walton, A. Z., and Stewart, J. D. (2004) Understanding and Improving NADPH-Dependent Reactions in *Escherichia coli* Cells. *Biotechnology Progress* **20**(2), 403-411.

Wang, F., and Lee, S. Y. (1998) High Cell Density Culture of Metabolically engineered *Escherichia coli* for the Production of Poly(3-hydroxybutyrate) in a Defined Medium. *Biotechnology and Bioengineering*, **58**(2-3), 325-8.

Watson, J. V. *Introduction to Flow Cytometry.* 1991. Cambridge University Press.

Watson, J. V. (1992) *Flow Cytometry Data Analysis. Basic Concepts and Statistics.* Cambridge University Press.

Weaver, J. L. (2000) Introduction to Flow Cytometry. *Methods*, **21**(3), 199-201.

Weaver, R. F., (1995) *Basic Genetics*. 2nd ed. Dubuque, Iowa

Willets, A., (1997) Structural Studies and Synthetic Applications of Baeyer-Villiger Monooxygenases. *Trends in Biotechnology* **15**, 55-62.

Willimsky, G., Bang, H., Fischer, G., and Marahiel, M. A. (1992). Characterization of cspB, a *Bacillus subtilis* Inducible Cold Shock Gene Affecting Cell Viability at Low Temperatures. *Journal of Bacteriology*, **174**(20), 6326-6235.

Winson, M. K., and Davey, H. M. (2000) Flow Cytometric Analysis of Microorganisms. *Methods*, **21,** 231-240.

Woodley, J. M. (2000) Advances in Enzyme Technology - UK contributions. *Advances in Biochemical Engineering/ Biotechnology*, **70,** 93-108.

Zambianchi, F., Pasta, P., Carrea, G., Colonna, S., Gaggero, N., and Woodley, J. M. (2002) Use of Isolated Cyclohexanone Monooxygenase from Recombinant *Escherichia coli* as a Biocatalyst for Baeyer-Villiger and Sulphide Oxidations. *Biotechnology and Bioengineering,* **78**, 489-496.

Zhao, R., Natarajan, A., and Srienc, F. (1999) A Flow Injection Flow Cytometry System for On-Line Monitoring of Bioreactors. *Biotechnology and Bioengineering*, **62**(5), 609-617.

Websites:

http://biology.berkeley.edu/crl/compensation.html. A close up view of FITC and PE Fluorescence overlap.
http://www.emdbiosciences.com/docs/NDIS/TB042-000.pdf) pET11a vector.